

DESIGN AND SYNTHESIS OF NOVEL ISOELECTRIC BUFFERS

A Dissertation

by

SANJIV KUMAR SHANKERDASS LALWANI

Submitted to the Office of Graduate Studies of
Texas A&M University
in partial fulfillment of the requirements for the degree of

DOCTOR OF PHILOSOPHY

August 2004

Major Subject: Chemistry

DESIGN AND SYNTHESIS OF NOVEL ISOELECTRIC BUFFERS

A Dissertation

by

SANJIV KUMAR SHANKERDASS LALWANI

Submitted to Texas A&M University
in partial fulfillment of the requirements
for the degree of

DOCTOR OF PHILOSOPHY

Approved as to style and content by:

Gyula Vigh
(Chair of Committee)

Ronald D. Macfarlane
(Member)

Manuel P. Soriaga
(Member)

Suryakant D. Waghela
(Member)

Emile A. Schweikert
(Head of Department)

August 2004

Major Subject: Chemistry

ABSTRACT

Design and Synthesis of Novel Isoelectric Buffers. (August 2004)

Sanjiv Kumar Shankerdass Lalwani, B.S., University of San Carlos, Philippines

Chair of Advisory Committee: Dr. Gyula Vigh

Hydrolytically stable, low- and high-pI isoelectric hydrogel membranes were prepared from poly(vinyl alcohol) (PVA) as alternatives to polyacrylamide-based isoelectric membranes that hydrolyze in acidic and basic solutions.

Low-pI membranes were made by attaching an isoelectric buffer of a well-defined pI value (such as iminodiacetic acid, IDA, aspartic acid, ASP or glutamic acid, GLU) to the PVA backbone and crosslinking the PVA strands, *in situ*. The pH in these membranes does not change significantly with slight variations in the amount of isoelectric buffer that gets incorporated. The pI values of these membranes were $1.7 < \text{pI} < 2.0$ (IDAPVA), $2.0 < \text{pI} < 2.6$ (ASPPVA) and $2.6 < \text{pI} < 3.4$ (GLUPVA). The membranes were used as anodic membranes in isoelectric trapping (IET) experiments.

Sugars, cyclodextrins (CDs), and certain polyhydroxy compounds have pK_a values between 11.5 and 14. Thus, high-pI hydrogels were obtained by incorporating (i) quaternary ammonium derivatives of β -CD (QCDPVA) (ii) quaternary ammonium groups and β -CD (CDQPVA) and (iii) quaternary ammonium groups alone (QPVA) into the crosslinked PVA hydrogels. All three membranes had pI values greater than 11 and served as effective cathodic membranes for the IET of small ampholytic molecules and proteins.

In pH-biased IET, proteins are collected into solutions of isoelectric buffers that set the pH to keep the proteins in a charged state affording high solubility and preventing precipitation. Thus, a series of isoelectric buffers (biasers) with high buffering capacity, high conductivity, and pI values covering the useful pH 2-10 range are needed.

Two sets of such buffers were designed (i) with pI values between the pK_a values of two carboxylic acid groups and (ii) with pI values between the pK_a values of the conjugate acid form of two amine groups. Six of these buffers were synthesized and their synthesis was optimized. The products were obtained in their pure, isoelectric form and were extensively characterized.

Deus ex machina!

By God's actions through me...

To...

Daddy, Amma, Didi and Bhau

in loving memory of ...

Papa and Mummy

and to the legacy of Prof. Gyula Vigh.

ACKNOWLEDGEMENTS

For the success of this endeavor, acknowledgement is due to the following.

In humility, I bow and thank God, for having chosen me to embark on this endeavor.

I am extremely indebted to my father, Shankerdass Lalwani. He singlehandedly faced several of life's ups and downs, and the jolts never got to me. For always encouraging me and believing in me. Daddy, my degree and my dissertation are the rewards of the years of sacrifice you have made.

My all-out gratitude is expressed to my advisor, Prof. Gyula Vigh, a true educator. Human languages fall short of vocabulary sufficient to describe how grateful I am to him and his efforts. After God and in line with my father, my respects go to Dr. Vigh. He has molded me into what I am today. It was his advising, not just in science but in life as well, that has gotten me where I am today and where I will get tomorrow. Dr. Vigh, it has been an honor to become a part of the Prof. Gyula Vigh legacy.

I thank my family, my grandmother, my sister – my first home tutor, my brother, my aunts, uncles, cousins, and Julie for always being supportive.

I thank my colleagues, members of Dr. Vigh's group senior to me: Brent, Silvia, Shulan, Kingsley; former members of the group: Carre, Adriana, Dawn, Pavel and Wenhong; and my fellow group members: Evan, Ann, Brian, Nellie, Omar, Roy and Peniel for their support, their insights and their fellowship.

I give credit to my friends, from chemistry and beyond, you guys kept me going during those rather “spicily” challenging (a more subtle term for frustrating) times in the lab.

I acknowledge Prof. Manuel P. Soriaga, for believing in me, recruiting me to join Texas A&M University and introducing me to a marvelous separations scientist par excellence.

I recognize those in the chemistry department who kept me going with my research, for the numerous favors I have asked and times when I became somewhat pushy: Dr. Steve Silber (NMR specialist), Dr. Joe Reibenspies (X-ray lab specialist), Dr. Vanessa Santiago (MS specialist), Bill Merka (Glass Shop in-charge), Sandy Manning (GSO secretary *cum* will-listen-to-grad-students-vent) and Donna and George of ‘the stockroom’.

Dei justiciam? Was this a trial by ordeal? ***Opusculum Dei?*** Was this God’s petty work (if there is such a thing)? ***Patria Dei!*** The significant and ground breaking contribution to chemistry that is described in this dissertation along with the coming together of all the people with their contributions mentioned above, encompass God’s country!

TABLE OF CONTENTS

	Page
1. INTRODUCTION	1
2. OBJECTIVES AND RATIONALE	4
2.1 Objectives	4
2.2 Rationale: Technical Realization of Isoelectric Separations at Hitherto Unattainable Levels (TRISHUL)	4
2.2.1 Membrane chemistry	4
2.2.2 Polymer backbone	9
2.2.3 Crosslinking	10
2.2.4 Chemical modifications	11
2.2.5 Low-pI membrane design	12
2.2.5.1 Isoelectric buffers	12
2.2.5.2 Linkers	16
2.2.6 High-pI membrane design	17
2.2.6.1 High-pK _a moieties	17
2.2.6.2 Linking	20
2.2.7 Substrate	21
2.3 Rationale: Materials for Optimized Systems of Electrophoretic Separations (MOSES)	22
2.3.1 Biased chemistry	22
2.3.1.1 Isoelectric concentration ($pH=pI C_{min}$)	22
2.3.1.2 Buffering capacity	24
2.3.1.3 Conductivity	26
2.3.2 Design for low-pI compounds	30
2.3.2.1 Low-pI range	30
2.3.2.2 Synthesis	33
2.3.2.2.1 Opportunistic	33
2.3.2.2.2 <i>De novo</i> synthesis	34
2.3.3 Design for high-pI compounds	37
2.3.3.1 High-pI range	37
2.3.3.2 Synthesis	38
2.3.3.2.1 Opportunistic (sulfation)	39
2.3.3.2.2 <i>De novo</i> synthesis	39

	Page
3. TRISHUL: SYNTHESIS OF LOW-pI, HYDROLYTICALLY STABLE, ISOELECTRIC MEMBRANES	42
3.1 IDAPVA	42
3.1.1 Synthesis	42
3.1.1.1 Optimization	43
3.1.1.1.1 Hydrogel composition	43
3.1.1.1.2 Curing conditions	44
3.1.1.1.3 Casting technique	46
3.1.1.1.4 Substrate	47
3.1.1.2 Final procedure	49
3.1.2 Testing	52
3.1.2.1 Trapping	52
3.1.2.2 Desalting	54
3.1.3 pI characterization	55
3.2 ASPPVA	58
3.2.1 Synthesis	58
3.2.1.1 Final procedure	58
3.2.2 Testing	61
3.2.2.1 Trapping	61
3.2.2.2 Desalting	63
3.2.3 pI characterization	63
3.3 GLUPVA	66
3.3.1 Synthesis	66
3.3.1.1 Final procedure	66
3.3.2 Testing	69
3.3.2.1 Trapping	69
3.3.2.2 Desalting	71
3.3.3 pI characterization	71
4. TRISHUL: SYNTHESIS OF HIGH-pI, HYDROLYTICALLY STABLE ISOELECTRIC HYDROGEL MEMBRANES	74
4.1 QCDPVA	74
4.1.1 Synthesis	74
4.1.1.1 Final procedure	74
4.1.2 Testing	77
4.1.2.1 Trapping	77
4.2 CDQPVA	79
4.2.1 Synthesis	79
4.2.1.1 Final procedure	79

	Page
4.2.2 Testing	82
4.2.2.1 Trapping	82
4.2.2.2 Desalting	84
4.2.2.3 Control experiments	87
4.3 QPVA	88
4.3.1 Synthesis	88
4.3.1.1 Final procedure	88
4.3.2 Testing	91
4.3.2.1 Trapping	91
4.3.2.2 Control experiments	93
4.4 Application	93
5. MOSES: SYNTHESIS OF LOW-pI ISOELECTRIC BUFFERS	96
5.1 Opportunistic	96
5.1.1 N,N-bis(carboxymethyl)dimethyl ammonium hydroxide, inner salt (BCDAH)	96
5.1.1.1 pI determination	99
5.1.1.2 Isoelectric crystallization	101
5.1.1.3 Characterization	104
5.1.1.4 Recapitulation	110
5.2 <i>De novo</i> synthesis	110
5.2.1 N,N-bis(carboxypropyl)diethyl ammonium hydroxide, inner salt (BCPDEAH)	111
5.2.1.1 Optimization	111
5.2.1.2 Step 1	112
5.2.1.2.1 Synthesis (tertiary amine intermediate)	112
5.2.1.2.2 Processing of the intermediate	115
5.2.1.3 Step 2	115
5.2.1.3.1 Synthesis (quaternary ammonium intermediate)	115
5.2.1.3.2 Processing of the intermediate	119
5.2.1.4 Step 3 (hydrolysis of the ester groups)	123
5.2.1.4.1 Basic hydrolysis	123
5.2.1.4.2 Acidic hydrolysis	123
5.2.1.5 pI determination	127
5.2.1.6 IET purification	127
5.2.1.7 Characterization	132
5.2.1.8 Recapitulation	132

	Page
6. MOSES: SYNTHESIS OF HIGH-pI ISOELECTRIC BUFFERS	138
6.1 Opportunistic	138
6.1.1 1,3-Bis(N,N-dimethylamino)-2-O-sulfo-propane (BDASP)	138
6.1.1.1 pI determination	139
6.1.1.2 Isoelectric crystallization	141
6.1.1.3 Characterization	144
6.1.1.4 Final procedure	144
6.1.1.5 Recapitulation	150
6.2 <i>De novo</i> synthesis	151
6.2.1 1,3-Dimorpholino-2-O-sulfo-propane (DMSP)	152
6.2.1.1 Optimization	152
6.2.1.2 Step 1	152
6.2.1.2.1 Synthesis of DMP	152
6.2.1.2.2 Processing of DMP	156
6.2.1.3 Step 2	159
6.2.1.3.1 Synthesis (sulfation)	159
6.2.1.4 pI determination	159
6.2.1.5 Isoelectric crystallization	161
6.2.1.6 Characterization	164
6.2.1.7 Final procedure	164
6.2.1.8 Recapitulation	171
6.2.2 1,3-Bis(dipropylamino)-2-O-sulfo-propane (BDPSP)	172
6.2.2.1 Step 1	173
6.2.2.1.1 Synthesis of BDPP	173
6.2.2.1.2 Processing of BDPP	174
6.2.2.2 Step 2	174
6.2.2.2.1 Synthesis (sulfation)	174
6.2.2.3 pI determination	176
6.2.2.4 Isoelectric crystallization	178
6.2.2.5 Characterization	181
6.2.2.6 Recapitulation	181
6.2.3 1,3-Dipiperidino-2-O-sulfo-propane (DPSP)	187
6.2.3.1 Step 1	187
6.2.3.1.1 Synthesis	187
6.2.3.1.2 Processing of DPP	190
6.2.3.2 Step 2	190
6.2.3.2.1 Synthesis (sulfation)	190
6.2.3.3 pI determination	192

	Page
6.2.3.4 Isoelectric crystallization	194
6.2.3.5 Characterization	197
6.2.3.6 Final procedure	197
6.2.3.7 Recapitulation	203
7. CONCLUSIONS	204
7.1 TRISHUL	204
7.1.1 Low-pI membranes	204
7.1.2 High-pI membranes	205
7.2 MOSES	206
7.2.1 Low-pI isoelectric buffers	207
7.2.2 High-pI isoelectric buffers	208
REFERENCES	211
VITA	217

LIST OF TABLES

TABLE		Page
1	List of acidic Immobiline compounds, their corresponding structures and pK_a values	7
2	List of basic Immobiline compounds, their corresponding structures and pK_a values of the conjugate acids	8
3	List of isoelectric buffers for low-pI membrane synthesis	12
4	pK_a and pI values of four IDA derivatives at 25°C and 0.1M ionic strength	13
5	Common high- pK_a acids and their lowest pK_a values	18
6	Common alkane carboxylic acids and aminoalkane carboxylic acids and their lowest pK_a values	32
7	PVA/base/GDGE combinations tested during the optimization process	44

LIST OF FIGURES

FIGURE		Page
1	pH of IDA, aspartic acid and glutamic acid solutions at increasing analyte concentrations	15
2	Solution pH as a function of the logarithm of isoelectric buffer concentration for buffers with the same pI but different ΔpK_a values	23
3	Buffering capacity (β) as a function of the logarithm of the buffer concentration for ampholytes of pI=3.8 with different ΔpK_a values	25
4	Species concentrations (a. monocationic, b. isoelectric and c. monoanionic) as a function of the ampholyte concentration for ampholytes of the same pI and different ΔpK_a s	28
5	Generic structure of the acidic isoelectric buffers that are to be synthesized	33
6	Generic <i>de novo</i> synthesis scheme for carboxylic acid-based isoelectric buffers	36
7	Generic structure of amine-based isoelectric buffers that are to be synthesized	38
8	Scheme for the <i>de novo</i> synthesis of amine-based isoelectric buffers	41
9	E-SEM images of the BFN4 grade PVA substrate	48
10	A cartoon representation of a possible structure of the IDAPVA hydrogel	51
11	Electropherograms for the aliquots from the trapping experiment with IDAPVA as the anodic membrane: (top) feed, (middle) after 60 min and (bottom) after 180 min	53
12	Electropherograms for the aliquots from the desalting experiment with IDAPVA as the anodic membrane: (top) feed, (middle) after 15 min, and (bottom) after 30 min	56

FIGURE		Page
13	Sample conductance and pH as a function of time during the desalting run with IDAPVA as the anodic membrane	57
14	A cartoon representation of a possible structure of the ASPPVA hydrogel	60
15	Electropherograms for the aliquots from the trapping experiment with ASPPVA as the anodic membrane: (top) feed, (middle) after 60 min and (bottom) after 180 min	62
16	Electropherograms for the aliquots from the desalting experiment with ASPPVA as the anodic membrane: (top) feed, (middle) after 15 min, and (bottom) after 30 min	64
17	Sample conductance and pH as a function of time during the desalting run with ASPPVA as the anodic membrane	65
18	A cartoon representation of a possible structure of the GLUPVA hydrogel	68
19	Electropherograms for the aliquots from the trapping experiment with GLUPVA as the anodic membrane: (top) feed, (middle) after 60 min and (bottom) after 180 min	70
20	Electropherograms for the aliquots from the desalting experiment with GLUPVA as the anodic membrane: (top) feed, (middle) after 15 min, and (bottom) after 30 min	72
21	Sample conductance and pH as a function of time during the desalting run with GLUPVA as the anodic membrane	73
22	A cartoon representation of a possible structure of the synthesized QCDPVA hydrogel	76
23	Electropherograms of the feed sample (top) and the sample after 1 hour (bottom) of trapping using QCDPVA as the cathodic membrane	78
24	A cartoon representation of a possible structure of the synthesized CDQPVA hydrogel	81

FIGURE		Page
25	Electropherograms of the feed sample (top), sample after 1 hour (middle) and sample after 2 hours (bottom) from the trapping experiment using CDQPVA as the cathodic membrane	83
26	Conductance, potential and pH traces of the sample stream for the duration of the desalting experiment using CDQPVA as the cathodic membrane	85
27	Electropherograms of the feed sample (top), sample after the 6 th pass (middle) and sample after the 16 th pass (bottom) for the desalting experiment using CDQPVA as the cathodic membrane	86
28	A cartoon representation of a possible structure of the synthesized QPVA hydrogel	90
29	Electropherograms of the feed sample (top), sample after 1 hour (middle) and sample after 3 hours (bottom) for the trapping experiment using QPVA as the cathodic membrane	92
30	Scanned image of an SDS-PAGE analysis of aliquots taken from the lysozyme trapping experiment (M=Markers, F=Feed stream samples, C=Collection stream samples, B=Blank, CA=Catholyte stream)	95
31	Synthesis scheme for BCDAH from MIDA and IM	97
32	¹ H-NMR spectra for the aliquots of the reaction mixture of BCDAH at 5, 15, and 22 hours of reaction time	98
33	CE traces for BCDAH in pH 1.5 and 1.7 BGEs	100
34	Electropherograms run in positive to negative polarity mode, for the crystal (top) and the mother liquor (middle) from the BCDAH crystallization experiment and the Peakmaster 5.0 simulation (bottom)	102
35	Electropherograms run in negative to positive polarity mode, for the crystal (top) and the mother liquor (middle) from the BCDAH crystallization experiment and the Peakmaster 5.0 simulation (bottom)	103

FIGURE		Page
36	^1H - (top panel) and ^{13}C - (bottom panel) NMR spectra of BCDAH	105
37	^1H - ^1H COSY spectrum for BCDAH	106
38	^1H - ^{13}C HETCOR spectrum for BCDAH	107
39	ESI-MS analysis of BCDAH	108
40	Ball-and-stick representation of the X-ray crystal structure for the single crystal of BCDAH	109
41	The <i>de novo</i> synthesis scheme of BCPDEAH	112
42	^1H -NMR spectra of the D_6 -acetone sample (top panel) and the D_2O sample (bottom panel) from the reaction mixture after 1 hour of heating	113
43	^{13}C -NMR spectra for the time course of the reaction during the synthesis of the tertiary amine intermediate	114
44	^1H -NMR spectrum (top panel) and the ^{13}C -spectrum (bottom panel) for the tertiary amine intermediate	116
45	^1H - ^{13}C HETCOR spectra for the tertiary amine intermediate and the corresponding assignments	117
46	^{13}C -NMR spectra for the time course of the reaction during the synthesis of the quaternary ammonium intermediate	118
47	^1H -NMR spectrum (top panel) and the ^{13}C -spectrum (bottom panel) for the quaternary ammonium intermediate	121
48	^1H - ^{13}C HETCOR spectrum for the quaternary ammonium intermediate and the corresponding assignments	122
49	^1H -NMR spectra for the reaction mixture before (top panel) and after (bottom panel) hydrolysis with NaOH	124
50	^{13}C -NMR spectra for the reaction mixture before (top panel) and after (bottom panel) hydrolysis with NaOH	125

FIGURE		Page
51	¹ H-NMR spectra for samples from the hydrolysis using HBr	126
52	Electropherograms for the determination of the pI of BCPDEAH	128
53	pH measurements of the feed stream (red dots) and receiving stream (blue squares) samples during IET of BCPDEAH	130
54	Conductance measurements for the feed stream (red curves) and the receiving stream (blue curves) samples during the IET separation of BCPDEAH	131
55	¹ H-NMR (top panel) and ¹³ C-NMR (bottom panel) spectra of BCPDEAH	133
56	¹ H- ¹ H COSY spectrum for BCPDEAH and the corresponding signal assignments	134
57	¹ H- ¹³ C HETCOR spectrum for BCPDEAH and the corresponding signal assignments	135
58	ESI-MS analysis of BCPDEAH in the positive (top panel) and the negative (bottom panel) ion modes	136
59	BDAP sulfation scheme	138
60	Electropherograms for BDASP in pH=7.8 and pH=9.6 BGEs	140
61	Electropherograms for the cation analysis of the crystallized BDASP (top panel) and the crystallization mother liquor (middle panel) compared to the electropherogram simulated using Peakmaster 5.0 (bottom)	142
62	Electropherograms for the anion analysis of the crystallized BDASP (top panel) and the crystallization mother liquor (middle panel) compared to the electropherogram simulated using Peakmaster 5.0 (bottom panel)	143
63	¹ H- (top panel) and ¹³ C- NMR spectra (bottom panel) for BDASP with tentative assignment of signals	145

FIGURE		Page
64	^1H - ^1H COSY spectrum for BDASP with the corresponding assignments	146
65	^1H - ^{13}C HETCOR spectrum for BDASP and the corresponding signal assignments	147
66	ESI-MS analysis of BDASP in the positive ion (top) and the negative ion (bottom) modes	148
67	Ball-and-stick image of the X-ray crystal structure of BDASP ...	149
68	Complete scheme for the synthesis of DMSP	153
69	^{13}C -NMR spectrum for the reaction mixture after 2 hours of heating, with tentative signal assignments	154
70	Selected section of the ^{13}C -NMR spectrum for the aliquots of the reaction mixture taken over the course of the reaction, showing a decrease in the signal for the amino alcohol intermediate (I) and increase in the signal for DMP (D)	155
71	^1H -NMR spectra for the solids (top panel) and the liquid (bottom panel) from DMP synthesis	157
72	^{13}C -NMR spectra for the solids (top panel) and the liquid (bottom panel) from DMP synthesis	158
73	Electropherograms for the determination of the pI of DMSP	160
74	Electropherograms for the analysis of cations in the crystallized DMSP (top panel) and the crystallization mother liquor (middle panel) compared to the electropherogram simulated using Peakmaster 5.0 (bottom panel)	162
75	Electropherograms for the analysis of anions in the crystallized DMSP (top panel) and the crystallization mother liquor (middle panel) compared to the electropherogram simulated using Peakmaster 5.0 (bottom panel)	163

FIGURE		Page
76	^1H - (top panel) and ^{13}C -NMR (bottom panel) spectra of DMSP with the tentative assignments	165
77	^1H - ^1H COSY spectrum of DMSP with the corresponding assignments	166
78	^1H - ^{13}C HETCOR spectrum of DMSP with the corresponding assignments	167
79	ESI-MS analysis of DMSP in the positive (top panel) and negative (bottom panel) ion modes	168
80	Ball-and-stick image of the single crystal X-ray structure of DMSP	169
81	Scheme for the complete synthesis of BDPSP	173
82	^1H - and ^{13}C -NMR spectra for BDPP and the corresponding tentative assignments	175
83	Electropherograms of BDPSP in pH 7.8 and pH 9.6 BGEs	177
84	Electropherograms for the analysis of cations in the crystallized BDPSP (top panel) and the crystallization mother liquor (middle panel) compared to the electropherogram simulated using Peakmaster 5.0 (bottom panel)	179
85	Electropherograms for the analysis of anions in the crystallized BDPSP (top panel) and the crystallization mother liquor (middle panel) compared to the electropherogram simulated using Peakmaster 5.0 (bottom panel)	180
86	^1H - (top) and ^{13}C - (bottom) NMR spectra for BDPSP and the tentative assignment of the signals	182
87	^1H - ^1H COSY spectrum of BDPSP with the corresponding assignments	183
88	^1H - ^{13}C HETCOR spectrum of BDPSP and the corresponding assignment of signals	184

FIGURE		Page
89	The ESI-MS spectra of BDPSP in the positive (top) and the negative (bottom) ion modes	185
90	Ball-and-stick image of the single crystal X-ray structure of BDPSP	186
91	Complete scheme for the synthesis of DPSP	188
92	¹ H- (top) and ¹³ C- (bottom) NMR spectra of the DPP reaction mixture	189
93	¹ H-NMR spectra for the two samples from the sulfation of DPP	191
94	Electropherograms for the determination of the pI of DPSP	193
95	Electropherograms for cation analysis of the crystallized DPSP (top panel) and the crystallization mother liquor (middle panel), and the electropherogram simulated using Peakmaster 5.0 (bottom)	195
96	Electropherograms for anion analysis of the crystallized DPSP (top panel) and the crystallization mother liquor (middle panel), and the electropherogram simulated using Peakmaster 5.0 (bottom)	196
97	¹ H- (top) and ¹³ C- (bottom) NMR spectra for DPSP and the corresponding assignments	198
98	¹ H- ¹ H COSY spectrum of DPSP with the corresponding assignments	199
99	¹ H- ¹³ C HETCOR spectrum of DPSP and the corresponding assignments	200
100	ESI-MS analysis of DPSP in the positive (top) and negative (bottom) ion modes	201

ABBREVIATIONS

1D	One dimensional
2D	Two dimensional
3PPA	3-Pyridinepropionic acid
A	Analyte band
ASP	Aspartic acid
ASPPVA	Hydrolytically stable, low-pI membranes made from PVA, ASP and GDGE
A.U.	Arbitrary units
AU	Absorbance units
Ave DS	Average degree of substitution
BCDAH	N,N-bis(carboxymethyl)dimethyl ammonium hydroxide, inner salt
BCPDEAH	N,N-bis(carboxypropyl)diethyl ammonium hydroxide, inner salt
BDAP	1,3-Bis(N,N-dimethylamino)-2-propanol
BDASP	1,3-Bis(N,N-dimethylamino)-2-O-sulfo-propane
BDPP	1,3-Bis(dipropylamino)-2-propanol
BDPSP	1,3-Bis(dipropylamino)-2-O-sulfo-propane
BGE	Background electrolyte
BS ⁻	Benzensulfonate anion
BSH	Benzenesulfonic acid
BTC	Benzenetricarboxylic acid
BzTMA ⁺	Benzyltrimethyl ammonium cation
BzTMAOH	Benzyltrimethyl ammonium hydroxide

CD	Cyclodextrin
CDQPVA	Hydrolytically stable, high-pI membranes made from PVA, β -CD, GTMA and GDGE
$\text{pH}=\text{pI}C_{\text{min}}$	Minimum concentration of the isoelectric buffer required to set the pH of the solution equal to the pI of the buffer; the isoelectric concentration.
CAR	Carnosine
CE	Capillary electrophoresis
COSY	Correlation spectroscopy
CTAOH	Hexadecyltrimethyl ammonium hydroxide
DEA	Diethylamine
DMF	Dimethylformamide
DMP	1,3-Dimorpholino-2-propanol
DMSO	Dimethylsulfoxide
DMSP	1,3-Dimorpholino-2-O-sulfo-propane
DPA	Dipropylamine
DPP	1,3-Dipiperidino-2-propanol
DPSP	1,3-Dipiperidino-2-O-sulfo-propane
EBB	Ethyl 4-bromobutyrate
EH	Epichlorohydrin
EOF	Electroosmotic flow
E-SEM	Environmental-Scanning Electron Microscopy
ESI-MS	Electrospray ionization – mass spectrometry
GDGE	Glycerol-1,3-diglycidyl ether, crosslinker used in membrane synthesis

GLU	Glutamic acid
GLUPVA	Hydrolytically stable, low-pI membranes made from PVA, GLU and GDGE
GTMA	Glycidyltrimethylammonium chloride
H ₂ SO ₄	Sulfuric acid
HBr	Hydrobromic acid
HCl	Hydrochloric acid
HETCOR	Heteronuclear correlation
HI	Hydroiodic acid
HIS	Histidine
HMMB	4-Hydroxy-3-(morpholinomethyl)benzoic acid
IDA	Iminodiacetic acid
IDAPVA	Hydrolytically stable, low-pI membranes made from PVA, IDA and GDGE
IEF	Isoelectric focusing
IET	Isoelectric trapping
IM	Iodomethane
IPG	Immobilized pH gradient
KOH	Potassium hydroxide
LiOH	Lithium hydroxide
L _d	Length of the capillary from the inlet to the detector
L _t	Total length of the capillary
LYS	Lysine

MABA	m-Aminobenzoic acid
MCE	Multicompartmental electrolyzer
MIDA	Methyliminodiacetic acid
MOR	Morpholine
MOSES	Materials for Optimized Systems of Electrophoretic Separations
MSH	Methanesulfonic acid
N1	First neutral marker band
N2	Second neutral marker band
NaCl	Sodium chloride
NaOH	Sodium hydroxide
NMR	Nuclear Magnetic Resonance
OH	Hydroxy group; alcohol group
PE	Polyethylene
PEG	Poly(ethylene glycol)
PIP	Piperidine
PP	Polypropylene
PPG	Poly(propylene glycol)
PreMCE	Pressure Mediated Capillary Electrophoresis
PS	Polysulfone
pTSA	p-Toluenesulfonic acid
PVA	Poly(vinyl alcohol)
PVAc	Poly(vinyl acetate)

QCD	Quaternary ammonium cyclodextrin
QCDPVA	Hydrolytically stable, high-pI membranes made from PVA, QCD and GDGE
QPVA	Hydrolytically stable, high-pI membranes made from PVA, GTMA and GDGE
SDS-PAGE	Sodium dodecylsulfate – polyacrylamide gel electrophoresis
SO ₃ •Pyr	Sulfur trioxide pyridine complex
T	Temperature
THF	Tetrahydrofuran
t _{inj}	Injection time
t _{migr}	Migration time
Tris	Tris(hydroxymethyl) aminomethane
TRISHUL	Technical Realization of Isoelectric Separations at Hitherto Unattainable Levels
t _{transf}	Transfer time
TYRA	Tyramine
U _{appl}	Applied potential
UV	Ultraviolet light

1. INTRODUCTION

Electrophoretic protein separations [1,2] are gaining acceptance as viable alternatives to chromatographic methods [3]. One of the more successful preparative electrophoretic methods, Isoelectric Trapping (IET) in multicompartmental electrolyzers (MCE), is based on the principles of isoelectric focusing (IEF). In IEF, ampholytic species are separated, in an applied electric field, in a pH gradient, based on the differences in their isoelectric points (pIs) [4]. Preparative IET in MCEs was first reported by Williams and Waterman [5] in 1929 and later, though independently conceived, by Tiselius for protein separations in 1941 [6]. In the Williams apparatus, 14 chambers were separated by parchment membranes. The chambers were filled with ampholyte solutions of different pHs, and a potential was applied. The Tiselius apparatus had an arrangement for simultaneous harvesting of the separated components from the chambers. Martin et al. further improved the MCE set-up for IET using isoelectric membranes made by attaching weak acid and weak base functionalities, in differing ratios, to crosslinked agarose gels [7]. In this set-up, sample solutions containing mixtures of proteins were recirculated through the separation compartments, external coolers and reservoirs. The electric field, orthogonal to the direction of the flow, moved proteins through the isoelectric membranes into separation compartments

This dissertation uses the style and format of *Electrophoresis*.

formed by isoelectric membranes bracketing the pI of the target protein. Another MCE of a different format, introduced by Faupel et al. [8], which later became commercially available as the Iso-Prime unit [9], was used to isolate proteins in their pure, isoelectric form between isoelectric membranes made by copolymerizing acrylamide, N,N'-methylenebisacrylamide, and sufficient amounts of the appropriate acrylamido weak acid or weak base derivatives (the buffering species) and an acrylamido strong acid or strong base derivative (the titrating species) [10,11], commercially available as Immobilines [12]. These Immobiline-based isoelectric membranes have been successfully used in a diverse set of applications [13-17].

To improve the mechanical stability of the membranes, the acrylamide copolymers have been supported on glass fiber filters [8,9,18], porous polyethylene discs [19,20] polysulfone membranes [21], and woven poly(ethylene terephthalate) substrates [22]. In a recent modification, use of copolymerized gel beads has been reported [23]. However, hydrolysis of the amide bonds [24] in polyacrylamide-based gels, especially at low and high pHs, is an inherent limitation [25]. Over time, the bisacrylamide crosslinker hydrolyzes at the amide bond, which breaks the crosslink and makes the gels soft. Soft gels do not withstand the mechanical stress caused by the hydraulic flow parallel to the gel surface. The anti-convective barrier formed by the gel is then breached and bulk mixing of the solutions from different chambers occurs. The acrylamido acidic and basic side groups also hydrolyze off from the gel, leaving carboxylic acid groups behind, unpredictably altering the pI value of the gel. The use of IET at low and high pHs is thus limited by the hydrolysis of polyacrylamide-based hydrogels.

Since the solubility of proteins in their pure, isoelectric form is significantly lower than in their charged form [26], conventional IET suffers from protein precipitation when the protein load is high, limiting the productivity of the process. Recently, the Gradiflow electrophoretic binary protein separation unit, the BF200 [27] has been modified to operate in IET mode [17,22]. This BF200IET unit was used for pH-biased IET [26]. In pH-biased IET, proteins are isolated into solutions of isoelectric buffers that establish a solution pH different from the pI of the target protein, keeping the protein in a charged state with a higher solubility [26]. These isoelectric buffers, termed as biasers, are selected such that they are good carrier ampholytes [4], and their pI is bracketed by the pI values of the membranes, while being different from the pI of the protein. A good carrier ampholyte is an ampholyte with an appreciable conductance in its isoelectric state, accompanied by a good buffering capacity [4] as a consequence of being isoelectric between two closely spaced pK values [28]. Currently, very few compounds are commercially available that meet these criteria, limiting the flexibility of pH-biased IET.

2. OBJECTIVES AND RATIONALE

2.1 Objectives

The need for an alternative membrane chemistry to make hydrolytically stable isoelectric membranes for IET has been long identified. Polyacrylamide-based isoelectric membranes have worked well, but significant hydrolysis of the amide bond in the gels at high and low pHs limit the utility of IET. With the success of pH-biased IET, there is now a demand for a series of isoelectric buffers that are good carrier ampholytes, with pI values covering the useful pH 2-10 range. Therefore, to fully utilize the potentials of IET, (i) hydrolytically stable, high and low pI isoelectric membranes and (ii) a family of good carrier ampholytes to function as biasers covering the useful pH range, need to be synthesized.

2.2 Rationale: Technical Realization of Isoelectric Separations at Hitherto Unattainable Levels (TRISHUL)

2.2.1 Membrane chemistry

A suitable isoelectric membrane for IET must be a gel membrane with (i) that has pores large enough to permit ions and macromolecules, such as proteins, to pass through and yet (ii) acts as an effective barrier against convective transfer of liquids between the adjacent compartments and (iii) contains immobilized acidic and basic functionalities that establish a buffered pH inside the membrane pores.

Certain hydrophilic polymers, upon hydration, take up large amounts of water and swell into gels, called hydrogels [29,30]. If such a hydrogel-forming monomer and a suitable difunctional crosslinker were copolymerized [10] or a prepolymer was reacted

with a difunctional crosslinker [29-32] hydrogels of defined pore sizes could be formed. Similarly, hydrogels with defined pI values could be made using appropriately functionalized acidic or basic compounds, either copolymerized or attached to the polymer backbone after polymerization [7, 8]. To make gel membranes with adequate mechanical strength, the hydrogels may be supported on porous substrates [7].

Several such hydrogel-forming polymers are currently available, and have been used in electrophoresis. Martin et al. used filter papers soaked in a hot agarose solution, followed by cooling, allowing gel formation. Agarose chains form an extensive hydrogen-bonded network (within the chains and between water and the chains) and form good hydrogels at room temperature. The filter paper-supported agarose membranes were soaked in aqueous sodium hydroxide, followed by overnight crosslinking with epichlorohydrin in xylene. The crosslinked gel membranes were then soaked in sodium hydroxide, followed by soaking in a solution of sodium chloroacetate to bind an acidic functional group to the backbone chains via an ether link. In the next step, the membranes were rinsed in a sodium hydroxide solution followed by soaking in an aqueous solution of diethanolamine and sodium hydroxide. Diethanolamine was connected to the polymer backbone as one end of epichlorohydrin was bound to the backbone and the other end reacted with the amine group or the alcohol groups. With this procedure, membranes with pI values between 4.8 and 5.5 were formed [7].

In another experiment, Martin et al. impregnated filter paper with an agarose solution, allowed the gel to set, and soaked the membrane in a basic solution of a carrier ampholyte [28] mixture. After this, the membrane was soaked in a xylene solution of

epichlorohydrin, overnight. By varying the composition of the carrier ampholyte mixture, membranes with pI values 4 to greater than 10 were obtained [7].

Bjellqvist et al. made polyacrylamide-based isoelectric hydrogels with immobilized pH gradients [10,12]. Acrylamido acidic and basic derivatives (commercially available as Immobilines [12]) were added in varying amounts to a solution of acrylamide and N,N-methylenebisacrylamide, over a 25 cm length to form a pH gradient. As the acrylamido acidic and basic derivatives copolymerized with acrylamide and N,N-methylenebisacrylamide, the pH gradient was immobilized on the hydrogel. These gels later became commercially available as IPG (**I**mmobilized **pH** **G**radient) gels and strips. Listed in Table 1 are the acidic Immobiline compounds, and in Table 2 are the basic Immobiline compounds, with their corresponding pK_a values.

Faupel et al. [8], using the same acrylamide-based chemistry, made IPG segments of pI 3.5-7.2 and pI 7.4-10. They constructed a segmented IPG apparatus with three chambers separated by the two IPG segment cylinders. The sample solution was recirculated through the chamber bracketed by the IPG segments. The anode containing

Table 1. List of acidic Immobiline compounds, their corresponding structures and pK_a values.

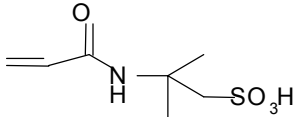
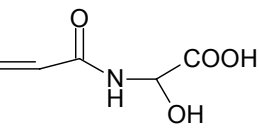
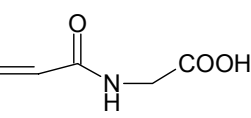
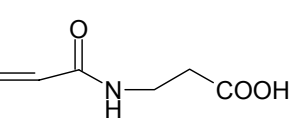
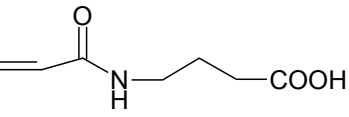
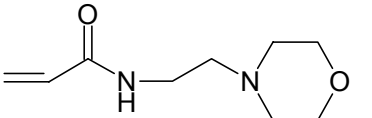
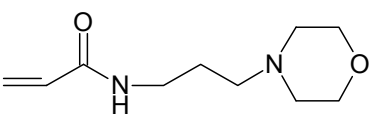
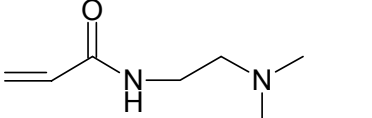
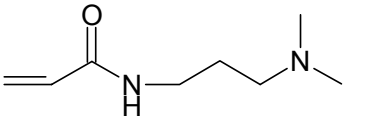
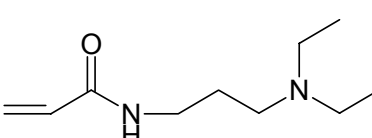
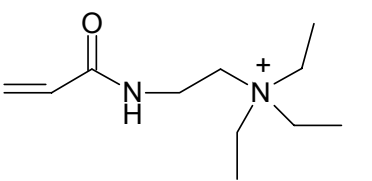
Name	Structure	pK _a
2-acrylamido-2-methylpropane sulfonic acid		1.2
2-acrylamido glycolic acid		3.1
N-acryloyl glycine		3.6
3-acrylamido propanoic acid		4.4
4-acrylamido butyric acid		4.6

Table 2. List of basic Immobiline compounds, their corresponding structures and pK_a values of the conjugate acids.

Name	Structure	pK_a
2-morpholino ethylacrylamide		6.2
3-morpholino propylacrylamide		7.0
N,N-dimethyl aminoethyl acrylamide		8.2
N,N-dimethyl aminopropyl acrylamide		9.3
N,N-diethyl aminopropyl acrylamide		10.3
QAE-acrylamide		>12

chamber was filled with the anolyte (an acid) and the cathode containing chamber with the catholyte (a base), and potential was applied. They trapped human adult hemoglobin ($7.2 < pI < 7.4$) in its pure isoelectric form between the two IPG segments. In a desalting experiment, they demonstrated the removal of Toluidine Blue (a cationic dye) and Bromophenol Blue (an anionic dye) from the sample chamber into the catholyte and anolyte chambers respectively [8]. Later, Wenger et al. [33] made acrylamide-based isoelectric gels with a well-defined, single pI value. They measured the electroosmotic flow (EOF) across the membranes as the pH surrounding the membranes (inside the membranes as well) was varied. By plotting the measured EOF values as a function of the pH, they found the pH where the EOF was zero. Since the EOF is zero when the number of positively charged and negatively charged species on the membrane surface are equal, the pH yielding a zero EOF was equal to the membrane pI value. The experimental pI values were found to be in good agreement with the desired values [33]. Polyacrylamide-based isoelectric gels of single pI values have been used in numerous diverse applications since then [16, 17, 23].

2.2.2 Polymer backbone

By definition, an isoelectric gel is hydrolytically stable if (i) the hydrogel forming polymer backbone, (ii) the crosslinking and (iii) the linking of the acidic and basic groups to the gel are resistant to hydrolysis.

One such stable, hydrogel forming polymer is poly(vinyl alcohol) (PVA) [29-32, 34]. PVA is produced by free radical polymerization of vinyl acetate, followed by either acidic or alkaline hydrolysis of the poly(vinyl acetate). Herrmann and Haehnel first

mentioned PVA in 1927 [35]. PVA is thermally stable up to 140°C, and forms films resistant to organic solvents. It is resistant to oxidation, and its films are stable over long periods of time. PVA films have high tensile strengths and 10 times more abrasion resistance than rubber [36, 37]. PVA is commercially available (more than 625,000 tons of PVA were manufactured in 2001), and relatively inexpensive (costing \$2.20/kg on average) [38].

To make isoelectric gel membranes from a hydrolytically stable polymer, the polymer must (i) form a hydrogel (thus be hydrophilic) (ii) be crosslinked and (iii) be derivatized with acidic and basic functionalities. Hydrophobic polymers such as polyethylene (PE), polypropylene (PP) and polystyrene (PS) do not form hydrogels. Very little chemical modification can be done on hydrophilic polymers such as poly(ethylene glycol) (PEG) and poly(propylene glycol) (PPG). PVA, however, forms hydrogels [30, 32, 34], has been crosslinked and has also been chemically modified in several ways [39-41].

2.2.3 Crosslinking

Dianhydrides prepared from maleic anhydride and diolefins crosslink PVA. Dialdehydes such as glutaraldehyde, were used to crosslink a thin PVA film in acidic media, inside fused silica capillaries [31]. A number of dianilinic dyes (Congo Red, Pontamine Bordeaux B, etc.) and a series of diphenols and triphenols (resorcinol, catechol, phloroglucinol, etc.), added to solutions of PVA form thermally reversible gels [34].

2.2.4 Chemical modifications

PVA undergoes chemical reactions very similar to those of low molecular weight aliphatic alcohols. Poly(vinyl hydrogen sulfate), a highly water soluble polymer, was made when PVA was reacted with sulfur trioxide [42]. Alkane and arene sulfonates of PVA were made by reacting the corresponding alkane or arene sulfonyl chlorides with PVA [43, 44]. In acidic solutions, aldehydes reacted with PVA formed acetals of PVA [31].

In basic solutions, PVA ethers were made using alkyl or aryl halides. In an aqueous, base catalyzed reaction of PVA with ethylene oxide, the hydroxyethyl ethers of PVA were formed [45]. Cyanoethylation of PVA with acrylonitrile was done using sodium hydroxide or sodium cyanide as catalyst [46, 47]. In the presence of alkoxides or alkalis, PVA was reacted with acid chlorides to form esters [48].

Given the hydrophilic nature, hydrolytic stability, and wide range of possible chemistries for chemical modification, PVA is an ideal polymer for the synthesis of hydrolytically stable, isoelectric hydrogel membranes. Production of such membranes and their use in IET would be feasible since PVA is inexpensive and commercially available in large quantities.

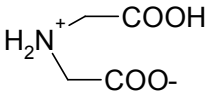
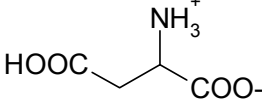
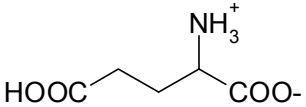
2.2.5 Low-pI membrane design

2.2.5.1 Isoelectric buffers

Martin et al. first introduced the concept of making isoelectric hydrogel membranes by grafting isoelectric buffers (in their case a mixture of carrier ampholytes) on a prepolymer (agarose) backbone [7]. To synthesize low-pI isoelectric hydrogels

from PVA in a similar manner, a low-pI, isoelectric buffer would have to be covalently attached to the PVA backbone. Three such isoelectric buffers that have (i) low, well defined pI values (ii) adequate buffering capacities (buffering groups with close pK_a values) [4] and (iii) a primary or secondary amino group that can be used to link these buffers to the PVA backbone, are listed in Table 3 [49, 50]. In basic media, compounds with amino groups can be attached to the PVA backbone using epihalohydrin, dihaloalkyl or diglycidyl linkers [7].

Table 3. List of isoelectric buffers for low-pI membrane synthesis.

Compound	Structure	pI	ΔpK_a
Iminodiacetic acid		2.20	0.81
Aspartic acid		2.77	1.7
Glutamic acid		3.17	2.01

This approach to make low pI, isoelectric hydrogel membranes from PVA is useful only if the pI of the isoelectric compound (i) does not change significantly upon immobilization or (ii) changes in a reproducible and predictable manner upon immobilization on the PVA backbone. Since linking of the isoelectric buffer to the PVA backbone occurs via the amino group, the influence of N-substitution on the pK_a values

of a series of N-substituted iminodiacetic acid (IDA) derivatives was studied. Listed in Table 4 are the pK_a and pI values of four N-substituted IDA derivatives [49, 50].

Table 4. pK_a and pI values of four IDA derivatives at 25°C and 0.1M ionic strength.

N-substituent	pK_{a1}*	pK_{a2}	pK_{a3}	pI
H	1.8	2.6	9.3	2.2
Methyl	1.9	2.3	9.6	2.1
Ethyl	1.6	2.2	9.9	1.9
n-Propyl	1.5	2.2	10.1	1.9
2-Hydroxyethyl	1.6	2.2	8.7	1.9

*tentative value

The pK_a value of the most acidic carboxylic acid group (pK_{a1}) decreases slightly as alkyl groups of increasing chain length replace hydrogen. pK_{a2} (for the second carboxylic acid group) decreases more significantly as a methyl group replaces the hydrogen, and from then on, is almost unaffected as the chain length of the substituent increases. pK_{a3} however (for the conjugate acid of the amine) is affected the most. The overall effect on the pI of the buffers (which is the average of the pK_a values of the two carboxylic groups) follows a similar trend with pK_{a2} . The pI values of N-substituted aspartic acid and glutamic acid derivatives can be expected to follow the same trend as the IDA derivatives, i.e., the N-substituted derivatives will have pI values lower than the

native isoelectric buffers. Thus, membranes made with these isoelectric buffers will have pI values slightly lower than or equal to the pI value of the unbound isoelectric buffer.

The pH of a solution of an isoelectric buffer, such as IDA varies with the buffer concentration, i.e., as the concentration of the isoelectric buffer increases, the pH of the solution approaches the true pI value of the isoelectric buffer. The pHs of solutions of three pure isoelectric buffers (IDA, aspartic acid and glutamic acid) were calculated using the Peakmaster 5.0 program [51, 52] taking the pK_a values from Ref 49 and 50. Figure 1 shows a plot of the calculated pH values of the three isoelectric buffers as a function of the logarithm of the respective buffer concentrations. As seen in Figure 1, at very low concentrations ($<1 \times 10^{-11}$ M) the pH of the solution is equal to the pH of distilled water. At higher isoelectric buffer concentrations, the pH of the solution approaches the pI of the buffer until the pH no longer changes (at and above 1.5×10^{-1} M). The minimum concentration at and above which the pH of a solution of an isoelectric buffer remains constant and is equal to the pI of the buffer ($^{pH=pI}C_{min}$) is a characteristic of the buffer (sometimes referred to as the isoelectric concentration of the buffer).

Forming isoelectric hydrogels by incorporating an isoelectric buffer on a prepolymer backbone has an advantage. If the amount of isoelectric buffer incorporated changes (but does not decrease below $^{pH=pI}C_{min}$) the pH inside the pores of the membrane does not change. If the concentration of the incorporated isoelectric buffer is lower than the isoelectric concentration (up to 50% less), the pH changes very slightly (about 0.1 pH unit). The pI values of isoelectric hydrogels currently being made using the

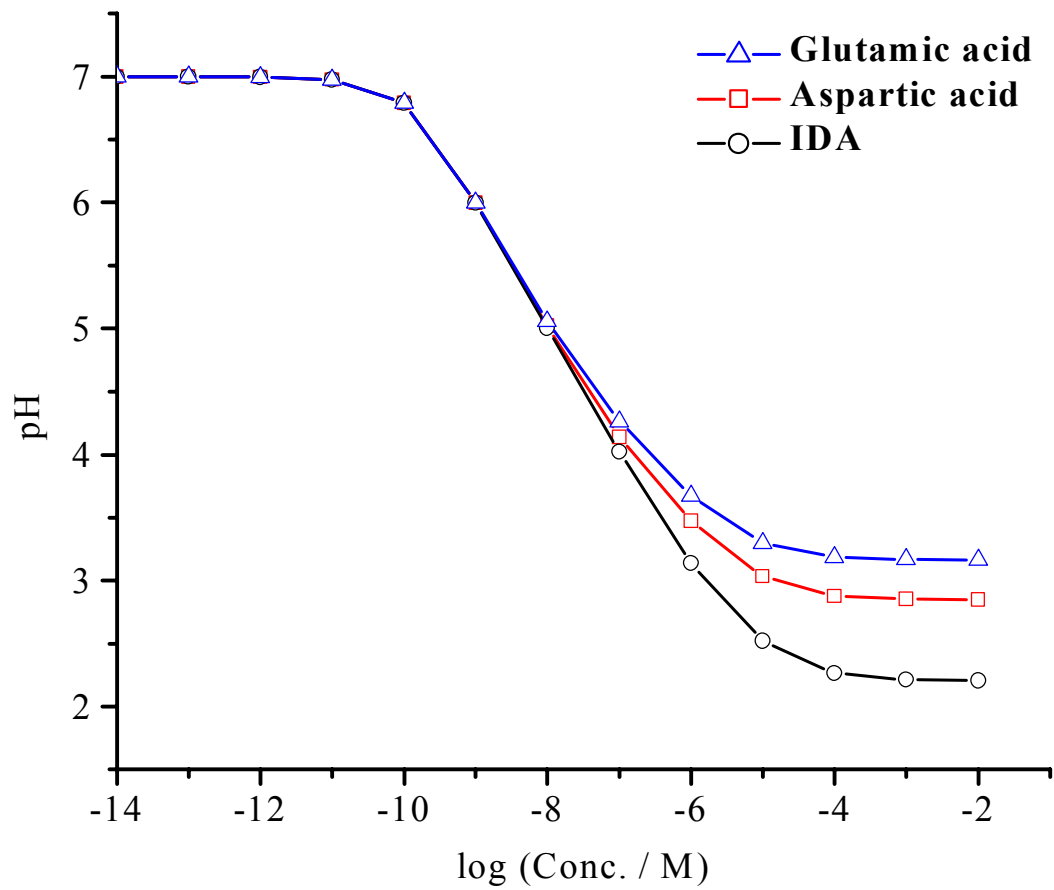


Figure 1. pH of IDA, aspartic acid and glutamic acid solutions at increasing analyte concentrations.

Immobiline chemicals alter significantly even with slight changes in the relative incorporation ratios of the acidic and basic functionalities.

There is a built-in limitation however to this approach of making isoelectric hydrogels. The pI of the hydrogel is set by the pI of the immobilized isoelectric buffer and cannot be tuned continuously, only stepwise, by changing the isoelectric buffer. However, if the hydrolytically stable, low-pI isoelectric hydrogel membrane is used as an anodic membrane (exposing it to low pH anolytes) in IET, the higher pI polyacrylamide-based isoelectric hydrogels, whose pI values can be tuned continuously, are isolated from the anolytes, and thus their hydrolysis is slowed-down. Stepwise tunability is a minimal limitation compared to the pragmatic benefits of hydrolytic stability, thus the low-pI PVA hydrogels can extend the utility of IET beyond the useful range of polyacrylamide-based isoelectric hydrogels.

2.2.5.2 Linkers

Glutaraldehyde (and other dialdehydes) can be used to crosslink PVA chains and immobilize the isoelectric buffers. In acidic media, glutaraldehyde can form acetals with PVA and via Schiff base formation with the amine, can link the isoelectric buffer to the backbone. However, glutaraldehyde readily oxidizes to form acid or hemi-acid functionalities [32] which will unpredictably alter the pI of the hydrogel.

Epichlorohydrin (and other epihalohydrins) can be used to crosslink PVA chains and immobilize the isoelectric buffers to the backbone in basic media, just as Martin et al. did with agarose and a carrier ampholyte mixture [7]. Similarly, dihaloalkyl linkers (such as the commercially available 1,3-dibromo-2-propanol, Aldrich Chemical Co.,

Inc.) can be used. Another alternative is to use a diglycidyl linker (such as glycerol-1,3-diglycidyl ether, Aldrich Chemical Co., Inc.) for immobilization and crosslinking.

Although all of the three kinds of linkers mentioned are hydrolytically stable, it is better, for simplicity sake, to use a linker that reacts with similar kinetics on both ends that form the link. Epoxy-ring opening, followed by nucleophilic attack and a proton transfer, is a much faster and more efficient reaction than a nucleophilic substitution reaction involving a halide leaving group. Thus, glycerol diglycidyl ether, a commercially available linker, was selected for the crosslinking of the PVA hydrogels and the immobilization of the isoelectric buffers.

2.2.6 High-pI membrane design

2.2.6.1 High-pK_a moieties

Since polyacrylamide-based chemistry can be used to make useful isoelectric hydrogels with pIs only as high as 11, hydrolytically stable isoelectric hydrogels of much higher pI values need to be synthesized. Weak acid or base functionalities with high-pK_a values are needed to make high-pI isoelectric hydrogels. The conjugate acids of organic weak bases (e.g., amines) can have pK_a values as high as 11 (e.g., piperidine) [50]. However, after N-substitution, the pK_a values decrease (by about 0.7 to 2 pH units, depending on the substituent). For high buffering capacity, the pI of the isoelectric membrane has to be close to the buffering range of the buffering species (pK_a ± 1). Thus, amines cannot be used to make high-pI (higher than 10), hydrolytically stable, isoelectric hydrogels. Sugars [53], cyclodextrins (CDs) [54, 55], and certain polyhydroxy compounds [56] are very weak acids and have pK_a values between 11.5 and 14. Listed

in Table 5 are some of these common, high- pK_a acids, and their lowest pK_a values. High buffering capacity, high pI, hydrolytically stable, isoelectric hydrogels can be made using these compounds.

Table 5. Common high- pK_a acids and their lowest pK_a values.

Compound	pK_a
Maltose	11.94
Lactose	11.98
Fructose	12.03
Mannose	12.08
Xylose	12.15
Glucose	12.28
Galactose	12.39
Dulcitol	13.43
Sorbitol	13.60
α -cyclodextrin (α -CD)	12.05
β -cyclodextrin (β -CD)	12.20
γ -cyclodextrin (γ -CD)	12.33

High-pI, PVA-based, isoelectric hydrogel membranes can be made if (i) as in the case of the low-pI membrane synthesis, a high-pI, isoelectric buffer (made from a high- pK_a acid listed in Table 5), is immobilized on the PVA backbone or (ii) a high- pK_a acid and a quaternary ammonium group are attached separately to the PVA backbone, followed by crosslinking of PVA. Since PVA is a polyhydroxy compound, some of the secondary alcohol groups of PVA might also have pK_a values in the 11-14 range as well. If this is true (and can only be determined experimentally), a third possible alternative to

making high-pI hydrogel membranes is to attach quaternary ammonium groups to the PVA backbone, followed by crosslinking. The pH in the pores of the membrane would be buffered by the PVA weak acid moieties.

A high pI, good buffering capacity, isoelectric buffer can be made using one of the high pK_a weak acids listed in Table 5, if the compound has (i) at least one amine group with a pK_a between 11 and 14 and at least one of the weak acid groups or (ii) at least one permanently charged quaternary ammonium group and at least two of the weak acid moieties (i.e., the ratio of the number of ammonium groups per weak acid group is less than 1). Since amines with pK_a values between 11 and 14 are very rare, the second design is more feasible. Reacting one of the CDs (preferably β -CD, the least expensive of the three) and attaching a quaternary ammonium group to it, will result in the desired quaternary ammonium cyclodextrin (QCD) isoelectric buffer. If any of the simple sugars were to be used, at least two sugar molecules and one quaternary ammonium group would have to be linked together, requiring multiple synthetic steps. Use of CDs is more practical since the presence of 6, 7 or 8 glucose units in a single molecule (whether α , β , or γ -CD) (i) decreases the number of synthesis steps and (ii) provides more binding sites for the quaternary ammonium group per molecule of the weak acid.

Reacting β -CD with trialkylammonium haloalkanes (such as trimethylammonium bromopropane, Aldrich Chemical Co., Inc.) in basic medium attaches the quaternary ammonium functionality to the CD via an ether link [57], due to nucleophilic substitution of the halogen. Similarly, glycidyl trialkylammonium groups can be used in basic media. Epoxy-ring opening, attachment to a hydroxy group on the

CD, followed by a proton transfer attaches the quaternary ammonium group, via an ether link, to the CD [58]. A third alternative is to first derivatize the CD to attach a better leaving group (such as tosylate) [59]. The derivatized CD can then react with a tertiary amine to form the quaternary ammonium group bound to the CD by a carbon-nitrogen covalent bond [59-61]. Quaternary ammonium groups can be attached to PVA in similar reactions. To make the three possible high-pI isoelectric hydrogels, the glycidyl trialkylammonium-based approach will be used, due to the faster epoxy reaction (compared to the haloalkanes) and simplicity of synthesis (compared to tosylation followed by reaction with an amine).

2.2.6.2 Linking

Solms and Egli first crosslinked a CD mixture into a block-polymer using epichlorohydrin in 1965 [62]. Water soluble CD polymers have been made with alkylene glycol diglycidyl ethers [63-65]. Szejtli et al. linked CDs to polymeric backbones such as cellulose [66] and PVA [39, 40] using epichlorohydrin under basic conditions.

To simplify the synthesis of the hydrolytically stable, high-pI isoelectric hydrogel membranes, the selected linker must (i) be hydrolytically stable (ii) link both QCD to PVA, native β -CD to PVA and (iii) crosslink PVA chains. Since the chosen quaternary ammonium group attachment (to the CD and PVA backbone) occurs in basic media, it is preferred that the linker reacts under the same conditions. Thus dihaloalkanes, epihalohydrins or diglycidyl derivatives have to be used. Since epoxy group reactions are faster, a diglycidyl linker is most suitable and will be used.

2.2.7 Substrate

Hydrogels supported on a porous substrate make membranes of better mechanical stability. A good substrate material is (i) hydrophilic, (ii) hydrolytically stable, (iii) does not have acidic or basic functionalities that would alter the overall pI of the membrane (iv) and preferably, binds covalently to the hydrogel matrix.

Polyacrylamide copolymers have been supported on glass fiber filters [8,9,18]. Silanol groups in glass are weak acids that contribute to the overall pI of the membrane. Porous polyethylene discs have been used [19,20] but are too hydrophobic. Polysulfone membranes have been tested [21] but polysulfones can slowly hydrolyze to form sulfonic acid functionalities. Woven poly(ethylene terephthalate) substrates have been used [22] but are prone to hydrolysis of the polyester backbone. None of these substrates are suitable for high and low pI isoelectric membranes. A woven substrate of PVA fibers is commercially available [67]. This PVA paper substrate has all the properties desired for the purpose of high and low pI hydrogel membranes. The paramount benefit of using a PVA paper substrate is its being chemically identical to the hydrogel matrix. Thus, being the most suitable substrate, PVA paper will be used.

2.3 Rationale: Materials for Optimized Systems of Electrophoretic Separations (MOSES)

2.3.1 Biased chemistry

An ideal isoelectric biased would have the properties of a good carrier ampholyte, as described by Vesterberg, i.e., have a high buffering capacity (β) [4] a requirement satisfied by being isoelectric between two closely spaced pK values [28].

2.3.1.1 Isoelectric concentration ($C_{\min}^{\text{pH}=\text{pI}}$)

At a sufficiently high concentration of the ampholyte, the pH of the solution, where the ampholyte is the only acidic or basic species, will be equal to the pI of the ampholyte. The minimum ampholyte concentration required to bring the solution pH equal to the ampholyte pI ($C_{\min}^{\text{pH}=\text{pI}}$) is a function of the pI and the difference between the two pK_a values (the ΔpK_a) that buffer at the pI.

Figure 2 shows a plot of solution pH calculated using Peakmaster 5.0 [51, 52] for a hypothetical isoelectric buffer with a pI=3.8 and $\Delta\text{pK}_a=1$ at different buffer concentrations. Similarly, values for the pH of hypothetical buffer solutions with the same pI (pI=3.8) but ΔpK_a values of 2, 3 and 4 were calculated and plotted.

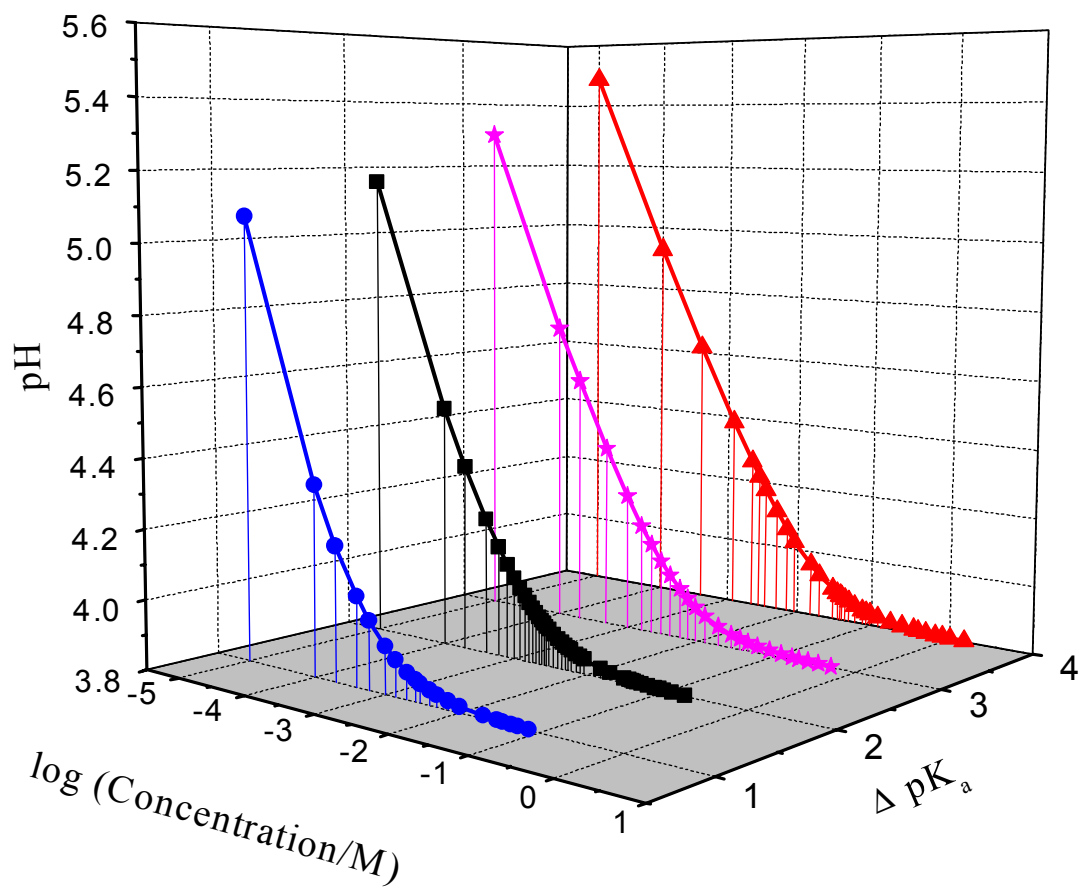


Figure 2. Solution pH as a function of the logarithm of isoelectric buffer concentration for buffers with the same pI but different ΔpK_a values.

It can be seen from Figure 2 that as the ΔpK_a increases, there is a significant increase in the $^{pH=pI}C_{min}$ of the ampholyte. For a $\Delta pK_a=1$, at 120 mM buffer concentration, the solution pH is 3.802. To reach the same pH, using an ampholyte with a $\Delta pK_a=3$, a buffer concentration of 800 mM is needed.

2.3.1.2 Buffering capacity

Van Slyke [68] defined β as the derivative $dCb/d(pH)$, where dCb represents the increase in strong base concentration to give a pH increase of $d(pH)$. For an isoelectric buffer, β is a function of the ΔpK_a between the buffering groups. Figure 3 is a plot of β as a function of ΔpK_a calculated for hypothetical ampholytes, in the following manner.

A set of increasing ampholyte concentrations was chosen and the resulting solution pH values were calculated using Peakmaster 5.0 [51, 52] for a hypothetical isoelectric buffer with a pI value of 3.8 and $\Delta pK_a = 1$. Then, the pH values of the solutions were recalculated assuming that they also contained 0.1 mM sodium hydroxide. From these pH values, the β values were calculated and plotted. This was also done for hypothetical ampholytes of the same pI value (3.8) but with ΔpK_a values of 2, 3, and 4.

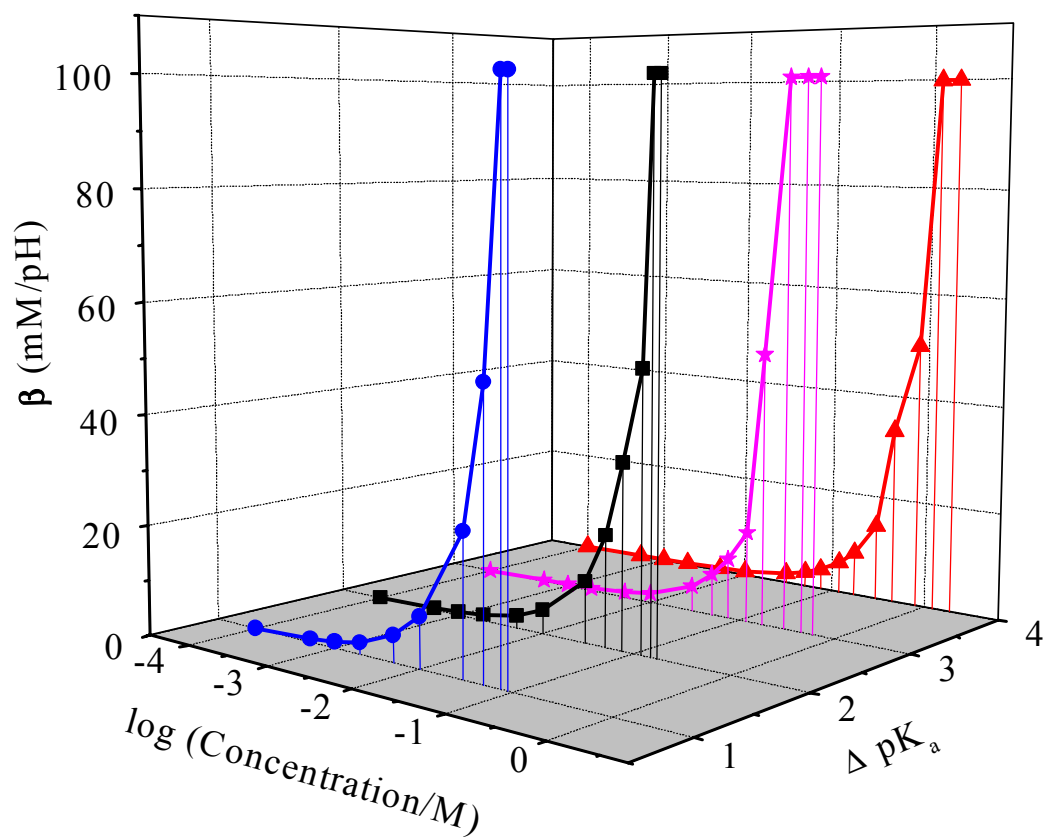


Figure 3. Buffering capacity (β) as a function of the logarithm of the buffer concentration for ampholytes of $pI=3.8$ with different ΔpK_a values.

Figure 3 indicates that at low isoelectric buffer concentrations (<2 mM), the influence of ΔpK_a is not significant. The amounts of the isoelectric buffer and the base are similar, thus, β is low and a drastic change in pH occurs in every solution. However, at higher concentrations (>10 mM), where a significant amount of the buffering species is present, the increase in β with the decrease in the ΔpK_a of the isoelectric buffer becomes evident. Also, at and above each isoelectric buffer's respective isoelectric concentration (also ΔpK_a dependent), the β value is the same for each buffer and the value does not change with an increase in the buffer concentration.

2.3.1.3 Conductivity

Fullarton and Kenny first proposed electrophoretic separations using low conductivity isoelectric buffers as background electrolytes (BGEs) [69]. Later, Hjertén et al. patented the concept of electrophoretic separations in low conductivity BGEs using isoelectric buffers with close pK_a values that have high buffering capacities [70].

Righetti et al. have proposed the concept that due to low conductivity, isoelectric buffer BGEs permit the use of high field strengths and result in minimum Joule heating. Thus, such buffers can be used for fast electrophoretic separations [68, 71-74].

However, Beckers [75], with a series of calculations, has shown that if the pK_a values of an isoelectric buffer are close, the conductivity of such a solution is high. Only if the pK_a values are far apart from each other will the conductivity of the solution be low. Thus, the conductivity of isoelectric buffer BGEs decreases only as buffering capacity is sacrificed. This agrees with the qualities of good carrier ampholytes proposed by Vesterberg and Svensson [4].

To test this concept, a set of increasing ampholyte concentrations was chosen and the concentrations of the respective species present in the solution were calculated using Peakmaster 5.0 [51, 52] for a hypothetical isoelectric buffer with a pI value of 3.8 and $\Delta pK_a = 1$. Then, the concentrations of the respective species were calculated for hypothetical ampholytes of the same pI value (3.8) but ΔpK_a values of 2, 3, and 4. Figure 4 shows the species concentration plots for each species.

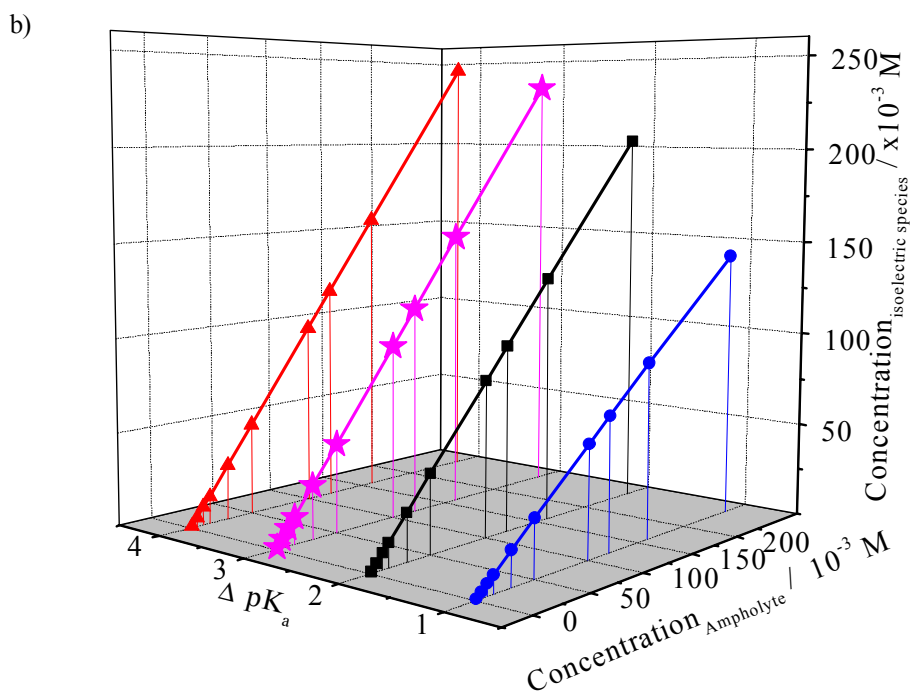
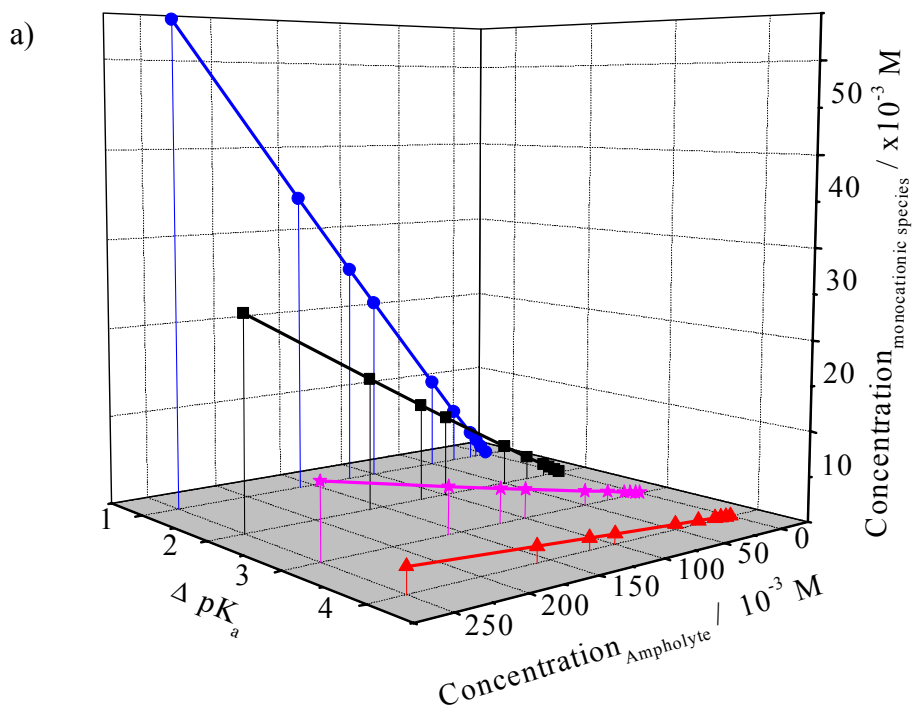


Figure 4. Species concentrations (a. monocationic, b. isoelectric and c. monoanionic) as a function of the ampholyte concentration for ampholytes of the same pI and different ΔpK_a s.

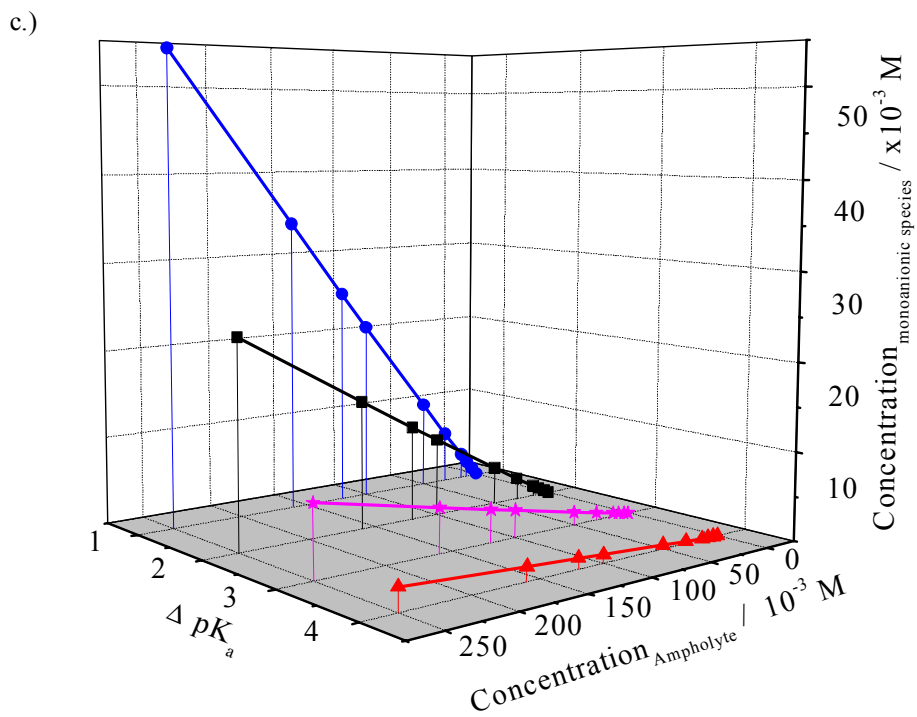


Figure 4. continued.

In Figures 4a and 4c (for the monocationic and monoanionic species, respectively) there is an increase in the concentration of the charged species, for the same ampholyte concentration, as the pK_a values come closer. The concentration of the isoelectric species correspondingly decreases as the pK_a values come closer, seen in Figure 4b. Thus, high conductivity is a consequence of the close pK_a values in an isoelectric buffer BGE, just as is high buffering capacity. These calculations support Beckers' claim that the existence of high buffering capacity, low conductivity isoelectric

buffers is a myth. However, the high conductivity of good isoelectric buffers can be beneficial in IET.

In an IET set-up, field strength varies over the distance between the electrodes as a function of the conductivity of the medium. The field strength is higher in the isoelectric membranes and its magnitude is difficult to manipulate. Field strength in (or potential drop across) the sample streams however, can be manipulated easily. Adding an ideal isoelectric biaser (i.e., one that has close pK_a values, thus having a high conductivity and a high buffering capacity at its pI) to the receiving stream increases the conductivity of the solution. Consequently, the field strength is low in the receiving stream. Similarly, if the conductivity in the feed stream is low, the field strength is high. As a result, transfer rates from the feed stream, across the membranes and to the receiving stream become faster.

2.3.2 Design for low-pI compounds

2.3.2.1 Low-pI range

An isoelectric buffer is made by coupling a weak acid and a weak base into one molecule. High buffering capacity and high conductivity isoelectric buffers (i.e., good carrier ampholytes) must have a small ΔpK_a (preferably 1 or 2). Most carboxylic acid pK_a values are in the 0.8 to 4.8 range. Most amines have pK_a values in the 8 to 11 range. Thus, it is obvious that isoelectric buffers that are also good carrier ampholytes cannot be made by simply coupling one carboxylic acid group with one amine group, i.e., most common amino acids (e.g., glycine, β -alanine, etc.) are not good carrier ampholytes.

Isoelectric buffers of a different design have two weak acid groups coupled to one weak base group. The pK_a values of the conjugate acids of the weak base must be at least 3 (preferably 4) units greater than the pK_a values of the weaker acidic group. The pI of such a buffer would fall between the pK_a values of the two weak acid groups [$pI=(pK_{a1} + pK_{a2})/2$]. The pK_a values of the two weak acids can be close (depending on the type of the functional group and its substituents) and thus, the molecule can act as a good carrier ampholyte. An example of such a compound is IDA (pK_a and pI values listed in Table 3).

Table 6 shows a list of common carboxylic acids and aminocarboxylic acids with their respective acidic pK_a values [49, 50]. First, it can be seen from Table 6 that the presence of the amine group has an influence on the pK_a of the carboxylic acid group (alkane carboxylic acid pK_a s are higher than the pK_a s of the corresponding aminocarboxylic derivatives). Also, this list indicates that the pK_a of the carboxylic acid is a function of the distance between the carboxylic acid group and the amine groups (the pK_a of the carboxylic acid increases with increasing distance from the amine). It can be predicted from these trends that isoelectric buffers of this design will have pI values between 1.5 and 4.0.

Table 6. Common alkane carboxylic acids and aminoalkane carboxylic acids and their lowest pK_a values.

Acid	pK_a
Carboxylic	
Formic	3.57
Acetic	4.56
Propanoic	4.69
Butanoic	4.63
Pentanoic	4.64
Hexanoic	4.63
Aminocarboxylic	
2-Aminoacetic	2.34
3-Aminopropanoic	3.54
4-Aminobutanoic	4.07
5-Aminopentanoic	4.20
6-Aminohexanoic	4.33

Isoelectric buffers with two acidic groups can also have a strong base functionality (such as a quaternary ammonium group) attached to the molecule. Aside from the pragmatic benefit of high buffering capacity and high conductivity due to close pK_a values, the permanently charged quaternary ammonium functionality is less prone to N-oxidation in comparison with amines. Figure 5 shows the generic structure for the acidic isoelectric buffers that are to be synthesized (with two carboxylic acid groups and an N-oxidation-resistant quaternary ammonium unit).

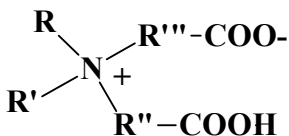


Figure 5. Generic structure of the acidic isoelectric buffers that are to be synthesized. R'' and R''' can be methylene to propylene.

2.3.2.2 Synthesis

2.3.2.2.1 Opportunistic

An opportunistic way to synthesize acidic isoelectric buffers according to the generic structure in Figure 5 is to alkylate the amine group of a pre-formed isoelectric species. As an example, one can alkylate IDA or methyliminodiacetic acid (MIDA) under basic conditions with an appropriate alkylating agent and form the N-oxidation-resistant derivative. Haloalkanes attach to nucleophiles (such as amines and alcohols) via nucleophilic substitution (S_N) of the halide leaving group for the nucleophile [24]. This reaction has been used to synthesize amines [53, 76], amino alcohols [77], aminocyano alcohols [78] and propargylic ammonium salts [79] with few complications. However, a similar reaction reported for N-alkylation of amino acids, required heating, longer reaction time and gave low yields [80-83]. In a different approach, acid derivatives (e.g., haloalkanoic acids or haloalkanoate esters) were attached onto amines via the S_N mechanism. Haloalkanoate ester attachment required shorter reaction times and lower temperatures than did the attachment of the haloalkanoic acid and provided better yields with fewer side products [84]. Haloalkanes of different chain lengths are

commercially available and are inexpensive. Iminodicarboxylic acids with pI values higher than IDA however are not available commercially. The oxidation resistant, quaternary ammonium derivative of IDA or MIDA can be made, but a different, and possibly *de novo* approach is needed for higher pI derivatives.

2.3.2.2.2 *De novo* synthesis

Michael addition

To make isoelectric buffers of pI values greater than the pI value of the quaternary ammonium derivative of IDA, carboxylic acid groups must be attached to amines via suitable carbon-nitrogen bond formation chemistries. Carbon-nitrogen bond formation followed by a proton transfer occurs according to the Michael addition reaction between amines and carboxylic acids with activated alkene groups [28]. By reacting acrylic acid with a mixture of different amines for 5 hours at 70°C, Vesterberg achieved close to 100% conversion. Due to the very slow rate of the reaction, heating is required which leads to formation of undesired colored side-products [28]. This reaction follows an anti-Markovnikov distribution [24], where the proton transfers to the proton-deficient carbon rather than the proton-rich carbon, which attaches to the amine [28]. The final product is obtained in its isoelectric form, which is an advantage of this reaction scheme. However, the reaction is limited to compounds with activated unsaturated bonds and minimal steric hindrance (for example, acrylic acid). Thus, iminodipropionic acid can be made in this manner, followed by alkylation (by nucleophilic substitution reaction) to make the quaternary ammonium derivative.

However, even higher pI derivatives (such as the iminodibutyric acid derivative) cannot be made using this synthetic scheme.

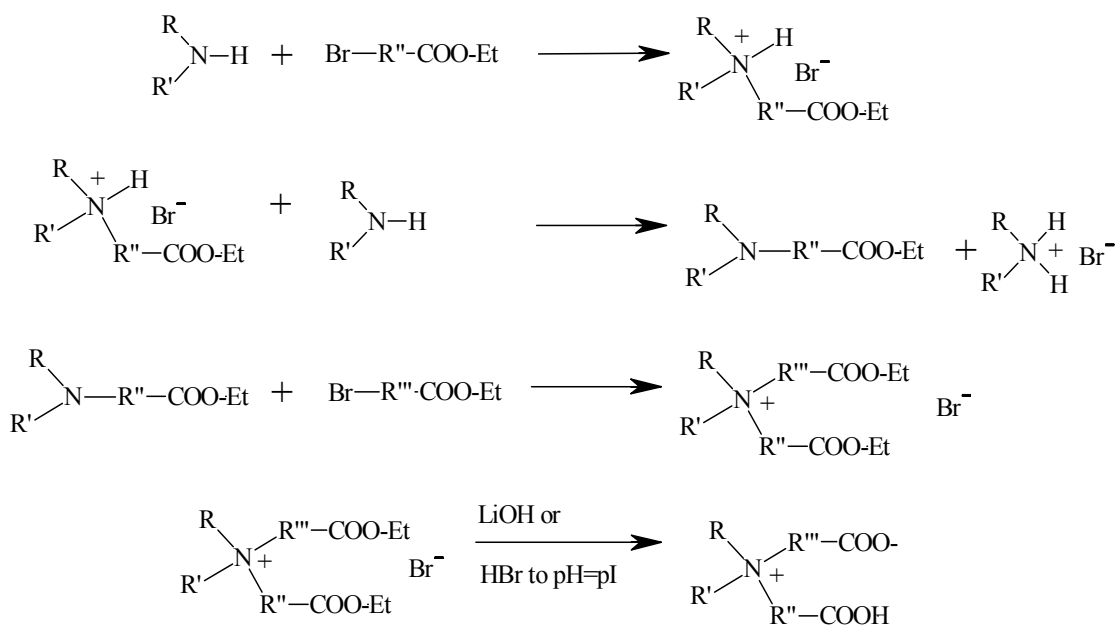
Nucleophilic substitution

Macka et al. synthesized a mixture of high molecular weight carrier ampholytes by reacting poly(ethyleneimine) (PEI) with chloroacetic acid via nucleophilic substitution reaction. PEI and sodium chloroacetate were heated in an oil bath at 80°C for 16 hours to form a mixture of macromolecular carrier ampholytes [85].

Haloalkylcarboxylic acids of different chain lengths and their sodium salts are commercially available. If a secondary amine was reacted with two equivalents of the same haloalkylcarboxylic acid (or salt), the isoelectric buffer species of choice would be formed. Similarly, an asymmetric compound with a unique pI would be formed if one equivalent of the amine was reacted with one equivalent of a haloalkylcarboxylic acid, followed by reaction with one equivalent of another haloalkylcarboxylic acid. This synthesis scheme has greater flexibility and broader applicability in terms of the derivatives that can be synthesized. A major disadvantage is that the isoelectric buffer is obtained in the salt form (due to the base and the released halide), requiring an additional salt removal step.

When the haloalkylcarboxylic acids or their salts are used, amide formation between the carboxylate and the amine is a possible side reaction. To avoid this, commercially available haloalkylcarboxylic acid alkyl esters (especially ethyl esters) can be used. Since the esters require hydrolysis either with base or acid [24] to form the free carboxylic acids, salt formation is still not avoided. Figure 6 illustrates the synthetic

scheme that will be used to make some of the carboxylic acid-based isoelectric buffers. This scheme however is limited. The highest aminocarboxylic acid pK_a value is at 4.3 (6-aminohexanoic acid) and thus, the pI value of the highest pI derivative could only be below that.



R'' and R''' = methylene to propylene

Figure 6. Generic *de novo* synthesis scheme for carboxylic acid-based isoelectric buffers

2.3.3 Design for high-pI compounds

2.3.3.1 High-pI range

The carboxylic acid-based design to synthesize isoelectric buffers is limited due to the narrow pK_a range of carboxylic acids. High buffering capacity, higher pI value isoelectric buffers cannot be made using one amine and one carboxylic acid (though the pI value would be high) due to the large ΔpK_a . Since pK_a values for amines range from 8.58 (morpholine) to 11.01 (piperidine), isoelectric buffers that act as good carrier ampholytes can be made using amines. Similarly to the carboxylic acid-based buffers, if two weak base groups (such as amines) and one acidic group (with a pK_a of at least 3, but preferably 4 units lower than the pK_a of the weaker base) were linked into one molecule, the compound pI value will fall between the pK_a values of the two amines ($pI = (pK_{a2} + pK_{a3})/2$). Depending on the choice of the amine (therefore the pK_a value), such a compound can qualify as a good carrier ampholyte.

The acidic functionality of such an isoelectric buffer can be either a weak acid group, such as a carboxylic acid group or a strong acid group, such as a sulfonic acid group. The permanent negative charge on the group which is independent of the solution pH and the conductivity contribution of the dicationic species, is a slight advantage of the latter.

2.3.3.2 Synthesis

In sulfation or sulfonation reactions, the reactant must have an alcohol group. A mixture of randomly substituted, polyanionic, cyclodextrin sulfonates has been synthesized by reacting the alcohol groups with alkyl sultones [86-88]. β -CD [86, 87] or γ -CD [88] was dissolved in an aqueous solution of sodium hydroxide. The appropriate alkane sultone was added and the mixture was heated for 24 hours at 47°C (for γ -CD) [88] or 70°C (for β -CD) [86, 87]. Haftendorn and Ulbrich-Hoffman synthesized diacylglycerol sulfate by reacting the diacylglycerol with sulfur trioxide pyridine complex in dry tetrahydrofuran [89]. Several mixtures of randomly sulfated cyclodextrins [90, 91], single-isomer sulfated cyclodextrins [92-98] and carbohydrate-based anionic surfactants [99] have been synthesized in a similar manner. Between the two, sulfation reactions are preferred due to their relative simplicity. Figure 7 shows the generic structure for amine-based isoelectric buffers that are to be synthesized (containing two amine groups and one sulfate group).

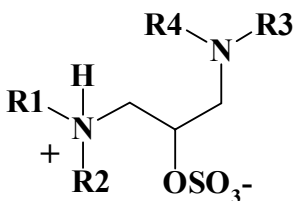


Figure 7. Generic structure of amine-based isoelectric buffers that are to be synthesized.

2.3.3.2.1 Opportunistic (sulfation)

An opportunistic approach to the synthesis of amine-based isoelectric buffers of the generic structure shown in Figure 7 is to sulfate the alcohol group of a species with two amine groups and one alcohol group. Although rare, two such compounds with the two amine groups and a small ΔpK_a value, are commercially available. Sulfating agents such as sulfur trioxide, stabilized as amine complexes, are also commercially available. In the reaction, sulfur trioxide forms a sulfate monoester with the hydroxy groups (such as alcohols) creating a monovalent, negatively charged species. Sulfating one of the two commercially available amine derivatives (using sulfur trioxide pyridine complex), the corresponding amine-based isoelectric buffers will be synthesized. However, a different, and most likely *de novo* approach is needed to make amine-based buffers of different pI values.

2.3.3.2.2 *De novo* synthesis

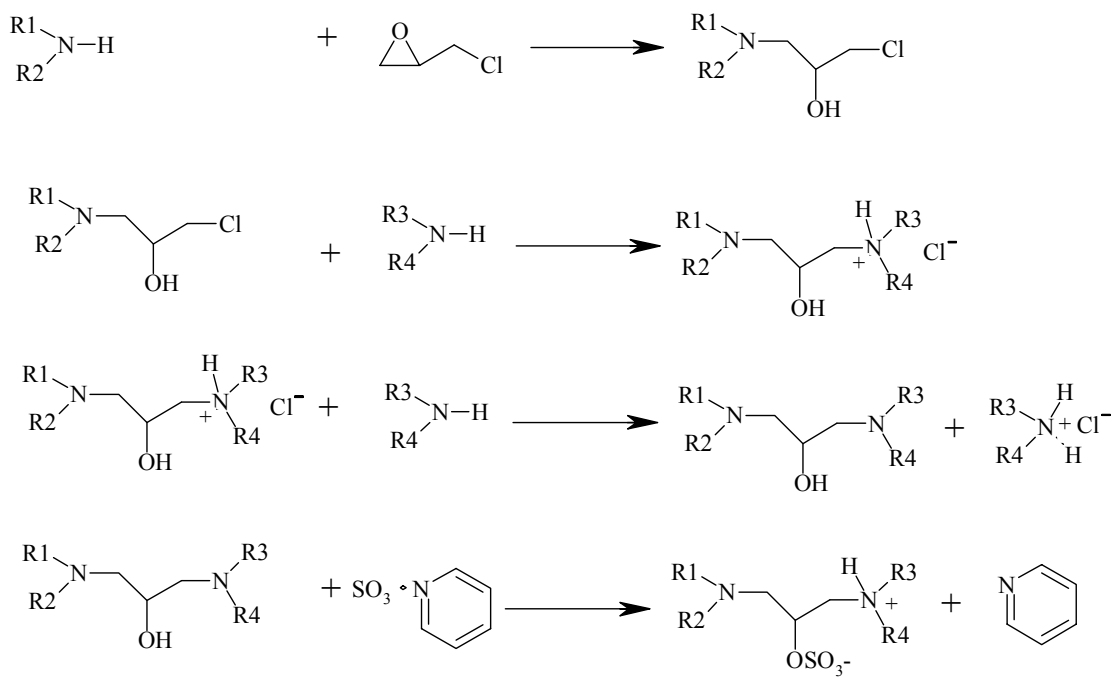
To synthesize a series of amine-based isoelectric buffers that conform to the generic structure in Figure 7 from amines of different pK_a values, an appropriate difunctional linker is needed. The linker must have (i) two sites to bind amines and (ii) an alcohol group to be sulfated.

Dihaloalkanols can be used to synthesize the appropriate diamine derivative for sulfation. By nucleophilic substitution, amines substitute the halide leaving group and form the corresponding diaminoalkanol. However, nucleophilic substitution reactions can be highly sensitive to steric hindrances and thus, can be slow.

Diepoxide linkers can also be used. Epoxy ring opening reactions, in basic conditions, followed by carbon-nitrogen bond formation and proton transfer, are relatively fast. In the process, two secondary alcohol groups are formed, which might become a problem. During sulfation (or sulfonation), two negative charges per molecule can form. Such a compound will not be an isoelectric buffer. Control of either the sulfation or sulfonation reactions to make the corresponding monoanionic species is extremely difficult.

Epihalohydrins, however, seem to be a good alternative. The faster reacting epoxy group can attach to one amine group and form one alcohol group in the reaction. The less reactive halide group from the amine bound alcohol then leaves and is substituted by a second amine group. Because of this difference in reactivities, it is also possible to make asymmetric diamino derivatives (compounds with two different amines linked). Also, controlled sulfation is not needed since the molecule has only one hydroxyl group that can be converted. Therefore, epichlorohydrin, an inexpensive, commercially available reagent will be used. Figure 8 illustrates the scheme for the *de novo* synthesis of amine-based isoelectric buffers.

An important point to consider is that secondary amines are the preferred amines in this synthesis scheme. Primary amines become secondary amines after attachment to the linker, and can form sulfonamides with sulfur trioxide during the sulfation step. Sulfonamido nitrogens are not basic nitrogens and thus, cannot be used to buffer in the desired pH ranges. Tertiary amines, after attachment, will form quaternary ammonium groups which are strong base functionalities and do not buffer.



R1-R4 alkyl groups

Figure 8. Scheme for the *de novo* synthesis of amine-based isoelectric buffers.

3. TRISHUL: SYNTHESIS OF LOW-pI, HYDROLYTICALLY STABLE, ISOELECTRIC MEMBRANES*

3.1 IDAPVA

3.1.1 Synthesis

The hydrogel forming solution was prepared as follows. Typically, a weighed, 150 mL beaker and two 230x190x6 mm, clean glass plates were heated in an oven to 80 °C. A 500 mL, three-neck, round bottom flask was fitted with an ice-water cooled condenser and a nitrogen purge line. A Teflon-coated magnetic stir bar was added to the flask. 60 mL deionized water, and weighed amounts of sodium hydroxide (NaOH) and IDA were added to the flask and brought to a boil in a heating mantle. PVA (average relative molecular mass ratio = 89,000-98,000) was weighed out and added to the hot solution. The system was purged with nitrogen, stirred and heated until all of the PVA dissolved.

A 40 g portion of the hot, viscous reaction mixture was weighed into the hot, 150 mL beaker, followed by the quick addition of the corresponding amount of glycerol-1,3-diglycidyl ether (GDGE, crosslinker). The reaction mixture was thoroughly mixed, manually, with a spatula and quickly cast above and below a 160x200mm piece of Grade BFN2 Papyrus PVA substrate. The membrane sheet was kept sealed until it cured. After

* Reprinted with permission from “High Buffering Capacity, Hydrolytically-Stable, Low-pI Isoelectric Membranes for Isoelectric Trapping Separations” by Lalwani, S., Shave, E., and Vigh, G., 2004. *Electrophoresis* (accepted). Copyright 2004, Wiley VCH.

curing, the membrane sheet was sloshed around in subsequent (typically five) batches of rinse water until the pH of the wash water remained neutral.

The IDAPVA membrane sheets were stored in deionized water at 4 °C until used. The IDAPVA membranes swelled to a final thickness of about 0.5 to 1.5 mm, depending on their buffering capacities. Since the amount of epoxide groups left-over in the IDAPVA membranes was not known, gloves were worn when the membranes were handled. IDAPVA membranes with the final size required for the separation cartridge of the BF200IET unit were cut with scissors. The used IDAPVA membranes were rinsed with water and disposed as solid waste.

3.1.1.1 Optimization

3.1.1.1.1 Hydrogel composition

Polyacrylamide-based isoelectric hydrogels are typically of 5% to 10%w/w in dry polymer [10,12]. Hydrogel-forming PVA solutions of 5, 10, 15, 17.5 and 20 g per 100 mL water, were tested. The (i) amount of PVA, (ii) NaOH concentration and (iii) GDGE concentration were optimized. Elasticity, tackiness and mechanical stability of the formed hydrogels were noted (qualitatively). The different combinations tested are listed in Table 7. As the PVA content of the solution was increased, all three properties improved. The 20g PVA per 100 mL water mixture resulted in the best hydrogels. Solutions with a higher PVA content could not be made due to the drastic increase in viscosity (an inherent property of the system) [34], making adequate mixing difficult.

Table 7. PVA/base/GDGE combinations tested during the optimization process. Optimized conditions are in bold.

Weight PVA (g)/ 100 mL water	NaOH concentration (M)	GDGE concentration (mM)
5	1	120
10	1	120
10	1	240
10	1	480
10	1	80
20	2	80
20	2	160
10	2	361
15	2	361
17.5	2.4	397
17.5	2.4	397
20	2.4	451
20	2.7	451

3.1.1.1.2 Curing conditions

Curing of the membranes was tested first at elevated temperatures in an oven. Membrane sheets cast in glass plate molds were initially heated in the oven at 85°C. Break-down of the PVA paper in the molds was observed (possibly due to melting). At

60°C oven temperature, the PVA paper remained intact, thus 60°C was used for all of the following experiments.

The PVA hydrogel forming solution was prepared and poured into five clean and dry glass vials. The vials were capped (to minimize drying) but not completely (to avoid expansion-driven rupture due to heating) and placed in the oven. Every hour, for four hours, one vial was taken out of the oven and the consistency of the hydrogel was checked (qualitatively). The fifth vial was left in the oven overnight and the gel was checked the next morning (after 14 hours of heating). The vial heated overnight had the best consistency, however, the gel was slightly yellow (indicating possible overheating and drying). Hence, membranes were cast in the molds and heated overnight in the oven at 60°C. The resulting membranes had a smooth, slippery surface, good mechanical stability and were slightly yellow.

Curing at room temperature was also tested. Membrane sheets were cast in the mold and cured for 12, 24, 40 and 48 hours at room temperature. The first two batches yielded turbid gels indicating incomplete reaction of the crosslinker. After 40 hours, the gels formed were clear and transparent, indicating that at least the majority, if not all of the crosslinker had reacted. Since the molds were not heated, the gels were colorless. There was no difference between the gel cured for 40 hours and 48 hours. However, the gel at the edges of the mold started to dry out. More drying was seen in the membranes cured for 48 hours than in the membranes cured for 40 hours. Portions of the gel not directly exposed to air (in between the glass plates) also had some drying (indicating a

wicking effect by the dry edge of the gel). To prevent this, membranes were left to cure in a styrafoam box with wet paper towels inside (to maintain a humid atmosphere).

3.1.1.1.3 Casting technique

It was observed that the thickness of the gel and the smoothness of its surface were dependent on the way the membrane sheet was cast. Initially, half of the hydrogel-forming solution was poured on a hot glass plate. The plate was tilted to evenly distribute the solution. Next, the PVA paper was lowered on the solution. As the paper became saturated with the solution, the remaining half of the solution was poured on another hot glass plate and distributed evenly. The two plates were then clipped together on the sides to squeeze out the excess liquid.

With this technique, the membrane sheets made were uneven. There was more gel in the middle of the plate (least compressed by the clips) than on the sides (where the clips work best). This indicated that the solution viscosity was so high that it forced the glass plates to slightly bend in the center.

To counter this effect, the solution was cast in the same manner, but the force was applied across the plate surface. Weights of up to 20 kg were placed on the plates (with the PVA paper and solution between them) to squeeze out the excess liquid. This often caused the paper to slide out from between the glass plates. If the solution did not get squeezed out, the paper would wrinkle resulting in wrinkled membranes.

Finally, the casting technique was modified such that the force used for compression was localized at a point rather than the entire plate (to generate a very high pressure for the same amount of force). First, the solution was poured, in the form of an

inverted “T” on a base-resistant plastic sheet such as PP or PE. Then, the PVA paper was lowered on the plastic sheet. A 1 mm thick poly(vinyl acetate) (PVAc) sheet was used to quickly push out the extra liquid from under the paper. The remaining half of the solution was then poured on the PVA paper. A second plastic sheet was lowered on the solution. A Teflon-coated rolling pin was then used to squeeze out the excess liquid. This way, even, smooth, and wrinkle-free IDAPVA hydrogel membranes were made.

3.1.1.1.4 Substrate

The PVA paper substrate was available in different thicknesses (Grade BFN1 to BFN 6, with 6 being the thickest). Membranes with different grades of PVA paper were made and their overall mechanical properties were compared.

Grade BFN1 was too thin, upon compression the paper tore. BFN2 made good membranes and was used in the first few batches. However, the membranes were too flimsy. In the modified BF200IET unit, the difference in flow rates between the sample and anolyte streams caused the membranes to bulge into and partially clog the separation compartment. Membranes of intermediate thickness were made using BFN3 grade paper. However, the membranes with BFN4 grade paper were sturdier and withstood the uneven pressure inside the BF200IET cartridge. Higher PVA paper grades (5 and 6) were not tested because they were too thick and additional sturdiness was not needed. Figure 9 shows Environmental-Scanning Electron Microscopy (E-SEM) images showing the weave of the BFN4 grade PVA paper with a cast hydrogel on it.

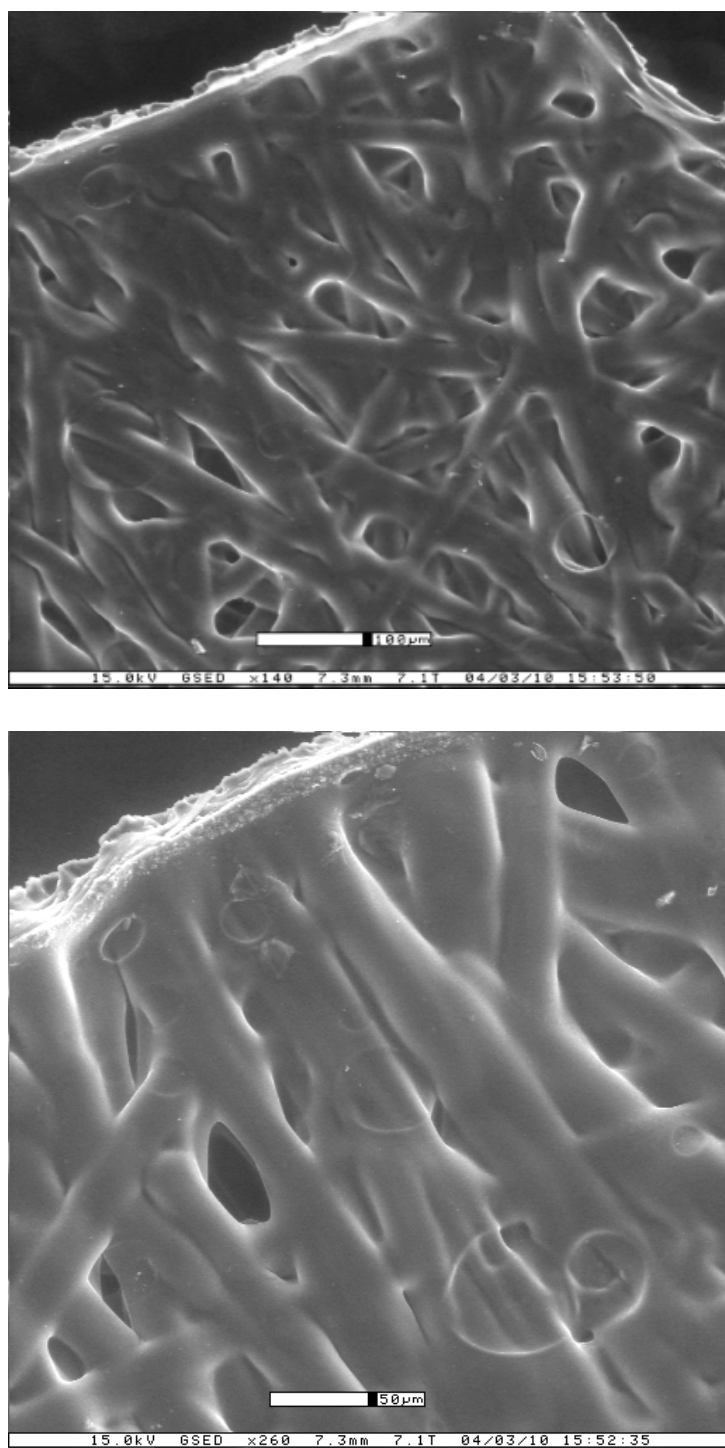


Figure 9. E-SEM images of the BFN4 grade PVA substrate. Scale: white bar is 100 μm wide in the top panel and 50 μm wide in the bottom panel.

3.1.1.2 Final procedure

The optimized procedure for synthesis of IDAPVA membranes (containing 165 mM IDA) is as follows. A 185x310 mm sheet of Grade BFN4 Papyrus PVA substrate was clipped in between two 190x320 mm PP sheets. The PP-PVA-PP sandwich was placed on a clean glass plate on the benchtop. The clips were taped to anchor the sandwich to the table.

A 150 mL beaker was heated in an oven to 80 °C. A 500 mL, three-neck, round bottom flask was fitted with an ice-water cooled condenser and a nitrogen purge line. A Teflon-coated magnetic stir bar was added to the flask. 60 mL deionized water, 7.49 g (0.187 mol) NaOH, and 1.32 g (0.010 mol) IDA were added to the flask and brought to a boil in a heating mantle. 12 g (0.273 mol OH equivalent) PVA was added to the hot solution, the system was purged with nitrogen, stirred and heated until all PVA dissolved.

A 40 g portion of the hot, viscous reaction mixture was weighed into the hot, 150 mL beaker, followed by the quick addition of 4.54 mL (5.58g, 0.027 mol) GDGE. The reaction mixture was thoroughly mixed, manually, with a spatula. The top PP sheet and the PVA sheet were lifted and about half of the beaker's content was poured on the lower PP sheet to form an inverted "T". The PVA sheet was slowly lowered and a 1mm thick PVAc sheet (scraper) was run over it to squeeze out the excess solution. The second half of the hot reaction mixture was then poured on the PVA sheet. The top PP sheet was then lowered and the Teflon-coated rolling pin was rolled over it to squeeze out the rest of the excess reaction mixture. The membrane sheet-sandwich was kept in a

covered styrafoam box with wet paper towels at room temperature for a total curing time of 40 hours. After curing, the PP sheets were carefully peeled under deionized water. The membrane was slosed around in subsequent (typically five) batches of rinse water until the pH of the wash water remained neutral. The membrane produced had clear, transparent salvage edges and a strong, even and slippery surface. Figure 10 shows a cartoon representation of a possible structure of the synthesized IDAPVA hydrogel.

The IDAPVA membrane sheets were stored in deionized water at 4 °C until used. The IDAPVA membranes swelled to a final thickness of about 0.5 to 1.5 mm, depending on their buffering capacities. Since the amount of epoxide groups left-over in the IDAPVA membranes was not known, gloves were worn when the membranes were handled. IDAPVA membranes with the final size required for the separation cartridge of the BF200IET unit were cut with scissors. Used IDAPVA membranes were rinsed with water and disposed as solid waste.

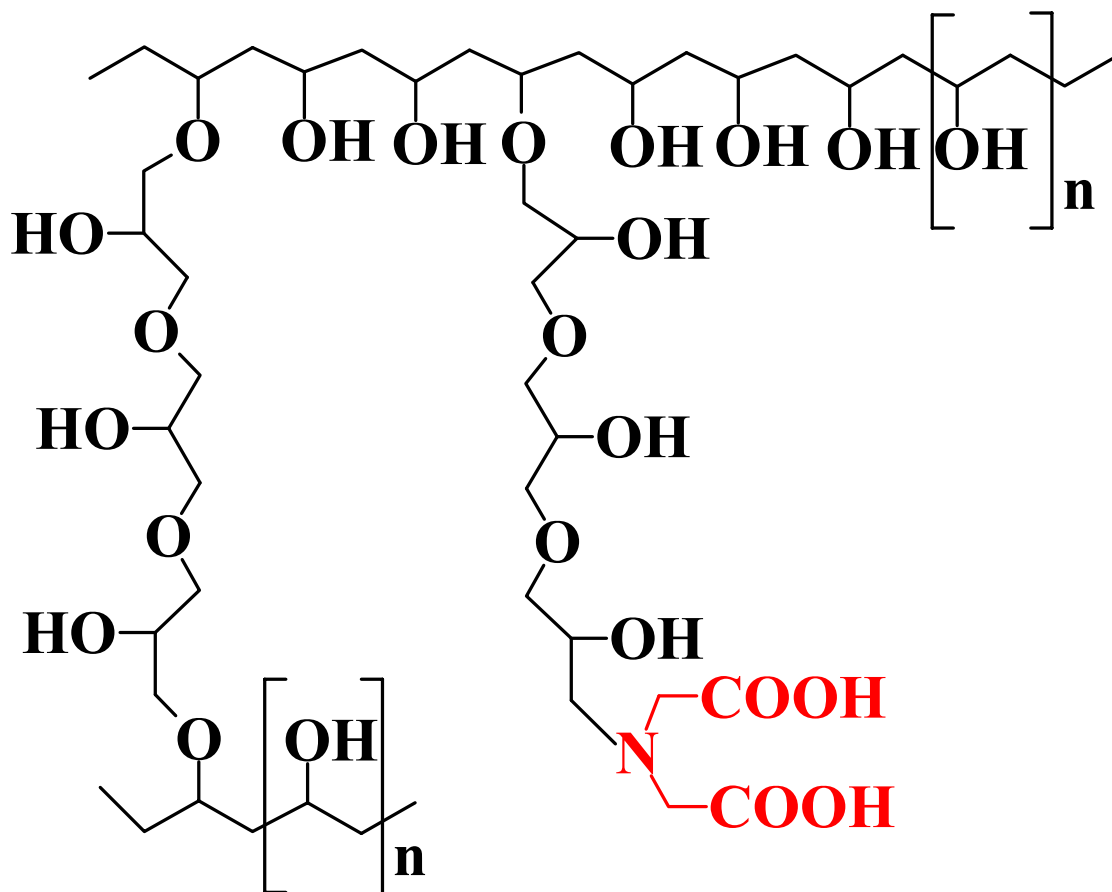


Figure 10. A cartoon representation of a possible structure of the IDAPVA hydrogel.

3.1.2 Testing

3.1.2.1 Trapping

The IDAPVA low-pI isoelectric membranes were tested as anodic membranes in the single separation compartment configuration of the BF200IET. The anolyte used was a 40 mM methanesulfonic acid solution (MSH) that contained 2.2 mM benzenesulfonic acid (BSH). If the anolyte entered any of the compartments by diffusion across the anodic membrane or by acid invasion or due to mechanical membrane failure, the presence of the UV absorbing BS^- would be easily detected by capillary electrophoresis (CE). The cathodic membrane was a high-pI isoelectric membrane. The catholyte used was a 200 mM NaOH solution that contained 2.5 mM benzyltrimethylammonium hydroxide (BzTMAOH). Similar to BS^- , the presence of the UV absorbing $BzTMA^+$ would be easily detected by CE if the catholyte entered any of the compartments by diffusion across the cathodic membrane or by base invasion or due to mechanical membrane failure. The anodic and cathodic membranes bracketed the single separation compartment.

The sample solution used in the trapping experiment contained the ampholytic analytes (i) 2 mM m-aminobenzoic acid (MABA, approximate pI = 3.9), (ii) 6 mM histidine (HIS, pI = 7.5) and (iii) 2 mM tyramine (TYRA, approximate pI = 10). Electrophoresis was continued in recirculating mode for 180 min, aliquots were collected at the exit ports every 30 min and analyzed by CE. A final potential of 98 V generated an electrophoretic current of 500 mA that corresponded to a current density of 33 mA/cm². Figure 11 shows the electropherograms for the starting sample (top panel),

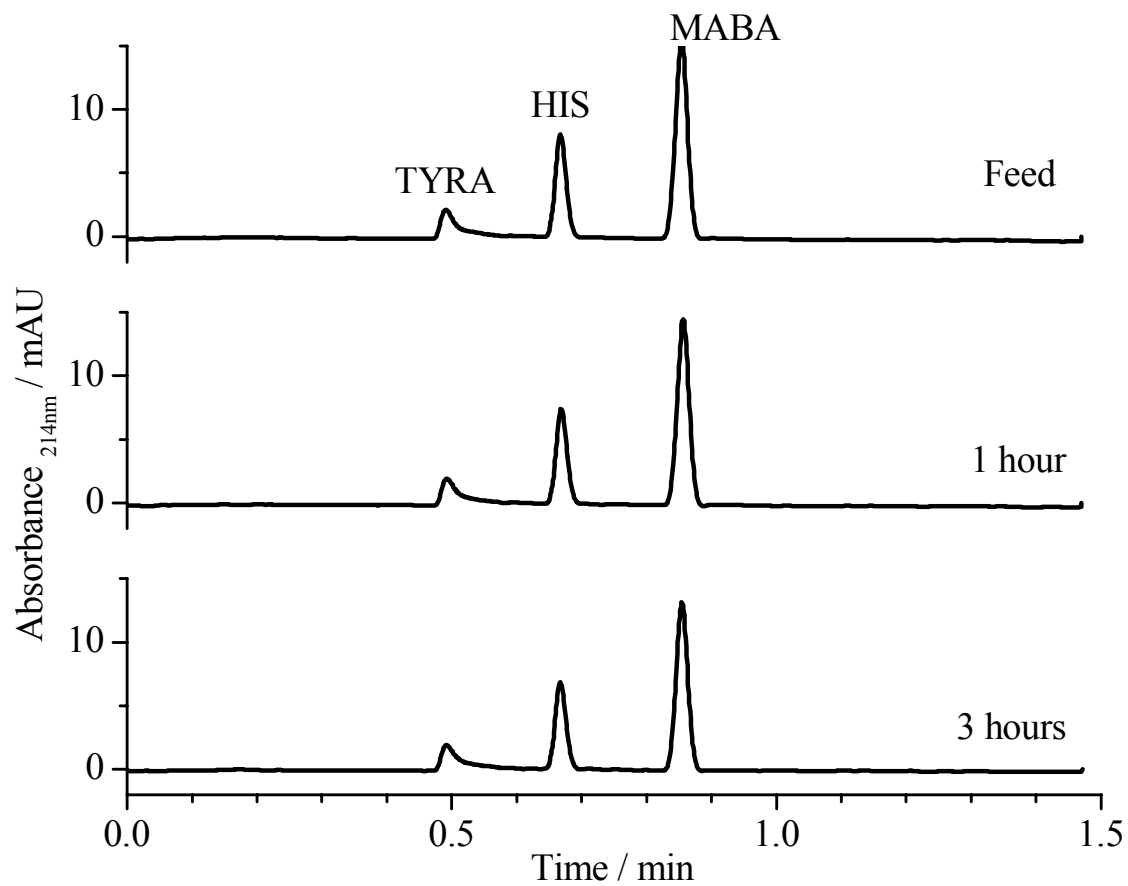


Figure 11. Electrochromatograms for the aliquots from the trapping experiment with IDAPVA as the anodic membrane: (top) feed, (middle) after 60 min and (bottom) after 180 min.

60 min sample (middle panel) and the 180 min sample (bottom panel). Clearly, MABA, HIS and TYRA were trapped for the duration of the 180 min run, and neither BS^- nor BzTMA^+ invaded the separation compartment.

3.1.2.2 Desalting

Next, the IDAPVA membrane was tested for IET desalting in the single separation compartment configuration of the Gradiflow BF200IET unit. The anolyte was 40 mM MSH solution and the catholyte was a 200 mM NaOH solution. The sample solution contained 10 mM benzyltrimethylammonium benzenesulfonate (a strong electrolyte salt), 2 mM MABA, 6 mM HIS and 2 mM TYRA. The UV absorbing strong electrolytes were selected to model the behavior of 10 mM sodium chloride (NaCl), because their analysis by CE was easier than indirect UV absorbance detection of Na^+ and Cl^- . IET was carried out at a constant current of 500 mA. Every 3 min, aliquots were taken from the recirculating sample solution and were analyzed by CE. The electropherograms for the 0 min (feed), 15 min and 30 min samples are shown in the top, middle and bottom panels of Figure 12.

Clearly, IET removed all strong electrolytes by 30 min and none of the amphoteric sample components were lost. The conductance and pH values of the recirculating sample solution are shown as a function of time in Figure 13. In the first part of the desalting phase, BzTMA^+ is removed at a faster rate than BS^- , hence the sample solution becomes temporarily more acidic than initially. After 30 min, removal of BS^- is complete, the pH and conductance return to the same, steady levels as observed at the end of the previous trapping experiment.

3.1.3 pI characterization

Two test solutions were made: (i) with 2 mM of a nominal pI 1.7 marker in 6 mM HIS and (ii) with 2 mM of a nominal pI 2.0 marker in 6 mM HIS. IET runs were completed with both solutions at a constant current of 500 mA, aliquots were taken at 10 min intervals and analyzed for the concentration of the respective acidic pI markers. The nominal pI = 1.7 marker left the separation compartment in 20 min, but the concentration of the nominal pI = 2.0 marker remained the same for 60 min indicating that the pI of the IDAPVA membrane was in the $1.7 < \text{pI} < 2.0$ range.

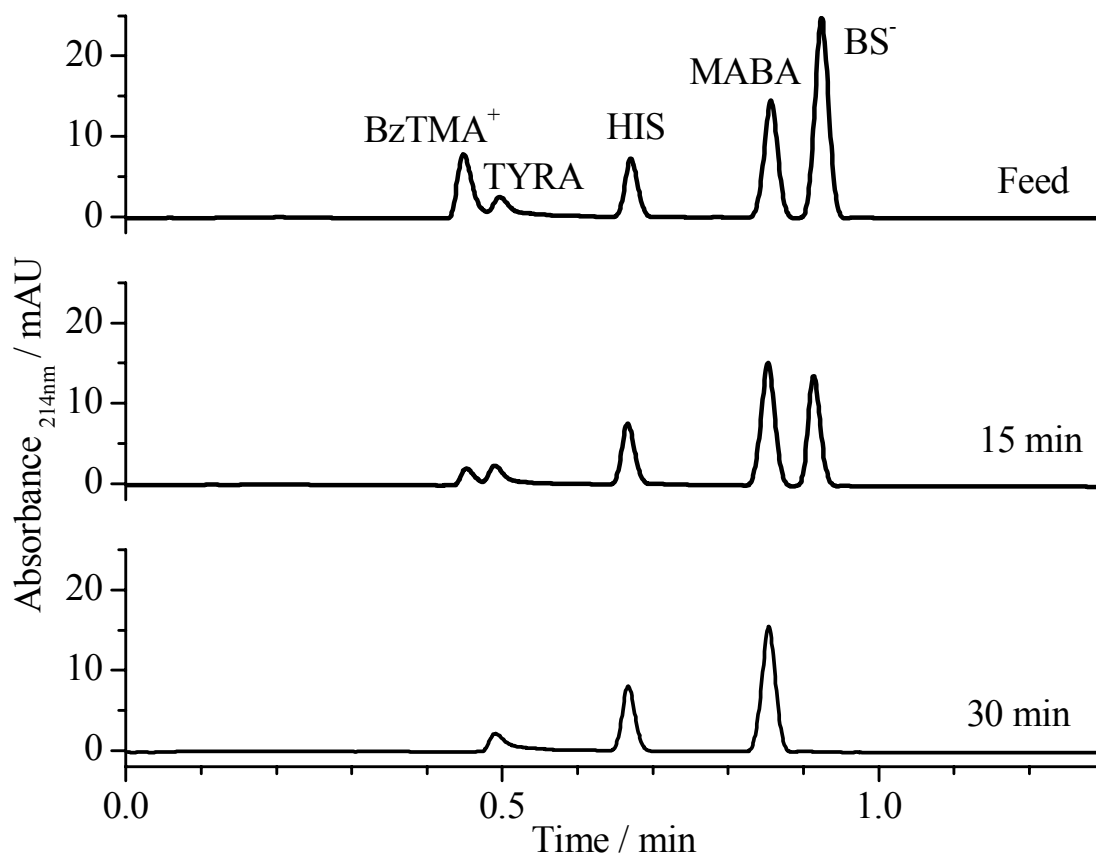


Figure 12. Electropherograms for the aliquots from the desalting experiment with IDAPVA as the anodic membrane: (top) feed, (middle) after 15 min, and (bottom) after 30 min.

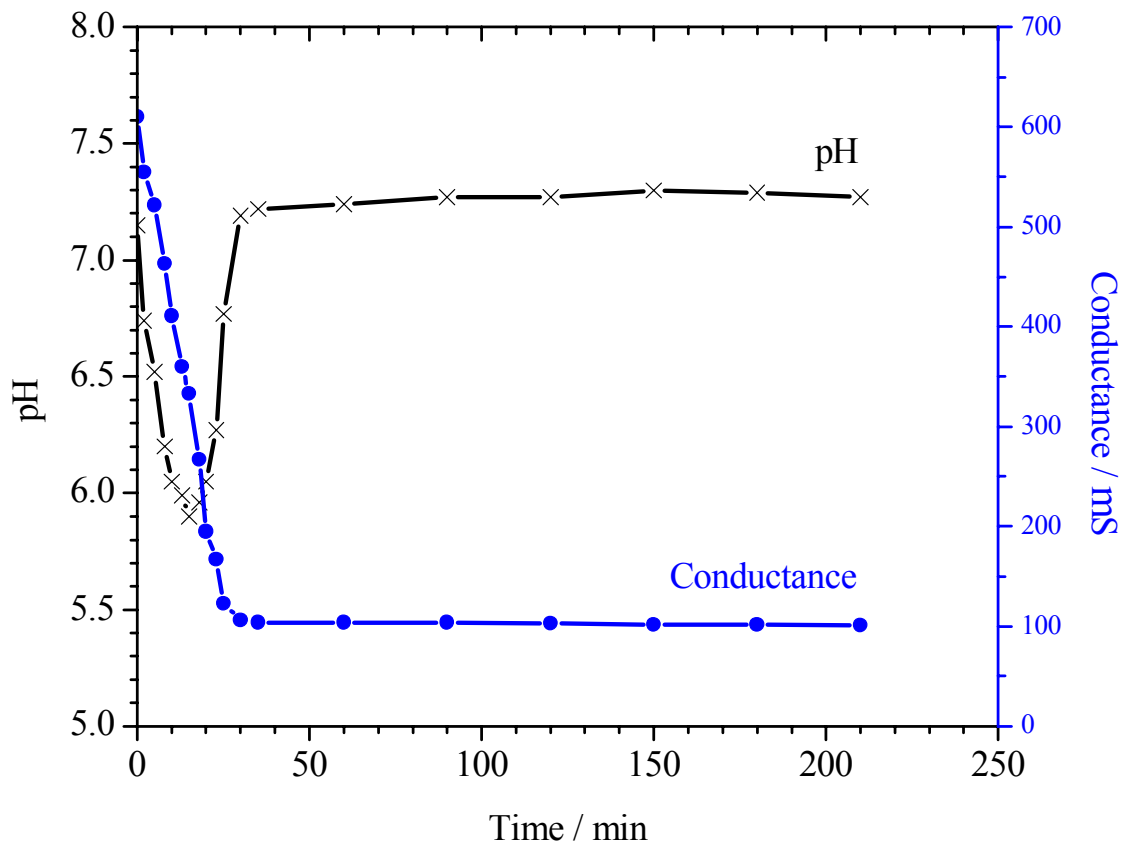


Figure 13. Sample conductance and pH as a function of time during the desalting run with IDAPVA as the anodic membrane.

3.2 ASPPVA

3.2.1 Synthesis

3.2.1.1 Final procedure

The optimized conditions for making IDAPVA membranes were used to make low pI hydrogels from aspartic acid (ASP) and PVA. The final procedure for the synthesis of the ASPPVA membranes (containing 165 mM ASP) is as follows. A 185x310 mm sheet of Grade BFN4 Papyrus PVA substrate was clipped in between two 190x320 mm PP sheets. The PP-PVA-PP sandwich was placed on a clean glass plate on the benchtop. The clips were taped to anchor the sandwich to the table.

A 150 mL beaker was heated in an oven to 80 °C. A 500 mL, three-neck, round bottom flask was fitted with an ice-water cooled condenser and a nitrogen purge line. A Teflon-coated magnetic stir bar was added to the flask. 60 mL deionized water, 7.49 g (0.187 mol) NaOH, and 1.32 g (0.010 mol) ASP were added to the flask and brought to a boil in a heating mantle. 12 g (0.273 mol OH equivalent) PVA was added to the hot solution, the system was purged with nitrogen, stirred and heated until all of the PVA dissolved.

A 40 g portion of the hot, viscous reaction mixture was weighed into the hot, 150 mL beaker, followed by the quick addition of 4.54 mL (5.58g, 0.027 mol) GDGE. The reaction mixture was thoroughly mixed, manually, with a spatula. The top PP sheet and the PVA sheet were lifted and about half of the beaker's content was poured on the lower PP sheet to form an inverted "T". The PVA sheet was slowly lowered and a 1 mm thick PVAc sheet (scraper) was run over it to squeeze out the excess solution. The

second half of the hot reaction mixture was then poured on the PVA sheet. The top PP sheet was then lowered and the Teflon-coated rolling pin was rolled over it to squeeze out the remaining excess reaction mixture. The membrane sheet-sandwich was kept in a covered styrafoam box with wet paper towels at room temperature for a total curing time of 40 hours. After curing, the PP sheets were carefully peeled under deionized water. The membrane was sashed around in subsequent (typically five) batches of rinse water until the pH of the wash water remained neutral. The membrane produced had clear, transparent salvage edges and a strong, even and slippery surface. Figure 14 shows a cartoon representation of a possible structure of the synthesized ASPPVA hydrogel.

The ASPPVA membrane sheets were stored in deionized water at 4 °C until used. The ASPPVA membranes swelled to a final thickness of about 0.5 to 1.5 mm, depending on their buffering capacities. Since the amount of epoxide groups left-over in the ASPPVA membranes was not known, gloves were worn when the membranes were handled. ASPPVA membranes with the final size required for the separation cartridge of the BF200IET unit were cut with scissors. The used ASPPVA membranes were rinsed with water and disposed as solid waste.

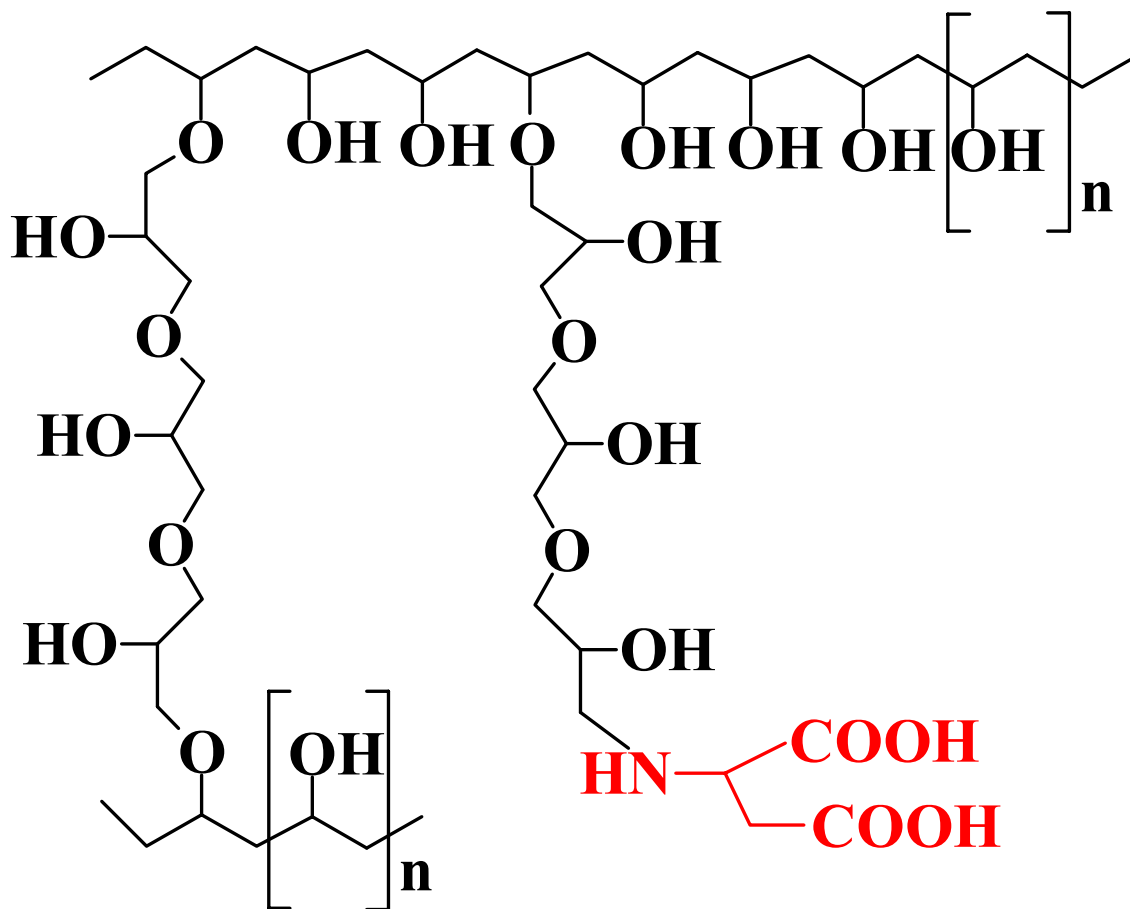


Figure14. A cartoon representation of a possible structure of the ASPPVA hydrogel.

3.2.2 Testing

3.2.2.1 Trapping

The ASPPVA isoelectric membranes were tested as the anodic membranes in the single separation compartment configuration of the BF200IET. The analyte used was a 40 mM MSH solution that contained 2.2 mM BSH. The cathodic membrane was a high-pI isoelectric membrane. The catholyte used was a 200 mM NaOH solution that contained 2.5 mM BzTMAOH. The presence of the UV absorbing BS^- or $BzTMA^+$ would be easily detected by CE if the analyte or the catholyte entered any of the compartments by diffusion across the membranes or by invasion or due to mechanical membrane failure. The anodic and cathodic membranes bracketed the single separation compartment.

The sample solution used in the trapping experiment contained the ampholytic analytes (i) 2 mM MABA (approximate pI = 3.9), (ii) 6 mM HIS (pI = 7.5) and (iii) 2 mM TYRA (approximate pI = 10). Electrophoresis was continued in the recirculating mode for 180 min, aliquots were collected at the exit ports every 30 min and analyzed by CE. A final potential of 90 V generated an IET current of 500 mA (corresponding to a current density of 33 mA/cm^2), indicating that the resistance of the ASPPVA membrane was slightly lower than that of the IDAPVA membrane. Results of the trapping experiments are shown in Figure 15 for the starting sample (top panel), 60 min sample (middle panel) and the 180 min sample (bottom panel). Clearly, MABA, HIS and TYRA were trapped by the ASPPVA membrane for the duration of the 180 min run, and neither BS^- nor $BzTMA^+$ invaded the separation compartment.

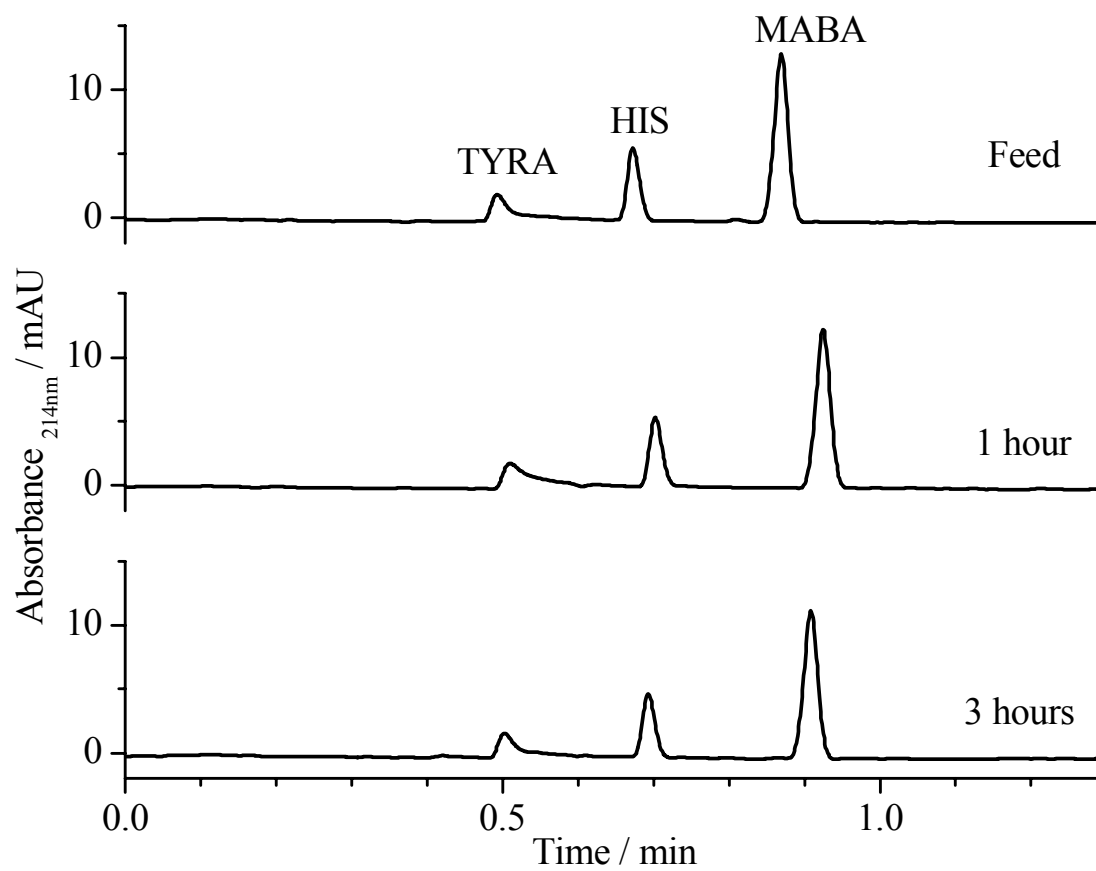


Figure 15. Electrochromatograms for the aliquots from the trapping experiment with ASPPVA as the anodic membrane: (top) feed, (middle) after 60 min and (bottom) after 180 min.

3.2.2.2 Desalting

Next, the ASPPVA membrane was tested for IET desalting using the Gradiflow BF200IET unit in the single separation compartment configuration. The anolyte and catholyte were 40 mM MSH and 200 mM NaOH solutions, respectively. The sample solution contained 10 mM benzyltrimethylammonium benzenesulfonate (a strong electrolyte salt), 2 mM MABA, 6 mM HIS and 2 mM TYRA. IET was carried out at a constant current of 500 mA. Every 3 min, aliquots were taken from the recirculating sample solution and were analyzed by CE. The electropherograms for the 0 min (feed), 15 min and 30 min samples are shown in the top, middle and bottom panels of Figure 16. Just as with the IDAPVA anodic membrane, BzTMA^+ was removed more rapidly than BS^- . The strong electrolyte salt was completely removed in less than 30 min and none of the ampholytic sample components were lost. The conductance and pH values of the recirculating sample solution are shown as a function of time in Figure 17. Both the conductance and the pH curves are similar to those obtained with the IDAPVA membrane.

3.2.3 pI characterization

The limiting pI values for the ASPPVA membrane were obtained in two successive experiments using 2 mM concentrations of acidic pI markers added to a 6 mM HIS solution. IET runs were completed with both solutions at a constant current of 500 mA, aliquots were taken at 10 min intervals and analyzed for the concentration of the respective acidic pI markers. The nominal pI = 2.0 marker left the separation compartment in 25 min, but the concentration of the nominal pI = 2.6 marker remained

the same for at least 60 min indicating that the pI of the ASPPVA membrane is in the 2.0 <math>< pI < 2.6</math> range.

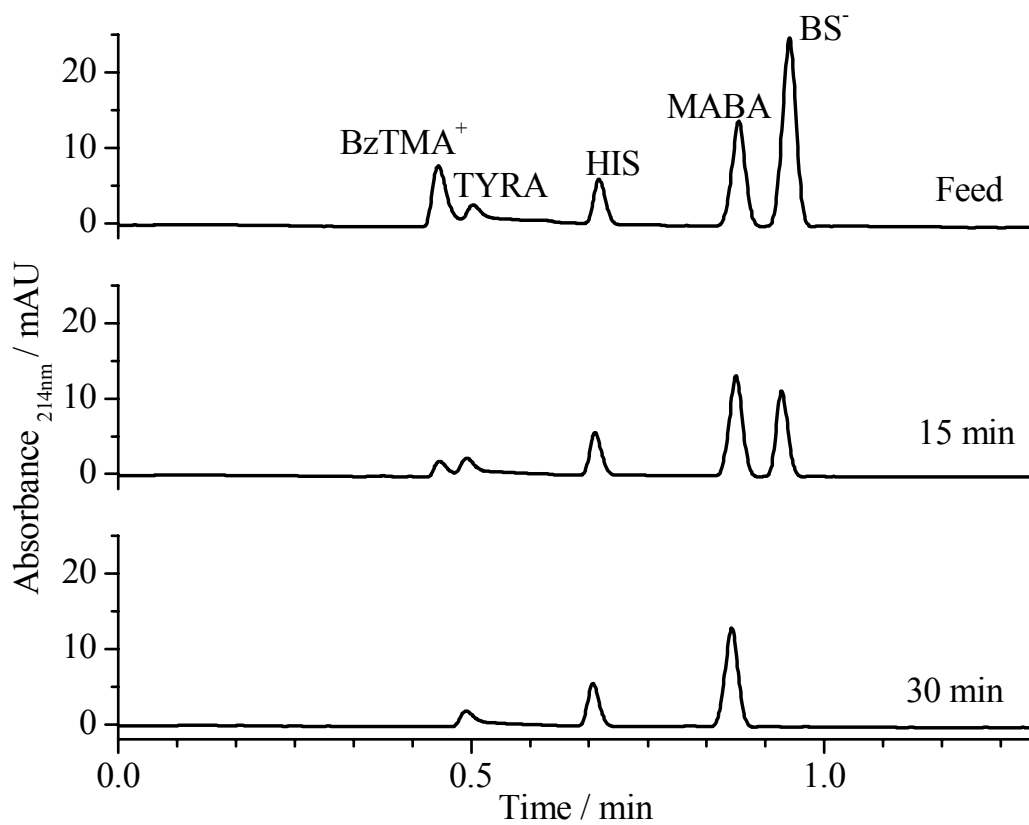


Figure 16. Electropherograms for the aliquots from the desalting experiment with ASPPVA as the anodic membrane: (top) feed, (middle) after 15 min, and (bottom) after 30 min.

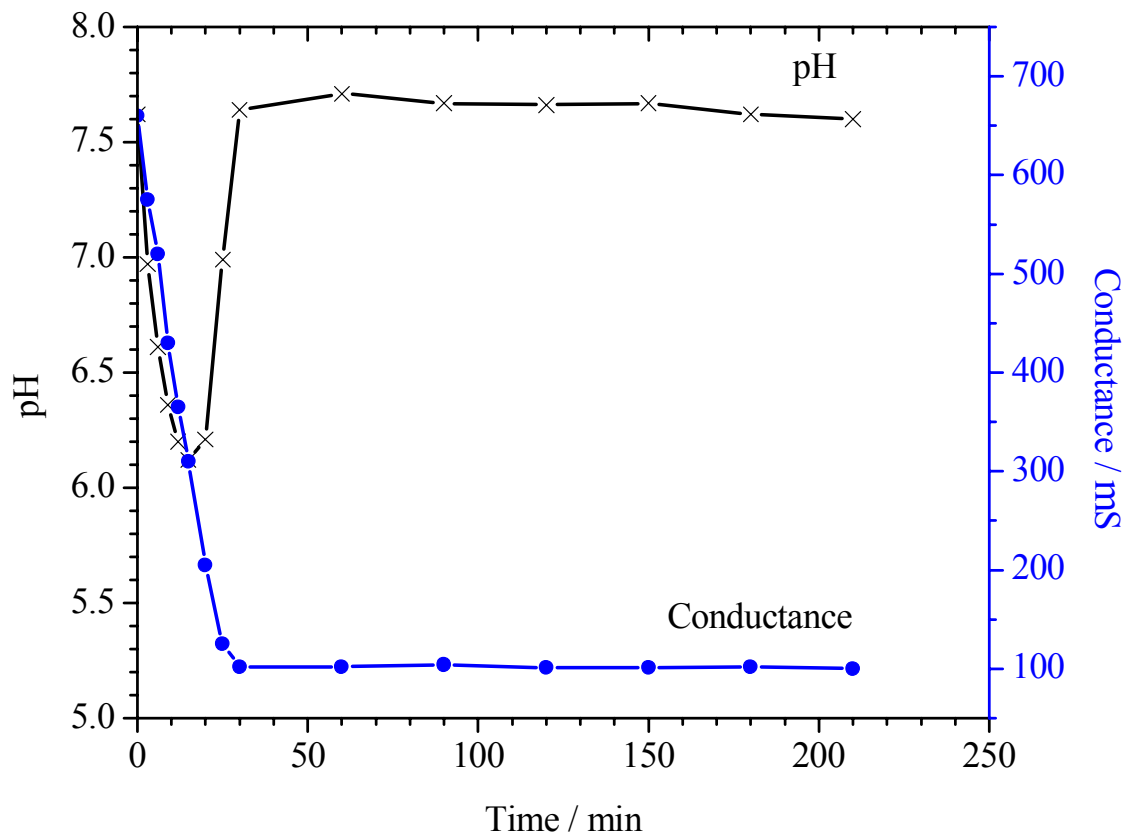


Figure 17. Sample conductance and pH as a function of time during the desalting run with ASPPVA as the anodic membrane.

3.3 GLUPVA

3.3.1 Synthesis

3.3.1.1 Final procedure

The conditions optimized for making IDAPVA membranes (also adapted for ASPPVA membranes) were used to make membranes from glutamic acid (GLU) and PVA. The final procedure for the synthesis of the GLUPVA membranes (containing 165 mM GLU) is as follows. A 185x310 mm sheet of Grade BFN4 Papyrus PVA substrate was clipped in between two 190x320 mm PP sheets. The PP-PVA-PP sandwich was placed on a clean glass plate on the benchtop. The clips were taped to anchor the sandwich to the table.

A 150 mL beaker was heated in an oven to 80 °C. A 500 mL, three-neck, round bottom flask was fitted with an ice-water cooled condenser and a nitrogen purge line. A Teflon-coated magnetic stir bar was added to the flask. 60 mL deionized water, 7.49 g (0.187 mol) NaOH, and 1.46 g (0.010 mol) GLU were added to the flask and brought to a boil in a heating mantle. 12 g (0.273 mol OH equivalent) PVA was added to the hot solution, the system was purged with nitrogen, stirred and heated until all PVA dissolved.

A 40 g portion of the hot, viscous reaction mixture was weighed into the hot, 150 mL beaker, followed by the quick addition of 4.54 mL (5.58g, 0.027 mol) GDGE. The reaction mixture was thoroughly mixed, manually, with a spatula. The top PP sheet and the PVA sheet were lifted and about half of the beaker's content was poured on the lower PP sheet to form an inverted "T". The PVA sheet was slowly lowered and a 1 mm

thick PVAc sheet (scraper) was run over it to squeeze out the excess solution. The second half of the hot reaction mixture was then poured on the PVA sheet. The top PP sheet was lowered and the Teflon-coated rolling pin was rolled over it to squeeze out the remaining excess reaction mixture. The membrane sheet-sandwich was kept in a covered styrafoam box with wet paper towels at room temperature for a total curing time of 40 hours. After curing, the PP sheets were carefully peeled under deionized water. The membrane was sloshed around in subsequent (typically five) batches of rinse water until the pH of the wash water remained neutral. The membrane produced had clear, transparent salvage edges and a strong, even and slippery surface. Figure 18 shows a cartoon representation of a possible structure of the synthesized GLUPVA hydrogel.

The GLUPVA membrane sheets were stored in deionized water at 4 °C until used. The GLUPVA membranes swelled to a final thickness of about 0.5 to 1.5 mm, depending on their buffering capacities. Since the amount of epoxide groups left-over in the GLUPVA membranes was not known, gloves were worn when the membranes were handled. GLUPVA membranes with the final size required for the separation cartridge of the BF200IET unit were cut with scissors. The used GLUPVA membranes were rinsed with water and disposed as solid waste.

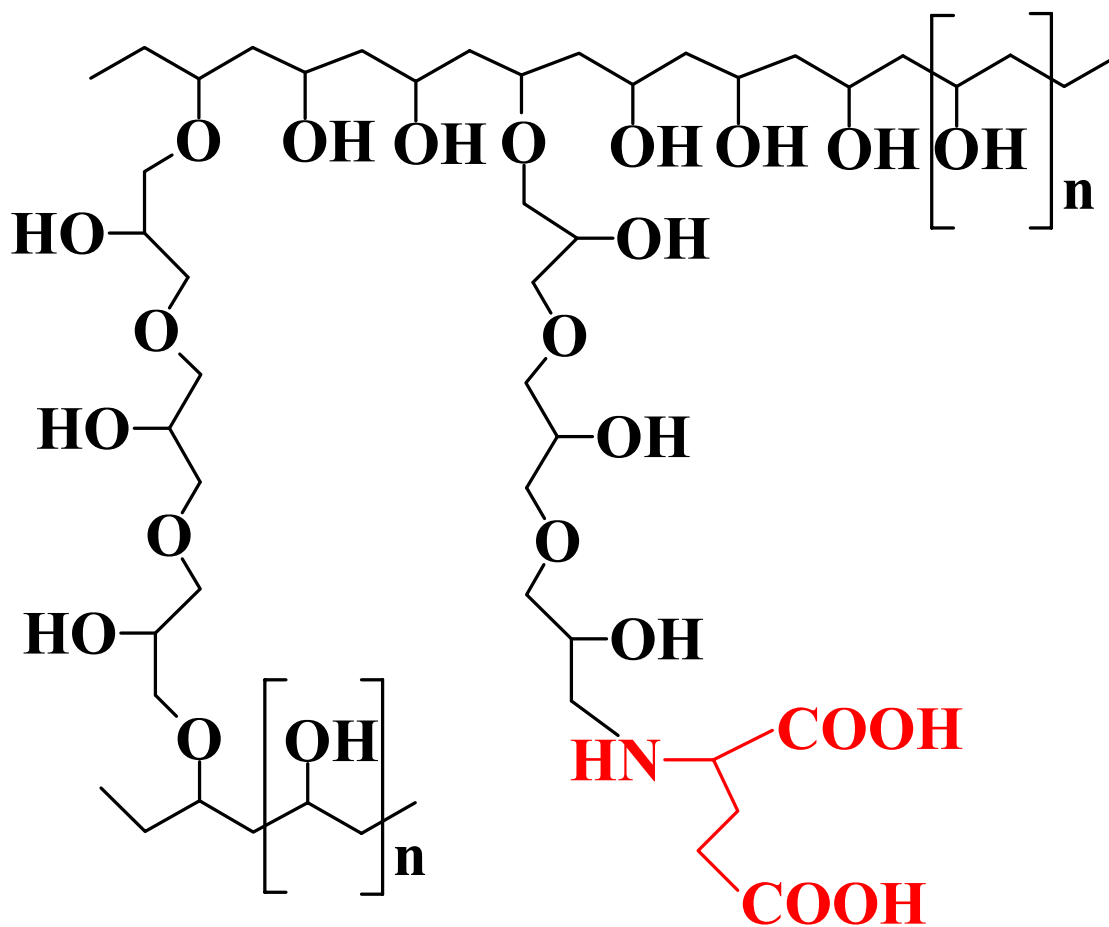


Figure 18. A cartoon representation of a possible structure of the GLUPVA hydrogel.

3.3.2 Testing

3.3.2.1 Trapping

The GLUPVA isoelectric membranes were tested as the anodic membranes in the single separation compartment configuration of the BF200IET (just as the IDAPVA and the ASPPVA membranes were tested). The cathodic membrane was a high-pI isoelectric membrane. The anolyte used was a 40 mM MSH solution containing 2.2 mM BSH. The catholyte used was a 200 mM NaOH solution containing 2.5 mM BzTMAOH. The BSH and BzTMAOH were added to indicate the presence of the anolyte or the catholyte in the sample stream (by diffusion across the cathodic membrane or by base invasion or due to mechanical membrane failure). The anodic and cathodic membranes bracketed the single separation compartment.

The sample solution used in the trapping experiment contained the ampholytic analytes (i) 2 mM MABA (approximate pI = 3.9), (ii) 6 mM HIS (pI = 7.5) and (iii) 2 mM TYRA (approximate pI = 10). Electrophoresis was continued in the recirculating mode for 180 min, aliquots were collected at the exit ports every 30 min and analyzed by CE. A final potential of 106 V generated an IET current of 500 mA (corresponding to a current density of 33 mA/cm²), indicating that the resistance of the GLUPVA membrane was slightly higher than that of both the IDAPVA and the ASPPVA membranes. Results of the trapping experiments are shown in Figure 19 for the starting sample (top panel), 60 min sample (middle panel) and the 180 min sample (bottom panel). Once again, MABA, HIS and TYRA were trapped by the GLUPVA membrane for the duration of the 180 min run, and neither BS⁻ nor BzTMA⁺ invaded the separation compartment.

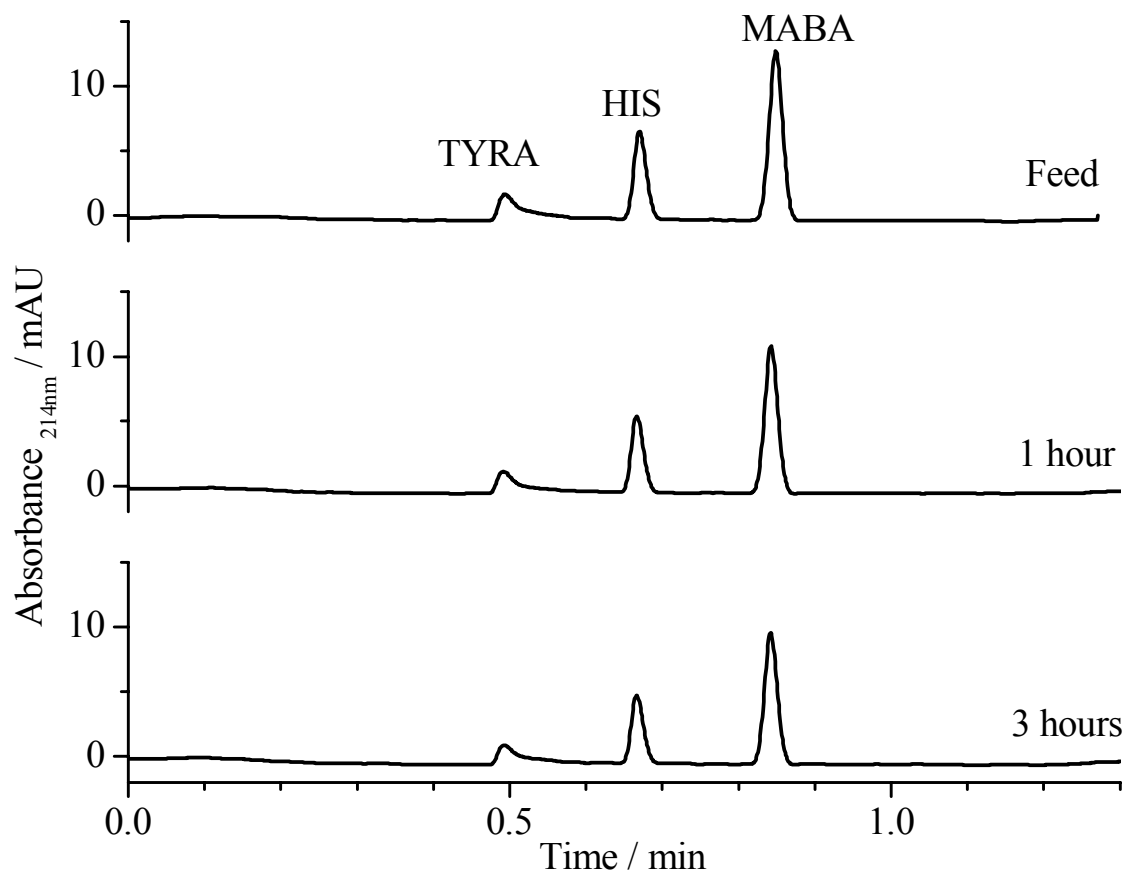


Figure 19. Electrochromatograms for the aliquots from the trapping experiment with GLUPVA as the anodic membrane: (top) feed, (middle) after 60 min and (bottom) after 180 min.

3.3.2.2 Desalting

The GLUPVA membrane was tested for IET desalting using the Gradiflow BF200IET unit in the single separation compartment configuration (just as the IDAPVA and ASPPVA membranes). The anolyte and catholyte were 40 mM MSH and 200 mM NaOH solutions, respectively. The sample solution contained 10 mM benzyltrimethylammonium benzenesulfonate (a strong electrolyte salt), 2 mM MABA, 6 mM HIS and 2 mM TYRA. IET was carried out at a constant current of 500 mA. Aliquots were taken from the recirculating sample solution every 3 min and were analyzed by CE. The electropherograms for the 0 min (feed), 15 min and 30 min samples are shown in the top, middle and bottom panels of Figure 20. Similarly to the desalting runs using IDAPVA and ASPPVA membranes, BzTMA^+ was removed more rapidly than BS^- . The strong electrolyte salt was once again completely removed in less than 30 min and none of the ampholytic sample components were lost. The conductance and pH values of the recirculating sample solution are shown as a function of time in Figure 21. Both curves are similar to those obtained with the IDAPVA and ASPPVA membranes.

3.3.3 pI characterization

The limiting pI values for the GLUPVA membrane were obtained in two successive experiments using 2 mM concentrations of the acidic pI markers in a 6 mM HIS solution. IET runs were completed for both solutions at a constant current of 500 mA. Aliquots were taken at 10 min intervals and analyzed for the concentration of the respective acidic pI markers. The nominal pI = 2.6 marker left the separation compartment in 25 min, but the concentration of nicotinic acid (NIC, approximate

pI=3.4) remained the same for at least 60 min indicating that the pI of the GLUPVA membrane is in the $2.6 < pI < 3.4$ range.

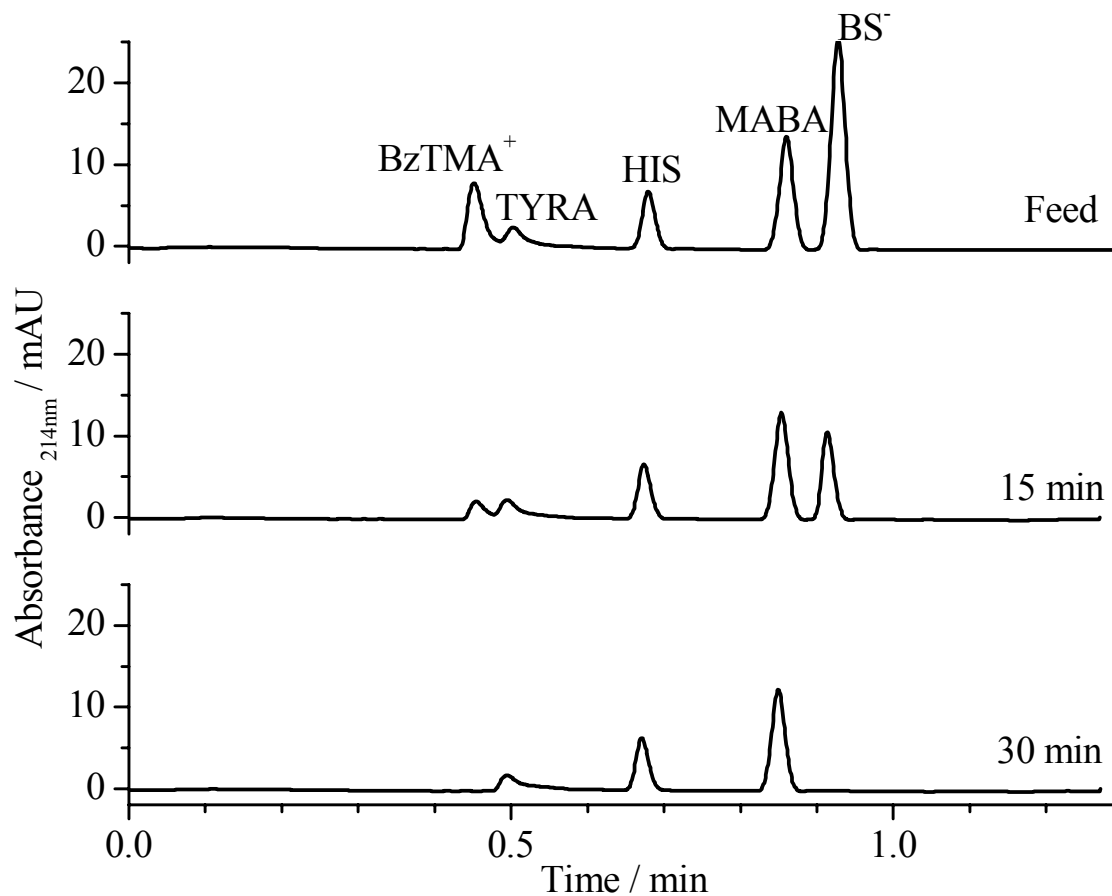


Figure 20. Electropherograms for the aliquots from the desalting experiment with GLUPVA as the anodic membrane: (top) feed, (middle) after 15 min, and (bottom) after 30 min.

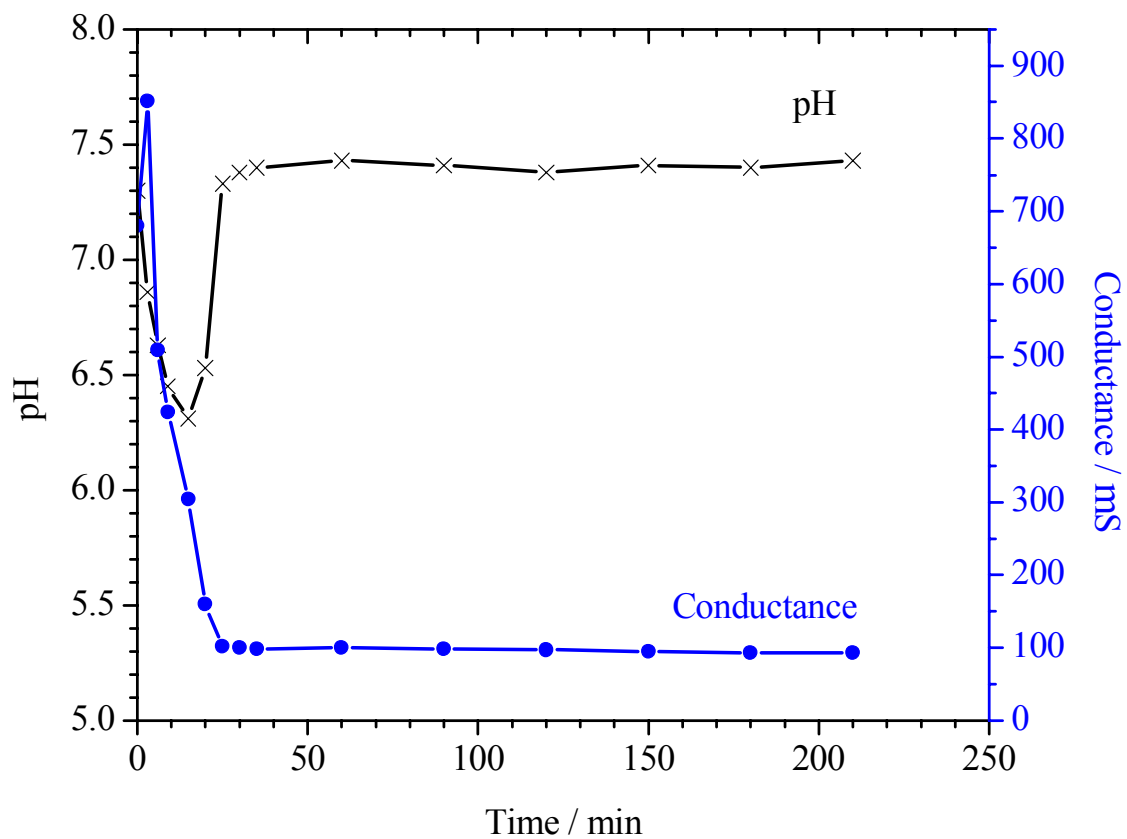


Figure 21. Sample conductance and pH as a function of time during the desalting run with GLUPVA as the anodic membrane.

4. TRISHUL: SYNTHESIS OF HIGH-pI, HYDROLYTICALLY STABLE ISOELECTRIC HYDROGEL MEMBRANES*

4.1 QCDPVA

4.1.1 Synthesis

4.1.1.1 Final procedure

High-pI membranes using quaternary ammonium cyclodextrins (QCDs), GDGE and PVA were made according to the following procedure. A 185x310 mm sheet of Grade BFN2 Papylon PVA substrate was clipped between two 190x320 mm PP sheets. The PP-PVA-PP sandwich was placed on a clean glass plate on the table. The clips were taped to anchor the sandwich to the table.

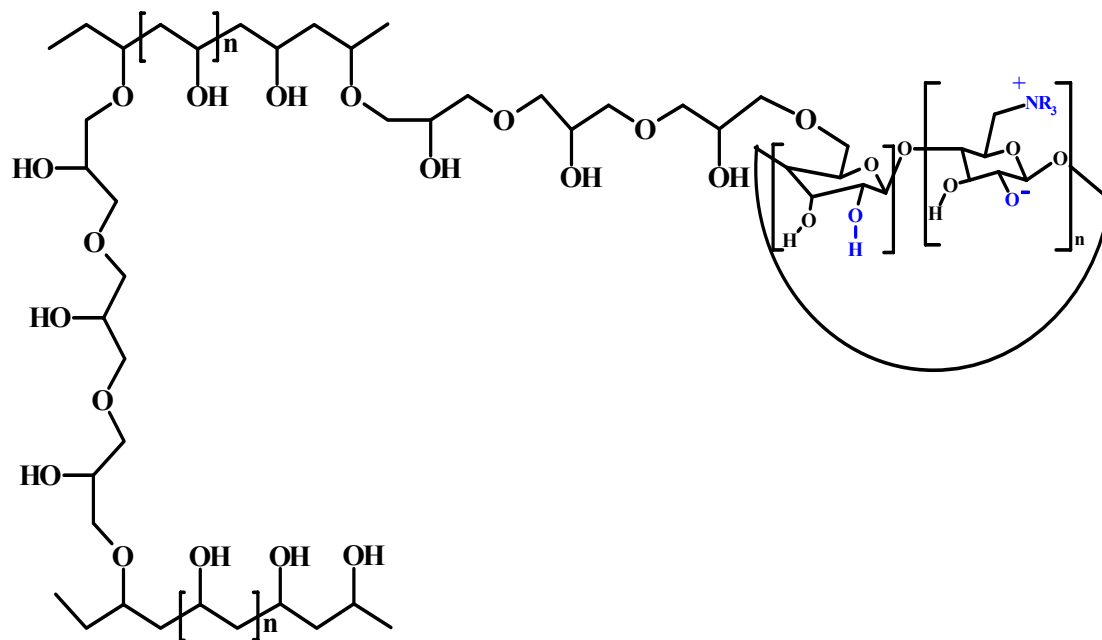
A 150 mL beaker was heated in an oven to 80 °C. A 500 mL, three-neck, round bottom flask was fitted with an ice-water cooled condenser and a nitrogen purge line. 80 mL deionized water and 3.2 g (80.2 mmol) NaOH were added to the flask and dissolved, followed by 8 g QCD (Ave. DS about 3.5), and brought to a boil in a heating mantle. 8 g (182 mmol OH equivalent) PVA was added to the hot solution, the system was purged with nitrogen, stirred and heated until all PVA dissolved.

An 80 g aliquot of the hot, viscous reaction mixture was weighed into the hot, 150 mL beaker, then 3.2 mL (3.5 g, 17 mmol) GDGE was quickly added to it and mixed well (manually) with a spatula. The top PP sheet and the PVA sheet were lifted and

* Reprinted with permission from “Alkali Stable High pI Isoelectric Membranes for Isoelectric Trapping Separations” by Lalwani, S., Shave, E., Fleisher, H.C., Nzeadibe, K., Busby, M.B., and Vigh, G., *Electrophoresis* 2004, 25, 2128-2138. Copyright 2004, Wiley VCH.

about half of the content of the beaker was poured on the lower PP sheet to form an inverted “T”. The PVA sheet was slowly lowered and a 1 mm thick PVAc sheet (scraper) was run over it to squeeze out the excess solution. The second half of the hot reaction mixture was then poured on the PVA sheet. The top PP sheet was then lowered and the Teflon-coated rolling pin was rolled over it to squeeze out the excess reaction mixture. The membrane-plastic sheet sandwich was kept in a covered styrafoam box with wet paper towels at room temperature for a total curing time of 40 hours. After curing, the PP sheets were carefully peeled under deionized water. The membrane was slosed around in subsequent (typically five) batches of rinse water until the pH of the wash water remained neutral. The membrane produced had clear, transparent salvage edges and a strong, even and slippery surface. Figure 22 shows a cartoon representation of a possible structure of the synthesized QCDPVA hydrogel.

The QCDPVA membrane sheets were stored in deionized water at 4°C until used. The QCDPVA membranes swelled to a final thickness typically between 0.4 and 0.7 mm. Since the amount of epoxide groups left-over in the QCDPVA membranes was not known, gloves were worn when the membranes were handled. QCDPVA membranes of the final size required for the separation cartridge of the BF200IET unit were cut with scissors. Used QCDPVA membranes were rinsed with water and disposed as solid waste.



R = alkyl group

Figure 22. A cartoon representation of a possible structure of the synthesized QCDPVA hydrogel.

4.1.2 Testing

4.1.2.1 Trapping

The high-pI isoelectric membranes produced from QCD, GDGE and PVA were tested as the cathodic membranes in the single separation compartment configuration of the BF200IET. The anolyte was a 5 mM BSH solution, the anodic membrane was a pI=3 polyacrylamide-based isoelectric membrane (Gradipore), and the catholyte was a 50 mM BzTMAOH solution. BSH and BzTMAOH were selected as strong electrolytes because both absorb UV light. If the electrode membranes failed during separation or if there was inadequate current to compensate for bulk flow-mediated or diffusion-mediated electrolyte invasion from the electrode compartments into the sample compartment, their presence could be easily detected by CE analysis of the collected fractions. The sample contained 5 mM MABA (approximate pI = 3.9), 5 mM HIS (pI = 7.5) and 5 mM TYRA (approximate pI = 10) as the ampholytic analytes. A potential of 60 V was applied generating an electrophoretic current of 300 mA that corresponded to a membrane current density of 20 mA/cm². Electrophoresis was continued in the recirculating mode for 1 hour, aliquots were collected at the exit ports and analyzed by CE. Figure 23 shows the results of the CE run for the starting sample (top panel, feed) and the 1hour sample (bottom panel). The ampholytic components, MABA, HIS and TYRA were trapped for the duration of the 1 hour long run, and neither BSH nor BzTMAOH invaded the separation compartment.

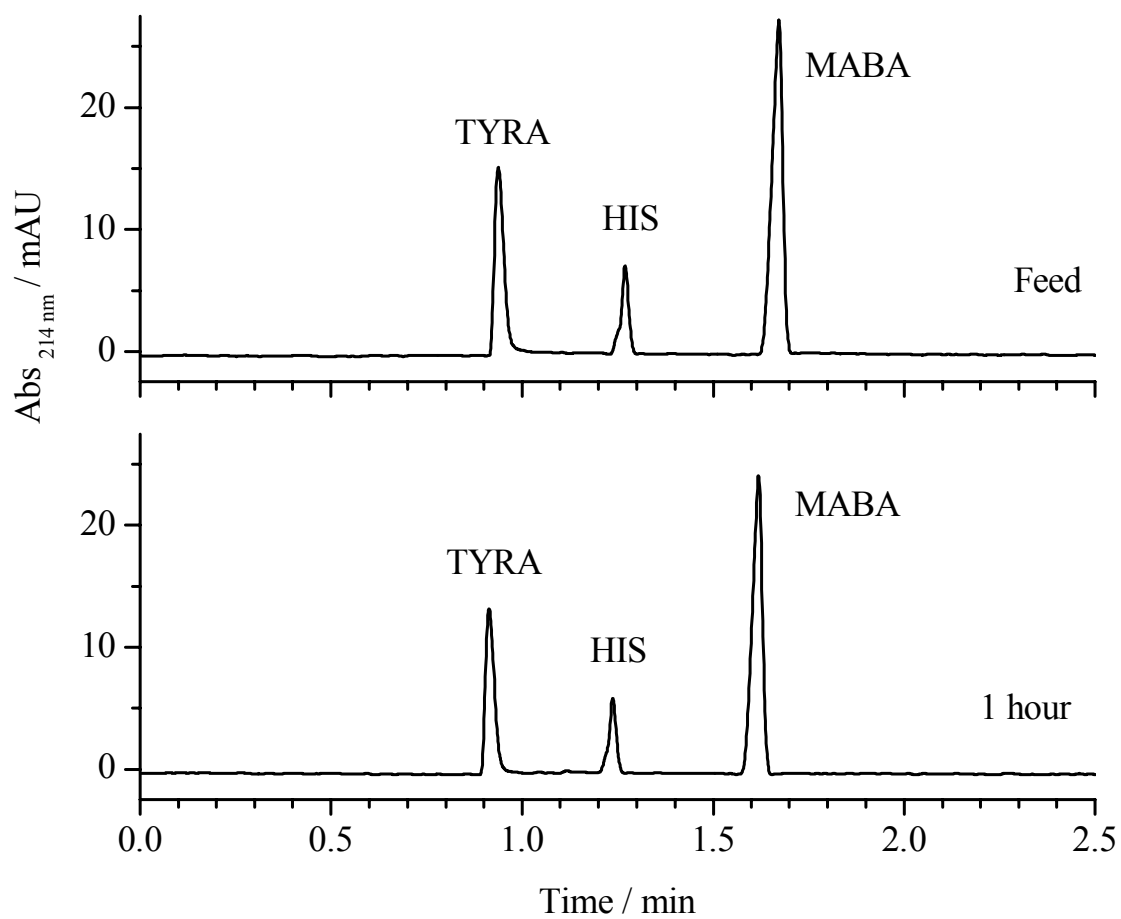


Figure 23. Electrochromatograms of the feed sample (top) and the sample after 1 hour (bottom) of trapping using QCDPVA as the cathodic membrane.

4.2 CDQPVA

4.2.1 Synthesis

4.2.1.1 Final procedure

High-pI membranes using glycidyltrimethylammonium chloride (GTMA), β -CD, GDGE and PVA were made according to the following procedure (conditions adapted from the optimized synthesis of IDAPVA membranes). A 185x310 mm sheet of Grade BFN4 Papyrus PVA substrate was clipped in between two 190x320 mm PP sheets. The PP-PVA-PP sandwich was placed on a clean glass plate on the table. The clips were taped to the table to anchor the sandwich.

A 150 mL beaker was heated in an oven at 80 °C. A 500 mL, two-neck, round bottom flask was fitted with an ice-water cooled condenser, a nitrogen purge line and a stir bar. 60 mL deionized water and 9.2 g (229 mmol) NaOH were added to the flask and the solution was warmed in a heating mantle. 10.9 g β -CD was added to the flask and heated until all β -CD dissolved. The solution was brought to a boil and 12 g (273 mmol OH equivalent) PVA was added to the hot solution. The system was purged with nitrogen, stirred and heated until all PVA dissolved. Then, 1.91 mL (2.16 g, 10 mmol) GTMA solution was added to the flask and the solution was stirred.

A 40 g aliquot of the hot, viscous reaction mixture was weighed into the hot, 100 mL beaker, then 4.1 mL (4.48 g, 22 mmol) GDGE was quickly added to it and mixed well (manually) with a spatula. The top PP sheet and the PVA sheet were lifted and about half of the content of the beaker was poured on the lower PP sheet to form an inverted "T". The PVA sheet was slowly lowered and 1 mm thick sheet of PVAc

(scraper) was run over it to squeeze out the excess solution. The second half of the hot reaction mixture was then poured on the PVA sheet. The top PP sheet was then lowered and the Teflon-coated rolling pin was rolled over it to squeeze out the rest of the excess reaction mixture. The membrane-plastic sheet sandwich was kept in a covered styrafoam box with wet paper towels at room temperature for a total curing time of 40 hours. After curing, the PP sheets were carefully peeled under deionized water. The membrane was sloshed around in subsequent (typically five) batches of rinse water until the pH of the wash water remained neutral. The membrane produced had clear, transparent salvage edges and a strong, even and slippery surface. Figure 24 shows a cartoon representation of a possible structure of the synthesized CDQPVA hydrogel.

The CDQPVA membrane sheets were stored in deionized water at 4°C until used. The CDQPVA membranes swelled to a final thickness typically between 0.4 and 0.7 mm. Since the amount of epoxide groups left-over in the CDQPVA membranes was not known, gloves were worn when the membranes were handled. CDQPVA membranes of the final size required for the separation cartridge of the BF200IET unit were cut with scissors. The used CDQPVA membranes were rinsed with water and disposed as solid waste.

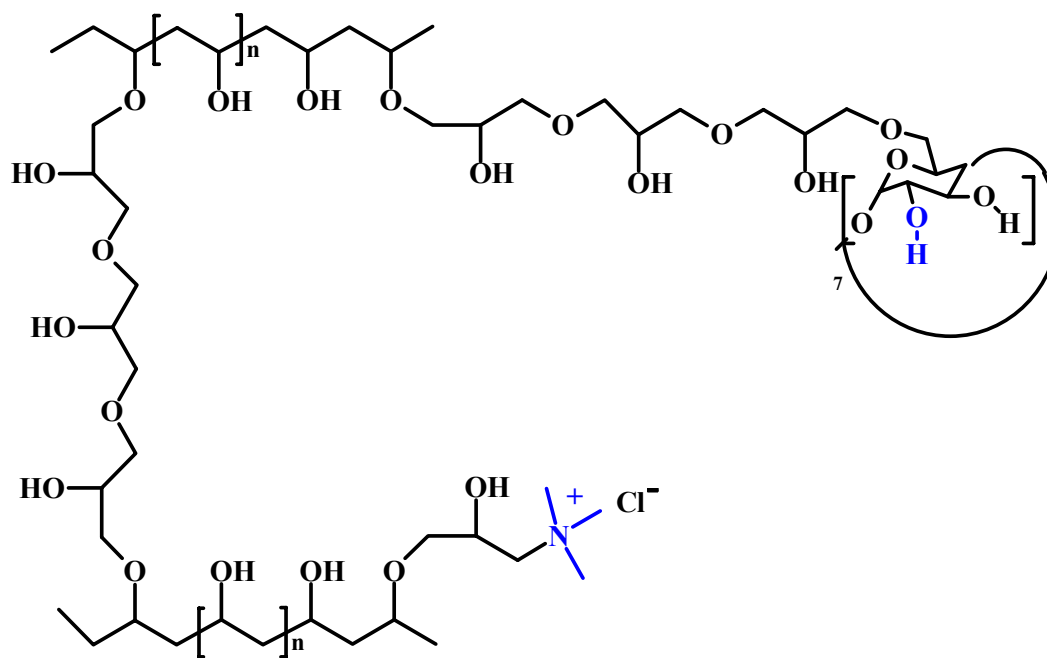


Figure 24. A cartoon representation of a possible structure of the synthesized CDQPVA hydrogel.

4.2.2 Testing

4.2.2.1 Trapping

CDQPVA membranes were tested as the cathodic membranes in trapping experiments, similarly to the QCDPVA membranes. The anolyte contained 5 mM BSH, and the catholyte contained a mixture of 200 mM BzTMAOH and 300 mM NaOH. The anodic membrane was a pI=3 polyacrylamide-based isoelectric membrane (Gradipore). The sample reservoir was filled with a 50 mL mixture that contained the ampholytic analytes: 1 mM 3-pyridinepropionic acid (3PPA, approximate pI = 4.8), 2 mM 4-hydroxy-3-(morpholinomethyl)benzoic acid (HMMB, approximate pI = 5.8) and 2 mM TYRA (approximate pI=10). A potential of 180 V was applied, generating an electrophoretic current of 500 mA that corresponded to a membrane current density of 33 mA/cm². Electrophoresis was continued in the recirculating mode for two hours, aliquots were collected at the exit ports and analyzed by CE. Figure 25 shows the results of the CE runs for the starting sample (top panel, feed), the 1 hour sample (middle panel) and the 2 hours sample (bottom panel). Clearly, 3PPA, HMMB and TYRA were trapped, and neither BSH nor BzTMAOH invaded the separation compartment.

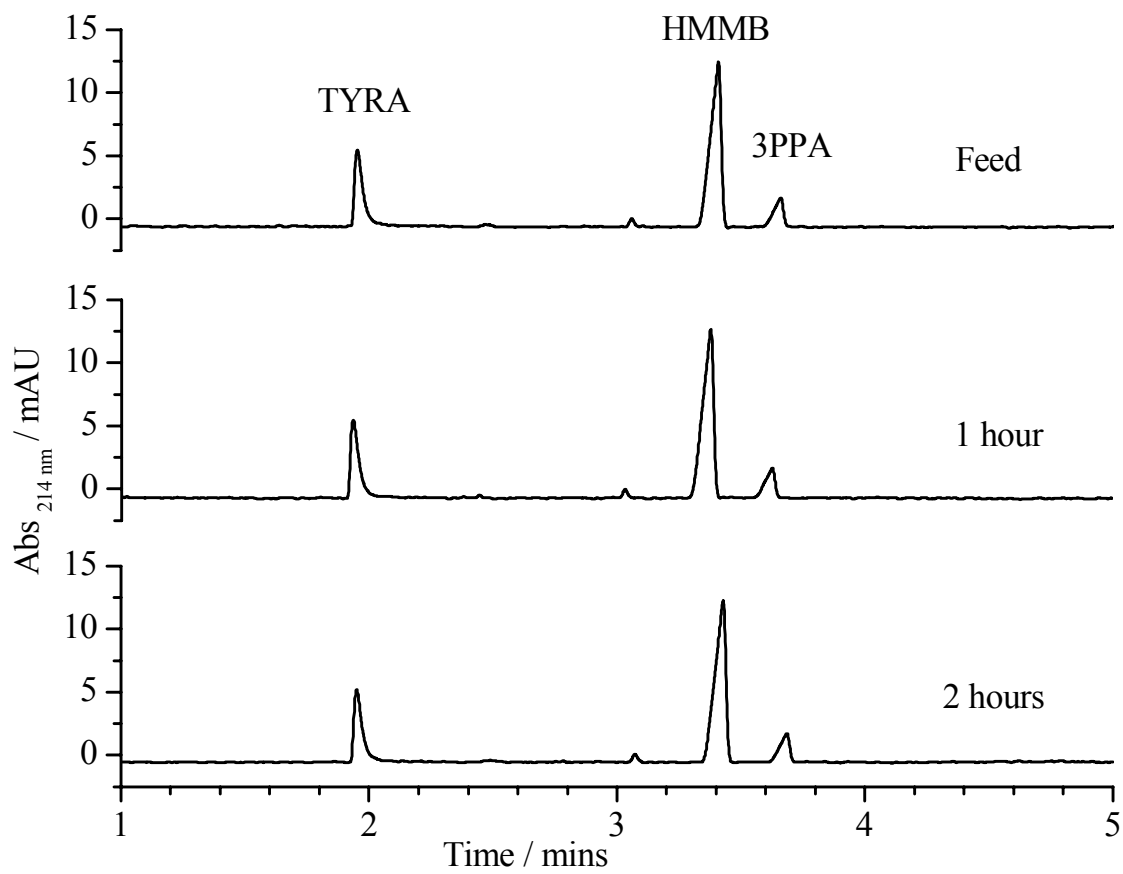


Figure 25. Electrochromatograms of the feed sample (top), sample after 1 hour (middle) and sample after 2 hours (bottom) from the trapping experiment using CDQPVA as the cathodic membrane.

4.2.2.2 Desalting

Next, the CDQPVA membrane was tested as a cathodic membrane in an IET desalting experiment. The BF200IET was set up in the single separation compartment mode, as in the trapping experiments, except that the anolyte was a 5 mM MSH solution and the catholyte was a 500 mM NaOH solution, both UV transparent solutions. UV absorbing BSH (10 mM) and BzTMAOH (10 mM) were added to a sample solution of 1 mM 3PPA, 2 mM HMMA, and 2 mM TYRA. The electrophoretic current was set at 800 mA that corresponded to a membrane current density of 53 mA/cm^2 , the separation was carried out in the pass-by-pass mode, and aliquots were taken at the end of each pass. The conductance and pH of each aliquot are plotted in Figure 26, along with the potential needed to generate a constant, 800 mA current, as a function of the pass number. By the 16th pass (corresponding to a total electrophoresis time of 27 min), the pH, conductance and potential values leveled off. The results of the CE analysis of the

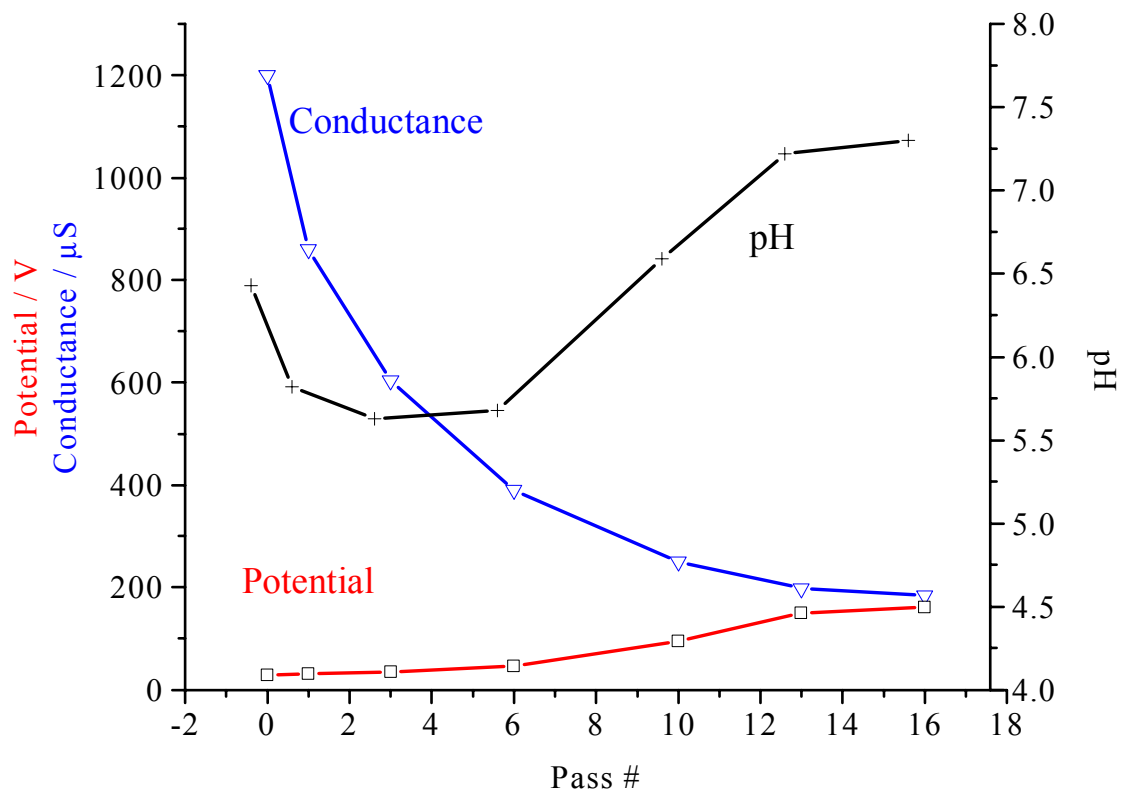


Figure 26. Conductance, potential and pH traces of the sample stream for the duration of the desalting experiment using CDQPVA as the cathodic membrane.

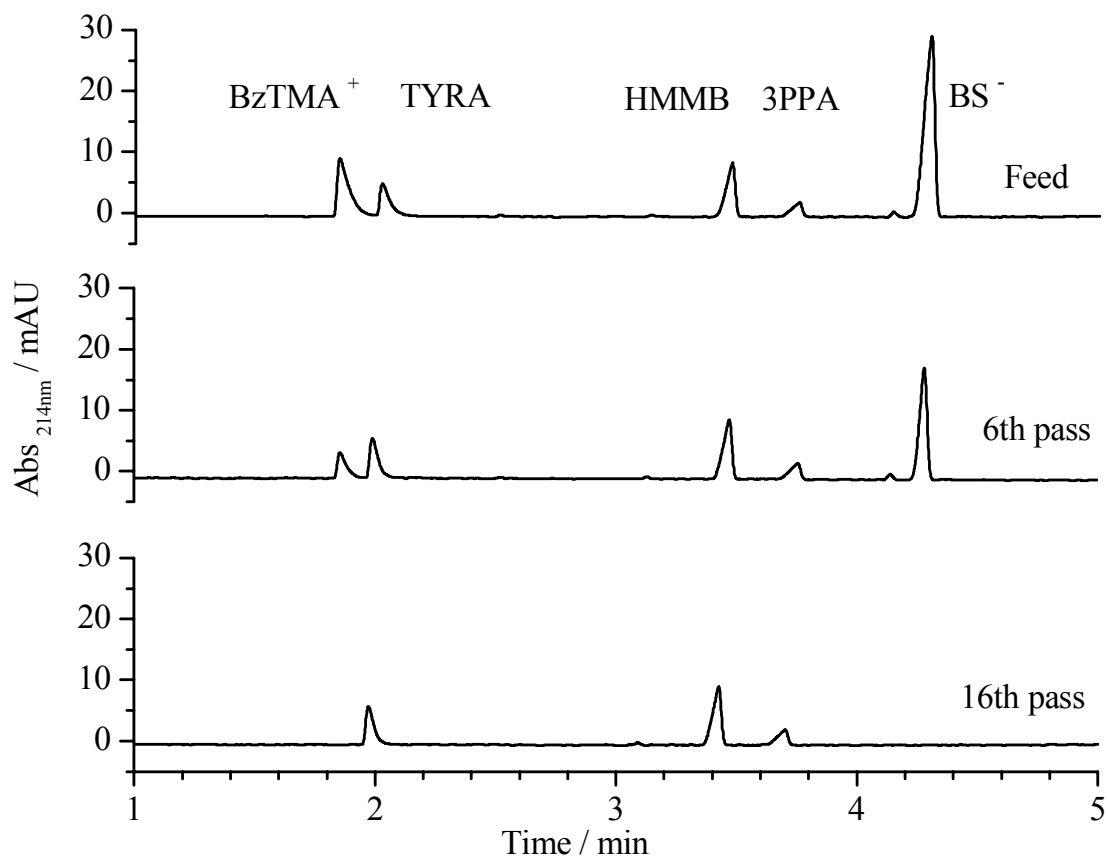


Figure 27. Electropherograms of the feed sample (top), sample after the 6th pass (middle) and sample after the 16th pass (bottom) for the desalting experiment using CDQPVA as the cathodic membrane.

aliquots are shown in Figure 27. The top panel is for the initial sample (feed), the middle panel is for the aliquot taken after the 6th pass, and the bottom panel is for the aliquot taken after the 16th pass. Clearly, BS^- and BzTMA^+ were removed from the sample by the end of the 16th pass and neither 3PPA, HMMB nor TYRA were lost from the sample stream indicating that CDQPVA acted as a proper, high pI isoelectric membrane.

4.2.2.3 Control experiments

When the electrophoretic current was reduced below 400 mA, the pH of the separation compartment began to increase slowly. BzTMA^+ appeared in the fractions taken from the sample stream and its concentration increased gradually with time indicating that the diffusive flux of BzTMAOH into the separation compartment was greater than the electrophoretic transport of BzTMA^+ out of the separation compartment.

When the experiment was repeated under the same conditions, except that the concentration of the strong base in the catholyte was reduced to 50 mM BzTMAOH , TYRA was lost from the separation compartment within 15 min. No TYRA was lost in 2 hour long runs when the concentration of the strong base in the catholyte was higher than 200 mM.

4.3 QPVA

4.3.1 Synthesis

4.3.1.1 Final procedure

High-pI membranes using GTMA, GDGE and PVA were made according to the following procedure (conditions adapted from the optimized synthesis of the IDAPVA membranes). A 185x310 mm sheet of Grade BFN4 Papyrus PVA substrate was clipped in between two 190x320 mm PP sheets. The PP-PVA-PP sandwich was placed on a clean glass plate on the table. The clips were taped to the table to anchor the sandwich.

A 150 mL beaker was heated in an oven at 80 °C. A 500 mL, two-neck, round bottom flask was fitted with an ice-water cooled condenser, a nitrogen purge line and a stir bar. 60 mL deionized water and 6.6 g (165 mmol) NaOH were added to the flask and the solution was warmed in a heating mantle. The solution was brought to a boil and 12 g (273 mmol OH equivalent) PVA was added to the hot solution. The system was purged with nitrogen, stirred and heated until all PVA dissolved. Then, 1.18 mL (1.34 g, 6 mmol) GTMA solution was added to the flask and the solution was stirred.

A 40 g aliquot of the hot, viscous reaction mixture was weighed into the hot, 100 mL beaker, 3 mL (3.3 g, 16 mmol) GDGE was quickly added to the mixture and was mixed well (manually) with a spatula. The top PP sheet and the PVA sheet were lifted and about half of the content of the beaker was poured on the lower PP sheet to form an inverted “T”. The PVA sheet was slowly lowered and the 1 mm thick PVAc sheet (scraper) was run over it to squeeze out the excess solution. The second half of the hot reaction mixture was then poured on the PVA sheet. The top PP sheet was then lowered

and the Teflon-coated rolling pin was rolled over it to squeeze out the remaining excess reaction mixture. The membrane-plastic sheet sandwich was kept in a covered styrafoam box with wet paper towels at room temperature for a total curing time of 40 hours. After curing, the PP sheets were carefully peeled under deionized water. The membrane was sloshed around in subsequent (typically five) batches of rinse water until the pH of the wash water remained neutral. The membrane produced had clear, transparent salvage edges and a strong, even and slippery surface. Figure 28 shows a cartoon representation of a possible structure of the synthesized QPVA hydrogel.

The QPVA membrane sheets were stored in deionized water at 4°C until used. The QPVA membranes swelled to a final thickness typically between 0.4 and 0.7 mm. Since the amount of epoxide groups left-over in the QPVA membranes was not known, gloves were worn when the membranes were handled. QPVA membranes with the final size required for the separation cartridge of the BF200IET unit were cut with scissors. Used QPVA membranes were rinsed with water and disposed as solid waste.

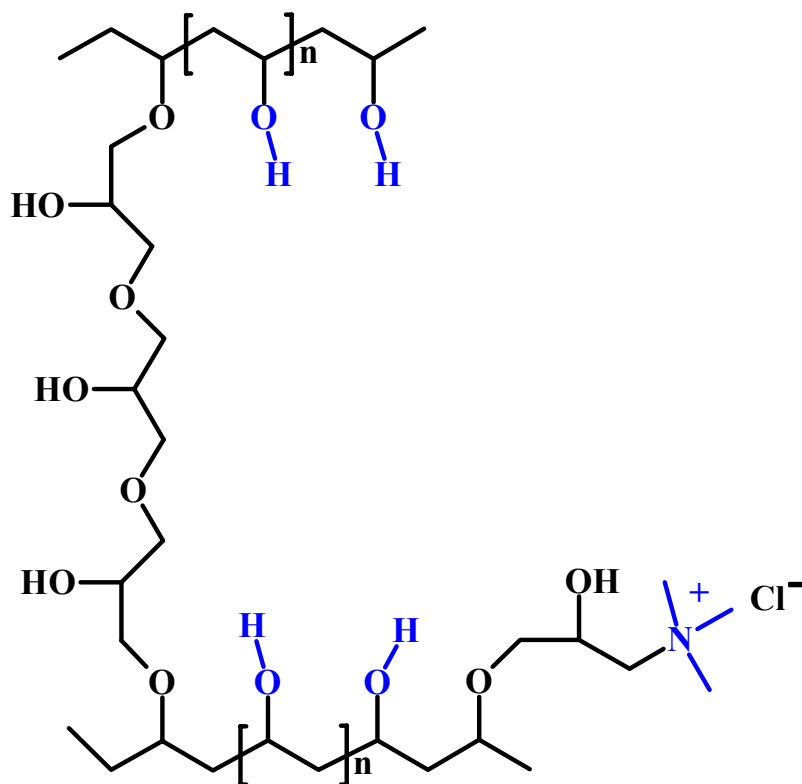


Figure 28. A cartoon representation of a possible structure of the synthesized QPVA hydrogel.

4.3.2 Testing

4.3.2.1 Trapping

Again, the suitability of the high pI, QPVA isoelectric membranes as the cathodic membranes in a trapping experiment, in the single separation compartment configuration of the BF200IET was tested. Because the QPVA membrane was expected to have a higher pI value than the QCDPVA and CDQPVA membranes, a more concentrated catholyte, containing 200 mM BzTMAOH and 800 mM NaOH was used. The anodic membrane was a pI=3 polyacrylamide-based isoelectric membrane (Gradipore). The anolyte composition remained the same, a 5 mM BSH solution. The sample solution contained 3 mM MABA, 7 mM HIS and 3 mM TYRA. An applied potential of 120V generated a constant current of 900 mA that corresponded to a membrane current density of 60 mA/cm^2 . The top panel in Figure 29 shows the results of the CE analysis of the starting sample (feed), the middle panel shows the analysis of the 1 hour sample, while the bottom panel shows the result for the 3 hours sample. Again, the ampholytic components were trapped and neither BSH nor BzTMAOH invaded the separation compartment.

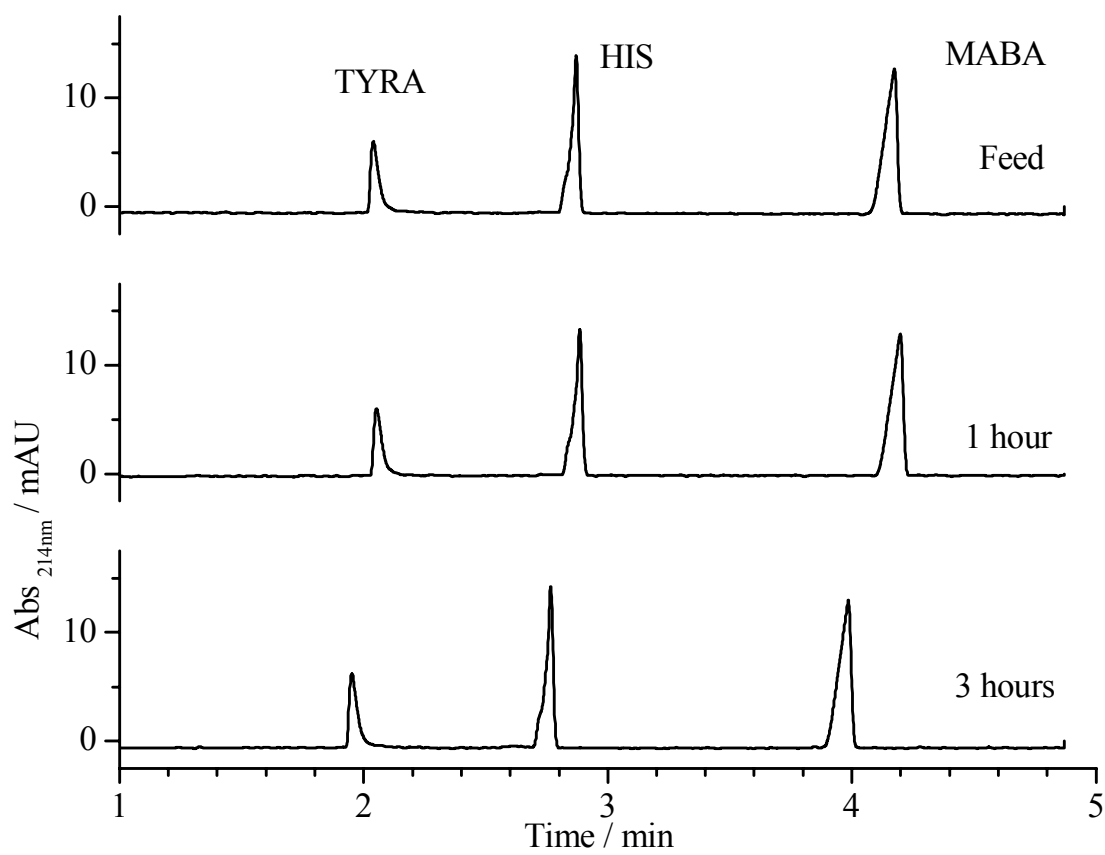


Figure 29. Electropherograms of the feed sample (top), sample after 1 hour (middle) and sample after 3 hours (bottom) for the trapping experiment using QPVA as the cathodic membrane.

4.3.2.2 Control experiments

When the trapping experiment was repeated under the same conditions, except that the strong base concentration in the catholyte was reduced to 100 mM (50 mM BzTMAOH and 50 mM NaOH), TYRA was lost within 10 min. With 50 mM BzTMAOH and 150 mM NaOH solution as the catholyte, TYRA was not lost and as long as the electrophoretic current was maintained higher than 200 mA, BzTMAOH did not invade the separation compartment.

4.4 Application

Finally, the QPVA membrane was used as the cathodic isoelectric membrane for the pH biased isoelectric trapping of the high pI fraction of chicken egg white (containing mostly lysozyme, pI = 10.7, MW = 14,300). The anodic membrane was a pI=3 polyacrylamide-based isoelectric membrane, the separation membrane was a pI=8 polyacrylamide-based isoelectric membrane (Gradipore), the cathodic membrane was QPVA. The anolyte was a 200 mL solution of 20 mM IDA, the catholyte a 200 mL solution of 200 mM NaOH. 1 mL chicken egg white was dissolved in a 50 mL portion of 10 mM GLU and 10 mM HIS and was filtered through a poly(ethylene terephthalate) paper. The filtered solution was loaded, without removing the natural salt content of egg white by dialysis, into the reservoir of the anodic separation compartment. The reservoir of the cathodic separation compartment was filled with a 20 mL portion of a solution that contained 10 mM carnosine (CAR) and 10 mM lysine (LYS). The separation was run in the recirculating mode, at a constant current of 200 mA that corresponded to a membrane current density of 13 mA/cm^2 , requiring initially 46 V, and leveling off at 484

V. Aliquots were taken every 10 minutes from both separation compartments and analyzed for lysozyme content by SDS-PAGE using a 4-20% m/m iGel (Gradipore), according to the manufacturers instructions. Figure 30 shows the scanned image of the GradiPure (Gradipore) stained gel. Lane 1 (M) contains the relative molecular mass markers (MBI Fermentas, Hanover, MD, USA), lanes 2 to 6 (F0 to F40) contain the aliquots taken from the anodic separation compartment at time 0, 10, etc. min, lanes 7 to 10 (C10 to C40) contain the aliquots taken from the cathodic separation compartment at time 10, 20, etc. min, lane 11 is a blank, and lane 12 contains an aliquot of the catholyte at the end of the separation. By 40 minutes, the majority of the lysozyme has been moved from the anodic separation compartment, through the pI 8 separation membrane, into the cathodic separation compartment, and was trapped there by the high pI QPVA membrane (no lysozyme was detected in the cathode compartment).

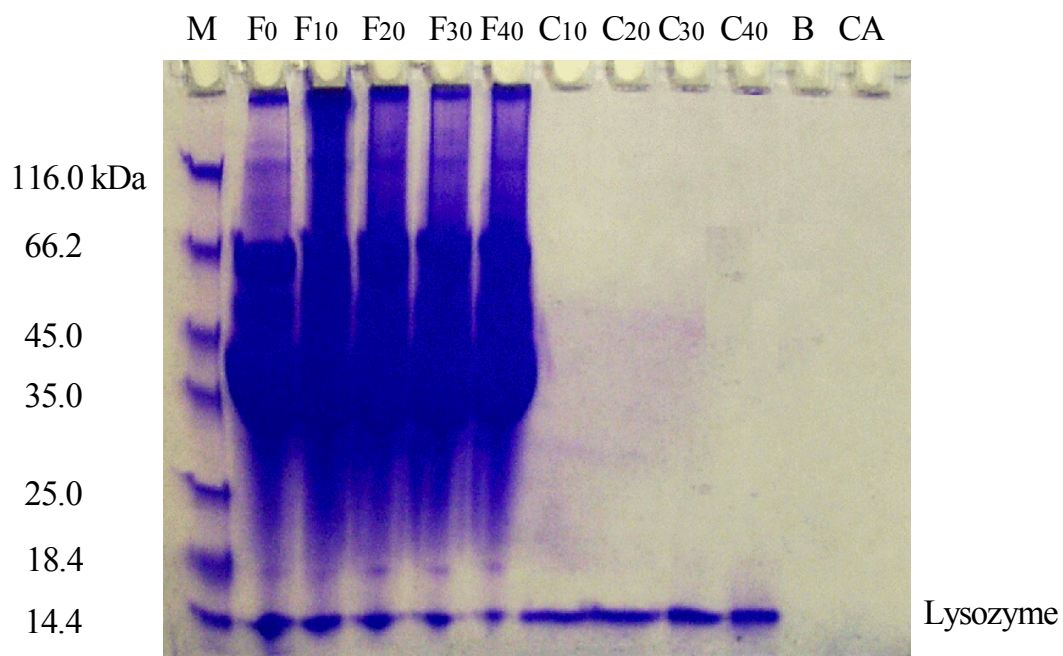


Figure 30. Scanned image of an SDS-PAGE analysis of aliquots taken from the lysozyme trapping experiment (M=Markers, F=Feed stream samples, C=Collection stream samples, B=Blank, CA=Catholyte stream).

5. MOSES : SYNTHESIS OF LOW-pI ISOELECTRIC BUFFERS

5.1 Opportunistic

5.1.1 N,N-bis(carboxymethyl)dimethyl ammonium hydroxide, inner salt (BCDAH)

The quaternary ammonium derivative of iminodiacetic acid was synthesized in the following manner (synthesis scheme illustrated in Figure 31). A clean, 2L, three-neck round bottom flask was fitted with an ice-water cooled condenser. 600 mL tetrahydrofuran (THF) and 500 mL deionized water were added to the flask. 5.0 g (0.034 mol) methyliminodiacetic acid (MIDA) were added to the flask and dissolved, followed by 3.8 g (0.068 mol) potassium hydroxide (KOH) and the mixture was warmed in a heating mantle. 2.35 mL (5.36 g, 0.038 mol) iodomethane (IM) was added to the warm solution and the mixture was stirred and heated continuously at 60°C for 5 hours. A sample from the reaction mixture was taken and analyzed by ¹H-NMR spectroscopy. Signals for unreacted MIDA were seen but IM signal was absent. IM could have hydrolyzed to form hydroiodic acid (HI) and methanol. Thus, sodium bicarbonate (NaHCO₃) was added to scavenge the acid formed in the hydrolysis of IM. More IM (3.0 mL, 6.84 g, 0.048 mol) was added to compensate for loss of IM (by hydrolysis or evaporation) and to increase the conversion of MIDA to BCDAH. Figure 32 shows the ¹H-NMR spectra of the reaction mixture after 5, 15 and 22 hours of reaction time.

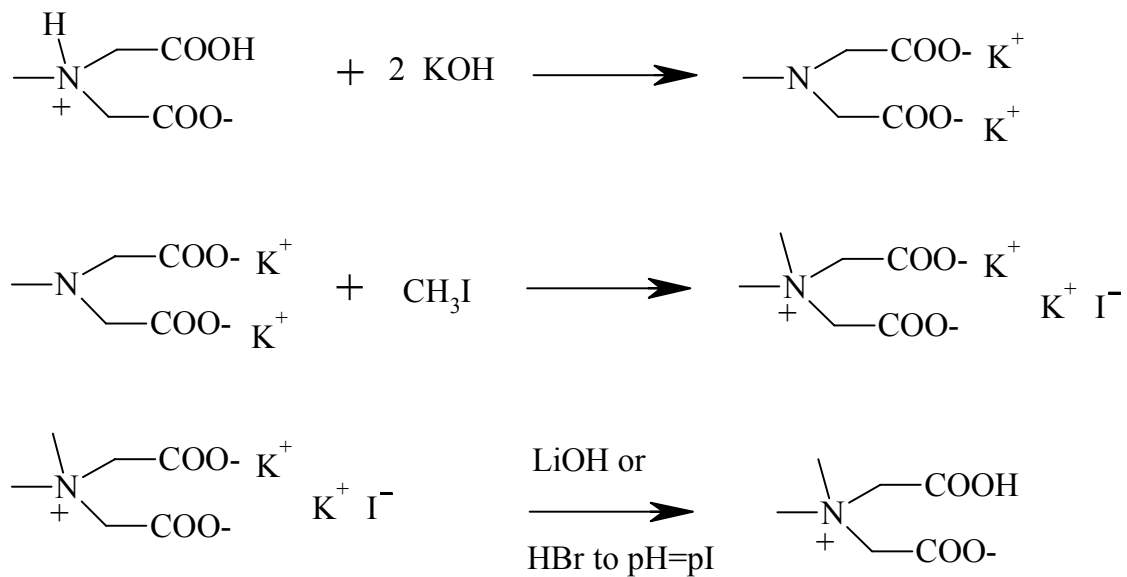


Figure 31. Synthesis scheme for BCDAH from MIDA and IM.

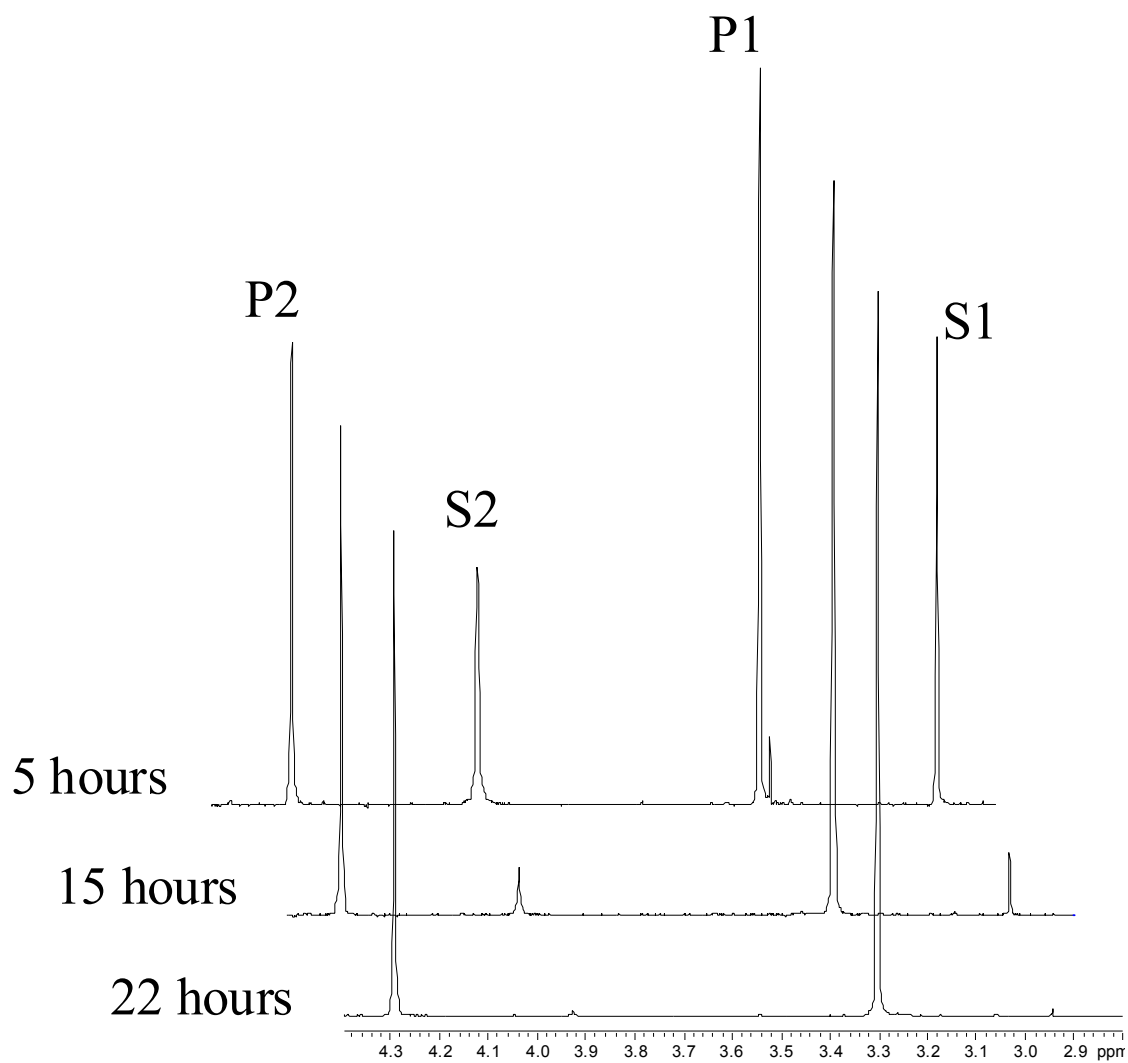


Figure 32. ¹H-NMR spectra for the aliquots of the reaction mixture of BCDAH at 5, 15 and 22 hours of reaction time. S1 – MIDA CH₃- signal, S2- MIDA -CH₂- signal, P1 – BCDAH CH₃- signal, and P2 – BCDAH -CH₂- signal.

After most of MIDA had been converted (>95%), THF was removed under reduced pressure followed by partial removal of water. The pI of BCDAH was then determined by CE

5.1.1.1 pI determination

The pI of BCDAH was determined using pressure-mediated capillary electrophoresis (PreMCE) [100] with the following conditions: 26 μm I.D. bare fused silica capillary, $L_t = 26.5$ cm, $L_d = 19.7$ cm, $t_{\text{inj}} = 1$ s, $t_{\text{transf}} = 20$ s, $t_{\text{migr}} = 1.80$ min, $U_{\text{appl}} = 10$ kV, positive to negative polarity, $T = 25$ °C and UV detector at 200 nm. Using dimethylsulfoxide (DMSO) as the neutral marker, a three band PreMCE with the sequence A-N1-N2, was carried out in phosphoric acid BGEs whose pH was increased with lithium hydroxide (LiOH) by approximately 0.1-0.2 pH units between pH=1 and pH=2. Figure 33 shows the CE traces for BCDAH in pH=1.5 and pH=1.7 BGEs and DMSO in pH=1.7 BGE (to mark the neutral position). Clearly, the pI of BCDAH is between 1.5 and 1.7.

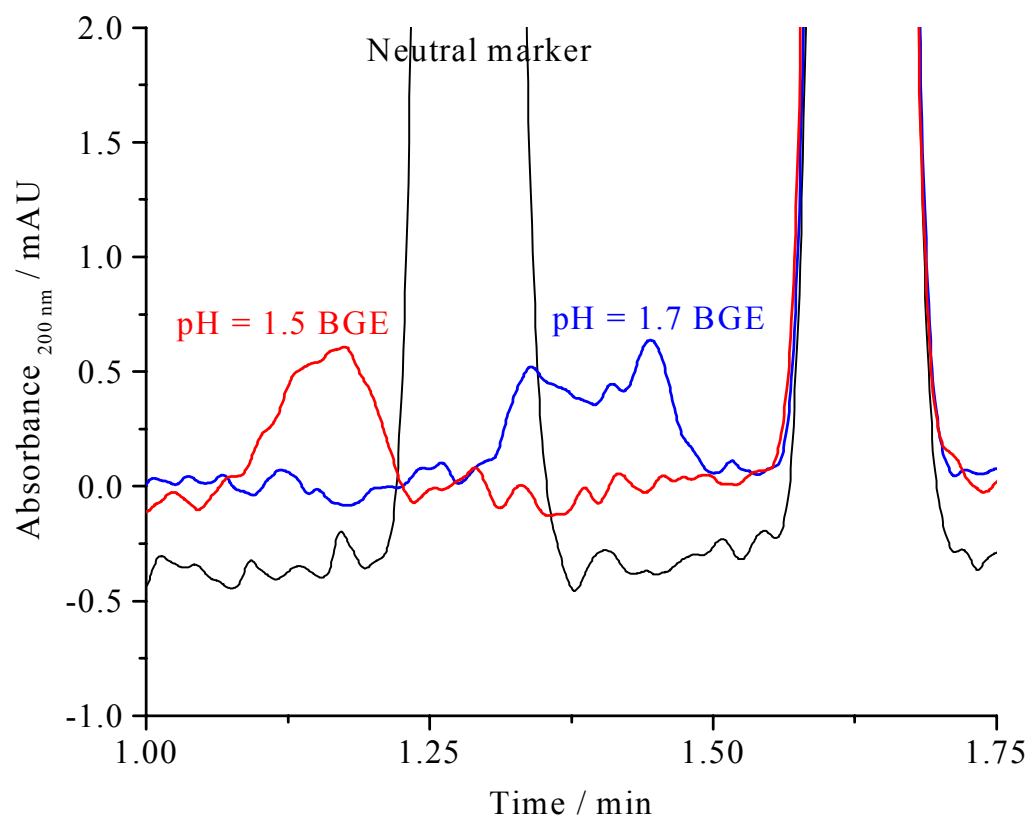


Figure 33. CE traces for BCDAH in pH 1.5 and 1.7 BGEs.

5.1.1.2 Isoelectric crystallization

The concentrated solution of BCDAH was titrated with hydrochloric acid (HCl) (and later with hydrobromic acid (HBr)) to pH=1.6. More water was removed under reduced pressure and the warm solution was cooled to crystallize the product in the salt-free form. Repeated crystallizations from water were done.

Product purity (in terms of inorganic salt content) was determined by indirect-UV detection CE. Using a 20 mM acetic acid BGE titrated with imidazole to pH=4.56, a 26 μm I.D. bare fused silica capillary, $L_t = 26.5$ cm, $L_d = 19.7$ cm at 25kV, positive to negative polarity, $T=25$ °C, and the UV detector at 214 nm, sodium and potassium ions were analyzed. Figure 34 shows the electropherograms of the crystallized product (top panel), the crystallization mother liquor (middle panel) and the electropherogram simulated by Peakmaster 5.0. Using a 20 mM β -alanine BGE titrated with p-toluenesulfonic acid (pTSA) to pH=3.35, a 26 μm I.D. bare fused silica capillary, $L_t = 25.7$ cm, $L_d = 19.3$ cm at 25kV, negative to positive polarity, $T=25$ °C, and the UV detector at 214 nm, bromide and iodide ions were analyzed. Results for the crystallized product (top panel), the crystallization mother liquor (middle panel) and the simulated electropherogram (by Peakmaster 5.0, bottom panel) are shown in Figure 35.

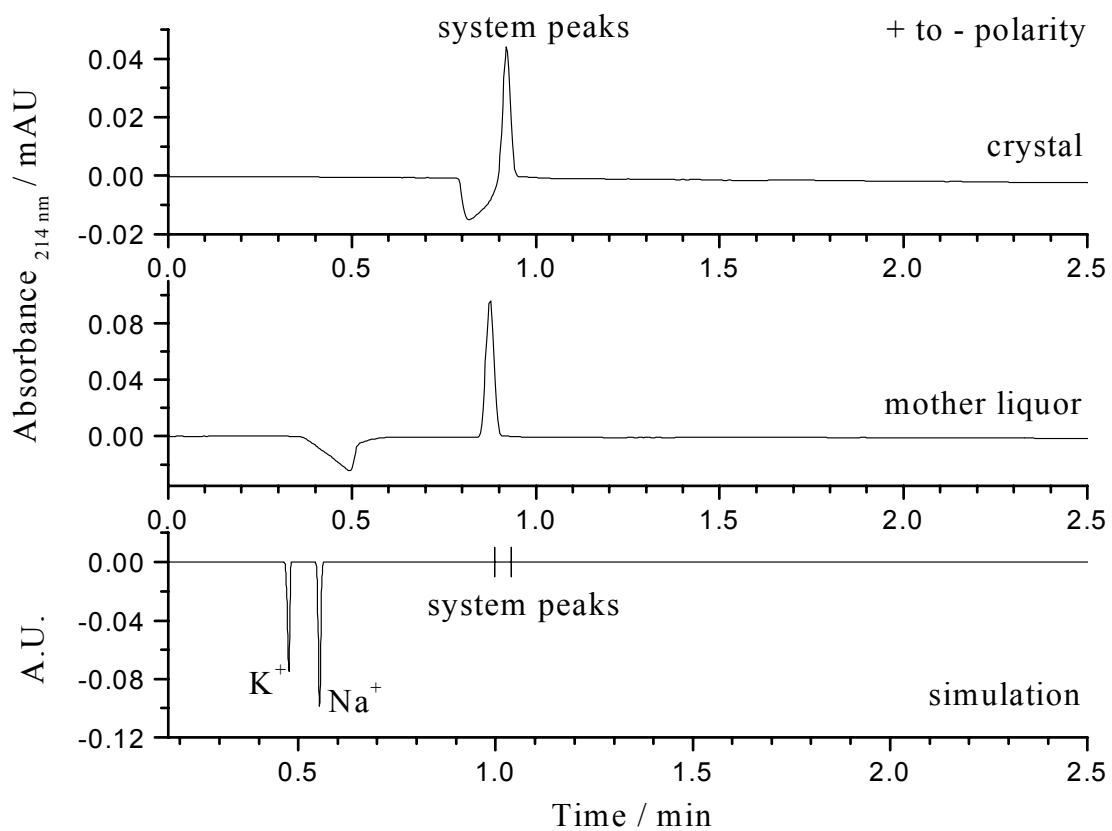


Figure 34. Electropherograms run in positive to negative polarity mode, for the crystal (top) and the mother liquor (middle) from the BCDAH crystallization experiment and the Peakmaster 5.0 simulation (bottom).

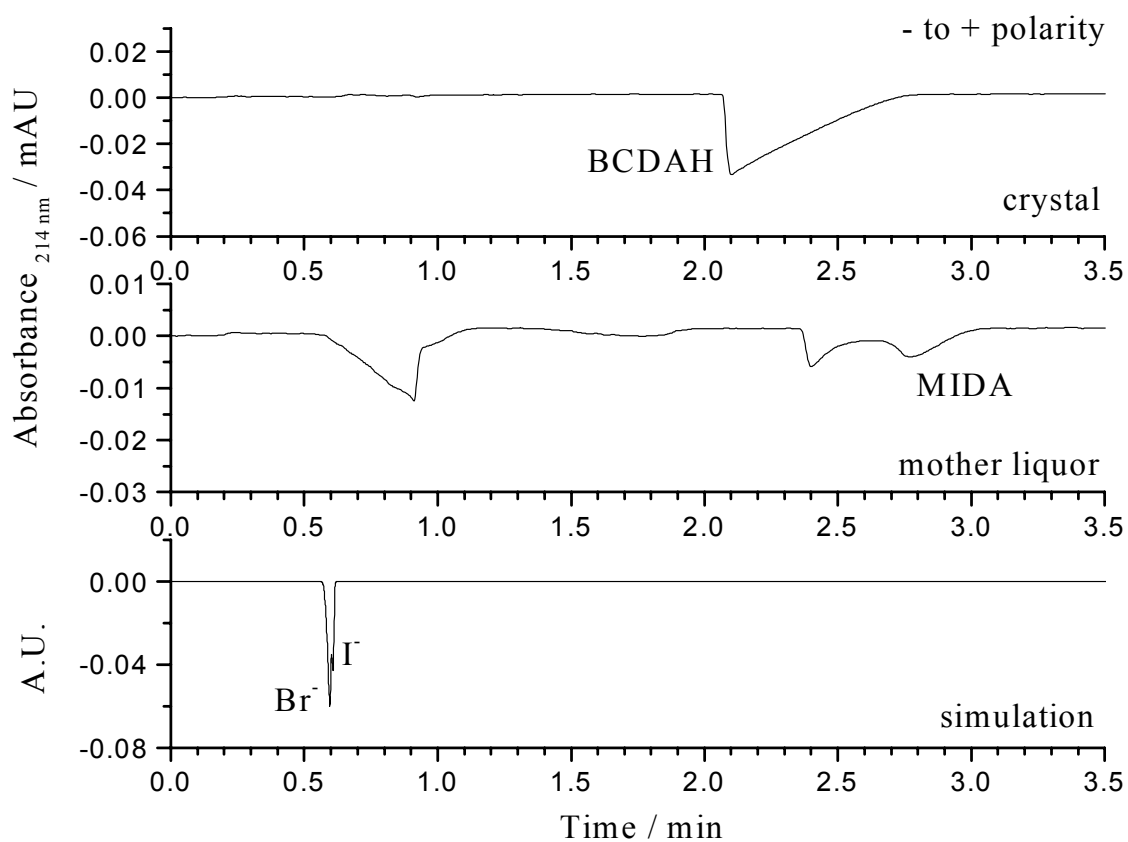


Figure 35. Electrochromograms run in negative to positive polarity mode, for the crystal (top) and the mother liquor (middle) from the BCDAH crystallization experiment and the Peakmaster 5.0 simulation (bottom).

5.1.1.3 Characterization

The final product was characterized by ^1H - and ^{13}C -NMR. Figure 36 shows the ^1H - and ^{13}C -NMR spectra and the tentative assignment of the signals. The product was also analyzed by ^1H - ^1H correlation spectroscopy (COSY) (spectra shown in Figure 37). This confirmed that the two proton signals were not coupled (thus not on neighboring carbon atoms). The ^{13}C assignments were confirmed using ^1H - ^{13}C Heteronuclear Correlation (HETCOR) NMR spectroscopy (spectra shown in Figure 38).

The identity and purity of the final product were confirmed by high resolution electrospray ionization – mass spectrometry (ESI-MS). The ESI-MS spectrum in positive ion mode is shown in Figure 39. Only signals corresponding to BCDAH (H^+ and K^+ adducts) are seen. Single crystals of the product were grown by slow and undisturbed cooling of a concentrated aqueous solution and their X-ray crystal structure was determined. An image of the X-ray crystal structure is shown in Figure 40.

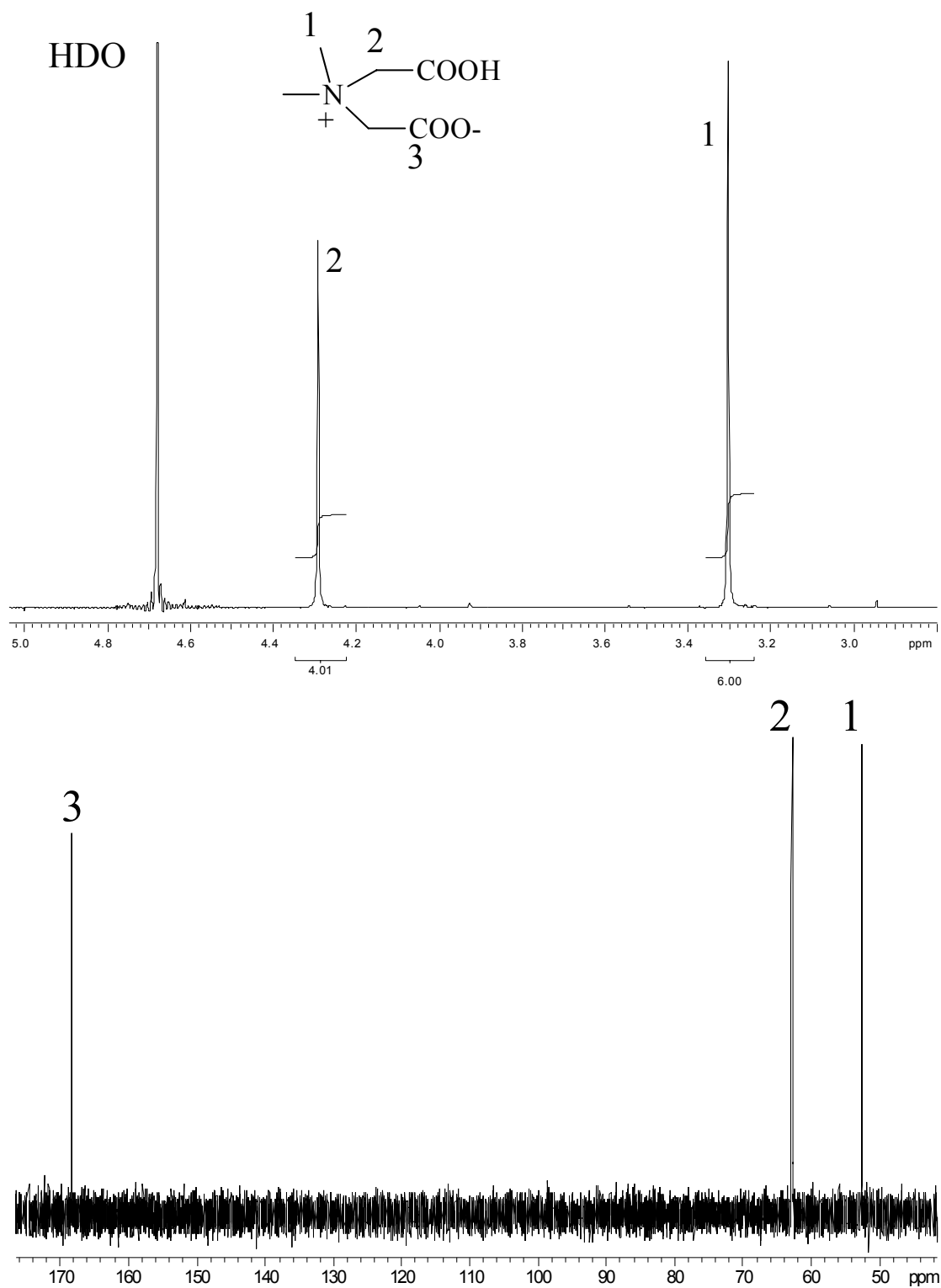
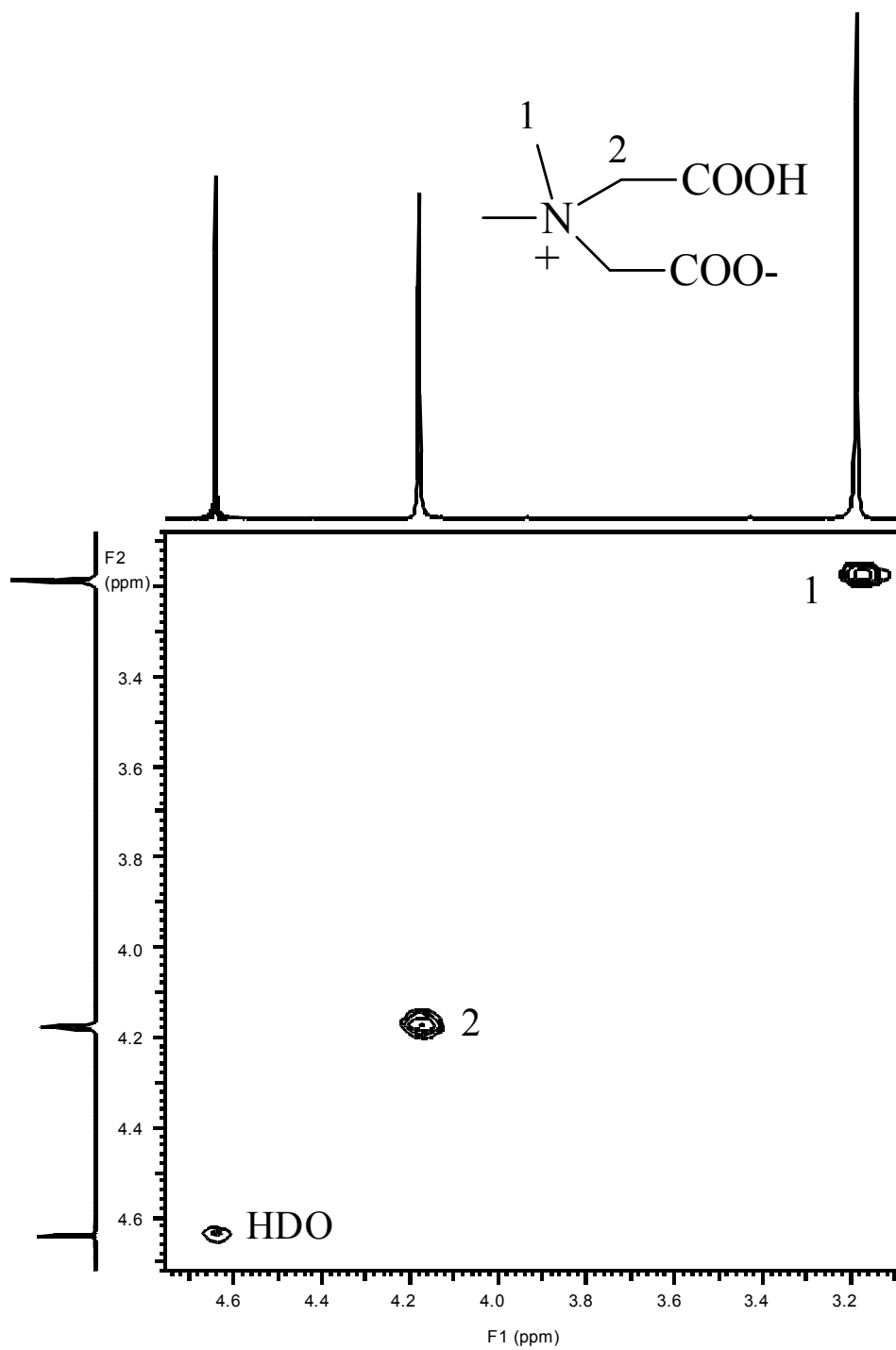


Figure 36. ^1H - (top panel) and ^{13}C - (bottom panel) NMR spectra of BCDAH.

Figure 37. ¹H-¹H COSY spectrum for BCDAH.

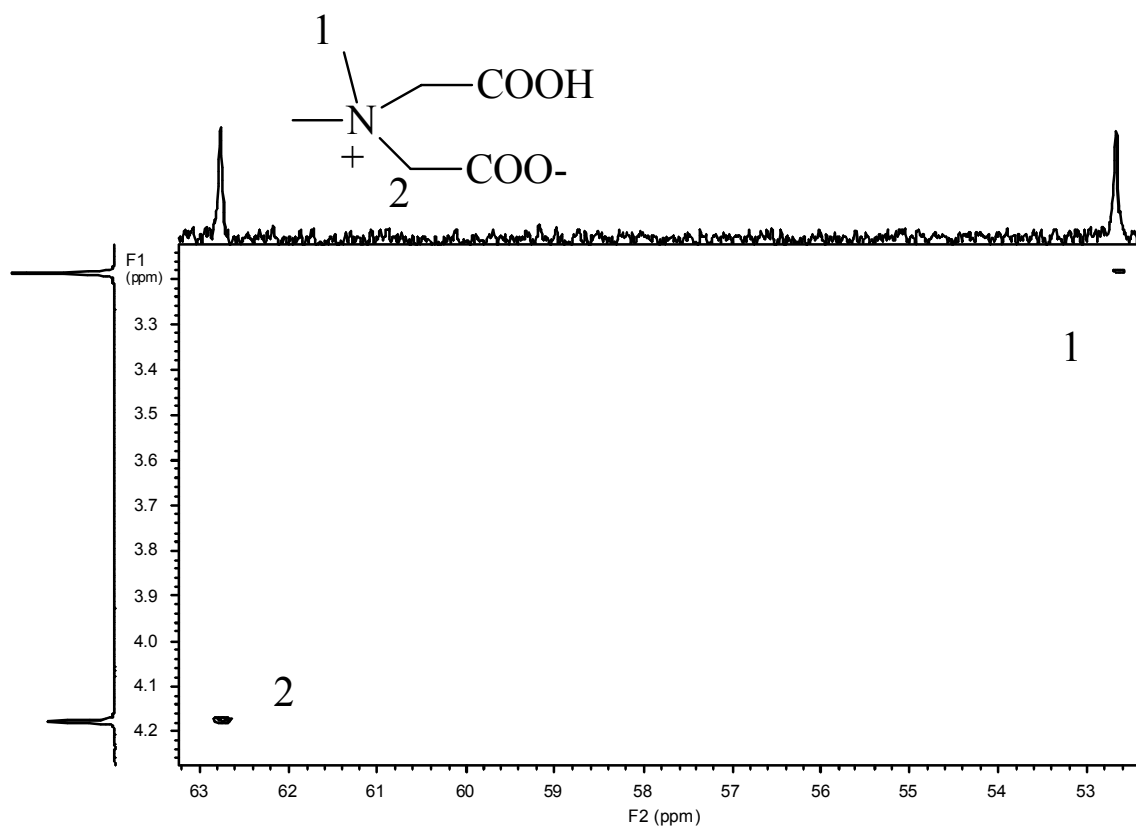


Figure 38. ^1H - ^{13}C HETCOR spectrum for BCDAH.

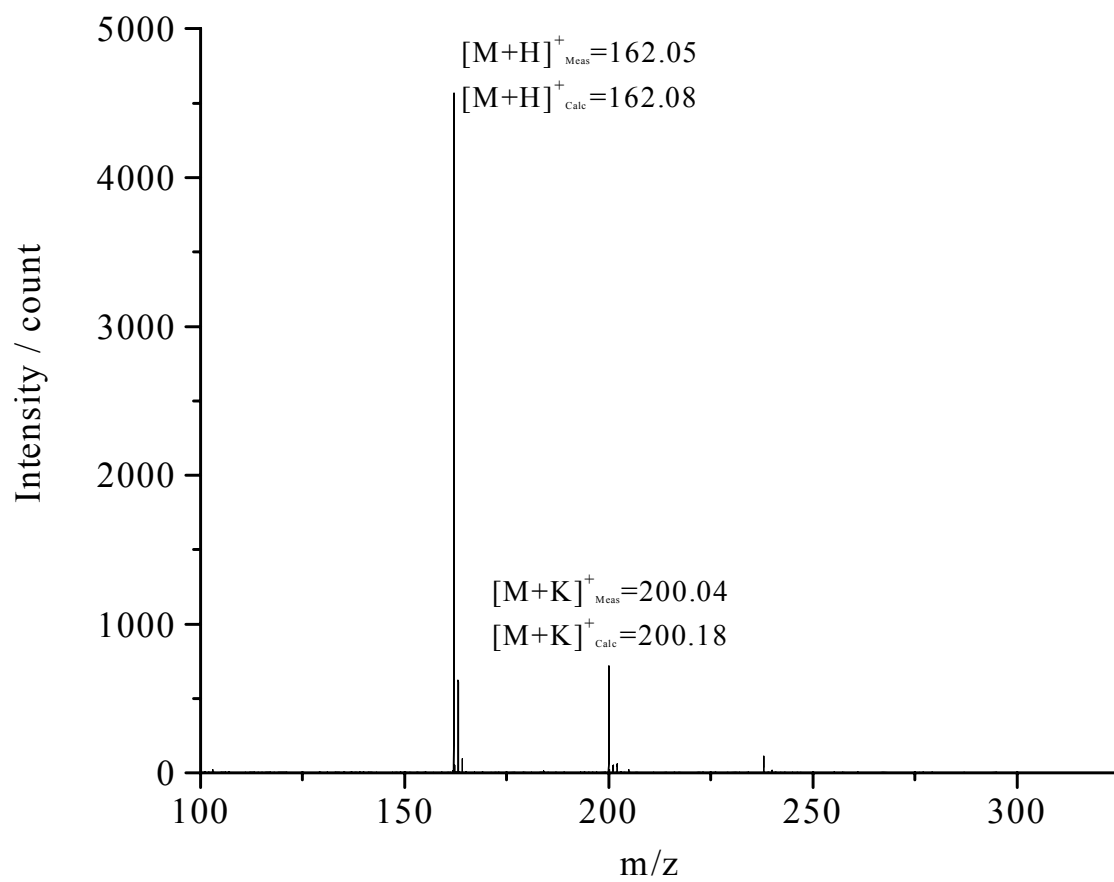


Figure 39. ESI-MS analysis of BCDAH.

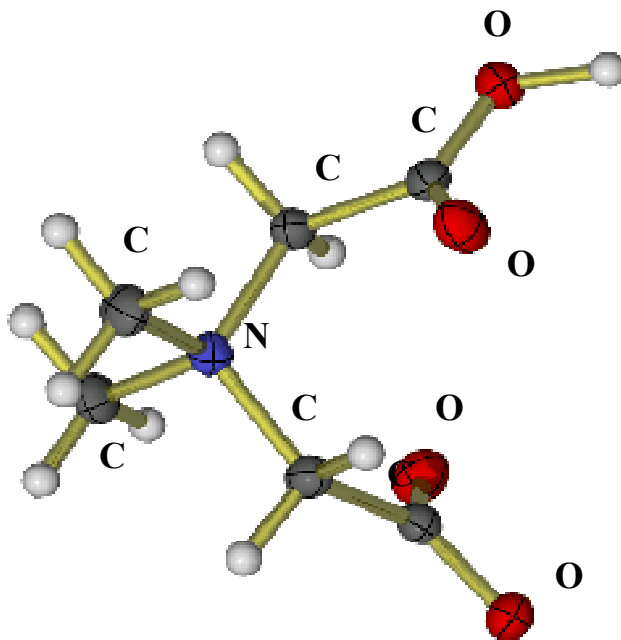


Figure 40. Ball-and-stick representation of the X-ray crystal structure for the single crystal of BCDAH.

5.1.1.4 Recapitulation

A unique, acidic isoelectric buffer, BCDAH, has been synthesized from MIDA and IM. Based on the design of the molecule, the two carboxylic acids in BCDAH have close pK_a values. Consequentially, solutions of BCDAH in its isoelectric state have high buffering capacity and high conductivity. The pI of BCDAH is between 1.5 and 1.7, being the most acidic isoelectric buffer so far reported (previously, cysteic acid was the most acidic known buffer with a pI of 1.85 [71, 72]). An additional characteristic of this buffer is its resistance to N-oxidation (not found in isoelectric buffers previously reported). BCDAH has been obtained in its pure, isoelectric form and has been well characterized by 1D and 2D-NMR, ESI-MS, CE and X-ray crystallography.

5.2 *De novo* synthesis

A family of carboxylic acid-based isoelectric buffers can be synthesized according to the following generic, *de novo* synthesis scheme. First, 2 equivalents of a moderately hydrophobic secondary amine are reacted with 1 equivalent of an alkylbromoalkanoate. As 1 equivalent of the amine reacts by nucleophilic substitution and attaches to the alkylalkanoate chain, forming a protonated, tertiary ammonium intermediate, simultaneously the second equivalent of the amine deprotonates the tertiary ammonium intermediate (pK_a of the secondary amine is slightly higher than the pK_a of the tertiary amine intermediate). As a result, the secondary ammonium bromide salt precipitates out from the hydrophobic reaction mixture and can be separated from the tertiary amine intermediate by filtration. Next, 1 equivalent of the tertiary amine intermediate is reacted with 1 equivalent of an alkyl bromoalkanoate (either the same as

the first one or a different one) to form a quaternary ammonium bromide salt intermediate. Finally, the ester functionalities can be hydrolyzed (with either an aqueous strong acid or strong base) to form the free carboxylic acids. The product can then be obtained in isoelectric form by crystallization from a concentrated aqueous solution titrated to the pH equal to the pI of the isoelectric buffer or by desalting in an IET set-up.

5.2.1 N, N-bis(carboxypropyl)diethyl ammonium hydroxide, inner salt (BCPDEAH)

5.2.1.1 Optimization

The necessary reaction conditions (reaction time and temperature) for the complete synthesis of BCPDEAH from diethylamine (DEA) and ethyl 4-bromobutyrate (EBB) were tested. The reactants were mixed and heated for one hour. A sample from the reaction mixture was taken and analyzed by ^1H - and ^{13}C -NMR spectroscopy, while the rest of the reaction mixture was frozen. After the analysis, the reaction mixture was thawed and heated for another hour. A sample was taken and analyzed in the same manner as previously, while the rest of the batch was frozen. This process was repeated until complete conversion of the starting material (determined from the NMR spectra) was seen. The intermediate was processed and the next reaction was set-up. Progress of the succeeding reactions was also monitored by ^1H - and ^{13}C -NMR. The complete synthesis scheme is shown in Figure 41.

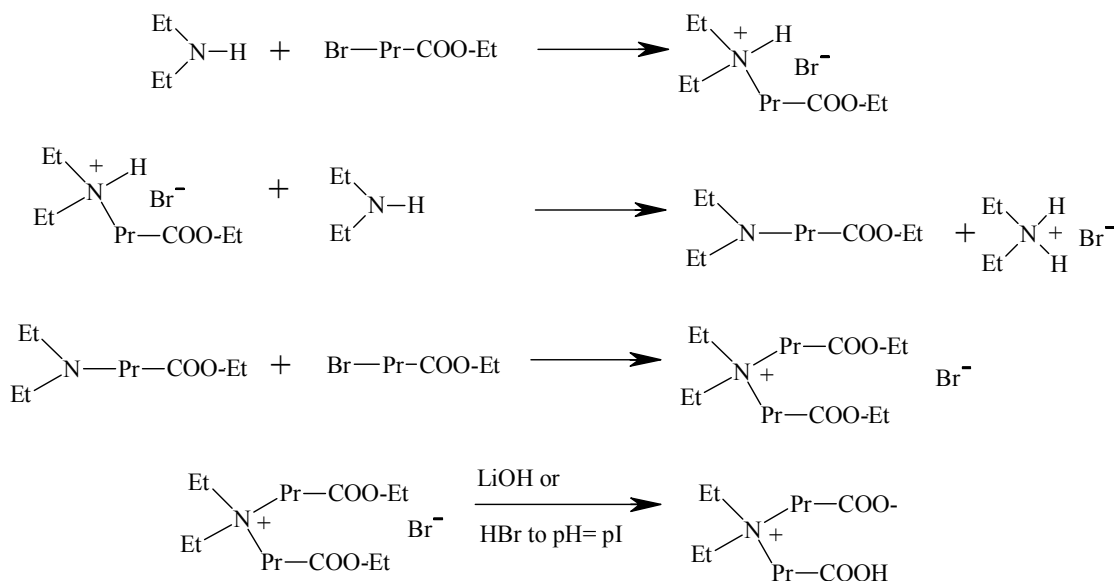


Figure 41. The *de novo* synthesis scheme of BCPDEAH.

5.2.1.2 Step 1

5.2.1.2.1 Synthesis (tertiary amine intermediate)

10.37g (0.142 mol) DEA was mixed with 13.5 g (0.069 mol) EBB in a 250mL round bottom flask fitted with an ice-water cooled condenser. The flask was warmed in a heating mantle with the rheostat set at 45 %. Heavy solid formation was observed within the first 30 minutes of heating. After one hour, a sample was taken, analyzed by ^1H -NMR with D_6 -acetone and D_2O as solvents for the liquid and the solid fractions, respectively. The spectra are shown in Figure 42. The spectrum for the sample containing the solids from the reaction mixture shows signals corresponding to DEA (must be for diethylammonium bromide since diethylamine is a liquid at room temperature). The spectrum for the liquid from the reaction mixture shows signals for

the unreacted DEA, unreacted EBB and a new set of signals. The unique, new signals were tentatively assigned to the tertiary amine intermediate and were monitored over the reaction time by ^{13}C NMR. Spectra taken during the course of reaction are shown in Figure 43.

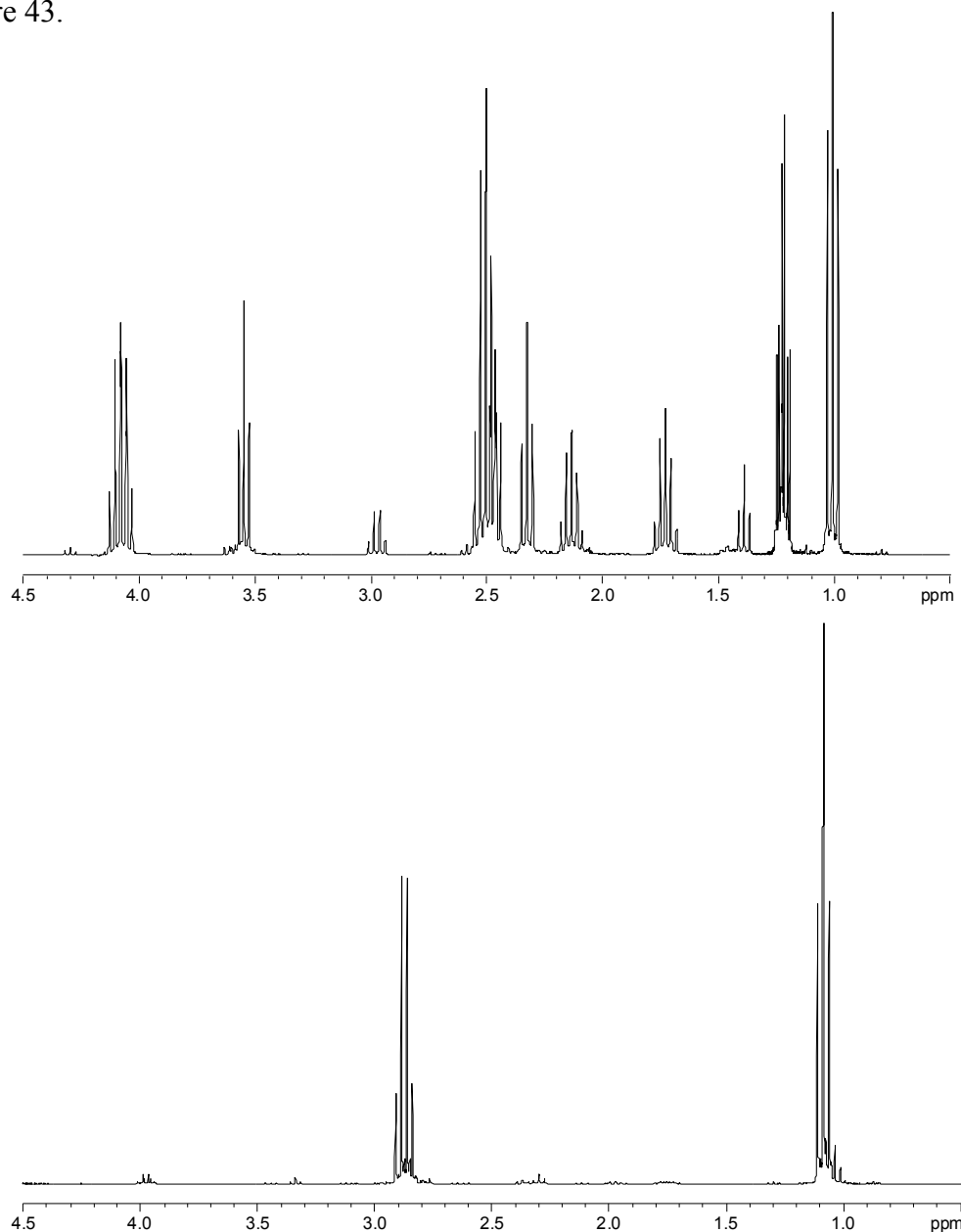


Figure 42. ^1H -NMR spectra of the D_6 -acetone sample (top panel) and the D_2O sample (bottom panel) from the reaction mixture after 1 hour of heating.

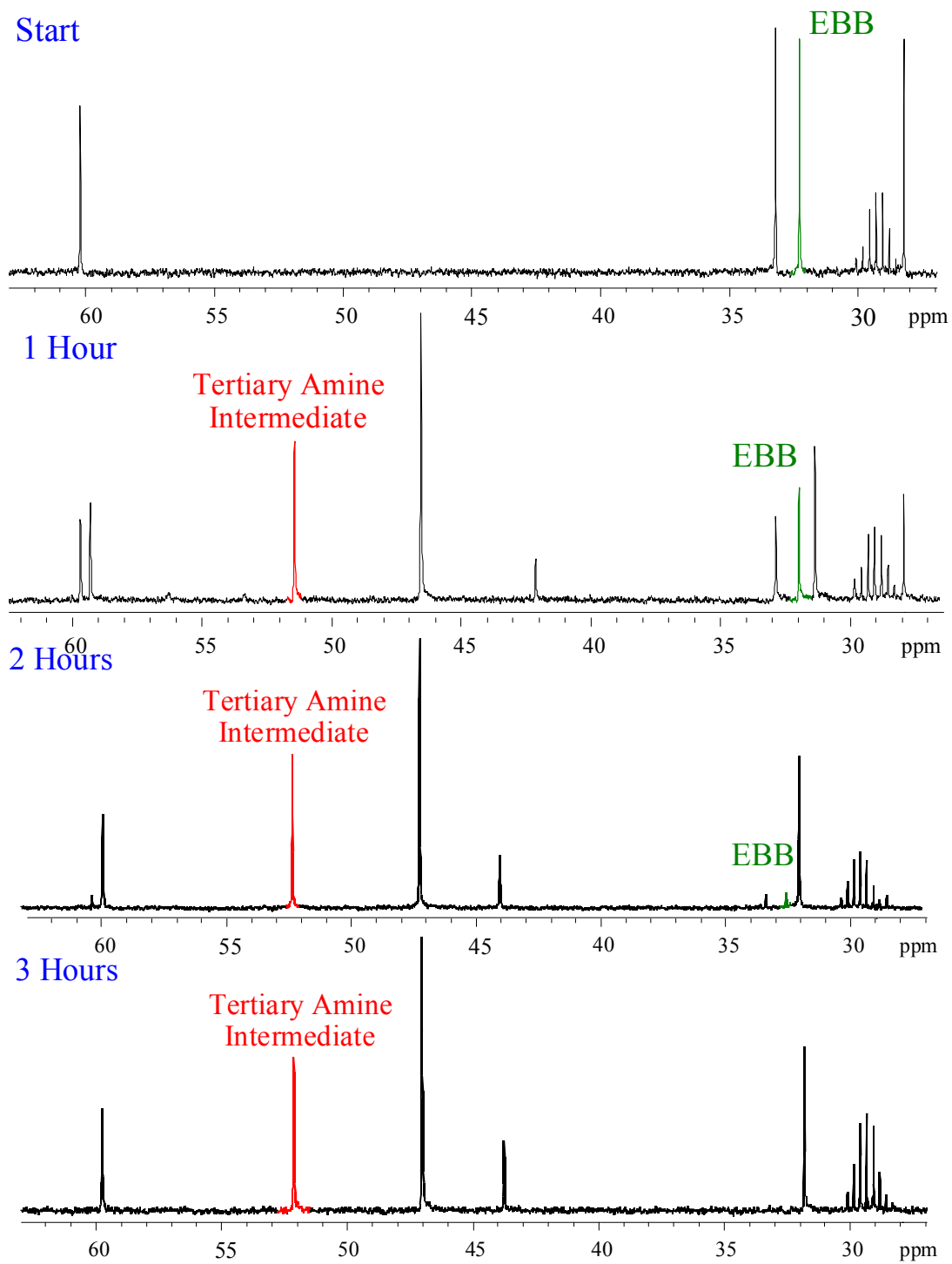


Figure 43. ^{13}C -NMR spectra for the time course of the reaction during the synthesis of the tertiary amine intermediate.

5.2.1.2.2 Processing of the intermediate

The reaction mixture was cooled to room temperature. 500 mL of acetone was added and the mixture was stirred into a homogenous slurry. The mixture was then filtered and the solids were washed with 25 mL of acetone, three times. Acetone and unreacted DEA were removed from the mixture under reduced pressure. The cooled mixture formed a small amount of white solids which was filtered-off; analysis showed it to be diethylammonium bromide. The processed tertiary amine intermediate was analyzed by ^1H -, ^{13}C -NMR spectroscopy (spectra in Figure 44) and the signals assigned tentatively were later confirmed by ^1H - ^{13}C HETCOR NMR (spectra in Figure 45).

5.2.1.3 Step 2

5.2.1.3.1 Synthesis (quaternary ammonium intermediate)

The whole batch of the tertiary amine intermediate from the previous step was mixed with 13.5 g (0.069 mol) ethyl 4-bromobutyrate (EBB) in a 250mL round bottom flask fitted with an ice-water cooled condenser. The flask was warmed in a heating mantle with the rheostat set at 45%. A sample was taken every thirty minutes and was analyzed by ^1H - and ^{13}C -NMR spectroscopy in D_6 -acetone. The spectrum for the reaction mixture showed signals for the unreacted tertiary amine intermediate, unreacted EBB and a new set of signals. The unique, new signals were tentatively assigned to the quaternary ammonium intermediate and were monitored over the reaction time by ^{13}C -NMR. Spectra taken during the course of the reaction are shown in Figure 46.

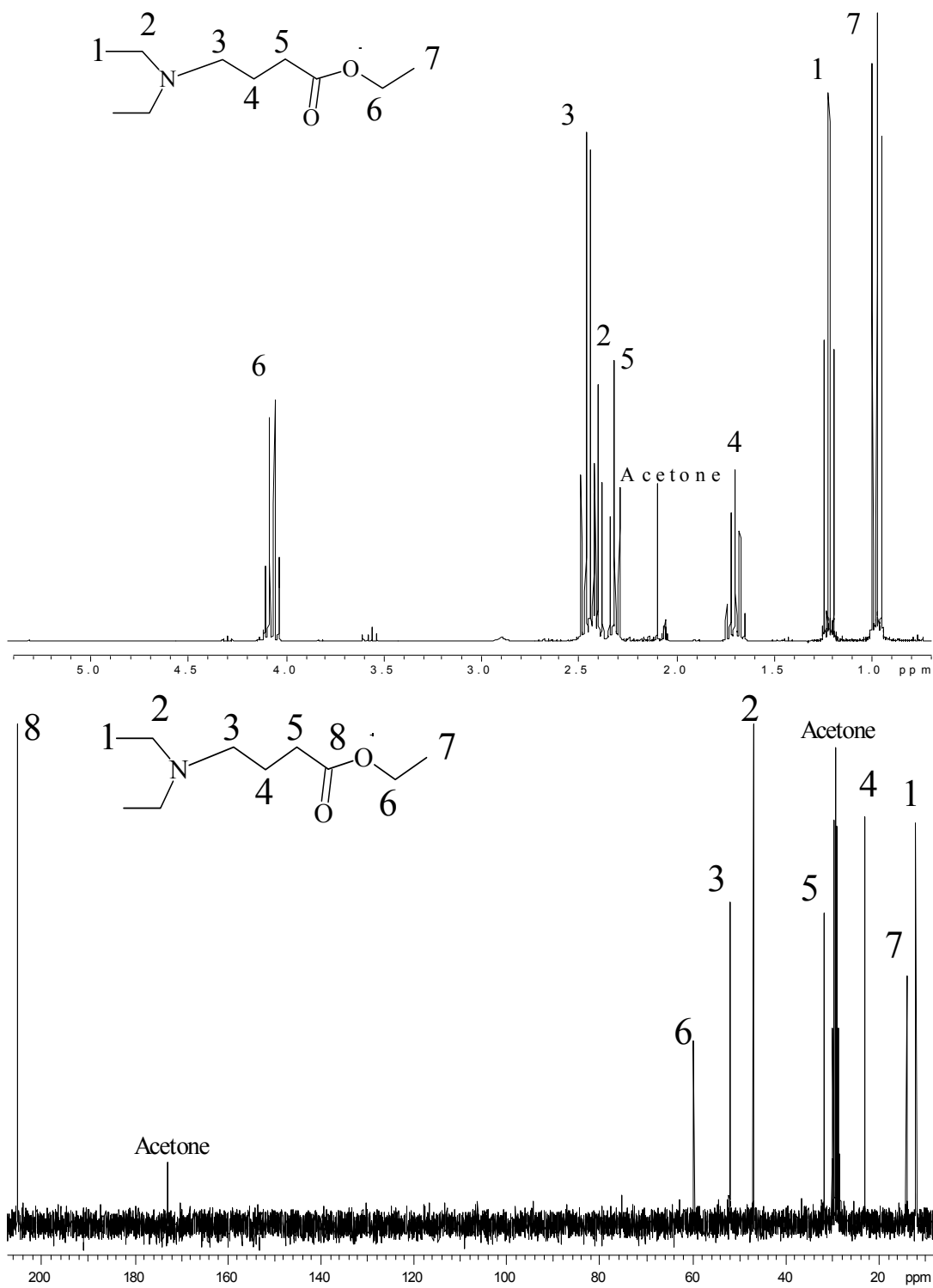


Figure 44. $^1\text{H-NMR}$ spectrum (top panel) and the $^{13}\text{C-NMR}$ spectrum (bottom panel) for the tertiary amine intermediate.

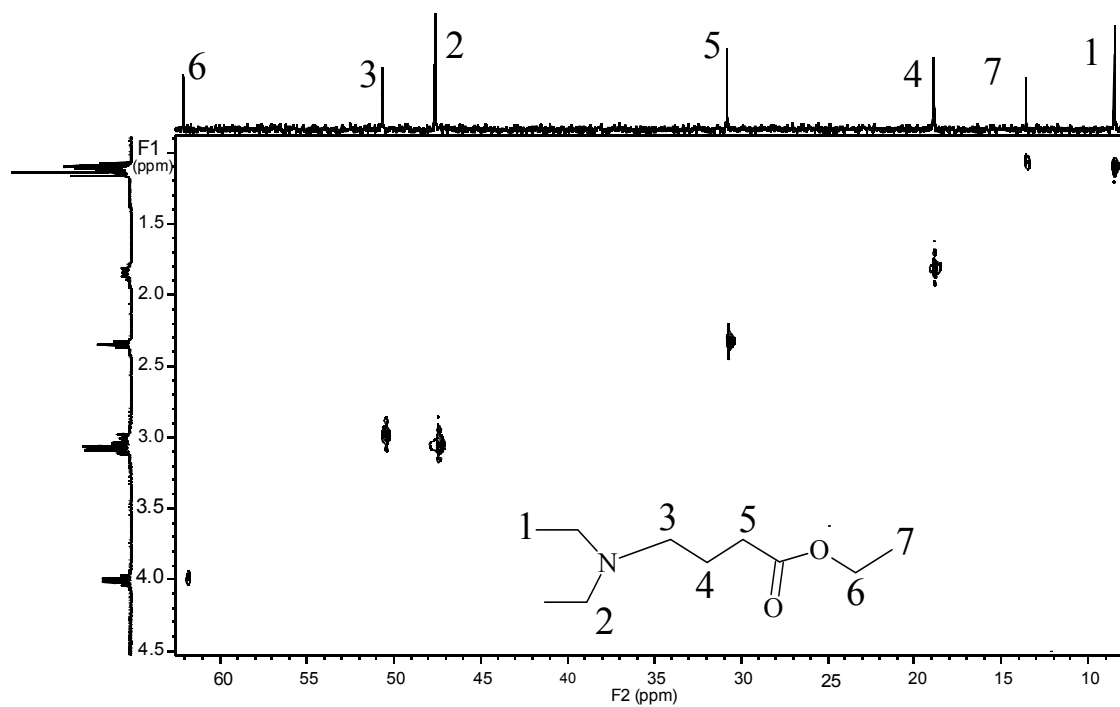


Figure 45. ^1H - ^{13}C HETCOR spectra for the tertiary amine intermediate and the corresponding assignments.

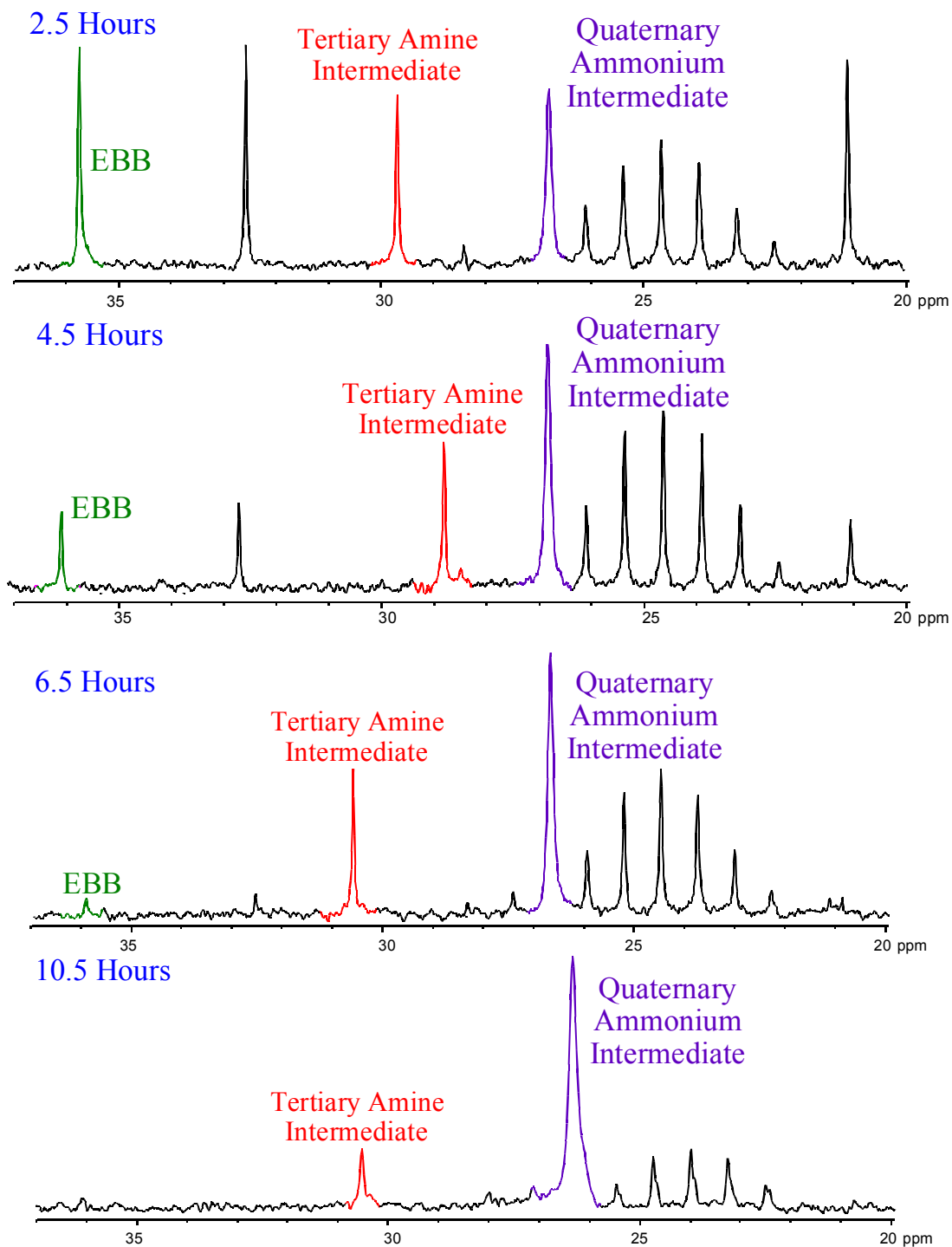


Figure 46. ^{13}C -NMR spectra for the time course of the reaction during the synthesis of the quaternary ammonium intermediate.

5.2.1.3.2 Processing of the intermediate

The reaction mixture was cooled to room temperature. 200 mL of deionized water were added and the mixture was stirred into a homogenous solution. An aliquot of the mixture was poured into a separatory funnel and dichloromethane was added into the funnel. The mixture was shaken vigorously, and the two phases were separated and analyzed by ^1H -NMR spectroscopy. The spectrum for the aqueous phase showed intense signals that were tentatively assigned to the quaternary ammonium intermediate. This indicated that the solubility of the quaternary ammonium intermediate in water was high, as expected. The spectrum of the organic phase showed very small signals for the quaternary ammonium intermediate, but intense signals for other species (unreacted EBB, unreacted tertiary ammonium intermediate, side products, etc.). This also indicated that solubilities of the contaminants in dichloromethane were high. Thus, there is indication of selective removal of the contaminants from the aqueous phase by solvent extraction with dichloromethane.

Similarly, an aliquot of the aqueous solution of the reaction mixture was shaken with methyl tert-butyl ether, the two phases were separated and analyzed by ^1H -NMR spectroscopy. From the spectra, it was seen that the aqueous phase retained the quaternary ammonium intermediate and the organic phase did not dissolve a significant amount of the quaternary ammonium intermediate. These indicated that there was a much more selective removal of contaminants from the aqueous phase by solvent extraction with methyl tert-butyl ether than with dichloromethane. However, a higher amount of the contaminants were retained in the aqueous phase when methyl tert-butyl

ether was used, indicating that the solubilities of the contaminants that in methyl tert-butyl ether were low.

Therefore, if dichloromethane was used for the processing of the reaction mixture, the contaminants would be removed in fewer extraction cycles and with less solvent. The disadvantage of the use of dichloromethane is the loss of some of the quaternary ammonium intermediate that gets extracted into the organic phase. With methyl tert-butyl ether, more solvent and more extraction cycles would be required to achieve the same level of purity, but the overall loss of the quaternary ammonium intermediate would be minimal. Thus, methyl tert-butyl ether was used to process the entire batch of the reaction mixture. The processed quaternary ammonium intermediate was analyzed by ^1H - and ^{13}C -NMR spectroscopy (spectra shown in Figure 47) and the signals assigned tentatively were later confirmed by ^1H - ^{13}C HETCOR NMR (spectra in Figure 48).

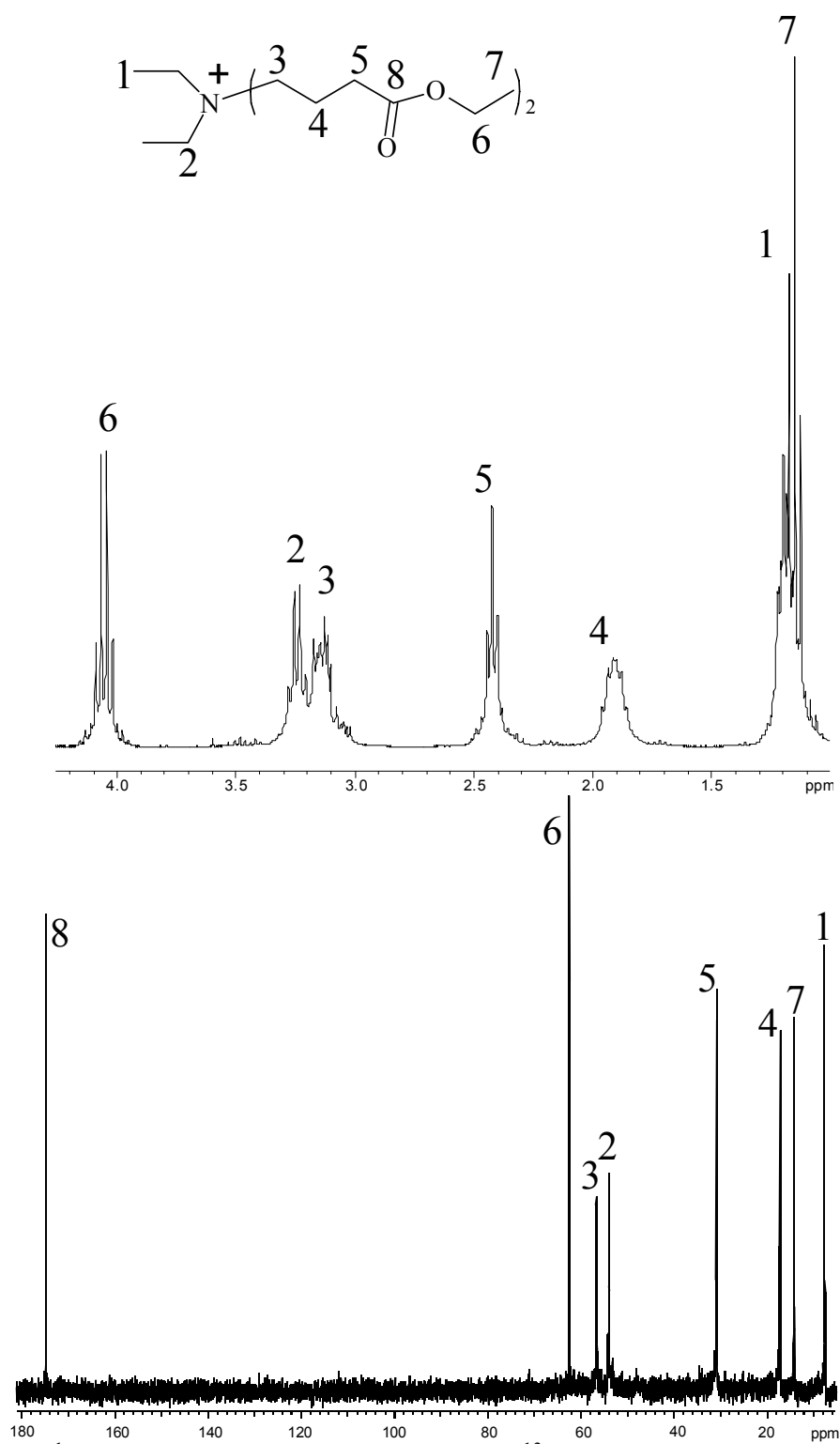


Figure 47. ^1H -NMR spectrum (top panel) and the ^{13}C -NMR spectrum (bottom panel) for the quaternary ammonium intermediate.

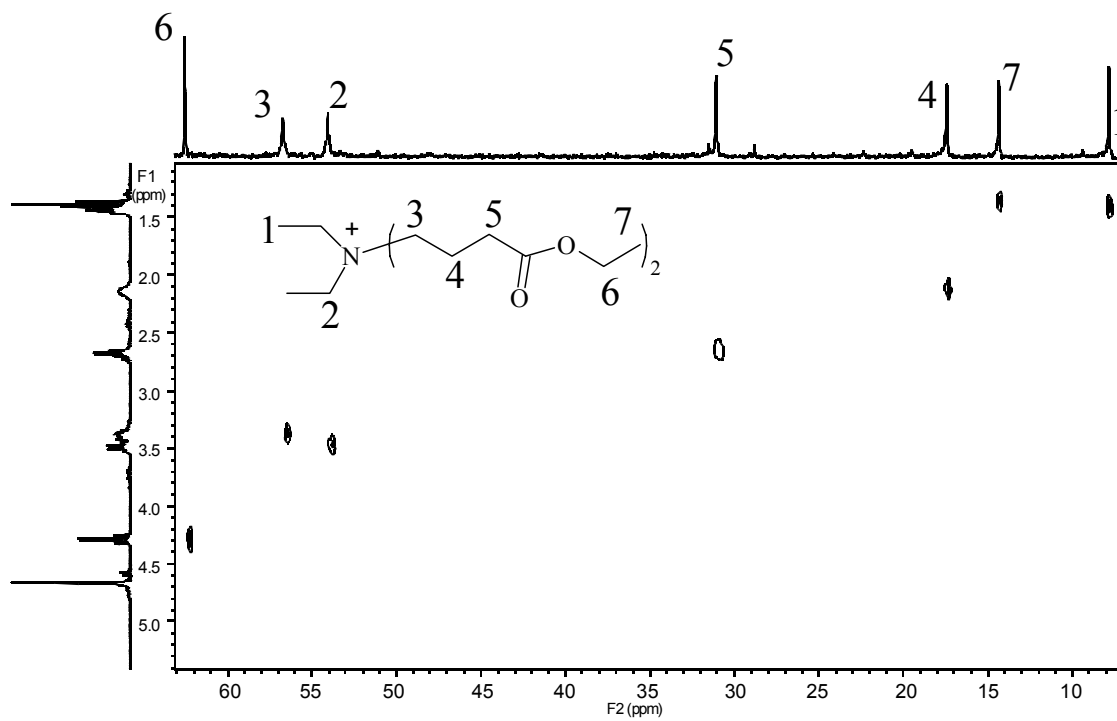


Figure 48. ^1H - ^{13}C HETCOR spectrum for the quaternary ammonium intermediate and the corresponding assignments.

5.2.1.4 Step 3 (hydrolysis of the ester groups)

5.2.1.4.1 Basic hydrolysis

11.2 g (0.28 mol) NaOH was dissolved in 100 mL deionized water and was mixed into the processed aqueous solution of the quaternary ammonium intermediate. The reaction mixture was left stirring at room temperature for 14 hours. Since the reaction is a classical, well established, well characterized ester saponification reaction, only the sample taken after 14 hours of reaction time was analyzed (no sampling or analysis done over the time course of the reaction). Figures 49 and 50 show the ^1H - and ^{13}C -NMR spectra, respectively, for the reaction mixture before and after hydrolysis. Complete hydrolysis was seen after 14 hours. Ethanol formed from the hydrolysis was removed under reduced pressure and the batch set-aside for further processing.

5.2.1.4.2 Acidic hydrolysis

Another batch of the reaction mixture, synthesized and processed in the same manner as previously, was set-up for hydrolysis with hydrobromic acid (HBr). Concentrated HBr was added into the reaction mixture to make a final solution of 300 mM HBr (pH~0.5). The flask was fitted with a Vigreux column and the solution was refluxed in an oil bath at 90°C. Hydrolysis was monitored by ^1H -NMR analysis of the aliquots of the reaction mixture; the spectra are shown in Figure 51. Complete hydrolysis was seen after 22 hours of heating followed by removal of the formed ethanol under reduced pressure. Since hydrolysis in acidic conditions was slower than in basic conditions, the latter was preferred.

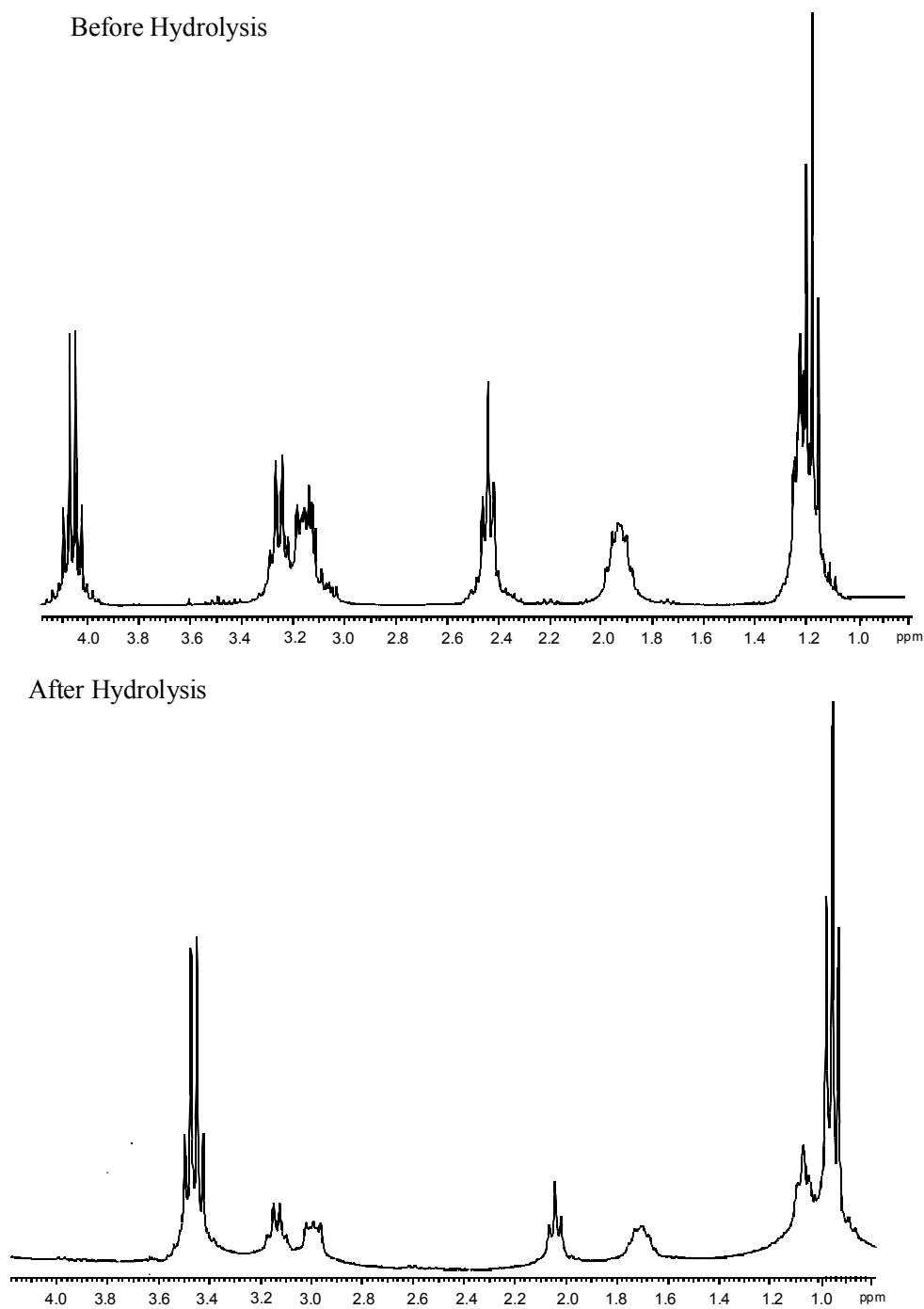


Figure 49. ^1H -NMR spectra for the reaction mixture before (top panel) and after (bottom panel) hydrolysis with NaOH.

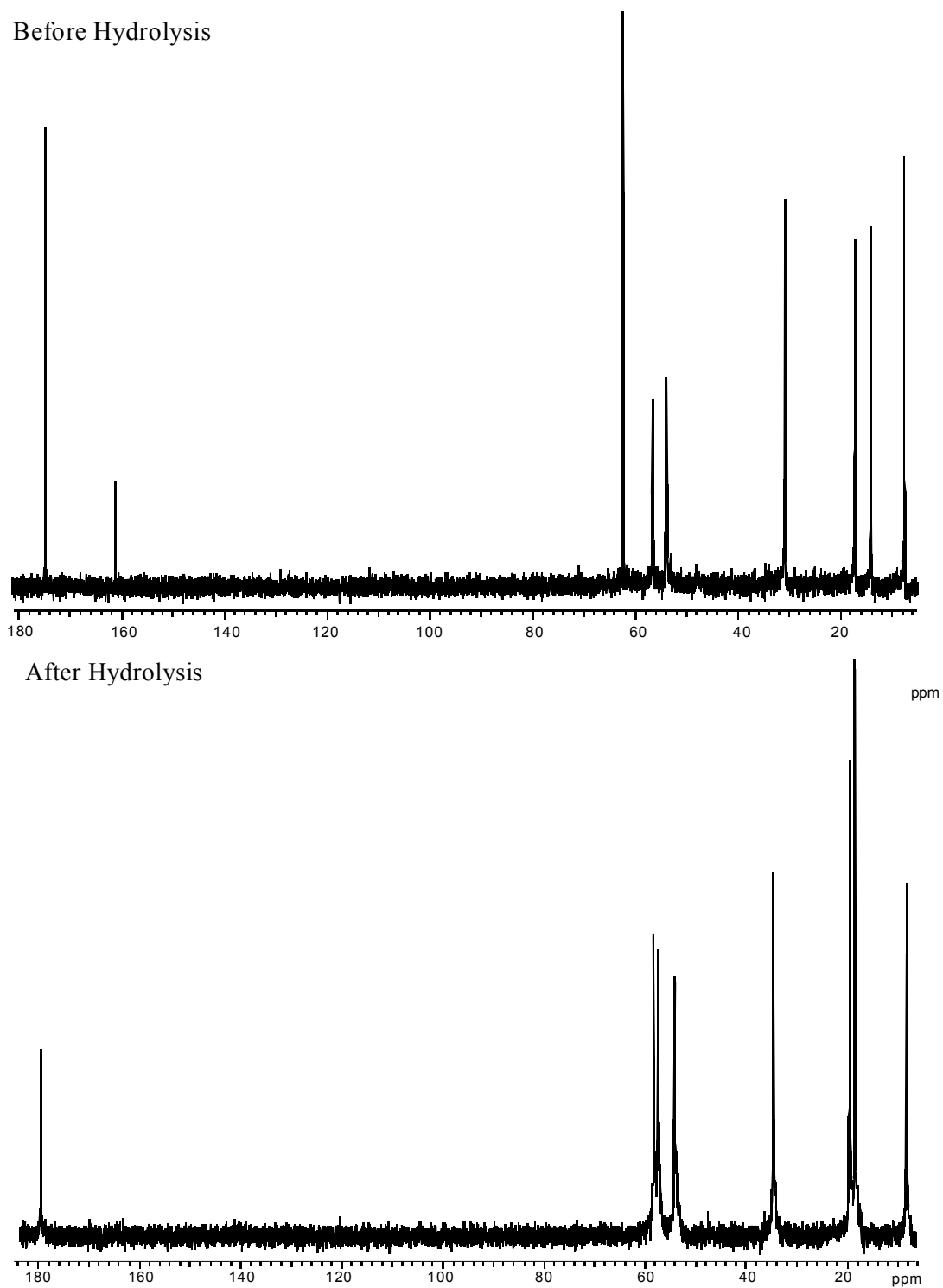


Figure 50. ^{13}C -NMR spectra for the reaction mixture before (top panel) and after (bottom panel) hydrolysis with NaOH.

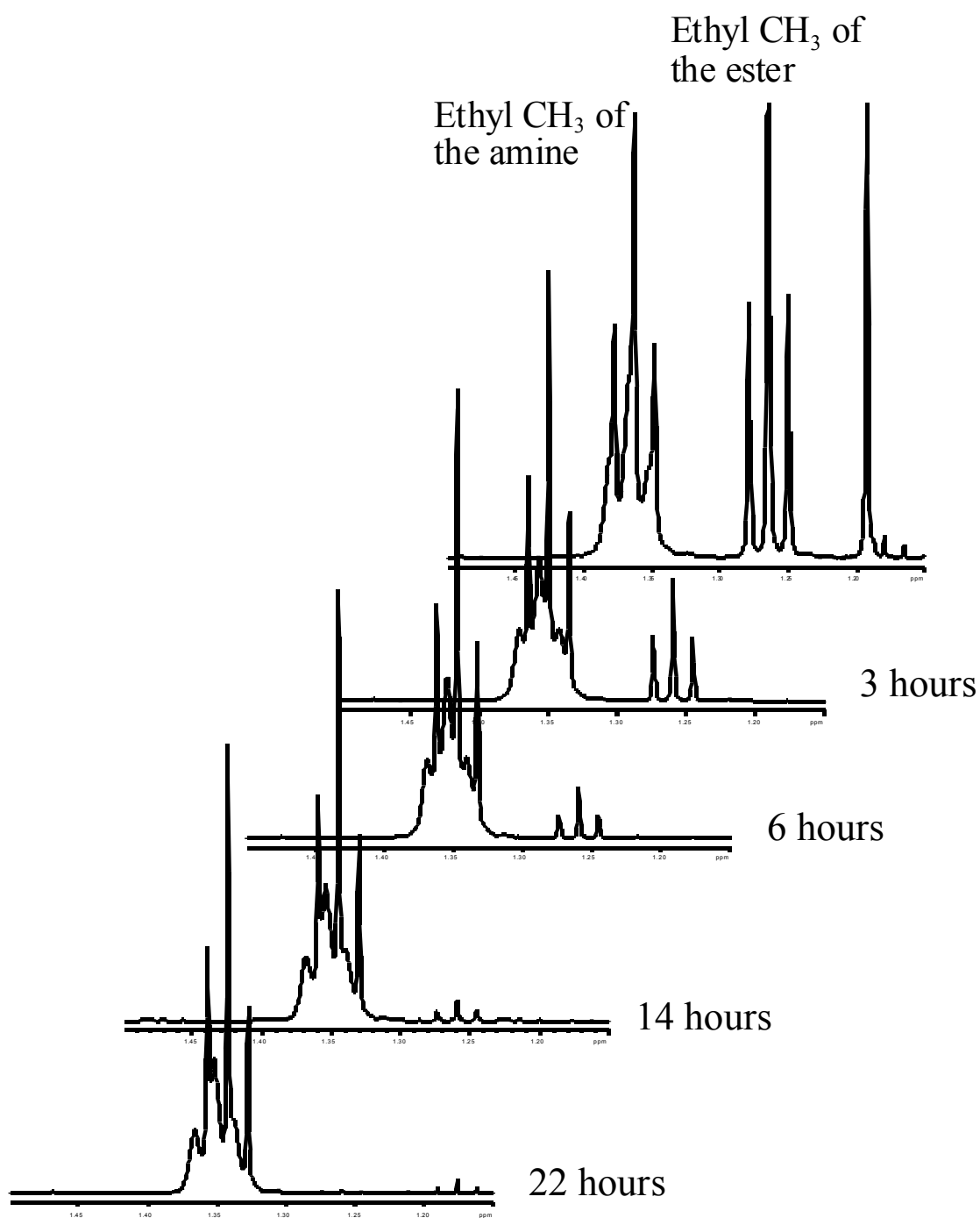


Figure 51. $^1\text{H-NMR}$ spectra for samples from the hydrolysis using HBr.

5.2.1.5 pI determination

The pI of BCPDEAH was determined using PreMCE [100] with the following conditions: 26 μm I.D. bare fused silica capillary, $L_t = 26.5$ cm, $L_d = 19.7$ cm, $t_{\text{inj}} = 1$ s, $t_{\text{transf}} = 30$ s, $t_{\text{migr}} = 1$ min, $U_{\text{appl}} = 10$ kV, positive to negative polarity, $T = 25$ °C, and UV detector at 200 nm. Using dimethylsulfoxide (DMSO) as the neutral marker, a three band PreMCE with the sequence A-N1-N2, was carried out in acetic acid BGEs whose pH was adjusted in 0.1-0.2 pH unit increments between pH=3.4 and pH=4.5 using NaOH. Figure 52 shows the CE traces for BCPDEAH in pH=3.4 and pH=3.9 BGEs and DMSO in pH=3.9 BGE (to mark the position of the neutral component). Clearly, the pI of BCPDEAH is between 3.4 and 3.9.

5.2.1.6 IET Purification

The BCDPEAH reaction mixture was desalted and the product obtained in its isoelectric form by IET using the BF200IET. The BF200IET was operated in a two chamber mode. IDAPVA was used as the anodic membrane (separating the anode compartment from the anodic separation compartment) and CDQPVA was used as the cathodic membrane (separating the cathode compartment from the cathodic separation

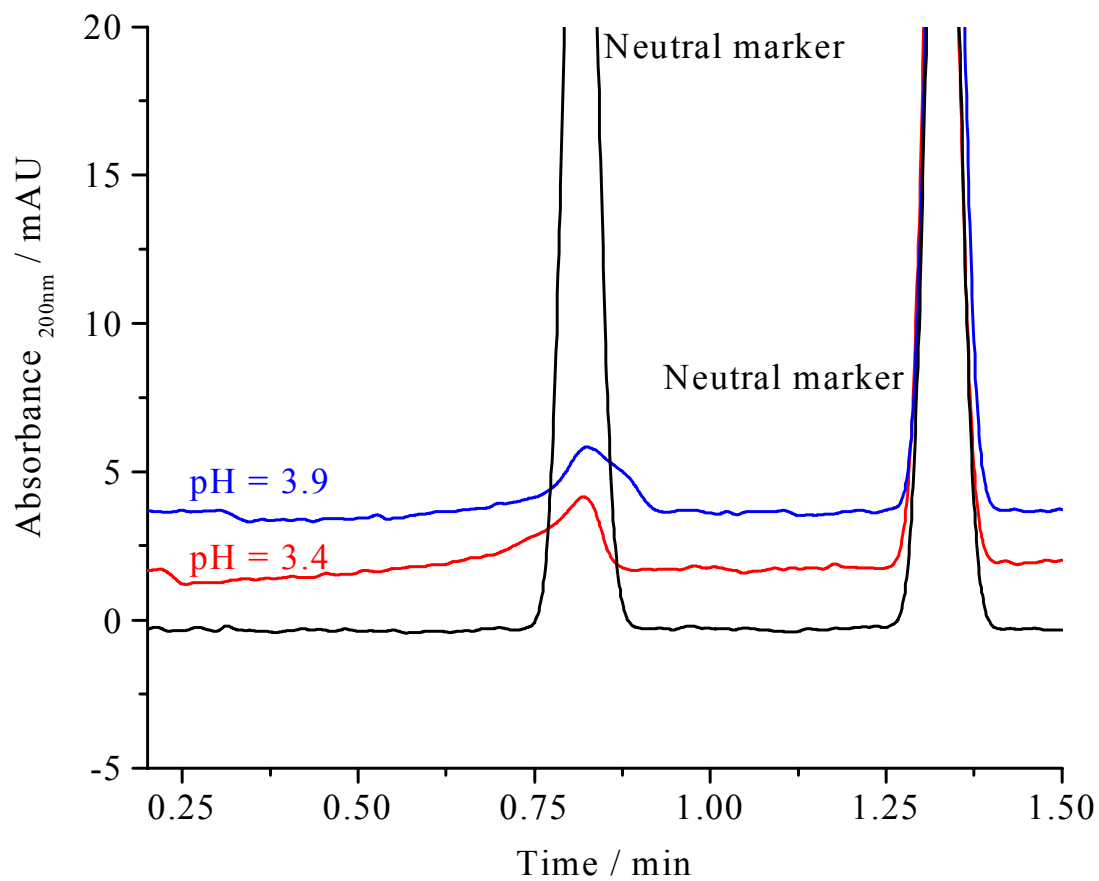


Figure 52. Electropherograms for the determination of the pI of BCPDEAH.

compartment). A $pI=3.7$ polyacrylamide-based isoelectric membrane was used as the separation membrane. The anolyte (a 100 mM sulfuric acid (H_2SO_4) solution) and the catholyte (a 200 mM NaOH solution) were recirculated in their respective compartments at a flow rate of 2L/min. The feed solution (containing the BCDPEAH reaction mixture) was recirculated in the anodic separation compartment and deionized water was recirculated in the cathodic separation compartment. Potential was applied across the chambers. For the first 3-5 minutes, an average current of 500 mA was generated. As the conductivity of the receiving stream increased (due to transfer of ions from the feed stream), the potential was increased and a constant current of 800 mA was maintained throughout the separation.

Aliquots from the feed and receiving streams were taken periodically and their pH and conductivity were measured. Figure 53 shows the pH curves for the feed and the receiving streams in one of the IET separations of BCDPEAH. Figure 54 shows the conductance measurements for similar IET separations of BCPDEAH. The samples were analyzed by CE using indirect UV detection. When the majority of BCDPEAH had transferred to the receiving stream, the separation was stopped and both solutions were collected. More of the solid, BCDPEAH reaction mixture was dissolved into the feed solution and processed in the same manner as previously. The collection streams were combined, water was removed under reduced pressure and the obtained BCDPEAH solids were characterized.

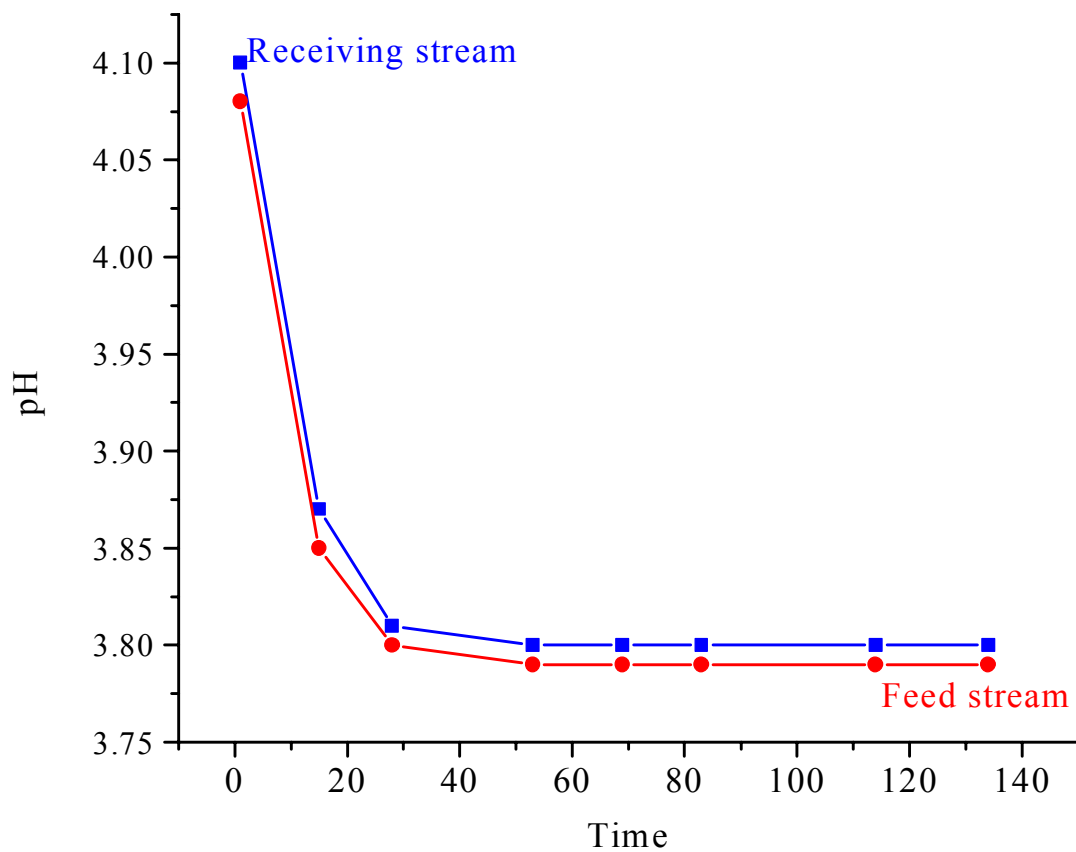


Figure 53. pH measurements of the feed stream (red dots) and receiving stream (blue squares) samples during IET of BCPDEAH.

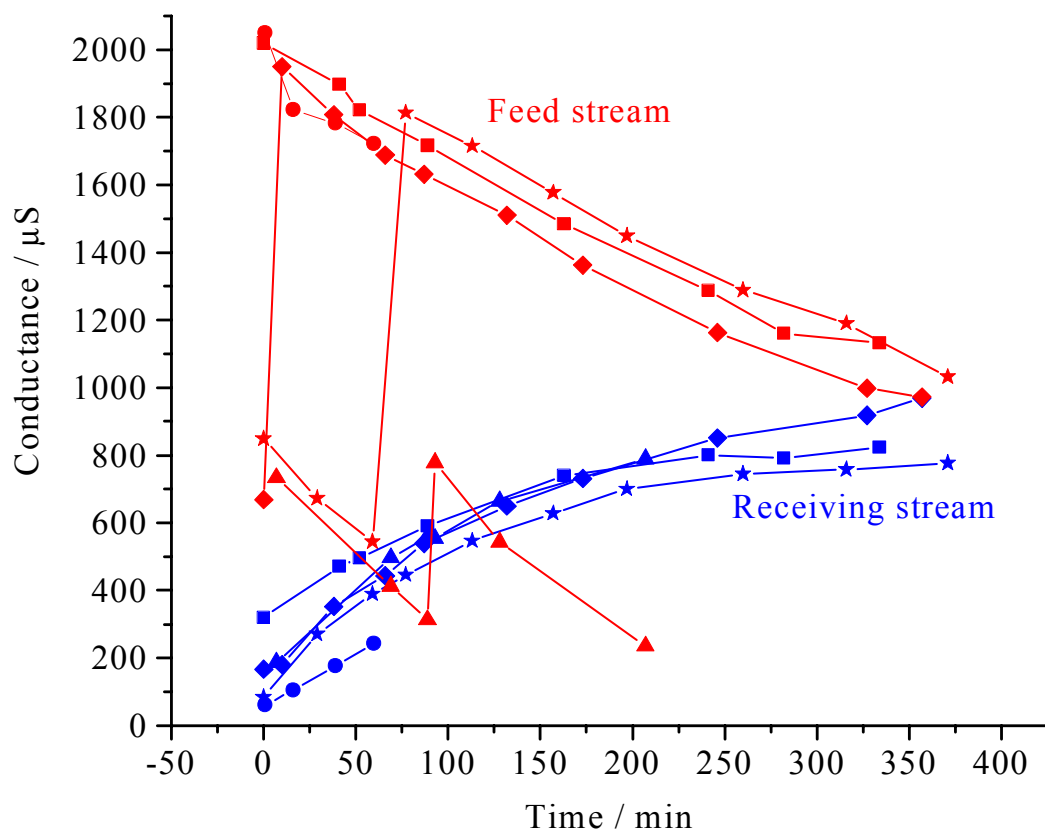


Figure 54. Conductance measurements for the feed stream (red curves) and the receiving stream (blue curves) samples during the IET separation of BCDPEAH.

5.2.1.7 Characterization

The final product was characterized by ^1H - and ^{13}C -NMR. Figure 55 shows the ^1H - and ^{13}C -NMR spectra and the tentative assignment of the signals. The product was analyzed by ^1H - ^1H COSY (spectra shown in Figure 56) to confirm the proton signal assignments. The ^{13}C assignments were confirmed using ^1H - ^{13}C HETCOR NMR spectroscopy (spectra shown in Figure 57).

The identity and purity of the final product were confirmed by high resolution ESI-MS. The ESI-MS spectra in positive and negative ion modes are shown in Figure 58. Only signals corresponding to BCPDEAH and its fragment ions are seen.

5.2.1.8 Recapitulation

A novel scheme has been designed for the *de novo* synthesis of carboxylic acid-based isoelectric buffers. According to the scheme, the isoelectric buffers have a permanently cationic quaternary ammonium functionality and two carboxylic acid functionalities. The pI value of the buffer will be between the pK_a values of the two

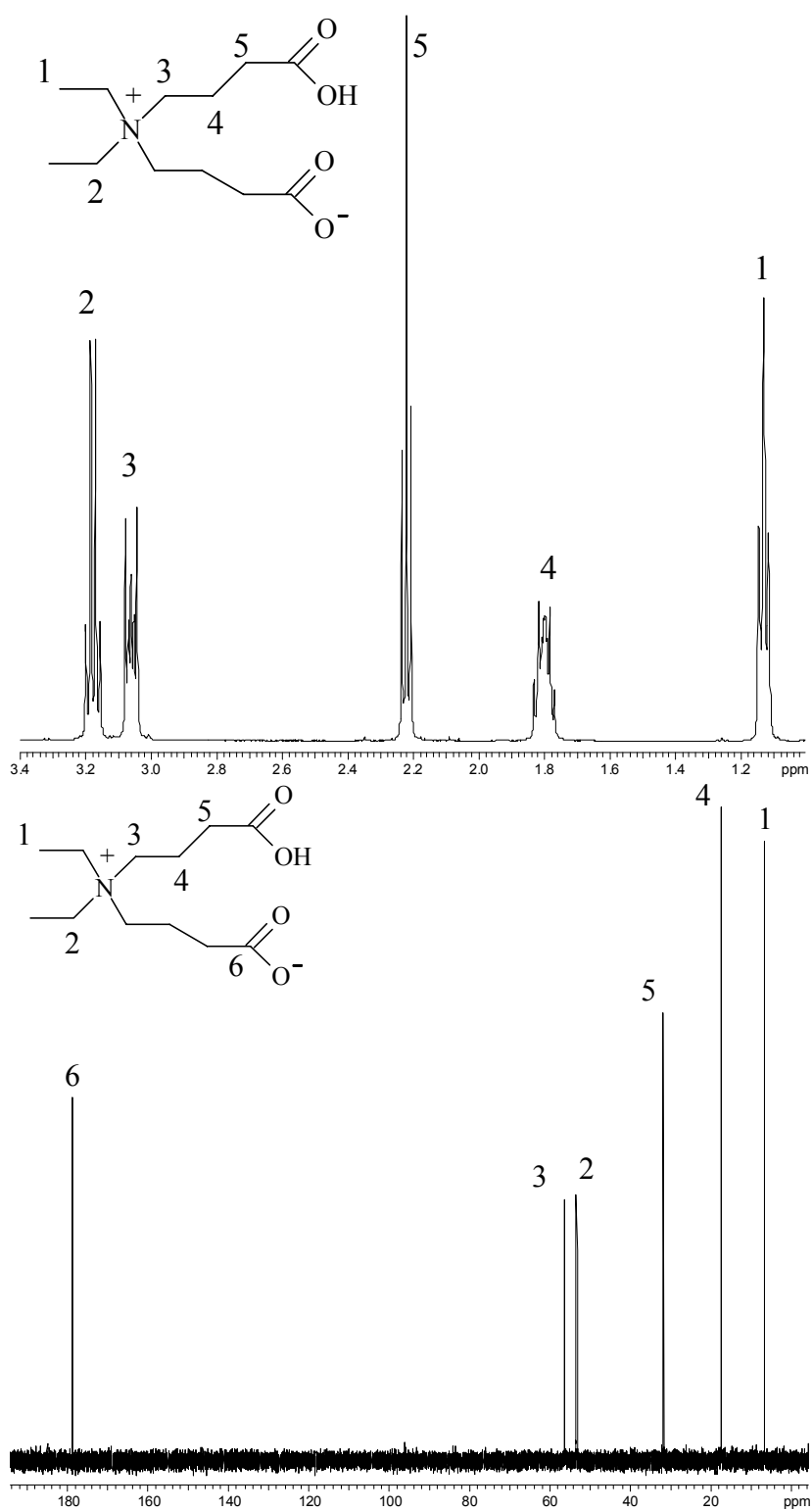


Figure 55. $^1\text{H-NMR}$ (top panel) and $^{13}\text{C-NMR}$ (bottom panel) spectra of BCPDEAH.

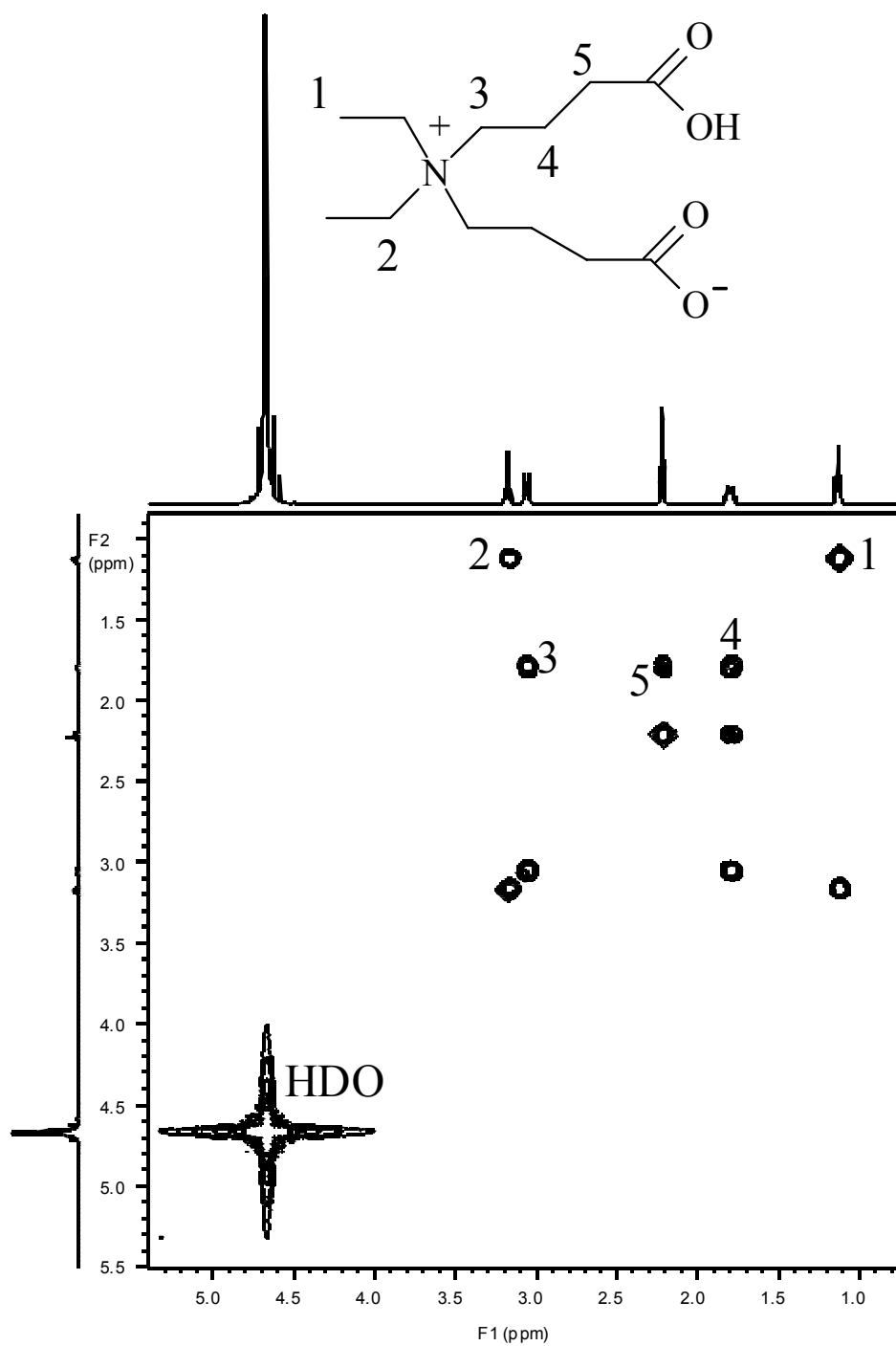


Figure 56. ^1H - ^1H COSY spectrum for BCPDEAH and the corresponding signal assignments.

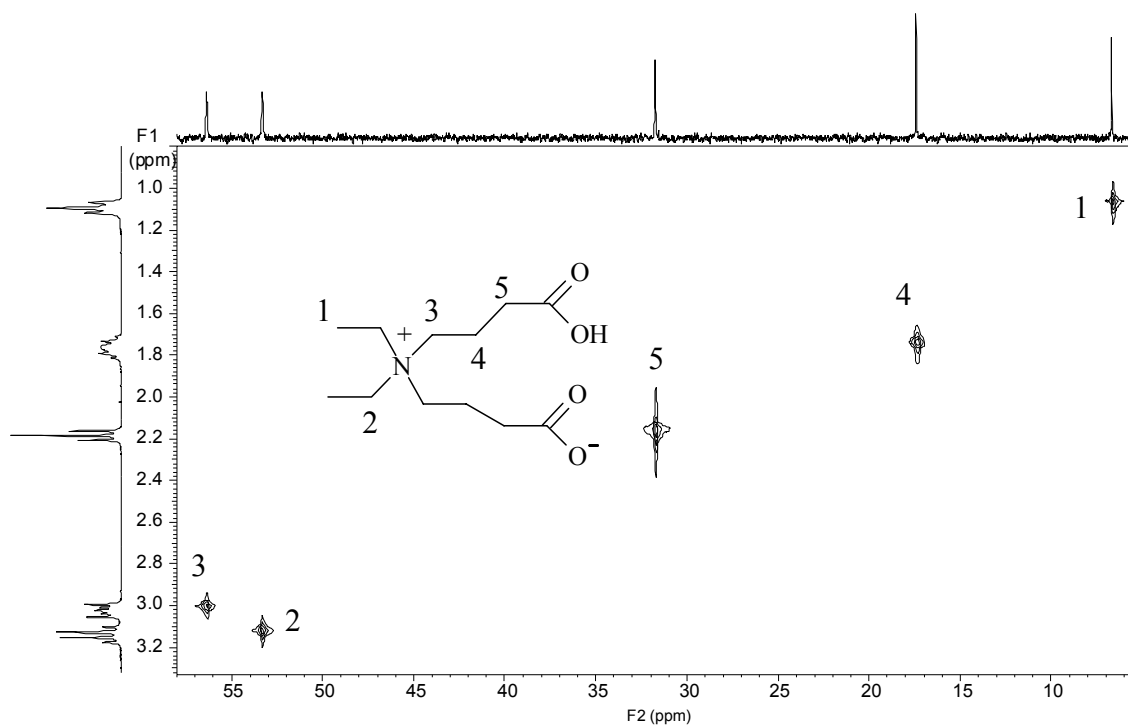


Figure 57. ^1H - ^{13}C HETCOR spectrum for BCPDEAH and the corresponding signal assignments.

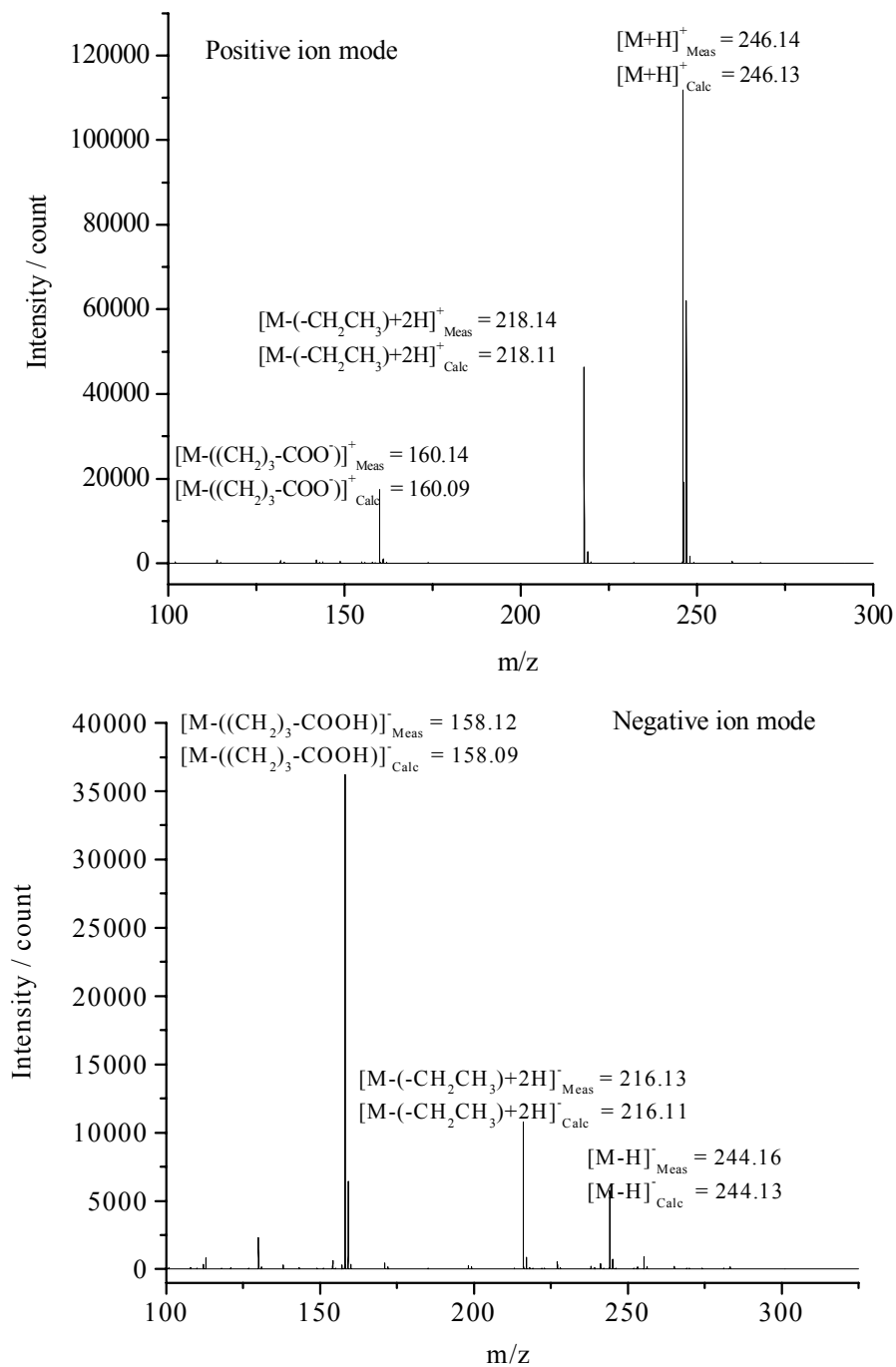


Figure 58. ESI-MS analysis of BCPDEAH in the positive (top panel) and the negative (bottom panel) ion modes.

carboxylic acid groups (the pK_a values vary with the length of the alkyl chain of the acid group). Buffers with both symmetric and asymmetric structures (in terms of the two carboxylic acid groups) can be made using this scheme.

BCPDEAH, a unique, acidic isoelectric buffer has been synthesized from DEA and EBB. Based on the design of the molecule, the two carboxylic acid groups in BCPDEAH have close pK_a values. Consequently, solutions of BCPDEAH in its isoelectric state have a high buffering capacity and high conductivity. The pI of BCPDEAH is between 3.4 and 3.9, making BCPDEAH the least acidic dicarboxylic acid-based isoelectric buffer so far reported (for buffers whose pI is between the pK_a values of the two carboxylic acid groups, glutamic acid was the least acidic known isoelectric buffer with a pI of 3.2). An additional characteristic of this buffer is its resistance to N-oxidation (not found in isoelectric buffers reported in the literature). BCPDEAH has been obtained in its pure, isoelectric form and has been well characterized by 1D- and 2D-NMR, ESI-MS and CE.

6. MOSES: SYNTHESIS OF HIGH-pI ISOELECTRIC BUFFERS

6.1 Opportunistic

6.1.1 1,3-Bis(N,N-dimethylamino)-2-O-sulfo-propane (BDASP)

1,3-Bis(N,N-dimethylamino)-2-O-sulfo-propane (BDASP) was synthesized by sulfation of the alcohol group of 1,3-bis(N,N-dimethylamino)-2-propanol (BDAP) (synthesis scheme shown in Figure 59) using sulfur trioxide pyridine complex ($\text{SO}_3 \cdot \text{Pyr}$). A clean, 250 mL, three-neck round bottom flask was fitted with an ice-water cooled condenser. 40 mL N,N-dimethylformamide (DMF) was added to the flask. 30.0 g (0.205 mol) BDAP was added and the flask was warmed in an oil bath to 65°C. 35.93 g (0.227 mol) $\text{SO}_3 \cdot \text{Pyr}$ was added to the warm solution and the mixture was stirred and heated continuously at 65°C for 3 hours. Heavy solid formation was observed after 1 hour of heating. Samples from the reaction mixture (taken every 30 min) were analyzed by CE using indirect UV detection and the decrease in the peak area for the unreacted BDAP was monitored. When the peak area did not change significantly between successive samples, more $\text{SO}_3 \cdot \text{Pyr}$ was added to the reaction mixture to compensate for loss of $\text{SO}_3 \cdot \text{Pyr}$ (forming sulfuric acid by hydrolysis), to increase the conversion of BDAP to BDASP.

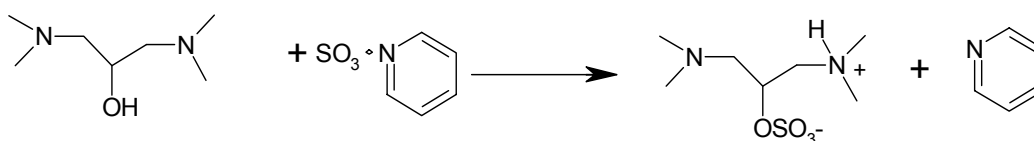


Figure 59. BDAP sulfation scheme.

After 3 hours of heating, the mixture was allowed to cool and 200 mL DMF was added to make a slurry. The slurry was filtered, the solids were dispersed in 500 mL acetone, and the acetone slurry was filtered. The solids were then dispersed in 500 mL ethyl alcohol followed by filtration of the slurry to obtain an off-white colored cake.

6.1.1.1 pI determination

The pI of BDASP was determined by indirect UV detection CE. Using a 26 μm I.D. bare fused silica capillary, $L_t = 26.1$ cm, $L_d = 19.7$ cm at 15kV in positive to negative polarity, $T = 25$ °C, and UV detector at 214 nm, conventional CE was carried out in a 20 mM tris(hydroxymethyl) aminomethane (Tris) BGE titrated to pH=7.8 with p-toluene sulfonic acid (pTSA) and a 20 mM benzylamine BGE titrated to pH=9.6 with pTSA. Figure 60 shows the electropherograms for BDASP in the two BGEs. Clearly, the pI of BDASP is between 7.8 and 9.6. The effective mobilities (μ^{eff} s) were calculated for BDASP in both CE runs, and were corrected for ionic strength suppression using Peakmaster 5.0. The corrected μ^{eff} s were plotted versus the BGE pH, and the pH at which the $\mu^{\text{eff}} = 0$ (thus the pI) was determined to be 8.0.

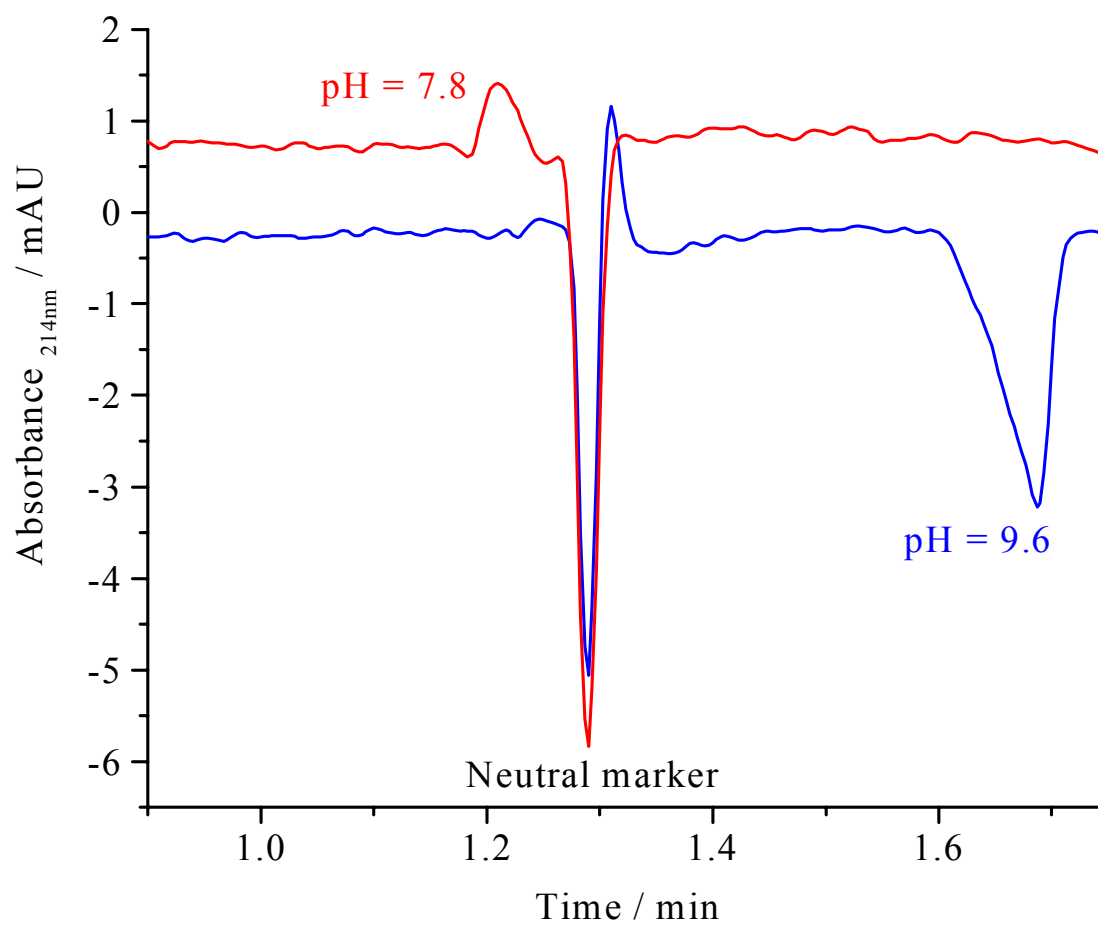


Figure 60. Electropherograms for BDASP in pH=7.8 and pH=9.6 BGEs.

6.1.1.2 Isoelectric crystallization

The solids were then dissolved into 200 mL deionized water and the solution was titrated with 5M lithium hydroxide (LiOH) to pH=8.0. Water was partially removed under reduced pressure and the warm solution was cooled to crystallize the product in the salt-free form.

Product purity (in terms of inorganic salt content) was determined by indirect-UV detection CE. Using a 20 mM acetic acid BGE titrated with imidazole to pH=4.56, run on a 26 μm I.D. bare fused silica capillary, $L_t = 26.5$ cm, $L_d = 19.7$ cm at 25kV, positive to negative polarity, $T=25$ °C, and the UV detector at 214 nm, lithium ions were analyzed. Figure 61 shows the electropherograms of the crystallized product (top panel) and the crystallization mother liquor (middle panel) and the electropherogram simulated by Peakmaster 5.0. Using a 20 mM Tris, 0.1 mM hexadecyltrimethyl ammonium hydroxide (CTAOH) BGE, titrated with benzenetricarboxylic acid (BTC) to pH=8.54, run on a 50 μm I.D. bare fused silica capillary, $L_t = 25.7$ cm, $L_d = 19.3$ cm at 25kV, negative to positive polarity, $T=25$ °C, and UV detector at 214 nm, sulfate ions were analyzed. Results for the crystallized product (top panel) and the crystallization mother liquor (middle panel) and the simulated electropherogram (bottom panel, using Peakmaster 5.0) are shown in Figure 62.

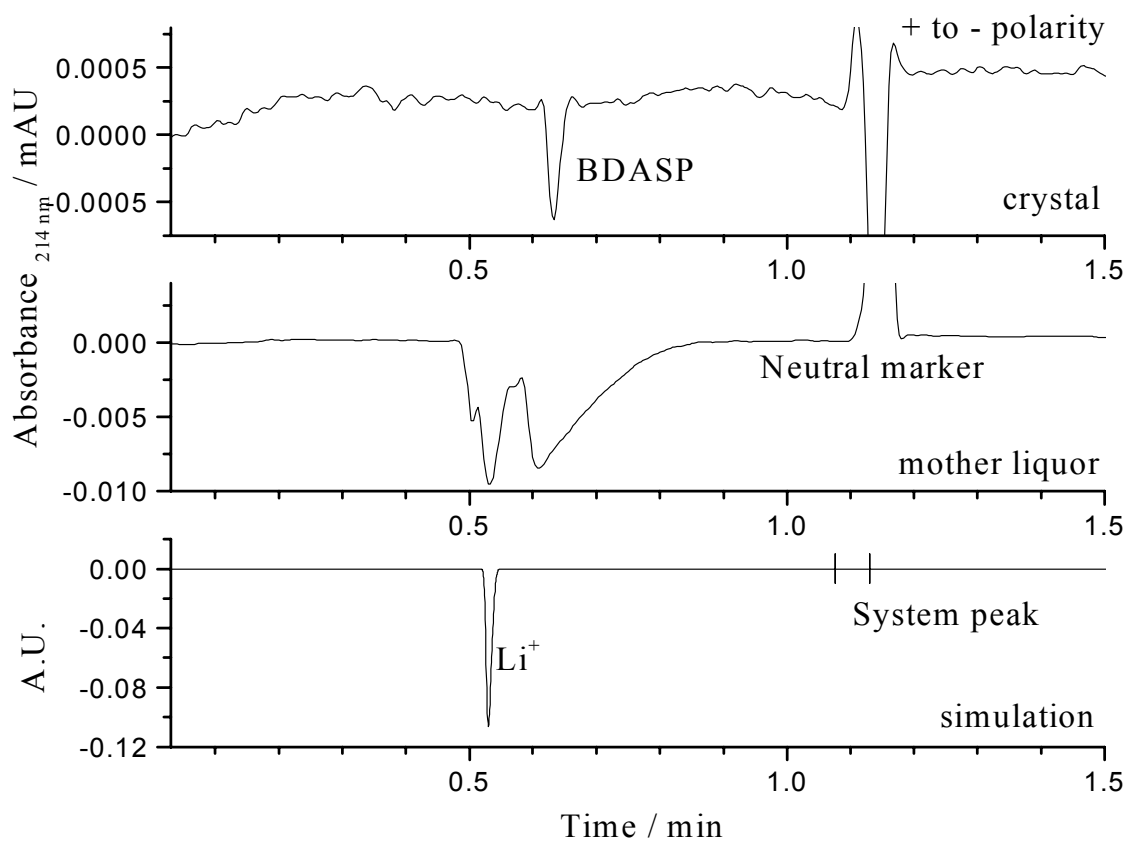


Figure 61. Electropherograms for cation analysis of the crystallized BDASP (top panel) and the crystallization mother liquor (middle panel) compared to the electropherogram simulated using Peakmaster 5.0 (bottom).

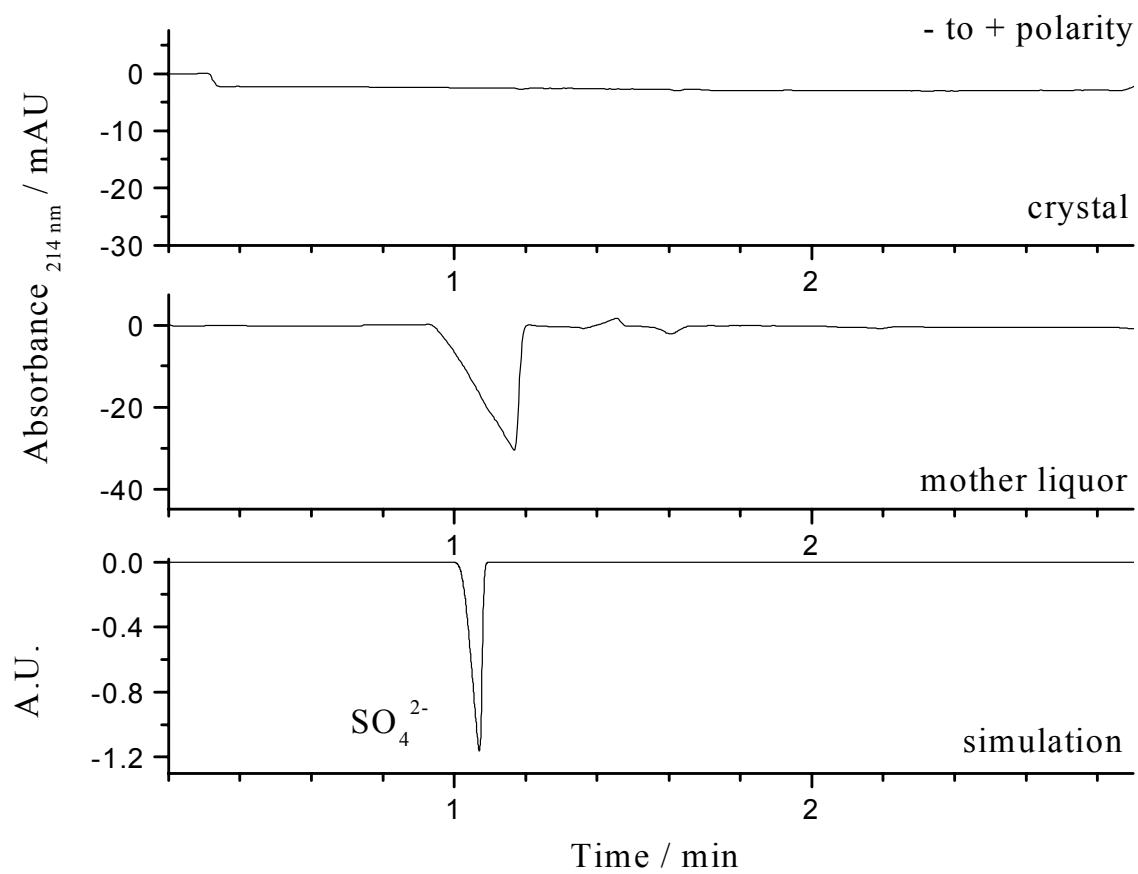


Figure 62. Electropherograms for anion analysis of the crystallized BDASP (top panel) and the crystallization mother liquor (middle panel) compared to the electropherogram simulated using Peakmaster 5.0 (bottom panel).

6.1.1.3 Characterization

The final product was characterized by ^1H - and ^{13}C -NMR. Figure 63 shows the ^1H - and ^{13}C -NMR spectra and the tentative assignment of the signals. Then, the product was analyzed by ^1H - ^1H COSY (spectra shown in Figure 64). This confirmed the proton signal assignments. The ^{13}C assignments were confirmed using ^1H - ^{13}C HETCOR NMR spectroscopy (spectra shown in Figure 65).

The identity and purity of the final product were confirmed by high resolution ESI-MS. The ESI-MS spectrum in the positive ion mode is shown in Figure 66. Only signals corresponding to BDASP and its Na^+ adduct are seen. Single crystals of the product were grown by slow and undisturbed cooling of a concentrated aqueous solution and its X-ray crystal structure was determined. An image of the X-ray crystal structure of BDASP is shown in Figure 67.

6.1.1.4 Final procedure

Step 1. Fit a clean, 250 mL, three-neck round bottom flask with an ice-water cooled condenser. Add 40 mL DMF to the flask, set the flask in an oil bath. Add 30.0 g (0.205 mol) BDAP into the flask and heat it to 65°C while stirring the solution with a half-inch football-shaped magnetic stir bar on a stir plate. To the warm, stirring solution add 35.93 g (0.227 mol) $\text{SO}_3\cdot\text{Pyr}$ and continuously heat and stir the mixture at 65°C for 4 hours. Take the flask off of the oil bath and set it to cool on a cork O-ring with paper towels underneath (to absorb the oil).

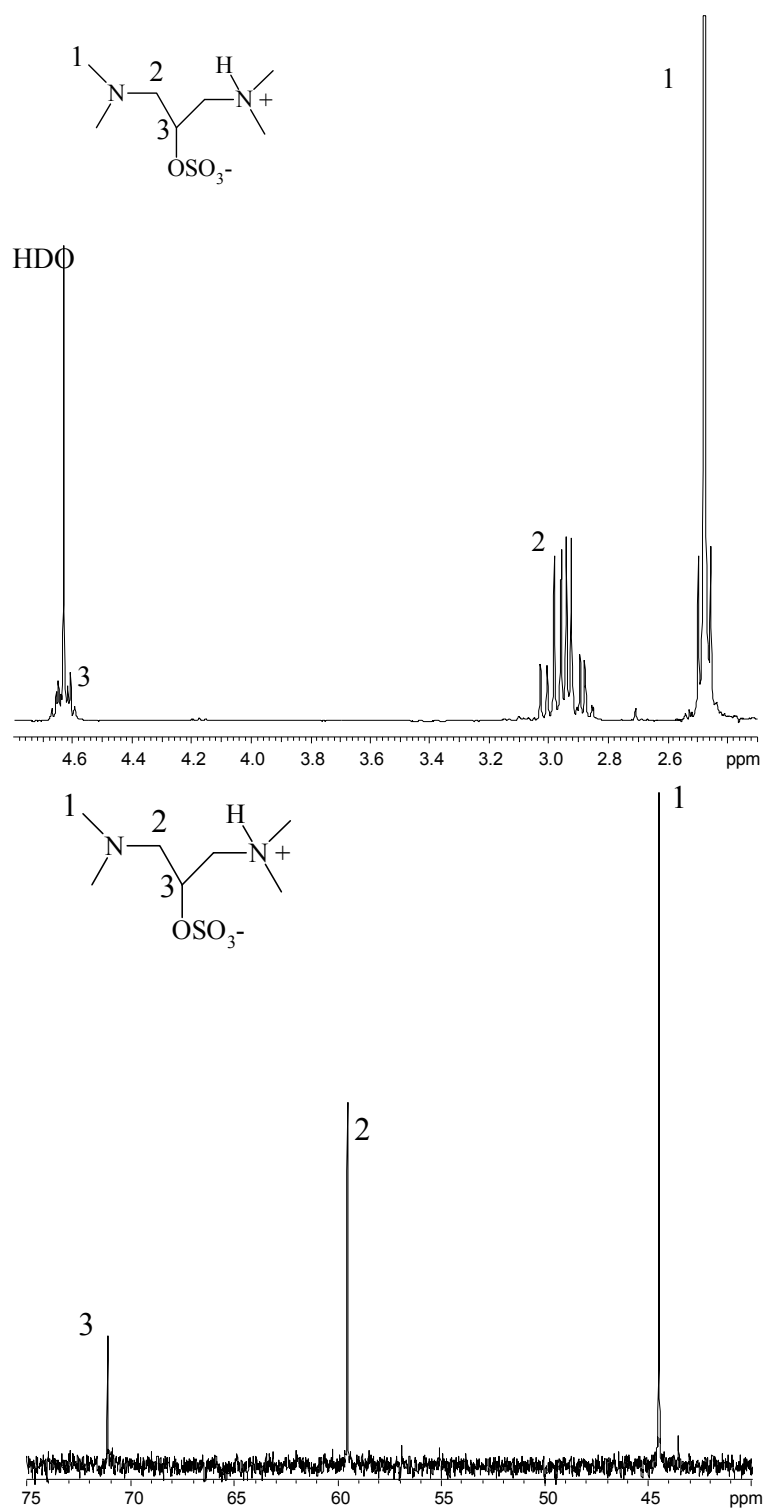


Figure 63. ¹H- (top panel) and ¹³C-NMR spectra (bottom panel) for BDASP with tentative assignment of the signals.

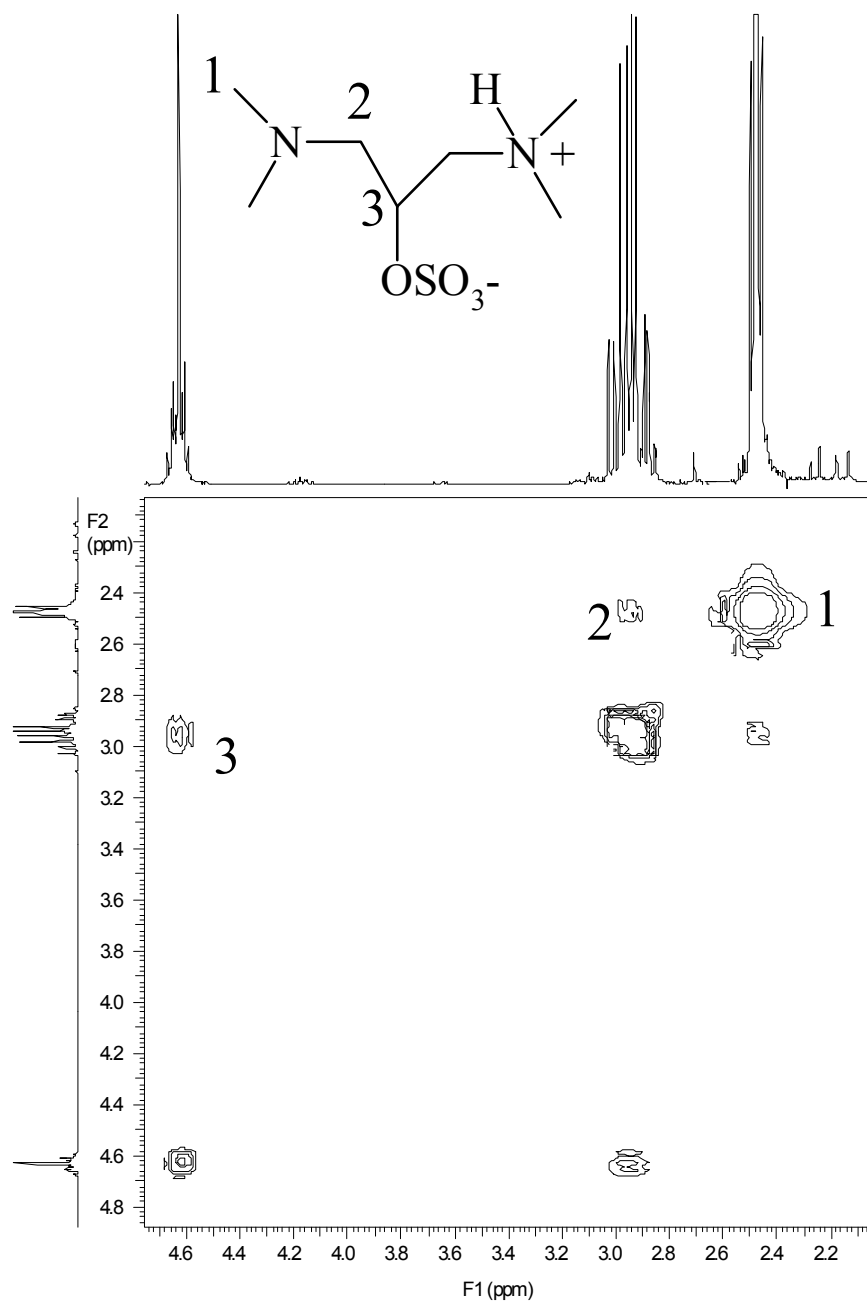


Figure 64. ^1H - ^1H COSY spectrum for BDASP with the corresponding assignments.

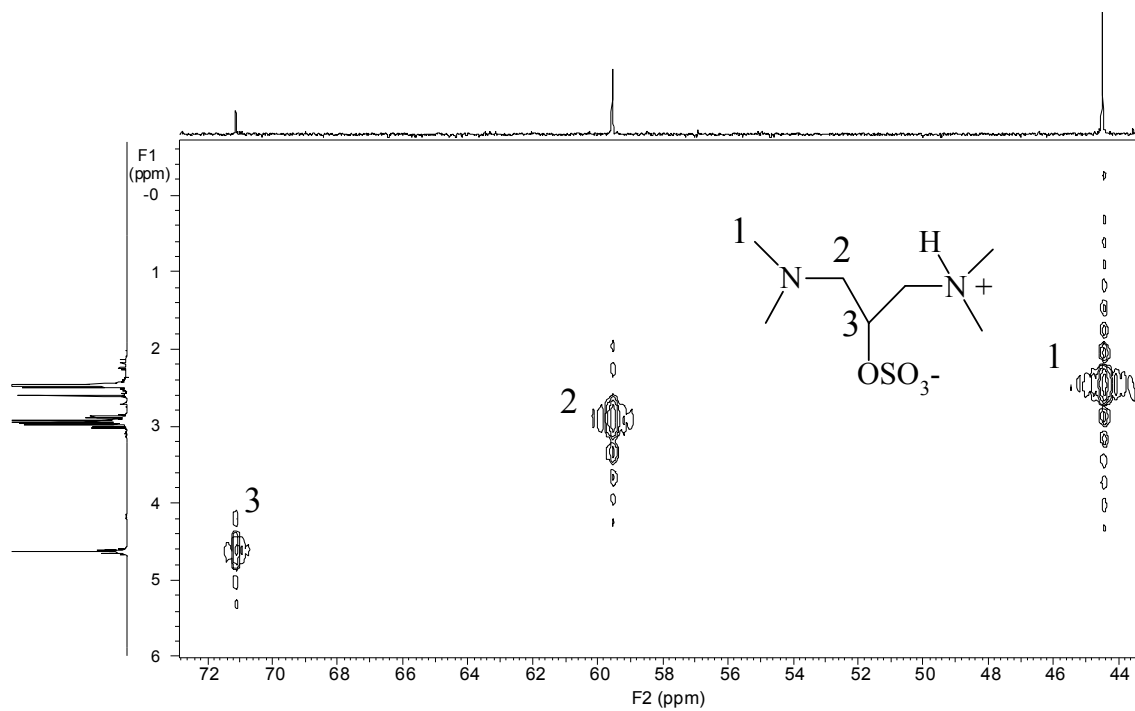


Figure 65. ^1H - ^{13}C HETCOR spectrum for BDASP and the corresponding signal assignments.

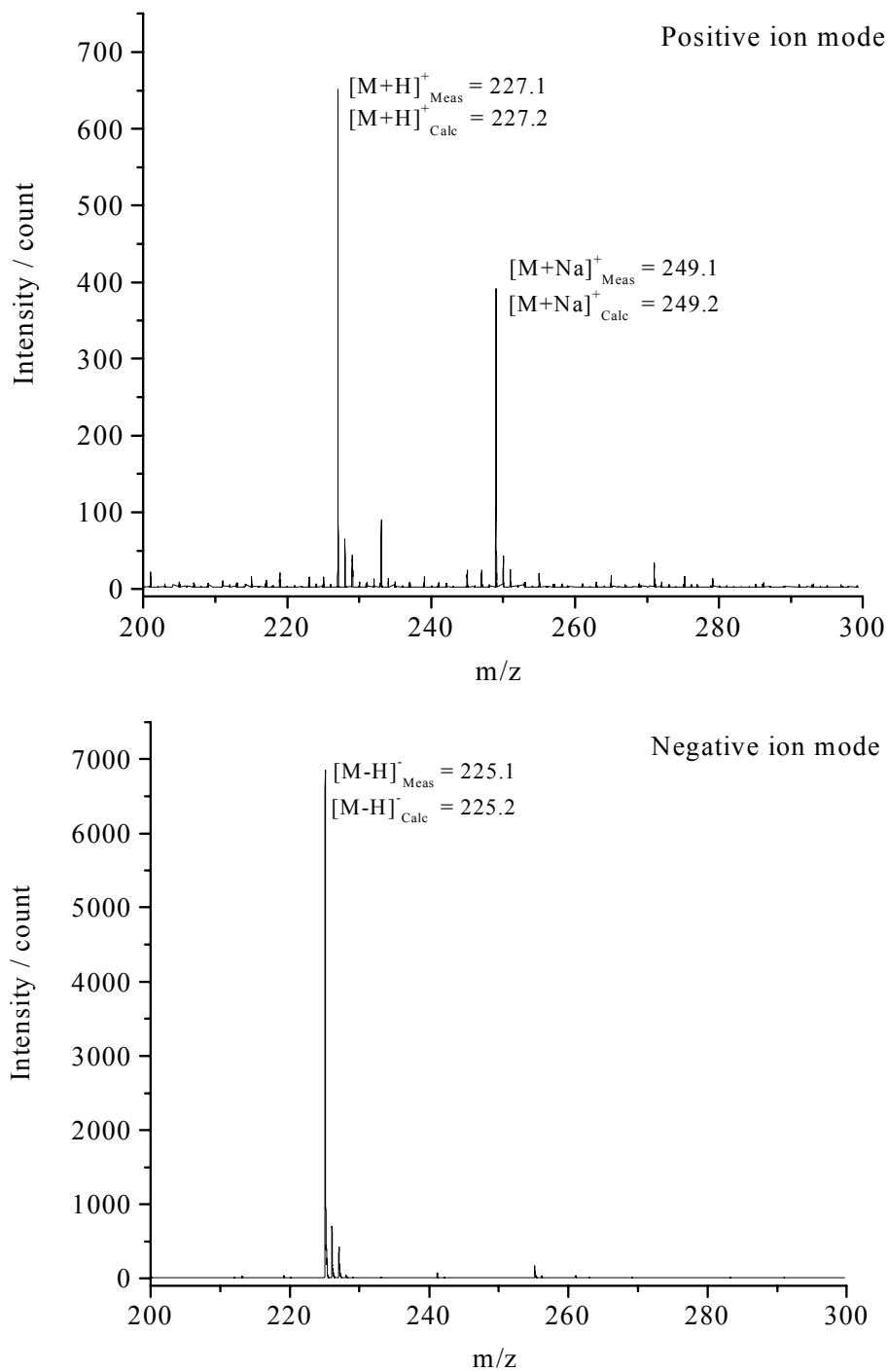


Figure 66. ESI-MS analysis of BDASP in the positive ion (top) and the negative ion (bottom) modes.

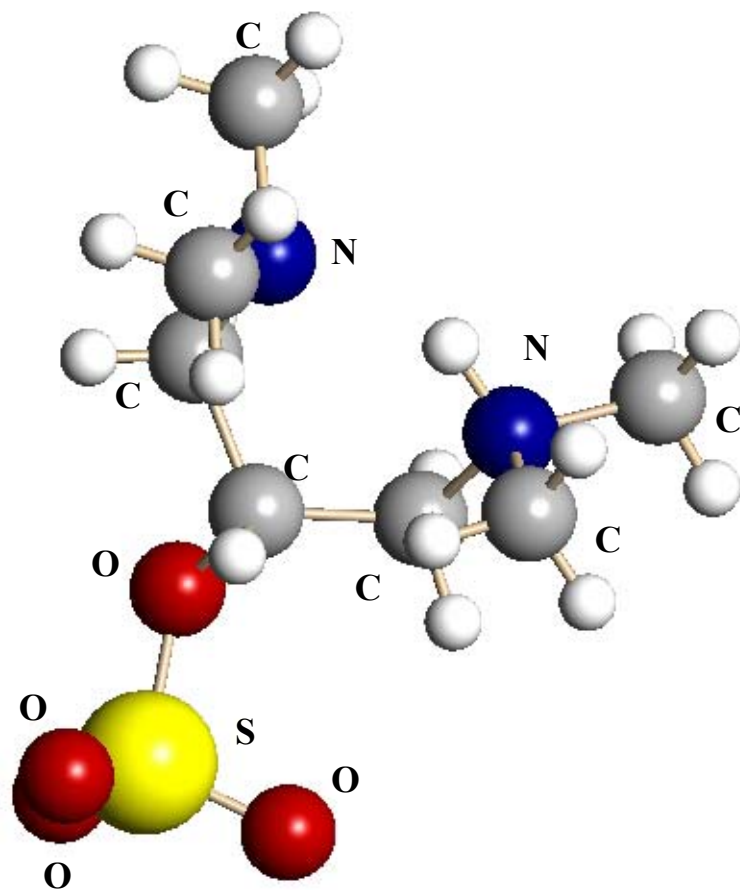


Figure 67. Ball-and-stick image of the X-ray crystal structure of BDASP.

Step 2. To the cooled reaction mixture, add 250 mL DMF and with the aid of a spatula, manually dislodge the solids and remove the chunks from the round bottom flask into a 500 mL beaker. Add 450 mL DMF into the beaker and make a slurry of the solids. Filter the slurry using a Buchner funnel and a suction flask. Remove the solid cake and filter paper from the funnel, and into another 500 mL beaker make a slurry with 450 mL acetone. Filter the slurry, make another slurry of the solids in 450 mL ethanol, and filter again. Let the solids dry inside the fume hood.

Step 3. Dissolve the solids in minimum volume (around 200 mL) of deionized water. Measure the pH of the solution and titrate it to pH=8.0 using a 5M LiOH solution (if the solution pH is below 8.0) or 2M sulfuric acid (H_2SO_4) (if the solution pH is above 8.0). Remove about 100 mL of water using a rotovap with the water bath set at 65°C. Let the solution cool in the fume hood with continuous stirring for 24 hours. Filter the slurry, wash the solid cake with cold ethanol a few times and let the cake dry in the fume hood. Analyze both the crystallization mother liquor and the solids by CE and repeat crystallization from deionized water if necessary.

6.1.1.5 Recapitulation

A unique, basic isoelectric buffer, BDASP, has been synthesized from BDAP and $SO_3 \cdot Pyr$. According to the design of the molecule, the two amino groups in BDASP have close pK_a values. Consequently, solutions of BDASP in its isoelectric state have a high buffering capacity and high conductivity. The pI of BDASP is between 7.8 and 9.6 (calculated to be 8.0). BDASP has been obtained in its pure, isoelectric form and has been well characterized by 1D and 2D-NMR, ESI-MS, CE and X-ray crystallography.

BDASP has been successfully synthesized several times, in a 1 g scale batch to a 40 g scale batch.

6.2 *De novo* synthesis

A family of amine-based isoelectric buffers can be synthesized according to the following generic, *de novo* synthesis scheme. First, 1 equivalent of a moderately hydrophobic secondary amine is reacted with 1 equivalent of epichlorohydrin. As the epoxide ring opens, a carbon-nitrogen bond forms, and the oxygen atom from the ring opening deprotonates the attached amine to form an alcohol. Next, the amino alcohol intermediate is reacted with 2 equivalents of a moderately hydrophobic secondary amine (either the same as the first one or a different one). As 1 equivalent of the amine reacts by nucleophilic substitution forming the protonated diamino alcohol intermediate, the second equivalent of the amine deprotonates the diamino alcohol intermediate (pK_a of the secondary amine is slightly higher than the pK_a of the diamino alcohol intermediate). The secondary ammonium chloride salt formed precipitates out from the hydrophobic reaction mixture and can be separated from the diamino alcohol intermediate by filtration. Finally, the diamino alcohol intermediate can be sulfated with $SO_3 \cdot Pyr$ to form the isoelectric buffer in the salt form. The product can then be obtained in isoelectric form by crystallization from a concentrated aqueous solution titrated to the pH equal to the pI of the isoelectric buffer.

6.2.1 1,3-Dimorpholino-2-O-sulfo-propane (DMSP)

6.2.1.1 Optimization

The necessary reaction conditions (reaction time and temperature) for the synthesis of 1,3-dimorpholino-2-propanol (DMP, the diamino alcohol intermediate) from morpholine (MOR) and epichlorohydrin (EH) were tested. The reactants were mixed and heated. A sample was taken periodically from the reaction mixture and analyzed by ^1H - and ^{13}C - NMR spectroscopy until complete conversion (determined from the NMR spectra) was seen. The intermediate was processed, and the next reaction was set-up. The complete scheme for the synthesis of DMSP is shown in Figure 68.

6.2.1.2 Step 1

6.2.1.2.1 Synthesis of DMP

30 g (0.344 mol) MOR was added into a 250mL round bottom flask fitted with an ice-water cooled condenser. 10.6 g (0.115 mol) EH was mixed with 20 mL THF and the solution was added into the flask with MOR. The flask was warmed in an oil bath set at 60°C . Heavy solid formation was observed within 1 hour of heating. A sample was taken after 2 hours, dissolved in D_4 -methanol, centrifuged and the supernatant solution was analyzed by ^1H - and ^{13}C -NMR. Tentative assignments were made on the ^{13}C -NMR spectrum and are shown in Figure 69. The unique, new signals were tentatively assigned to the products of the reaction (both the amino alcohol intermediate and DMP) and were monitored over the reaction time by ^{13}C -NMR. Selected sections of the ^{13}C -NMR spectrum for aliquots taken from the reaction mixture over the course of the reaction are shown in Figure 70. It can be seen from Figure 70 that (i) it is possible

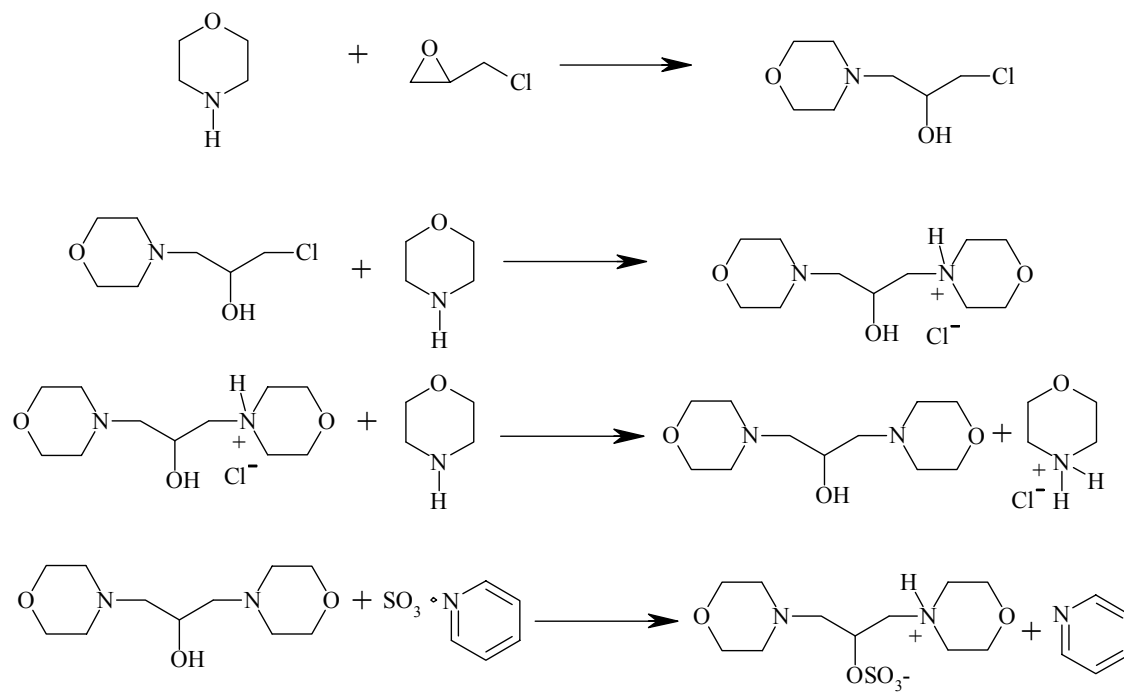


Figure 68. Complete scheme for the synthesis of DMSP.

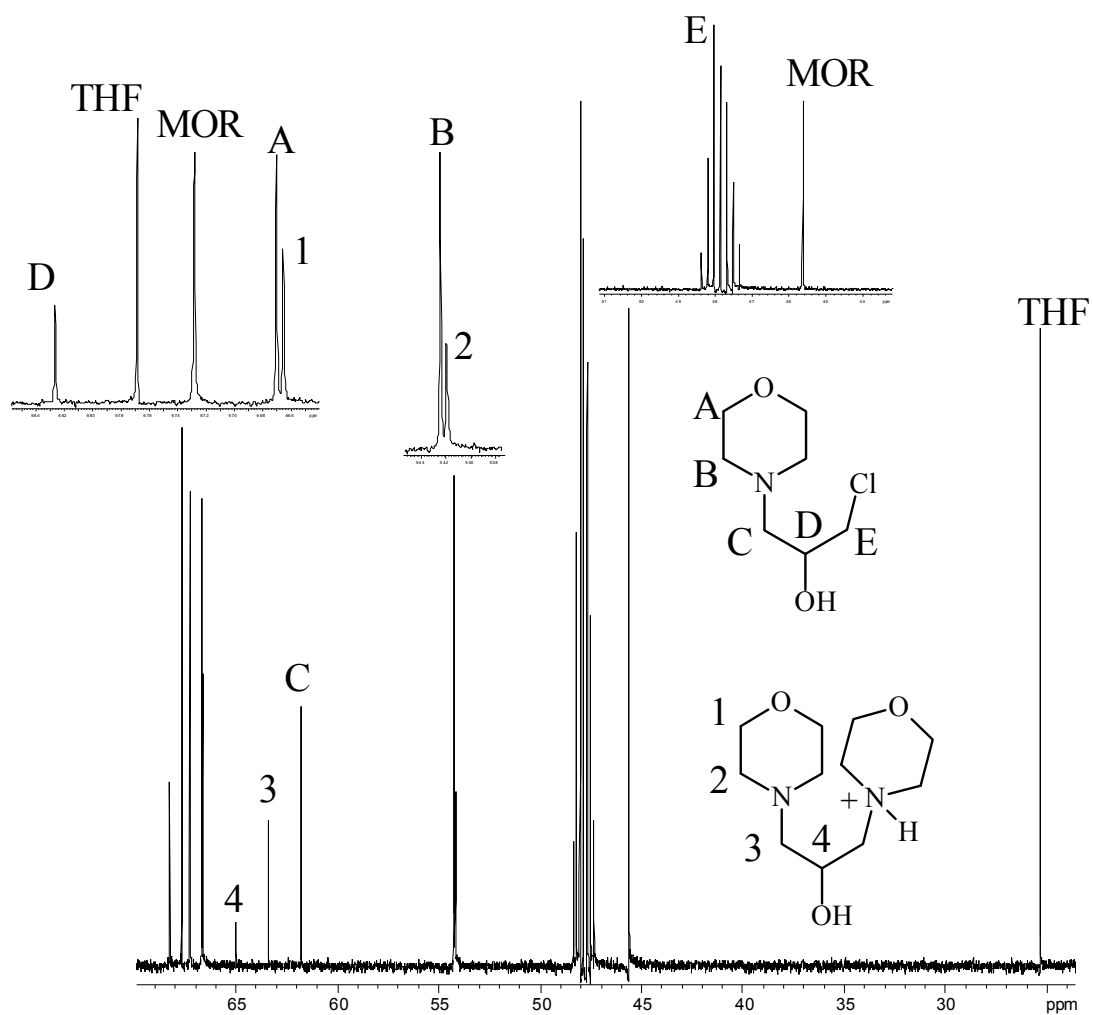


Figure 69. ^{13}C -NMR spectrum for the reaction mixture after 2 hours of heating, with tentative signal assignments.

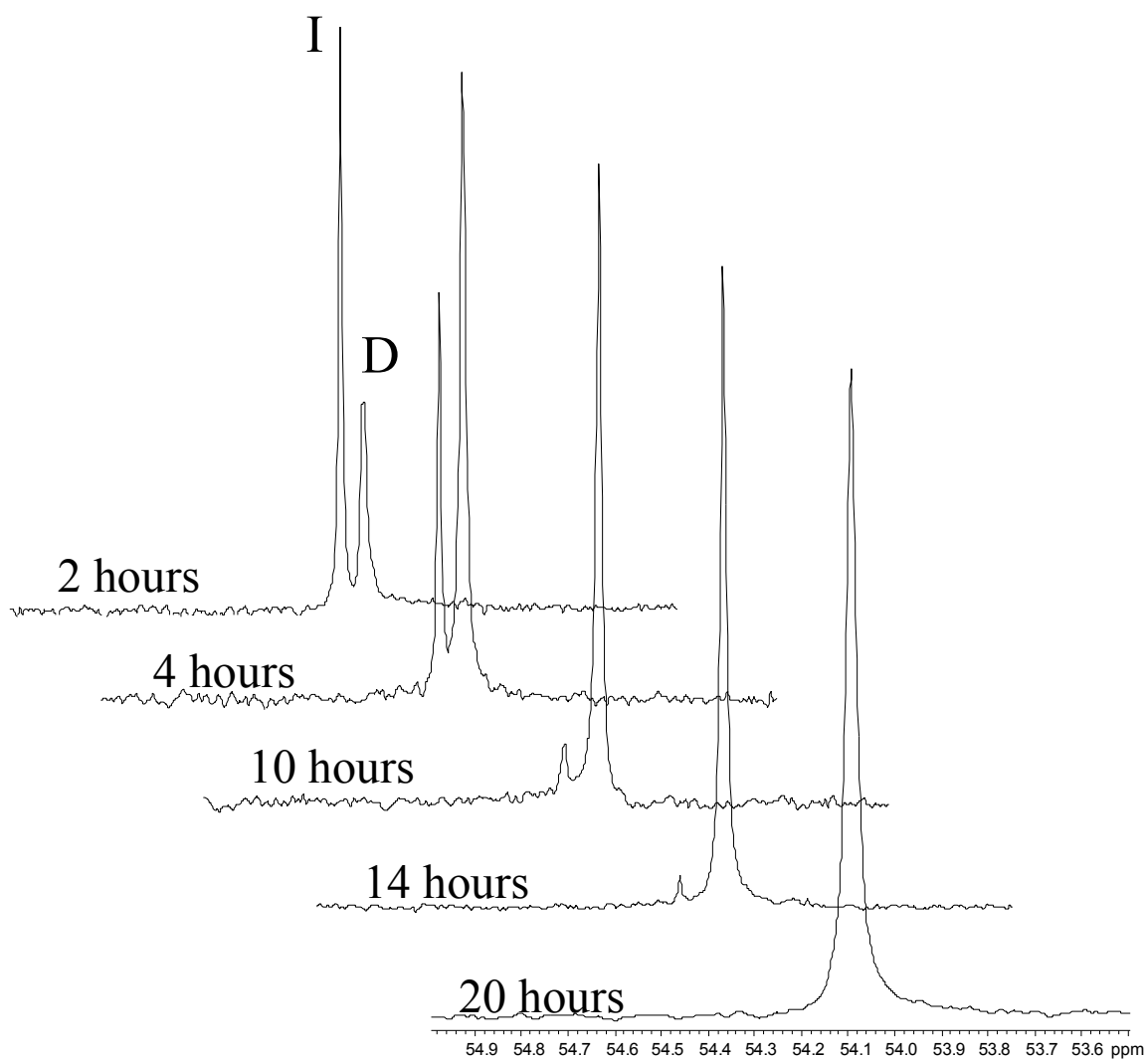


Figure 70. Selected section of the ^{13}C -NMR spectrum for aliquots of the reaction mixture taken over the course of the reaction, showing a decrease in the signal for the amino alcohol intermediate (I) and increase in the signal for DMP (D).

to synthesize and isolate the amino alcohol intermediate for the synthesis of the asymmetric diamino alcohol intermediates and (ii) that the reaction for the synthesis of the diamino alcohol intermediate is complete in 22 hours.

6.2.1.2.2 Processing of DMP

Acetone was added to the DMP reaction mixture and the slurry was filtered. Acetone was removed from the filtrate under reduced pressure to yield a reddish viscous liquid. The solids from the filtration were dissolved in D₂O while the viscous solution was mixed into D₄-methanol and both samples were analyzed by ¹H- and ¹³C-NMR. The ¹H- and ¹³C-NMR spectra are shown in Figure 71 and Figure 72, respectively.

The spectra for the solids correspond to that of MOR, most likely morpholinium chloride (since MOR is liquid at room temperature), THF, acetone and D₄-methanol. The spectra for the liquid correspond with the tentative assignments made for DMP, and also show a slight carry-over of MOR (either in the free amine or salt form). Assignments were made on the DMP spectra based on the results of the integration of peak areas.

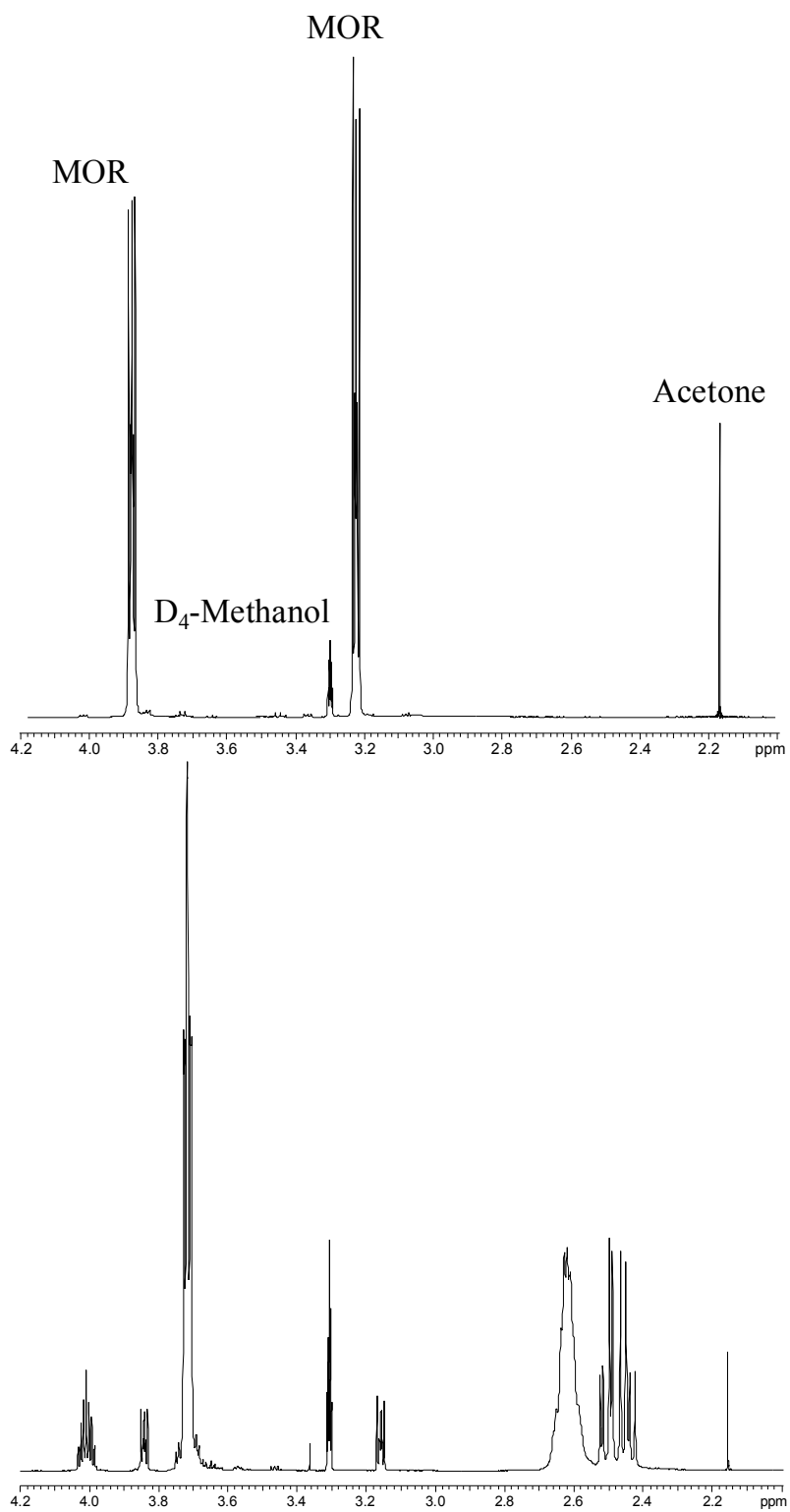
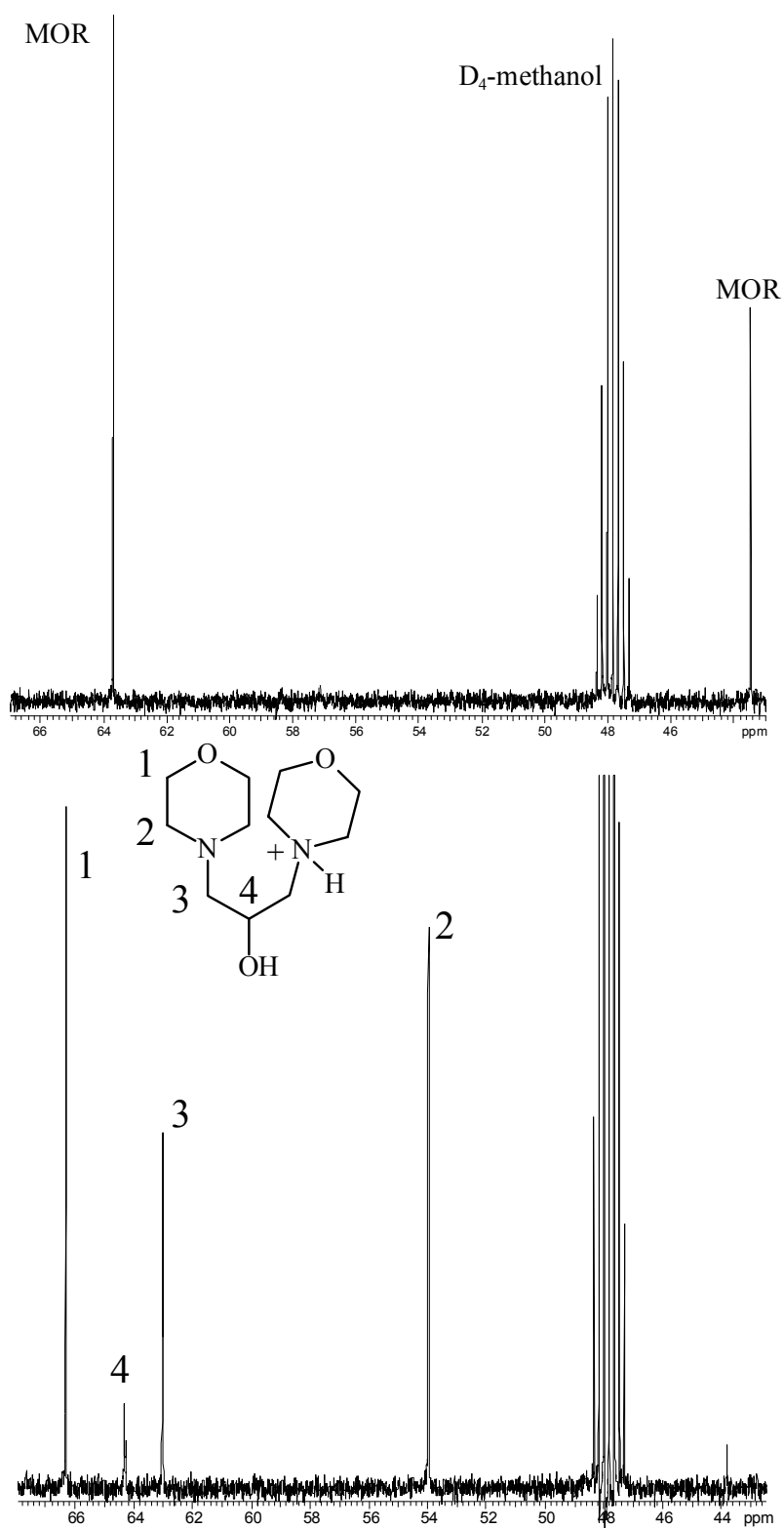


Figure 71. $^1\text{H-NMR}$ spectra for the solids (top panel) and the liquid (bottom panel) from DMP synthesis.



6.2.1.3 Step 2

6.2.1.3.1 Synthesis (sulfation)

Conditions for the sulfation of DMP were adapted from the optimized conditions for the synthesis of BDASP. A clean, 250 mL, three-neck round bottom flask was fitted with an ice-water cooled condenser. 40 mL N,N-dimethylformamide (DMF) was added to the flask. 5 g (0.022 mol) DMP was added and the flask was warmed in an oil bath to 65 °C. 3.85 g (0.024 mol) SO₃•Pyr was added to the warm solution and the mixture was stirred and heated continuously at 65 °C for 4 hours. Heavy solid formation was observed after 1 hour of heating.

After 4 hours of heating, the mixture was allowed to cool and 100 mL DMF was added to make a slurry. The slurry was filtered, the solids were dispersed in 500 mL acetone, and the acetone slurry was filtered. The solids were then dispersed in 500 mL ethyl alcohol followed by filtration of the slurry to obtain an off-white colored cake. A sample of the solids was dissolved in D₂O and the solution was analyzed by ¹H- and ¹³C-NMR. Complete conversion was seen and the signals were tentatively assigned.

6.2.1.4 pI determination

The pI of DMSP was determined by indirect UV detection CE. Using a 26 μm I.D. bare fused silica capillary, L_t = 26.1 cm, L_d = 19.7 cm at 15kV in positive to negative polarity, T=25 °C, and the UV detector at 214 nm, conventional CE was carried out in a 20 mM acetic acid BGE titrated to pH=4.6 with imidazole and a 20 mM pyridine BGE titrated to pH=6.1 with pTSA. Figure 73 shows the electropherograms for DMSP in the two BGEs. Clearly, the pI of DMSP is between 4.6 and 6.1. The effective

mobilities (μ^{eff} s) were calculated for DMSP in both CE runs, and were corrected for ionic strength suppression using Peakmaster 5.0. The corrected μ^{eff} s were plotted versus the BGE pH, and the pH at which the $\mu^{\text{eff}} = 0$ (thus the pI) was determined to be 5.8.

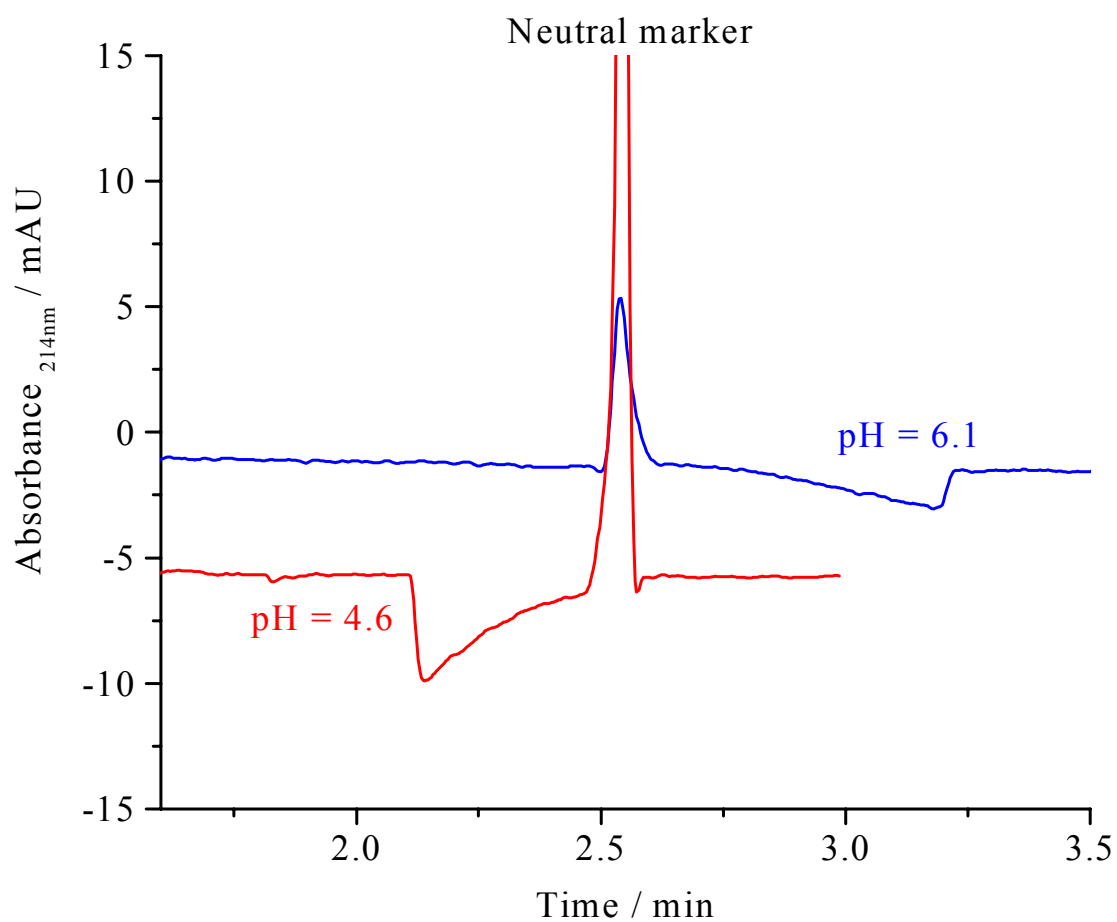


Figure 73. Electropherograms for the determination of the pI of DMSP.

6.2.1.5 Isoelectric crystallization

The solids were dissolved into 200 mL deionized water and the solution was titrated with a 10% LiOH solution to pH=5.8. Water was partially removed under reduced pressure and the warm solution was cooled to crystallize the product in the salt-free form.

Product purity (in terms of inorganic salt content) was determined by indirect-UV detection CE. Using a 20 mM acetic acid BGE titrated with imidazole to pH=4.5, run on a 26 μ m I.D. bare fused silica capillary, $L_t = 26.5$ cm, $L_d = 19.7$ cm at 25kV, positive to negative polarity, $T=25$ °C, and UV detector at 214 nm, lithium ions were analyzed. Figure 74 shows the electropherograms of the crystallized product (top panel) and the crystallization mother liquor (middle panel) and the electropherogram simulated by Peakmaster 5.0 (bottom panel). Using a 20 mM Tris, 0.1 mM CTAOH BGE titrated to pH=8.5 with BTC, run on a 50 μ m I.D. bare fused silica capillary, $L_t = 25.7$ cm, $L_d = 19.3$ cm at 10 kV, negative to positive polarity, $T=25$ °C, and UV detector at 214 nm, sulfate ions were analyzed. Results for the crystallized product (top panel) and the crystallization mother liquor (middle panel) and the simulated electropherogram (bottom, using Peakmaster 5.0) are shown in Figure 75.

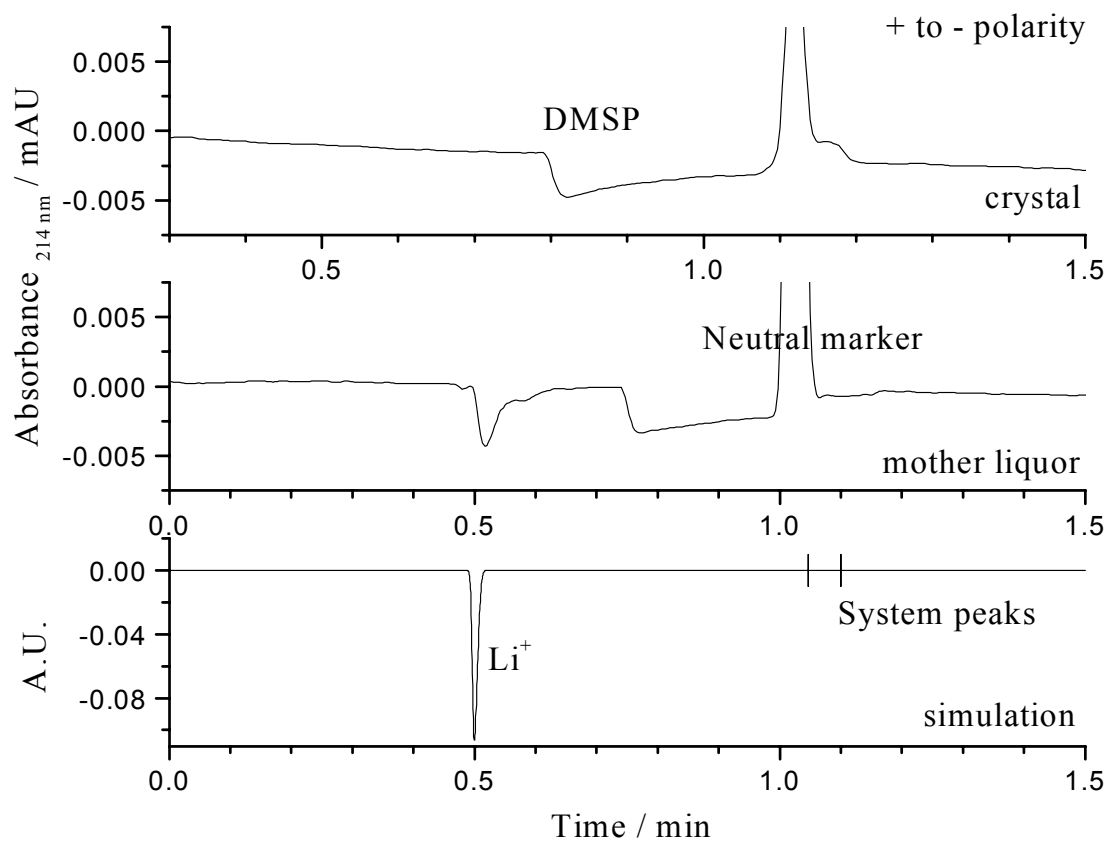


Figure 74. Electropherograms for the analysis of cations in the crystallized DMSP (top panel) and the crystallization mother liquor (middle panel) compared to the electropherogram simulated using Peakmaster 5.0 (bottom panel).

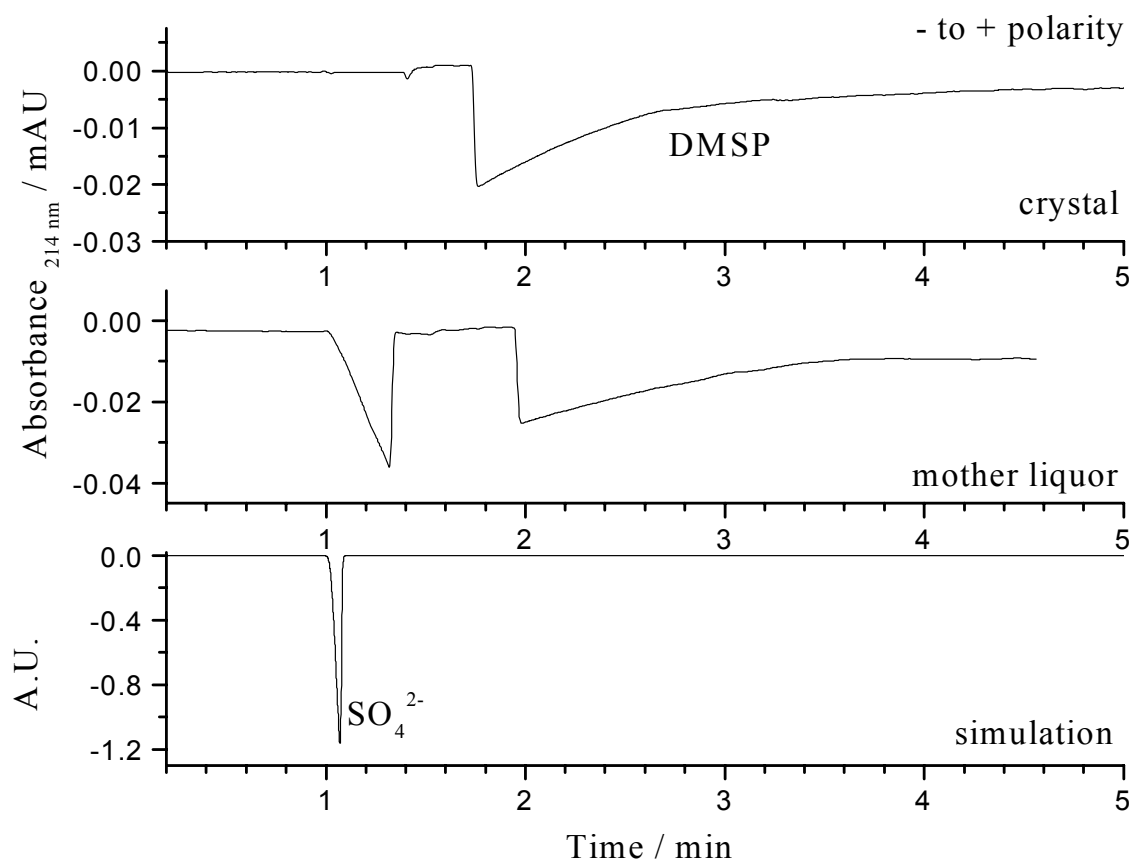


Figure 75. Electropherograms for the analysis of anions in the crystallized DMSP (top panel) and the crystallization mother liquor (middle panel) compared to the electropherogram simulated using Peakmaster 5.0 (bottom panel).

6.2.1.6 Characterization

The final product was characterized by ^1H - and ^{13}C -NMR. Figure 76 shows the ^1H - and ^{13}C -NMR spectra and the tentative assignment of the signals. Then, the product was analyzed by ^1H - ^1H COSY (spectra shown in Figure 77). This confirmed the proton signal assignments. The ^{13}C assignments were confirmed using ^1H - ^{13}C HETCOR NMR spectroscopy (spectra shown in Figure 78).

The identity and purity of the final product were confirmed by high resolution ESI-MS. The ESI-MS spectra in the positive and negative ion modes are shown in Figure 79. Only signals corresponding to DMSP (and the corresponding adducts and fragment ions) are seen. Single crystals of DMSP were grown by slow and undisturbed cooling of a concentrated aqueous solution of DMSP and its X-ray crystal structure was determined. An image of the X-ray crystal structure is shown in Figure 80.

6.2.1.7 Final procedure

Step 1. Fit a clean, 3 L, three-neck round bottom flask with an ice-water cooled condenser. Add 750 g (8.61 mol) MOR to the flask, set the flask in an oil bath. Mix together 265.5 g (2.87 mol) EH and 500 mL THF. Slowly add the EH solution into the flask and heat to 65°C , while stirring the solution with a mechanical stirrer. Take samples periodically and monitor the increase in the amount of DMP (and the corresponding decrease in the amount of the amino alcohol intermediate) by NMR. Depending on whether more MOR or more EH is needed, add the corresponding amount into the reaction flask. Stirring continuously, heat the reaction mixture for a minimum

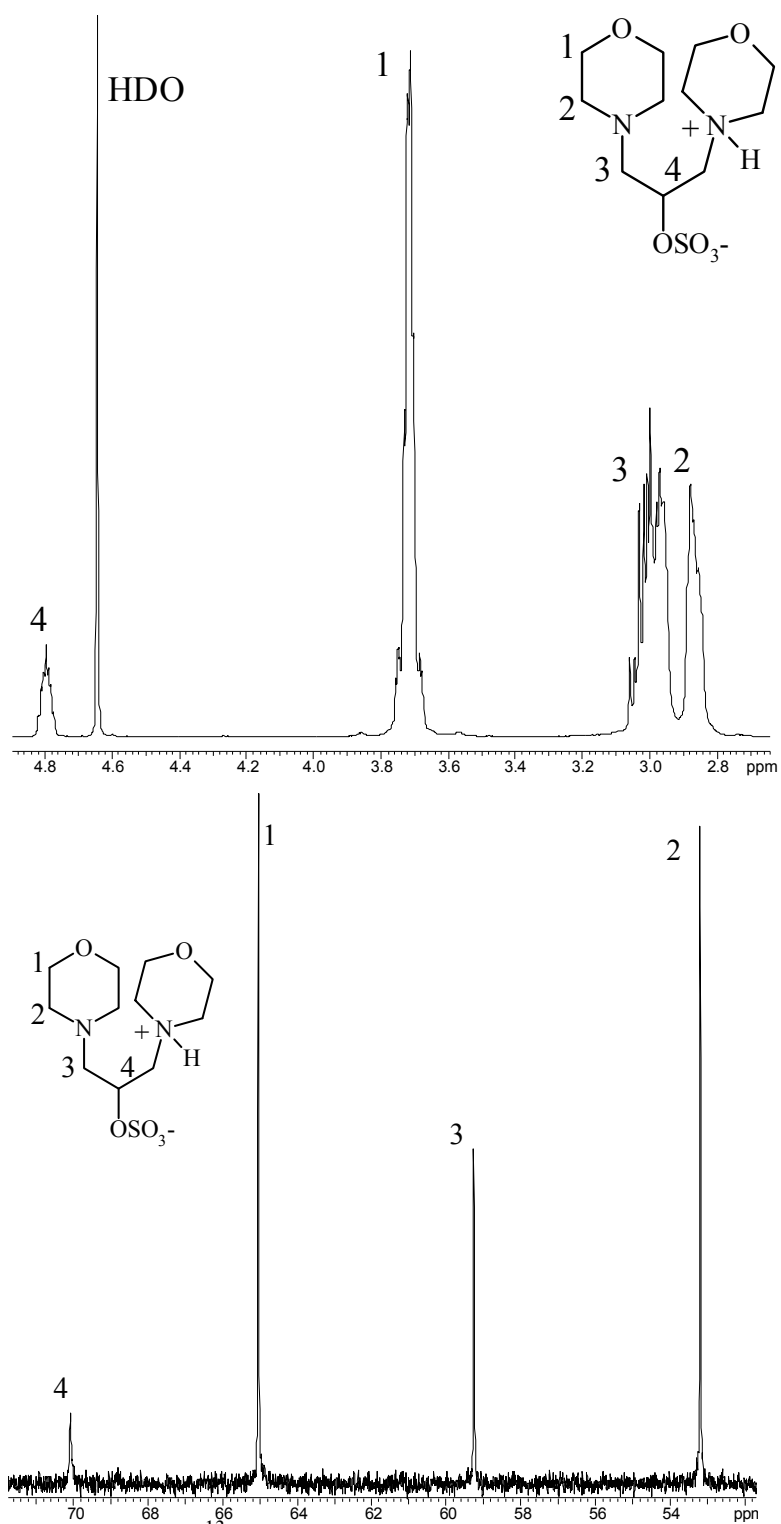


Figure 76. ^1H - (top panel) and ^{13}C -NMR (bottom panel) spectra of DMSP with the tentative assignments.

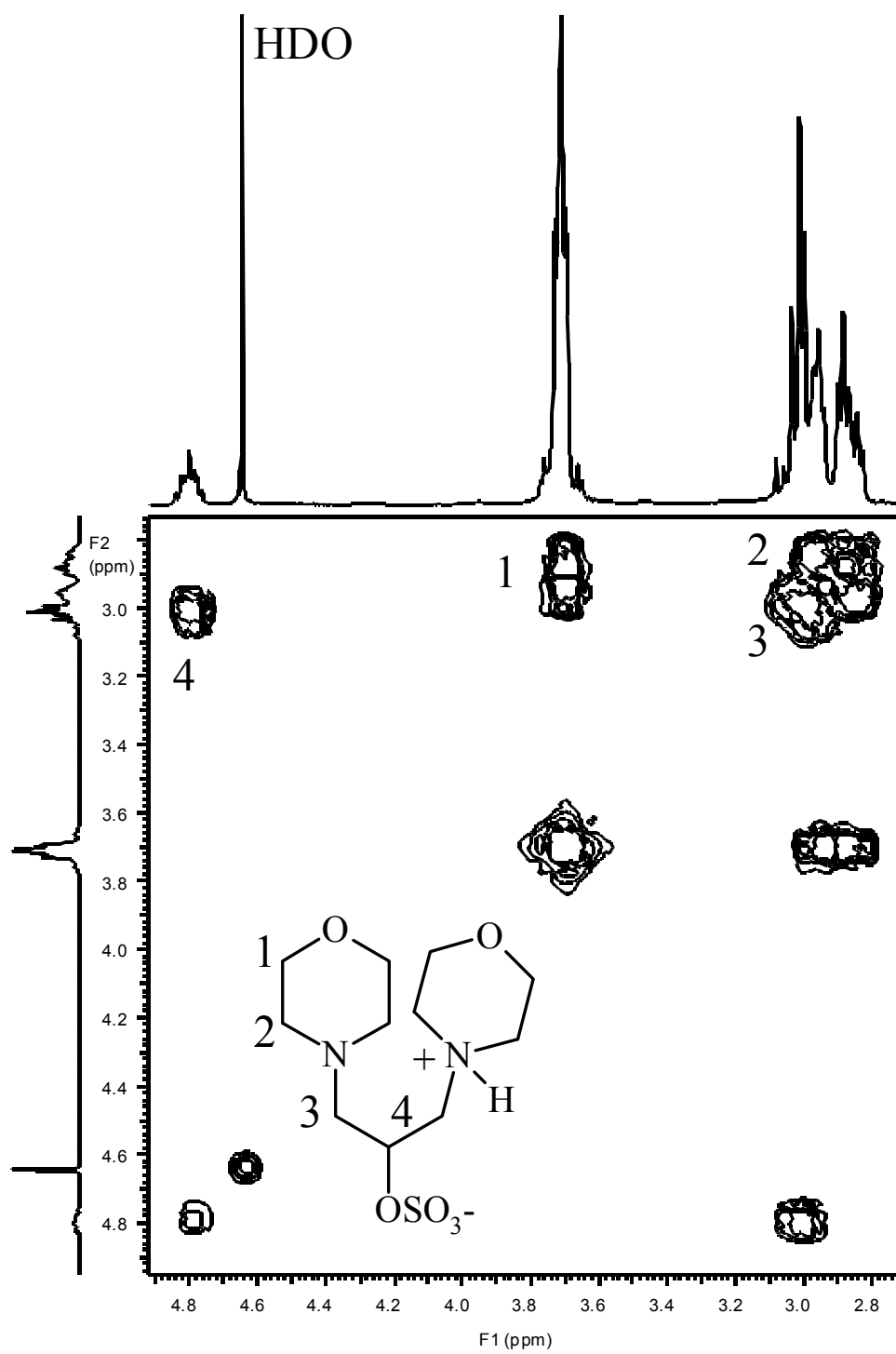


Figure 77. ^1H - ^1H COSY spectrum of DMSP with the corresponding assignments.

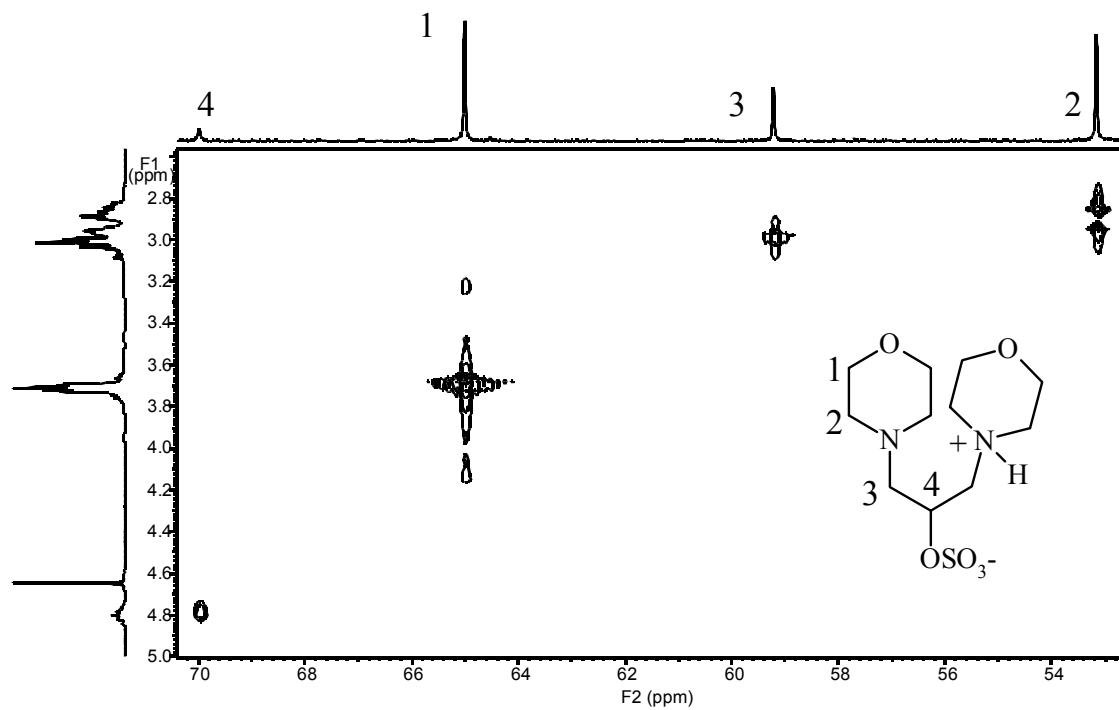


Figure 78. ^1H - ^{13}C HETCOR spectrum of DMSP with the corresponding assignments.

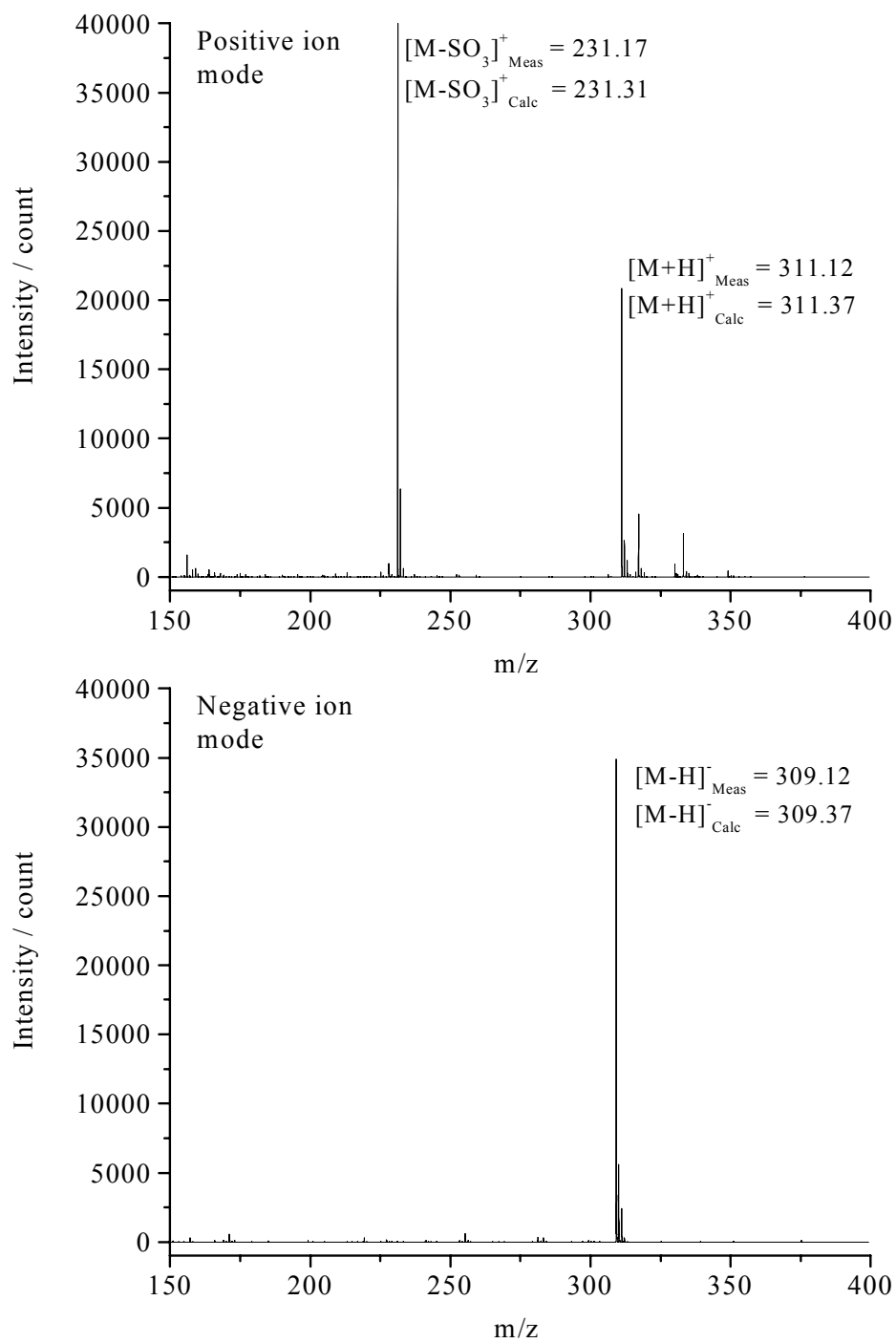


Figure 79. ESI-MS analysis of DMSP in the positive (top panel) and the negative (bottom panel) ion modes.

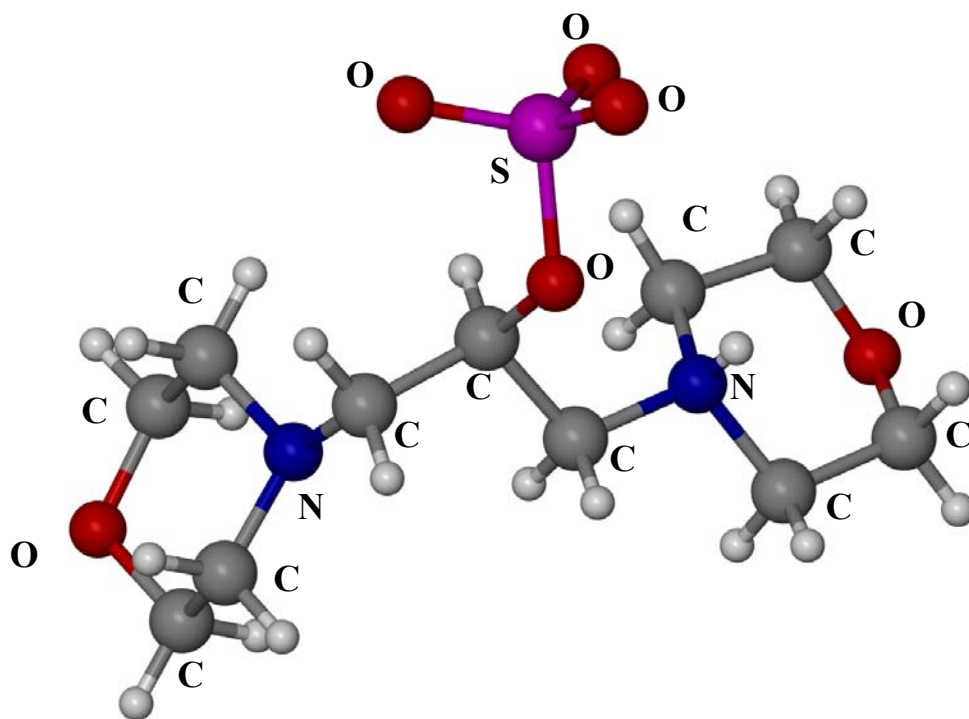


Figure 80. Ball-and-stick image of the single crystal X-ray structure of DMSP.

of 22 hours. At the end of the reaction, take the flask off of the oil bath and set it to cool on a cork O-ring with paper towels underneath (to absorb the oil).

Into the cool reaction mixture, add enough acetone to form a slurry of a thin consistency. Filter the slurry using a Buchner funnel and a suction flask. Remove acetone and THF under reduced pressure.

Step 2. (adapted from sulfation of BDAP). Fit a clean, 5L, three-neck round bottom flask with an ice-water cooled condenser. Add 500 mL DMF to the flask, set the flask in an oil bath. Add the processed DMP from step 1 into the flask and heat it to 65°C while stirring the solution with a mechanical stirrer. To the warm, stirring solution add 466.1 g (2.87 mol) SO₃•Pyr and continuously heat and stir the mixture at 65°C for 4 hours. Take the flask off of the oil bath and set it to cool on a cork O-ring with paper towels underneath (to absorb the oil).

Step 3. To the cooled reaction mixture, add 700 mL DMF and with the aid of the mechanical stirring rod and a spatula, manually dislodge the solids and remove the chunks from the round bottom flask into a 5 L beaker. Add 1L DMF into the beaker and make a slurry of the solids. Filter the slurry using a Buchner funnel and a suction flask. Remove the solid cake and filter paper from the funnel and add them into another 5 L beaker and make a slurry with another 1L DMF. Repeat until the DMF filtrate comes out pale yellow. Then, remove the solid cake and filter paper from the funnel and add them into another 5 L beaker and make a slurry with 1L of acetone. Filter the slurry, and make another slurry of the solids in 1L of ethanol, and filter again. Let the solids dry inside the fume hood.

Step 4. Split the solids into two batches and dissolve each batch in a minimum volume (around 2L) of deionized water. Measure the pH of the solution and titrate it to pH=5.8 using a 10% LiOH solution (if the solution pH is below 5.8) or 2M H₂SO₄ (if the solution pH is above 5.8). Remove about half of the water using a rotovap with the water bath set at 65°C. Let the solution cool in the fume hood with continuous stirring for 24 hours. Filter the slurry, wash the solid cake with sufficient amounts of cold ethanol a few times and let the cake dry in the fume hood. Analyze both the crystallization mother liquor and the solids by CE and repeat crystallization from deionized water if necessary.

Then, combine the two crystallized batches and recrystallize it from deionized water. Filter off the first crop of crystals, wash the cake with sufficient amounts of cold ethanol a few times, let the solids dry and analyze them by CE. Remove more water from the crystallization mother liquor to get a second crop of crystals. Analyze each crop of crystals, and combine the similar ones. Repeat the concentration followed by crystallization steps until co-crystallization of DMSP and any of the salt contaminants is observed.

6.2.1.8 Recapitulation

A novel scheme has been designed for the *de novo* synthesis of amine-based isoelectric buffers. According to the scheme, the isoelectric buffers have an anionic sulfate group and two amino groups. The pI value of the buffer will be between the pK_a values of the two amino groups (the pK_a values vary with the amine used). Buffers with

both symmetric and asymmetric structures (in terms of the two amino groups) can be made using this scheme.

A unique, isoelectric buffer, DMSP, has been synthesized from MOR and EH followed by reaction with $\text{SO}_3 \cdot \text{Pyr}$. According to the design of the molecule, the two amino groups in DMSP have close pK_a values. Consequently, solutions of DMSP in its isoelectric state have a high buffering capacity and high conductivity. The pI of DMSP is between 4.6 and 6.1 (calculated to be 5.8). For isoelectric buffers where the pI value is between the pK_a values of two amino groups (such as in lysine with a pI of 9.9) DMSP is the least basic isoelectric buffer reported so far. DMSP has been obtained in its pure, isoelectric form and has been well characterized by 1D and 2D-NMR, ESI-MS, CE and X-ray crystallography. DMSP has been successfully synthesized several times, in a 1 g scale batch to a 500 g scale batch.

6.2.2 1,3-Bis(dipropylamino)-2-O-sulfo-propane (BDPSP)

The reaction conditions (reaction time and temperature) for the synthesis of 1,3-bis(dipropylamino)-2-propanol (BDPP, the diamino alcohol intermediate) from dipropylamine (DPA) and epichlorohydrin (EH) were adapted from the synthesis of DMP. The reactants were mixed and heated. A sample from the reaction mixture was taken periodically and analyzed by ^1H - and ^{13}C -NMR spectroscopy until complete conversion (determined from the NMR spectra) was seen. The intermediate was processed, and the next reaction was set-up. The complete scheme for the synthesis of BDPSP is shown in Figure 81.

6.2.2.1 Step 1

6.2.2.1.1 Synthesis of BDPP

7.5 g (0.074 mol) DPA was added into a 50 mL round bottom flask fitted with an ice-water cooled condenser. 2.3 g (0.025 mol) EH was mixed with 5 mL THF and the solution was added into the flask with DPA. The flask was warmed in an oil bath set at 65°C. Heavy solid formation was observed within 1 hour of heating. After 22 hours of heating, the reaction mixture was cooled.

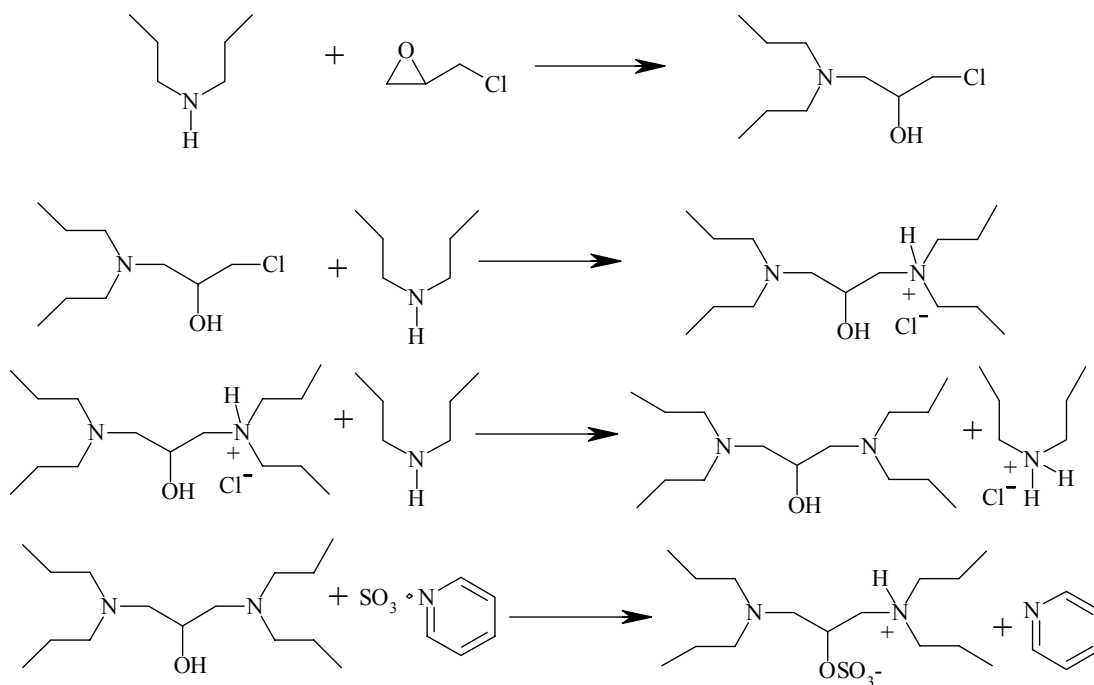


Figure 81. Scheme for the complete synthesis of BDPP.

6.2.2.1.2 Processing of BDPP

Acetone was added to the BDPP reaction mixture and the slurry was filtered. Samples were taken from the filtrate and the solids and were analyzed by ^1H - and ^{13}C -NMR. Five new, unique signals (aside from the reactant signals) were seen, indicating complete conversion of the amino alcohol intermediate to BDPP. Acetone was removed from the filtrate under reduced pressure to yield a yellow viscous liquid. ^1H - and ^{13}C -NMR spectra for BDPP are shown in Figure 82 with the tentative assignment of the signals. The processed BDPP was used for the next reaction.

6.2.2.2 Step 2

6.2.2.2.1 Synthesis (sulfation)

Conditions for the sulfation of BDPP were adapted from the optimized conditions for the synthesis of BDASP and DMSP. A clean, 50 mL, three-neck round bottom flask was fitted with an ice-water cooled condenser. 10 mL DMF was added to the flask. 5 g (0.022 mol) BDPP was added and the flask was warmed in an oil bath to 65°C . 3.9 g (0.025 mol) $\text{SO}_3\cdot\text{Pyr}$ was added to the warm solution and the mixture was stirred and heated continuously at 65°C for 4 hours. Heavy solid formation was observed after 1 hour of heating.

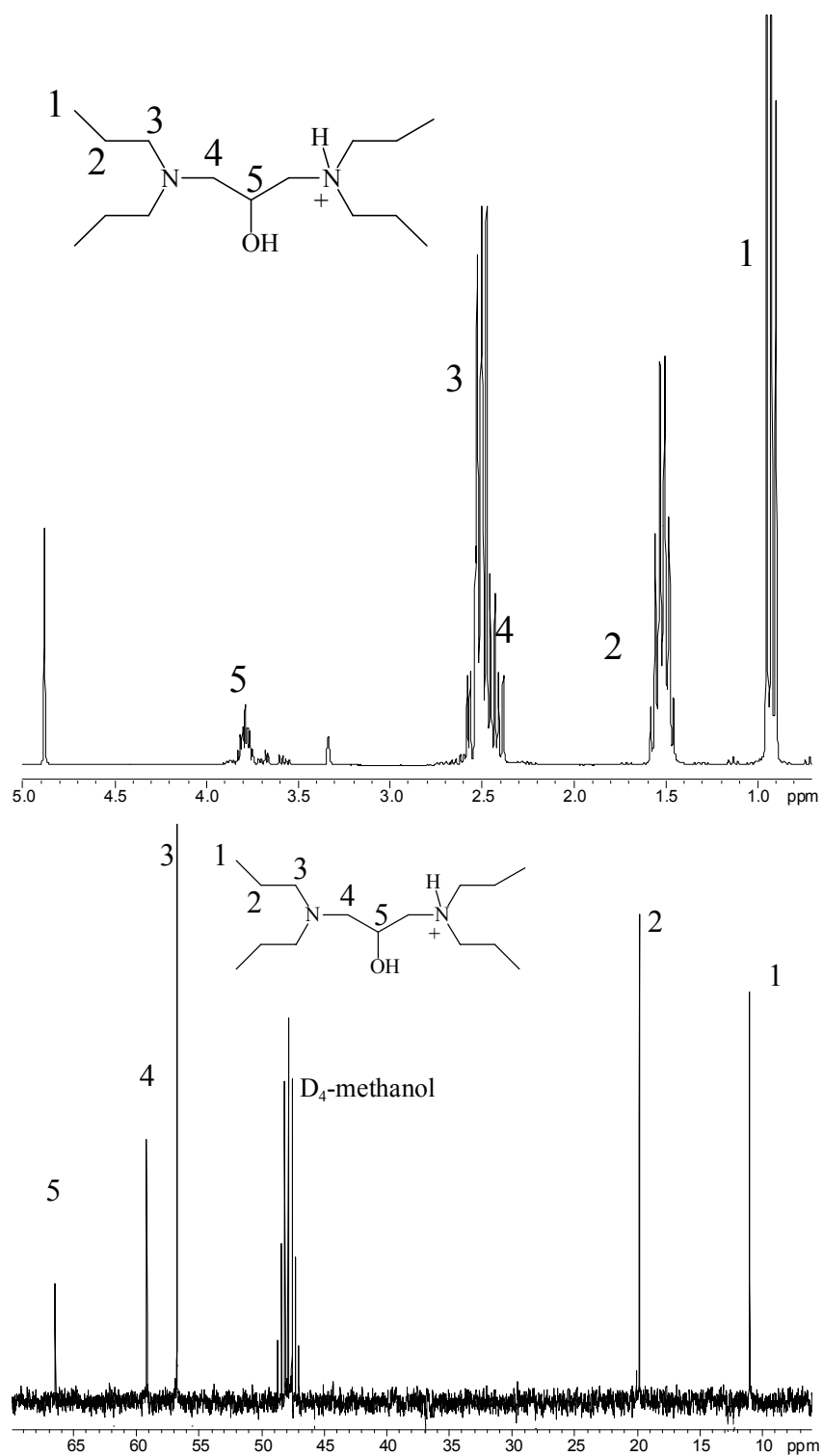


Figure 82. $^1\text{H-}$ and $^{13}\text{C-}$ NMR spectra for BDPP and the corresponding tentative assignments.

After 4 hours of heating, the mixture was allowed to cool. A sample of the solids was dissolved in D₂O and the solution was analyzed by ¹H- and ¹³C-NMR which showed 93% conversion of BDPP to BDPSP. 5 mL DMF was added to the solids to make a slurry. The slurry was filtered and the solids were suspended in 50 mL acetone, and the acetone slurry was filtered. The solids were then dispersed in 50 mL ethyl alcohol followed by filtration of the slurry to obtain an off-white colored cake. A sample of the solids was dissolved in D₂O and the solution was analyzed by ¹H- and ¹³C-NMR. Almost complete removal of the contaminants was seen.

6.2.2.3 pI determination

The pI of BDPSP was determined by indirect UV detection CE. Using a 26 μm I.D. bare fused silica capillary, L_t = 26.1 cm, L_d = 19.7 cm at 15kV in positive to negative polarity, T=25 °C, and UV detector at 214 nm, conventional CE was carried out in a 20 mM Tris BGE titrated to pH=7.8 with pTSA and a 20 mM benzylamine BGE titrated to pH=9.6 with pTSA. Figure 83 shows the electropherograms for BDPSP in the two BGEs. Clearly, the pI of BDPSP is between 7.8 and 9.6. The effective mobilities (μ^{eff}s) were calculated for BDPSP from both CE runs, and were corrected for ionic strength suppression using Peakmaster 5.0. The corrected μ^{eff}s were plotted versus the BGE pH, and the pH at which the μ^{eff} = 0 (thus the pI) was determined to be 8.7.

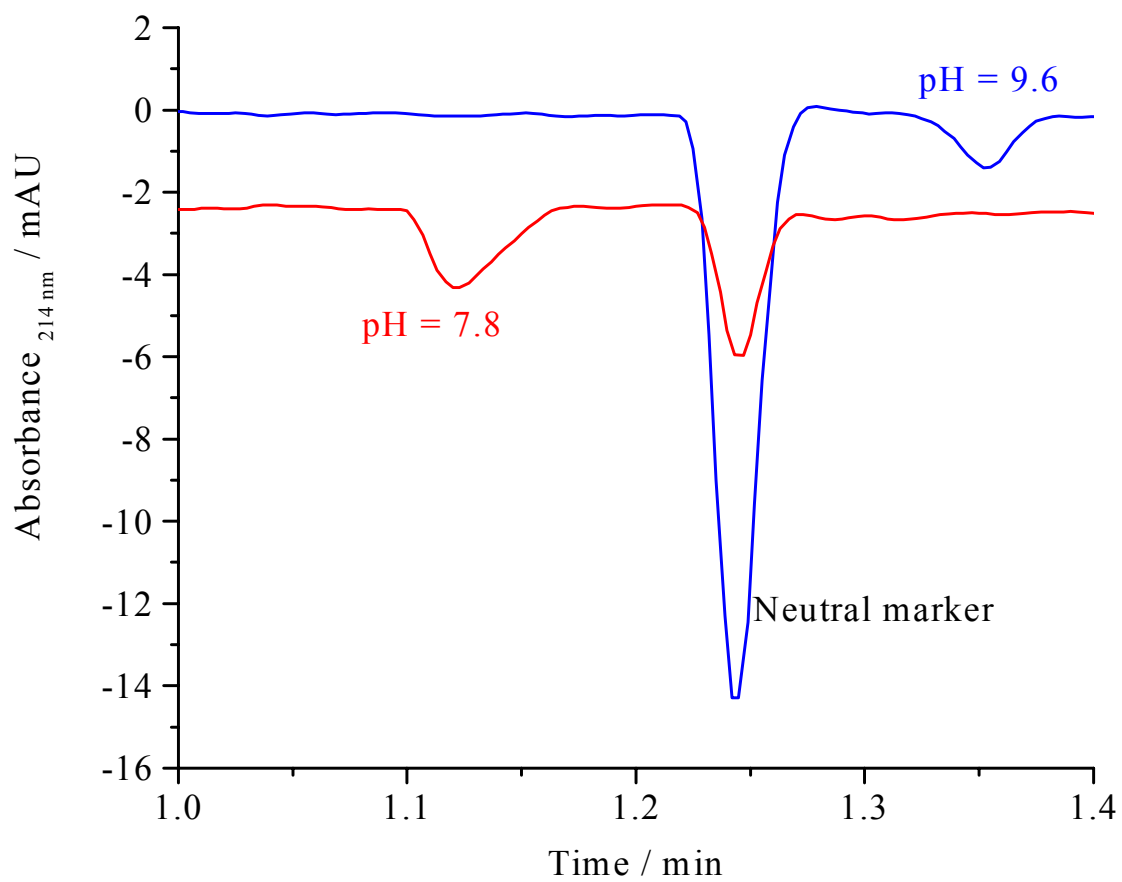


Figure 83. Electropherograms of BDPSP in pH 7.8 and pH 9.6 BGEs.

6.2.2.4 Isoelectric crystallization

The solids were then dissolved in 50 mL deionized water and the solution was titrated with a 10% LiOH solution to pH=8.7. Water was partially removed under reduced pressure and the warm solution was cooled to crystallize BDPSP in the salt-free form.

Product purity (in terms of inorganic salt content) was determined by indirect-UV detection CE. Using a 20 mM acetic acid BGE titrated with imidazole to pH=4.5, run on a 26 μ m I.D. bare fused silica capillary, L_t = 26.5 cm, L_d = 19.7 cm at 25kV, positive to negative polarity, T=25 °C, and UV detector at 214 nm, lithium ions were analyzed. Figure 84 shows the electropherograms of the crystallized product (top panel) and the crystallization mother liquor (middle panel), and the electropherogram simulated using Peakmaster 5.0 (bottom panel). Using a 20 mM Tris, 0.1 mM CTAOH BGE titrated with BTC to pH=8.5 BGE, run on a 50 μ m I.D. bare fused silica capillary, L_t = 25.7 cm, L_d = 19.3 cm at 10 kV, negative to positive polarity, T=25 °C, and UV detector at 214 nm, sulfate ions were analyzed. Results for the crystallized product (top panel) and the crystallization mother liquor (middle panel), and the simulated electropherogram (bottom, using Peakmaster 5.0) are shown in Figure 85.

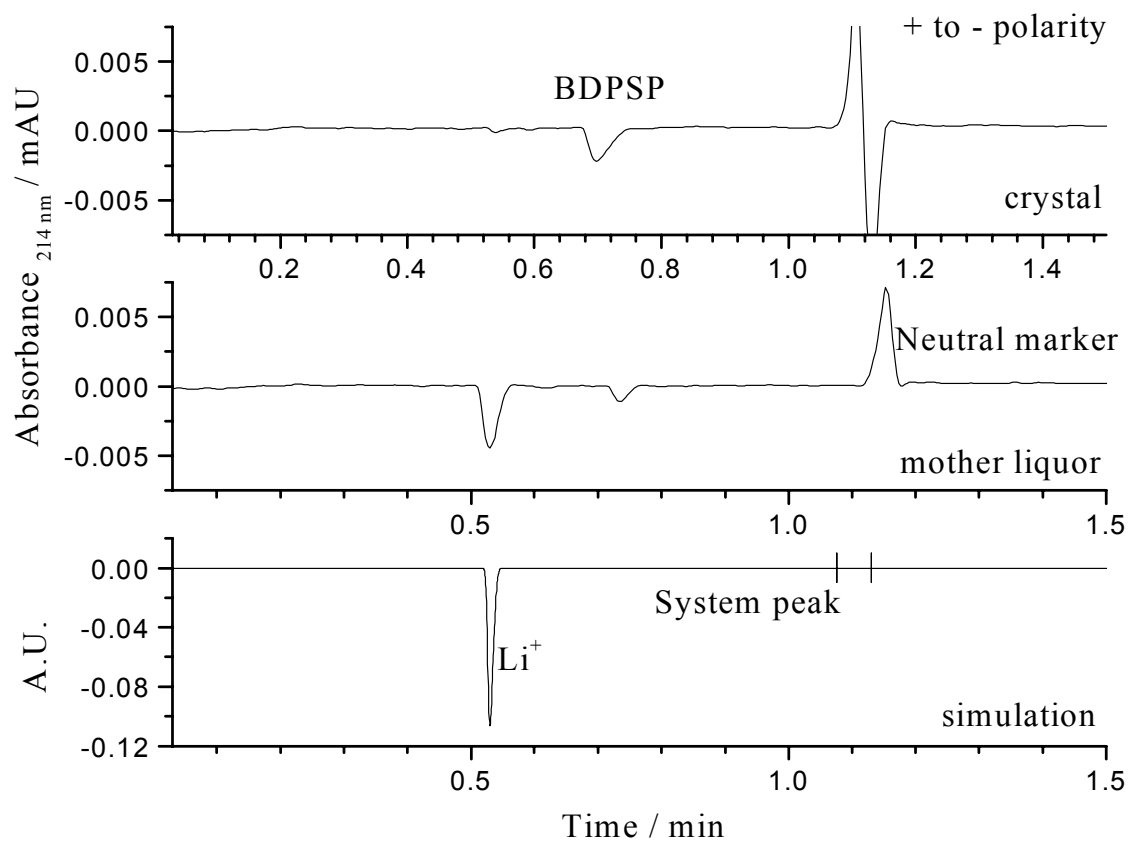


Figure 84. Electropherograms for the analysis of cations in the crystallized BDPSP (top panel) and the crystallization mother liquor (middle panel) compared to the electropherogram simulated using Peakmaster 5.0 (bottom panel).

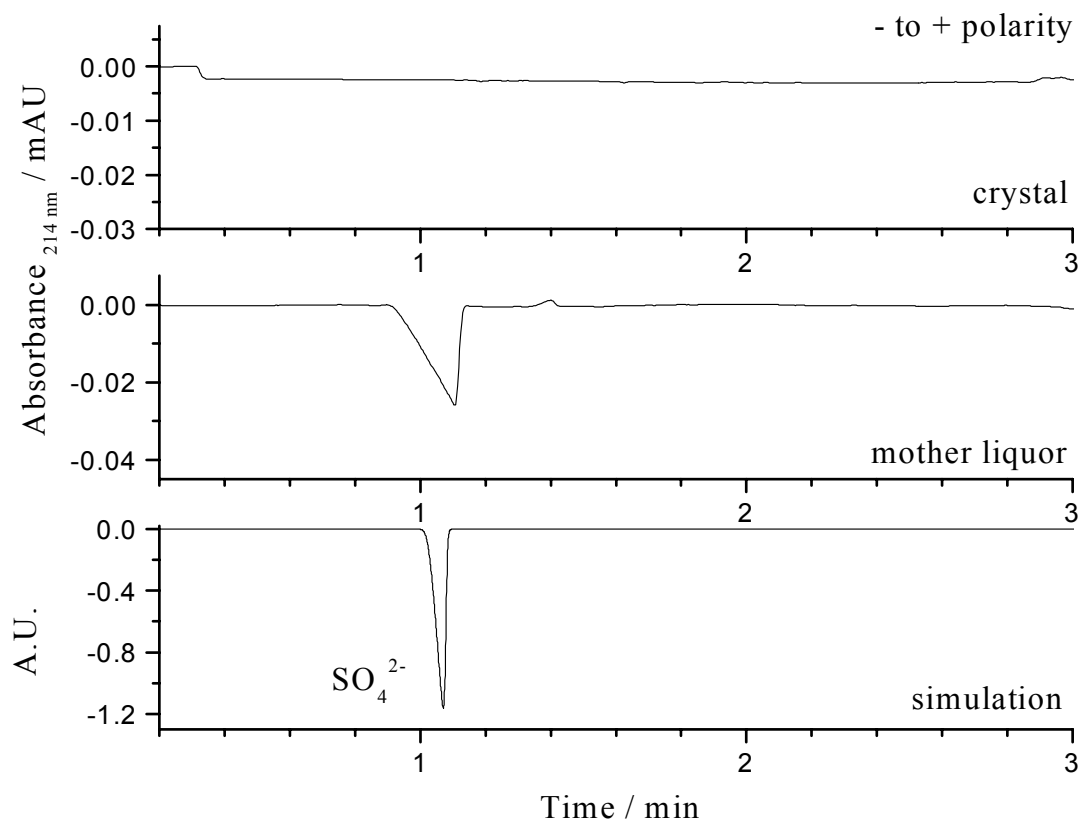


Figure 85. Electropherograms for the analysis of anions in the crystallized BDPSP (top panel) and the crystallization mother liquor (middle panel) compared to the electropherogram simulated using Peakmaster 5.0 (bottom panel).

6.2.2.5 Characterization

The final product was characterized by ^1H - and ^{13}C -NMR. Figure 86 shows the ^1H - and ^{13}C -NMR spectra and the tentative assignment of the signals. Then, the product was analyzed by ^1H - ^1H COSY (spectra shown in Figure 87). This confirmed the proton signal assignments. The ^{13}C assignments were confirmed using ^1H - ^{13}C HETCOR NMR spectroscopy (spectra shown in Figure 88).

The identity and purity of the final product were confirmed by high resolution ESI-MS. The ESI-MS spectra in the positive and negative ion modes are shown in Figure 89. Only signals corresponding to BDPSP (and the corresponding fragment ions) are seen. Single crystals of DMSP were grown by slow and undisturbed cooling of a concentrated aqueous solution of DMSP and its X-ray crystal structure was determined. An image of the X-ray crystal structure is shown in Figure 90.

6.2.2.6 Recapitulation

A unique, basic isoelectric buffer, BDPSP, has been synthesized from DPA and EH followed by reaction with $\text{SO}_3\cdot\text{Pyr}$. According to the design of the molecule, the two amino groups in BDPSP have close pK_a values. Consequently, solutions of BDPSP in its isoelectric state have a high buffering capacity and high conductivity. The pI of BDPSP is between 7.8 and 9.6 (calculated to be 8.7). BDPSP has been obtained in its pure, isoelectric form and has been well characterized by 1D and 2D-NMR, ESI-MS and CE and X-ray crystallography.

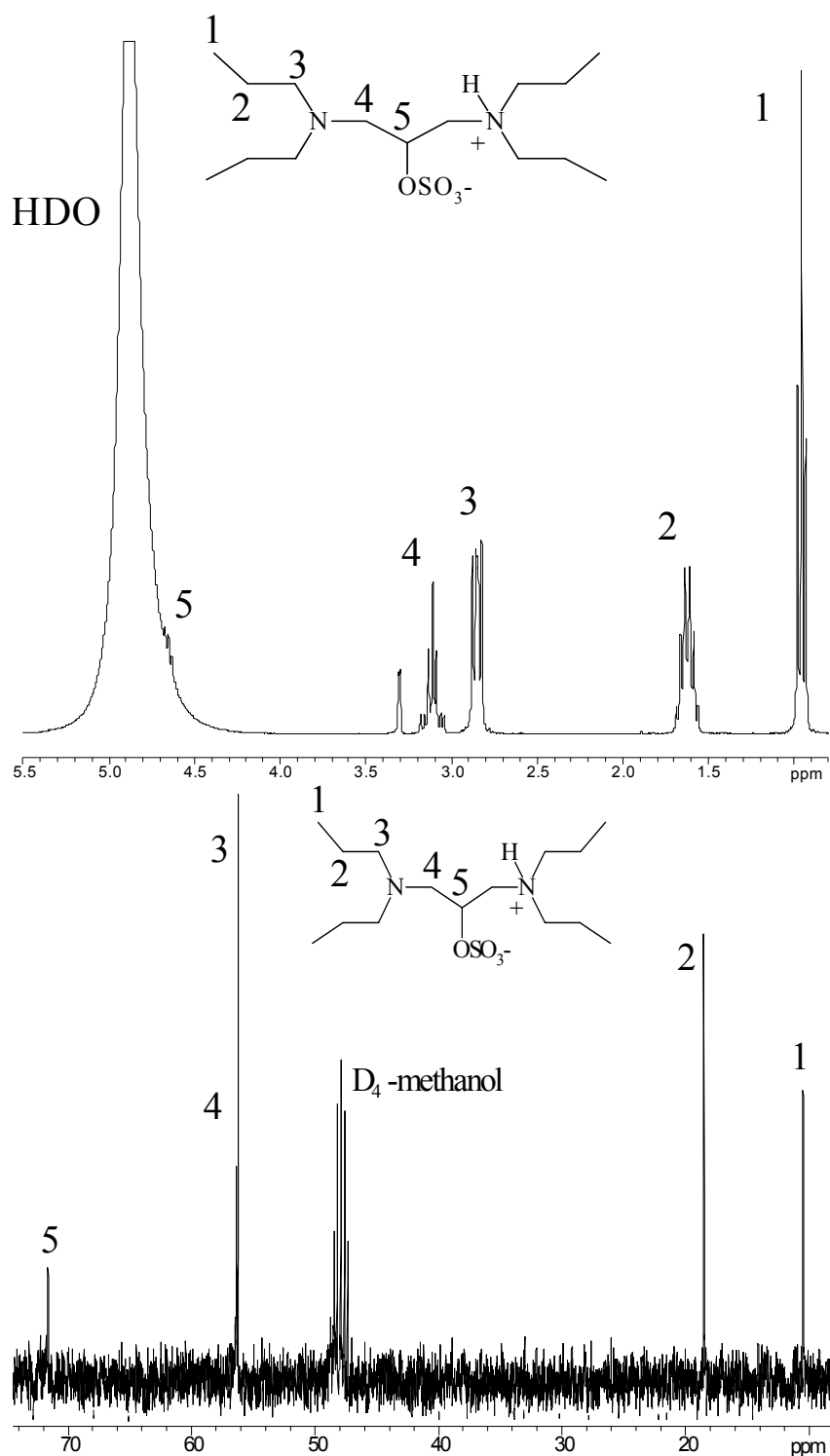


Figure 86. ^1H - (top) and ^{13}C - (bottom) NMR spectra for BDPSP and the tentative assignment of the signals.

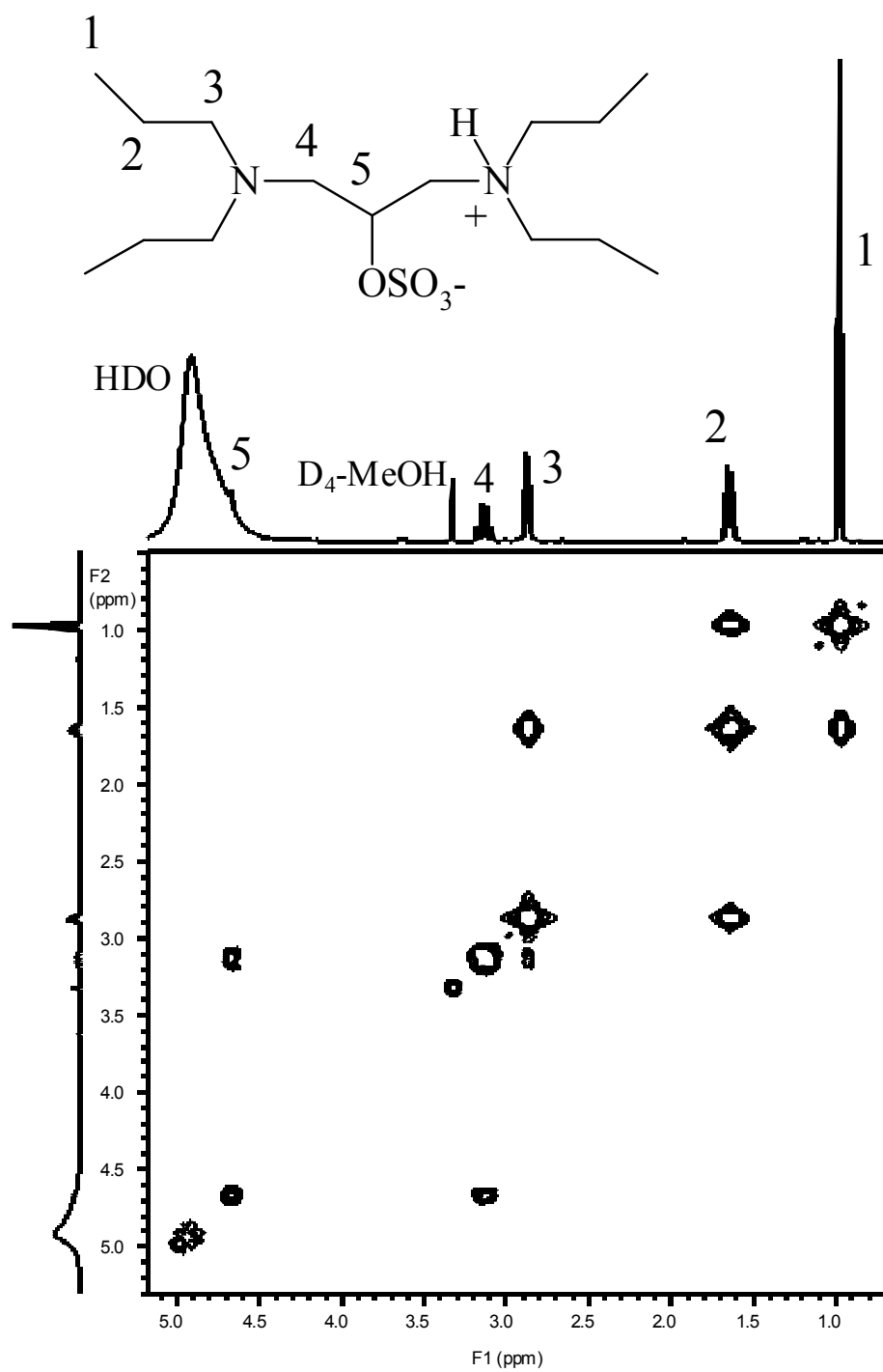


Figure 87. ^1H - ^1H COSY spectrum of BDPSP with the corresponding assignments.

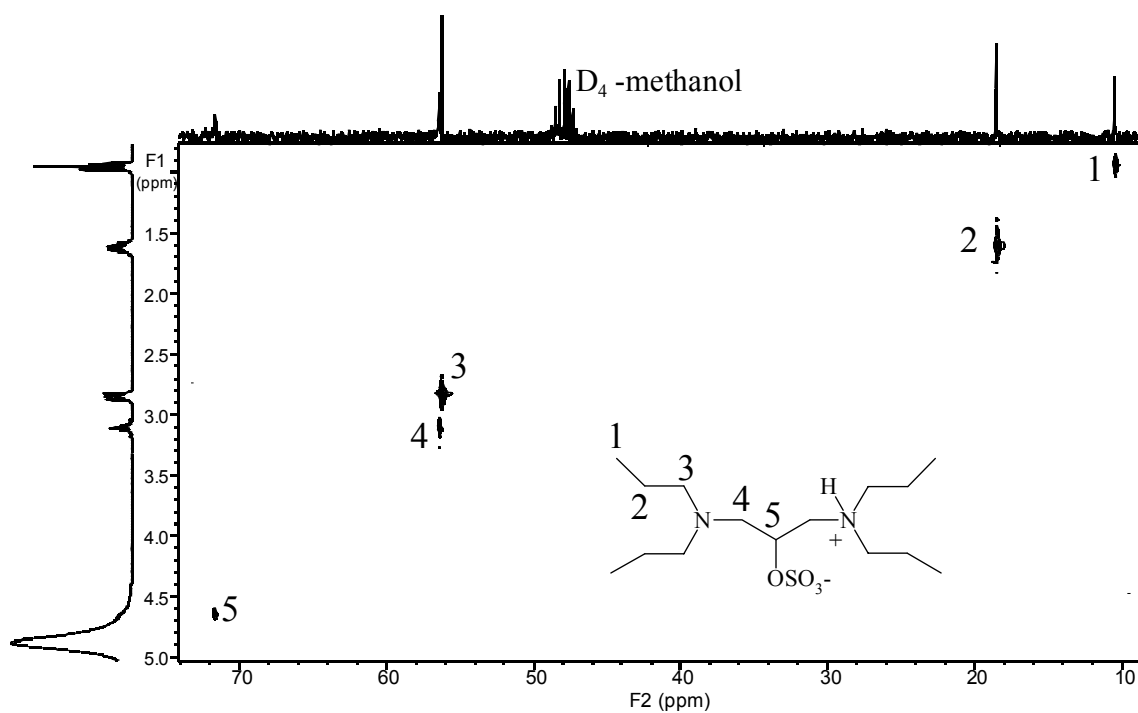


Figure 88. ^1H - ^{13}C HETCOR spectrum of BDPSP and the corresponding assignment of signals.

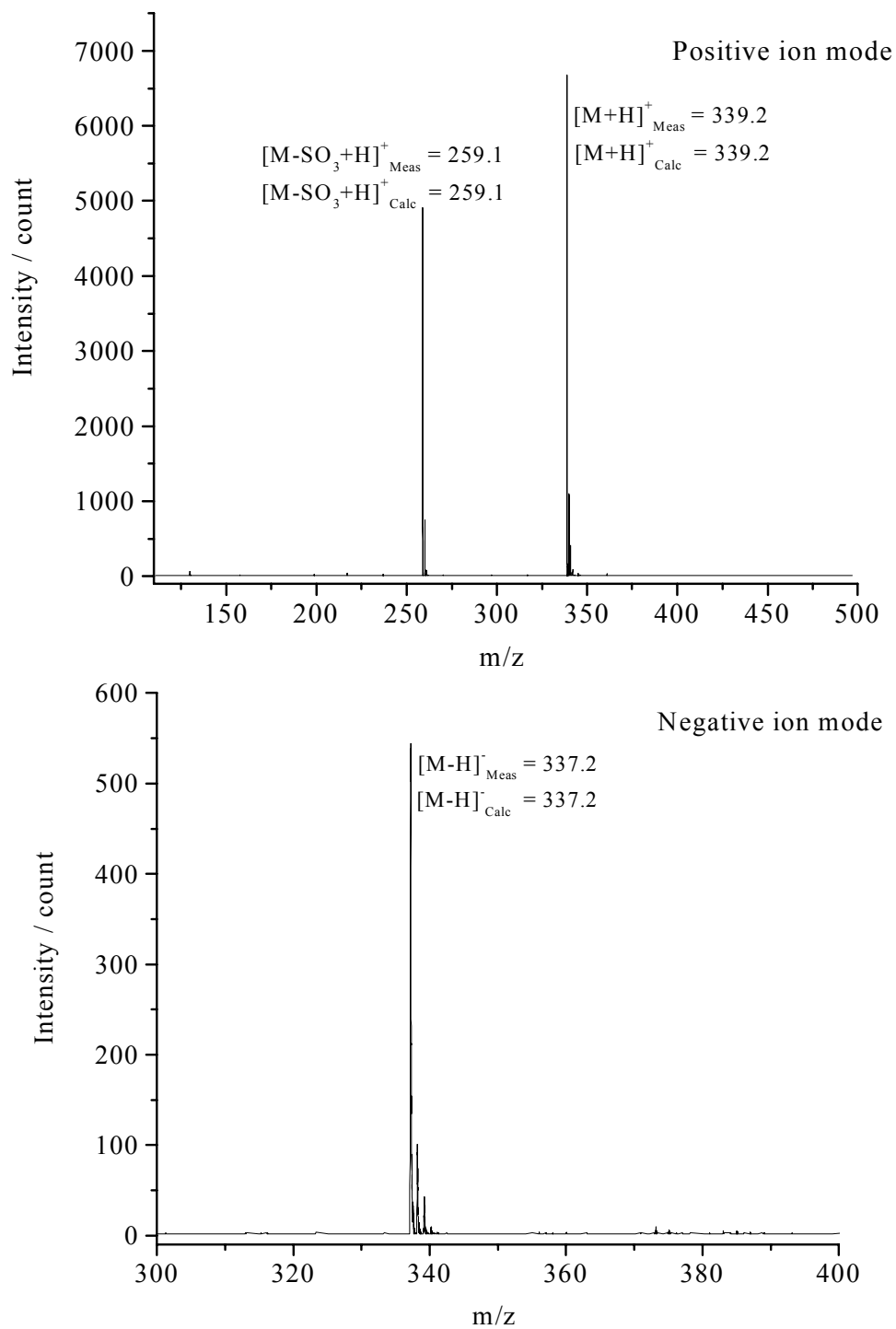


Figure 89. The ESI-MS spectra of BDPSP in the positive (top) and the negative (bottom) ion modes.

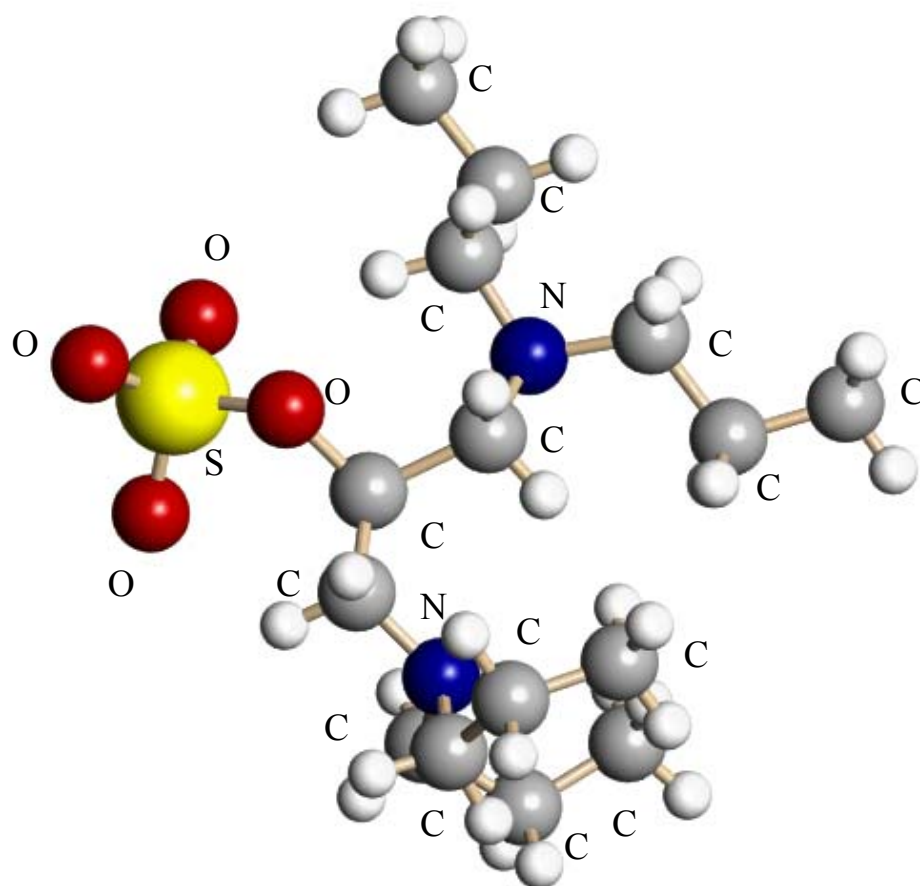


Figure 90. Ball-and-stick image of the single crystal X-ray structure of BDPSP.

6.2.3 1,3-Dipiperidino-2-O-sulfo-propane (DPSP)

6.2.3.1 Step 1

6.2.3.1.1 Synthesis

The reaction conditions (reaction time and temperature) for the synthesis of 1,3-dipiperidino-2-propanol (DPP, the diamino alcohol intermediate) from piperidine (PIP) and epichlorohydrin (EH) were adapted from the synthesis of DMP. The reactants were mixed and heated. A sample from the reaction mixture was taken periodically and analyzed by ^1H - and ^{13}C -NMR spectroscopy until complete conversion (determined from the NMR spectra) was seen. The intermediate was processed, and the next reaction was set-up. The complete scheme for the synthesis of DPSP is shown in Figure 91.

Step 1. Synthesis of DPP

7.5 g (0.088 mol) PIP was added into a 50 mL round bottom flask fitted with an ice-water cooled condenser. 2.7 g (0.029 mol) EH was mixed with 5 mL THF and the solution was added into the flask with PIP. The flask was warmed in an oil bath set at 65°C . Heavy solid formation was observed within 1 hour of heating. After 22 hours of heating, the reaction mixture was cooled. A sample was taken from the mixture and analyzed by ^1H - and ^{13}C -NMR (spectra shown in Figure 92). Five new, unique signals (aside from the reactant signals) were seen, indicating complete conversion of the amino alcohol intermediate to DPP.

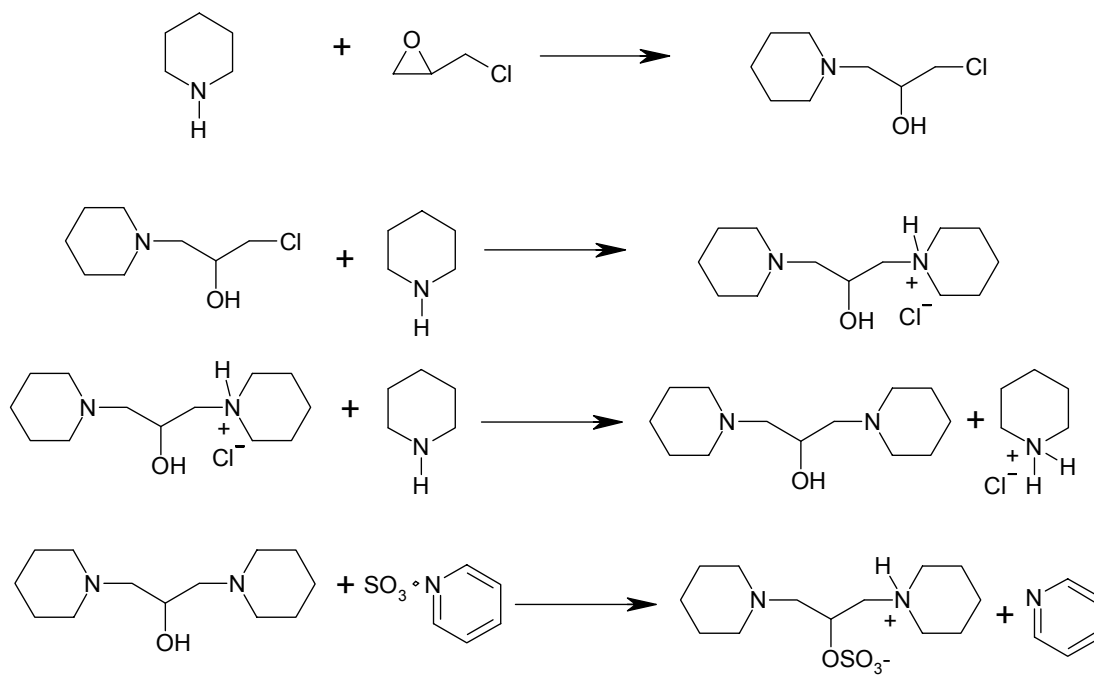


Figure 91. Complete scheme for the synthesis of DPSP.

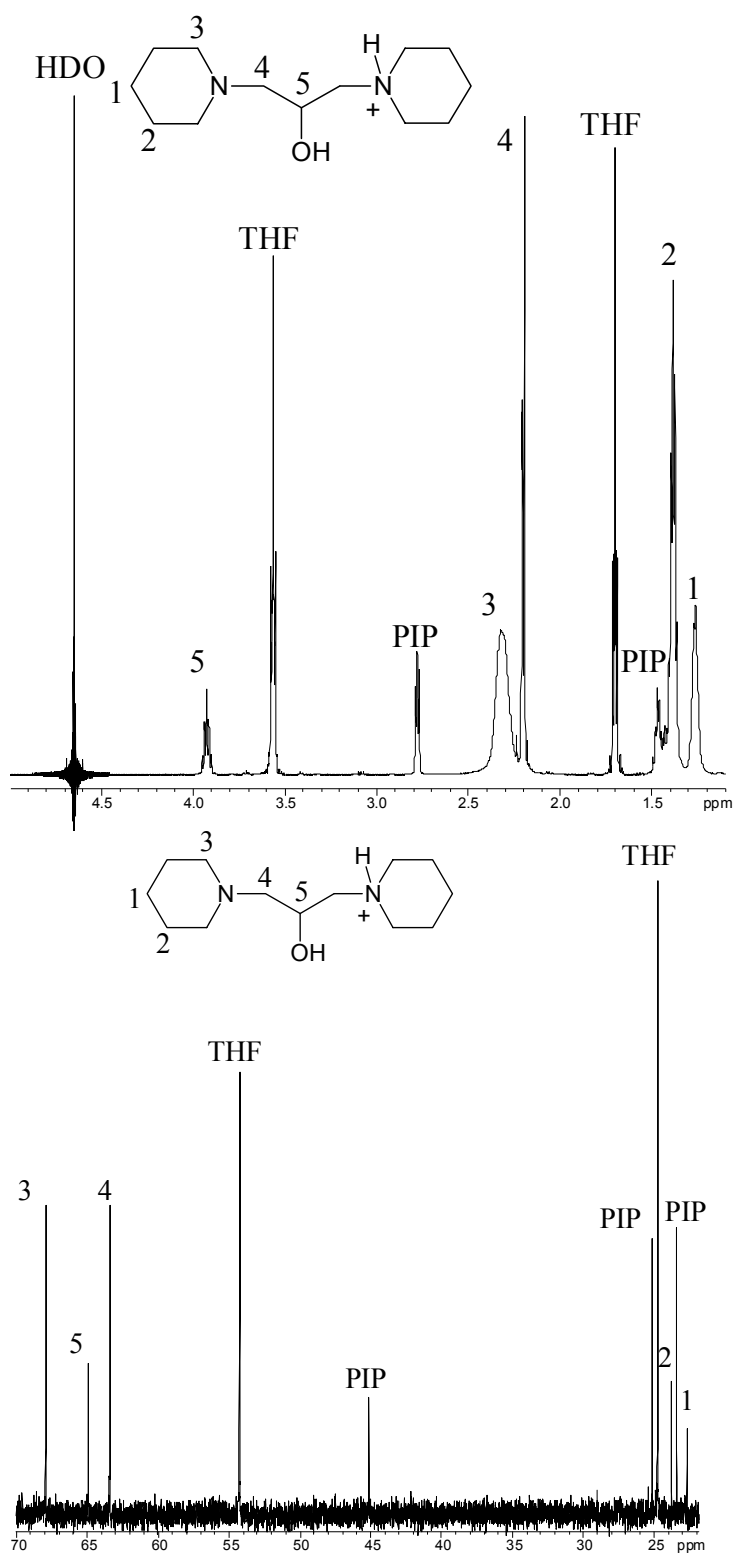


Figure 92. ^1H - (top) and ^{13}C - (bottom) NMR spectra of the DPP reaction mixture.

6.2.3.1.2 Processing of DPP

Acetone was added to the DPP reaction mixture and the slurry was filtered.

Acetone was removed from the filtrate under reduced pressure to yield a reddish viscous liquid. The processed DPP was set-up for the next reaction.

6.2.3.2 Step 2

6.2.3.2.1 Synthesis (sulfation)

The conditions for the sulfation of DPP were adapted from the optimized conditions for the synthesis of BDASP and DMSP. A clean, 50 mL, three-neck round bottom flask was fitted with an ice-water cooled condenser. 10 mL DMF was added to the flask. 5 g (0.026 mol) DPP was added and the flask was warmed in an oil bath to 65°C. 4.62 g (0.029 mol) SO₃•Pyr was added to the warm solution and the mixture was stirred and heated continuously at 65°C for 4 hours. Heavy solid formation was observed after 1 hour of heating.

After 4 hours of heating, the mixture was allowed to cool. A sample of the solids was dissolved in D₂O and the solution was analyzed by ¹H- and ¹³C-NMR which showed 60% conversion of DPP to DPSP. Another 3.70 g (0.023 mol) SO₃•Pyr was added and the mixture was heated for another 4 hours at 65°C. The reaction mixture was cooled and a sample was analyzed by ¹H- and ¹³C-NMR, which showed complete conversion. All this indicated that the system (DMF and possibly, DPP) had a significant amount of water, which competitively consumed SO₃•Pyr by hydrolysis. Figure 93 shows the ¹H-NMR spectra for the two sulfation samples.

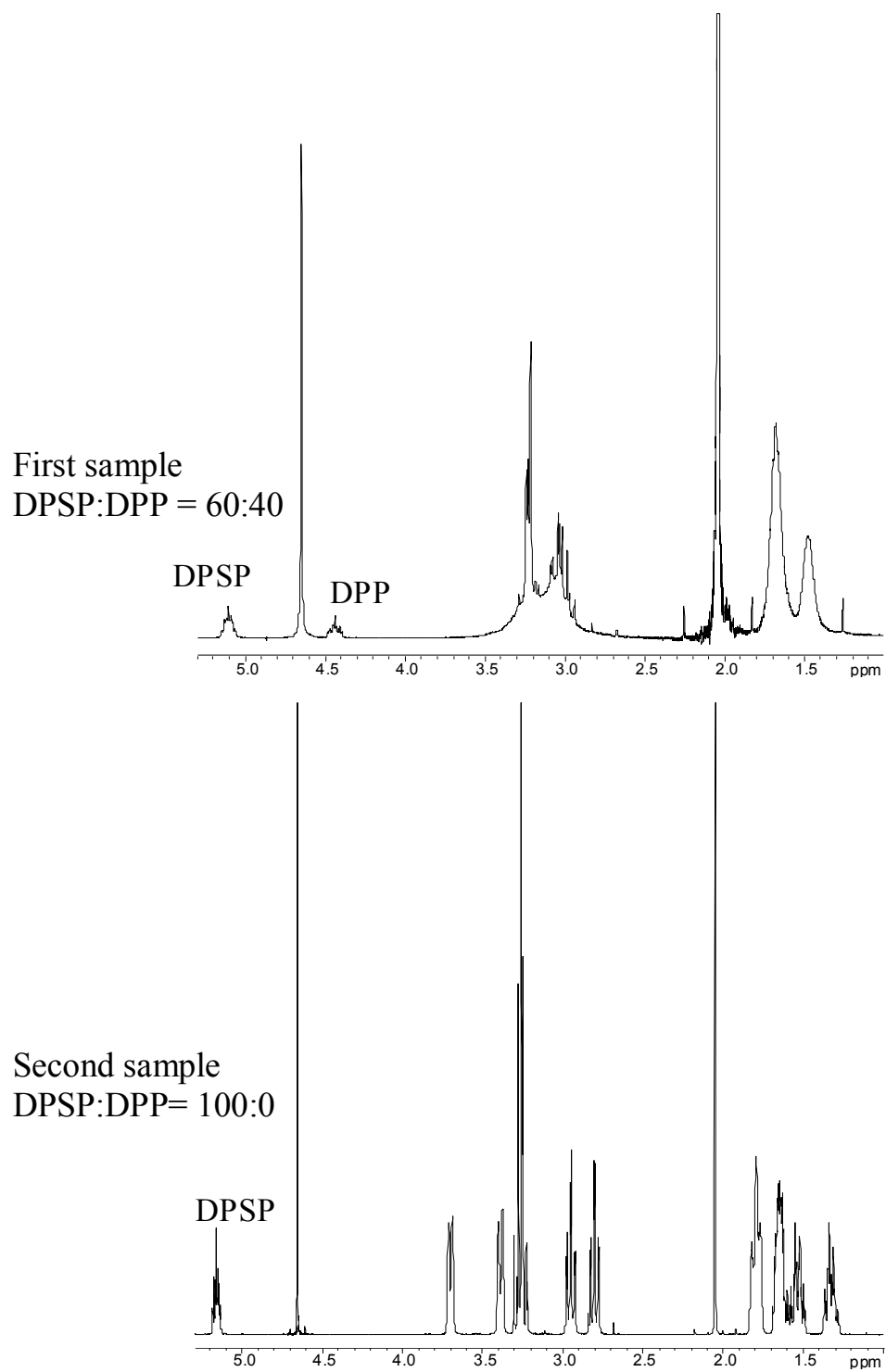


Figure 93. ^1H -NMR spectra for the two samples from the sulfation of DPP.

50 mL DMF was added to make a slurry. The slurry was filtered, the solids were dispersed in 100 mL acetone, and the acetone slurry was filtered. The solids were then dispersed in 100 mL ethyl alcohol followed by filtration of the slurry to obtain an off-white colored cake. A sample of the solids was dissolved in D₂O and the solution was analyzed by ¹H- and ¹³C-NMR. Almost complete removal of the contaminants was seen and signals were assigned tentatively.

6.2.3.3 pI determination

The pI of DPSP was determined by indirect UV detection CE. Using a 26 μm I.D. bare fused silica capillary, L_t = 26.1 cm, L_d = 19.7 cm at 15kV in positive to negative polarity, T=25 °C and UV detector at 214 nm, conventional CE was carried out in a 20 mM Tris BGE titrated to pH=7.8 with pTSA and a 20 mM benzylamine BGE titrated to pH=9.6 with pTSA. Figure 94 shows the electropherograms for DPSP in the two BGEs. Clearly, the pI of DPSP is between 7.8 and 9.6. The effective mobilities (μ^{eff} s) were calculated for DPSP in both CE runs, and were corrected for ionic strength suppression using Peakmaster 5.0. The corrected μ^{eff} s were plotted versus the pH of the BGE, and the pH at which the $\mu^{\text{eff}} = 0$ (thus the pI) was determined to be 8.9.

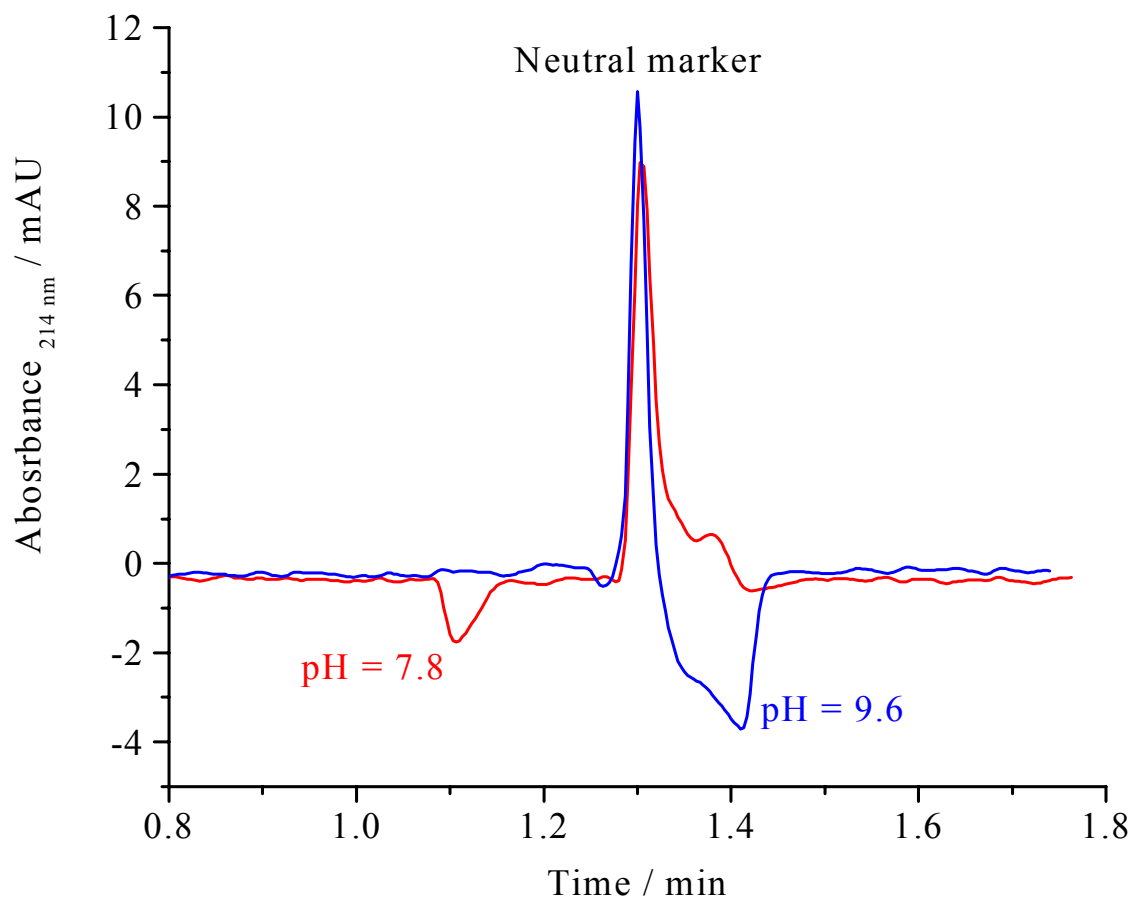


Figure 94. Electropherograms for the determination of the pI of DPSP.

6.2.3.4 Isoelectric crystallization

The solids were then dissolved into 50 mL deionized water and the solution was titrated with a 10% LiOH solution to pH=8.9. Water was partially removed under reduced pressure and the warm solution was cooled to crystallize the product in the salt-free form.

Product purity (in terms of inorganic salt content) was determined by indirect UV detection CE. Using a 20 mM acetic acid BGE titrated with imidazole to pH=4.5, run on a 26 μm I.D. bare fused silica capillary, $L_t = 26.5$ cm, $L_d = 19.7$ cm at 25kV, positive to negative polarity, $T=25$ °C and UV detector at 214 nm, lithium ions were analyzed. Figure 95 shows the electropherograms of the crystallized product (top panel) and the crystallization mother liquor (middle panel), and the electropherogram simulated using Peakmaster 5.0 (bottom panel). Using a 20 mM Tris, 0.1 mM CTAOH BGE titrated to pH=8.5 with BTC, run on a 50 μm I.D. bare fused silica capillary, $L_t = 25.7$ cm, $L_d = 19.3$ cm at 10 kV, negative to positive polarity, $T=25$ °C and UV detector at 214 nm, sulfate ions were analyzed. Results for the crystallized product (top panel) and the crystallization mother liquor (middle panel), and the simulated electropherogram (bottom, using Peakmaster 5.0) are shown in Figure 96.

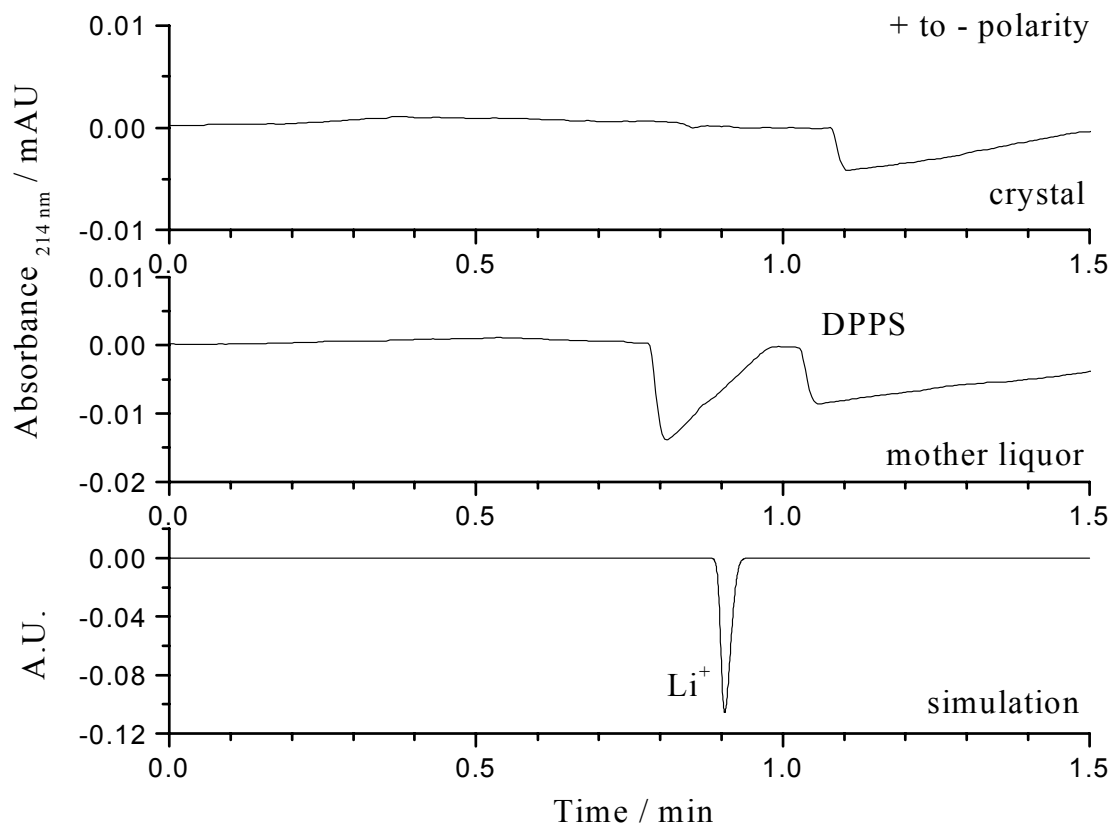


Figure 95. Electrochromograms for cation analysis of the crystallized DPSP (top panel) and the crystallization mother liquor (middle panel), and the electrochromogram simulated using Peakmaster 5.0 (bottom).

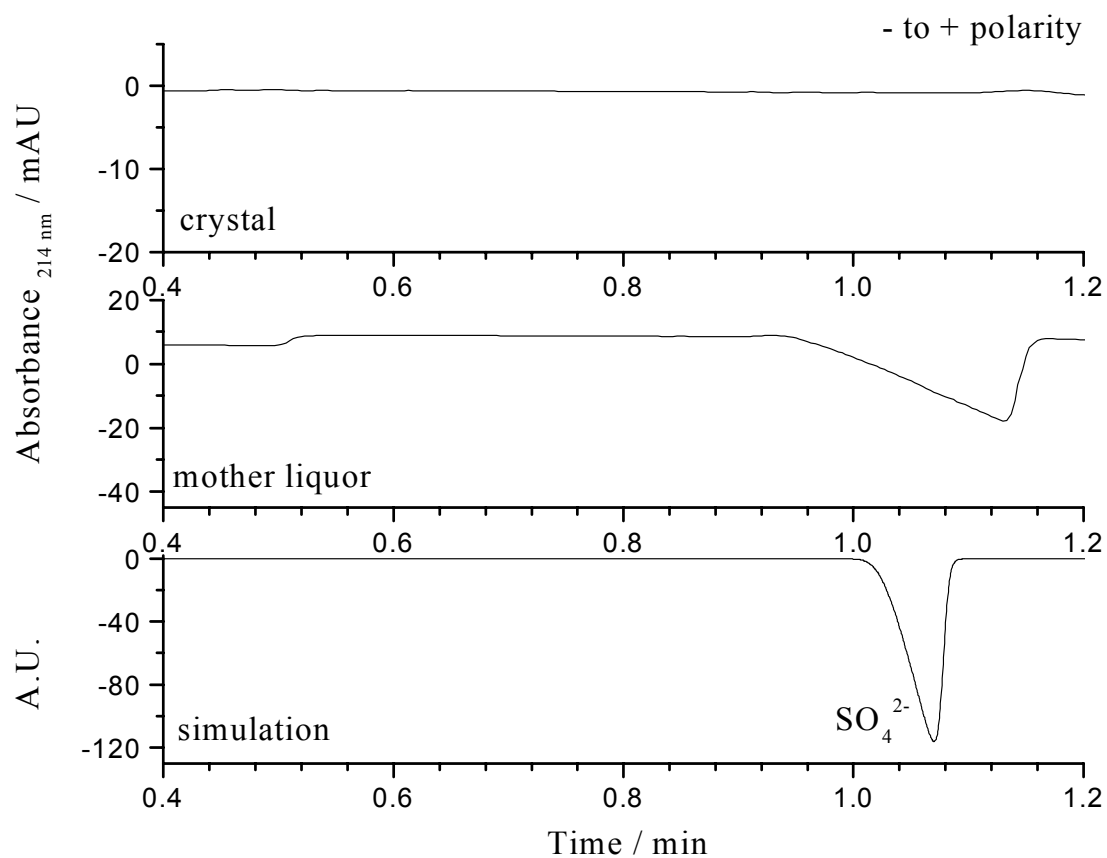


Figure 96. Electropherograms for anion analysis of the crystallized DPSP (top panel) and the crystallization mother liquor (middle panel), and the electropherogram simulated using Peakmaster 5.0 (bottom).

6.2.3.5 Characterization

The final product was characterized by ^1H - and ^{13}C -NMR. Figure 97 shows the ^1H - and ^{13}C -NMR spectra and the tentative assignment of the signals. Then, the product was analyzed by ^1H - ^1H COSY (spectra shown in Figure 98). This confirmed the proton signal assignments. The ^{13}C assignments were confirmed using ^1H - ^{13}C HETCOR NMR spectroscopy (spectra shown in Figure 99).

The identity and purity of the final product were confirmed by high resolution ESI-MS. The ESI-MS spectra in the positive and negative ion modes are shown in Figure 100. Only signals corresponding to DPSP and its fragment ions are seen.

6.2.3.6 Final procedure

Step 1. Fit a clean, 1 L, three-neck round bottom flask with an ice-water cooled condenser. Add 90 g (1.06 mol) PIP to the flask, set the flask in an oil bath over a magnetic stirrer. Mix together 32.6 g (0.352 mol) EH and 100 mL THF. Slowly add the EH solution into the flask and heat to 65°C while stirring the solution with a one-inch football-shaped magnetic stir bar. Take samples periodically and monitor the increase in the amount of DPP (and the corresponding decrease in the amount of the amino alcohol intermediate). Depending on whether more PIP or more EH is needed, add the corresponding amount into the reaction flask. Stirring continuously, heat the reaction mixture for a minimum of 22 hours. At the end of the reaction, take the flask off of the oil bath and set it to cool on a cork O-ring with paper towels underneath (to absorb the oil).

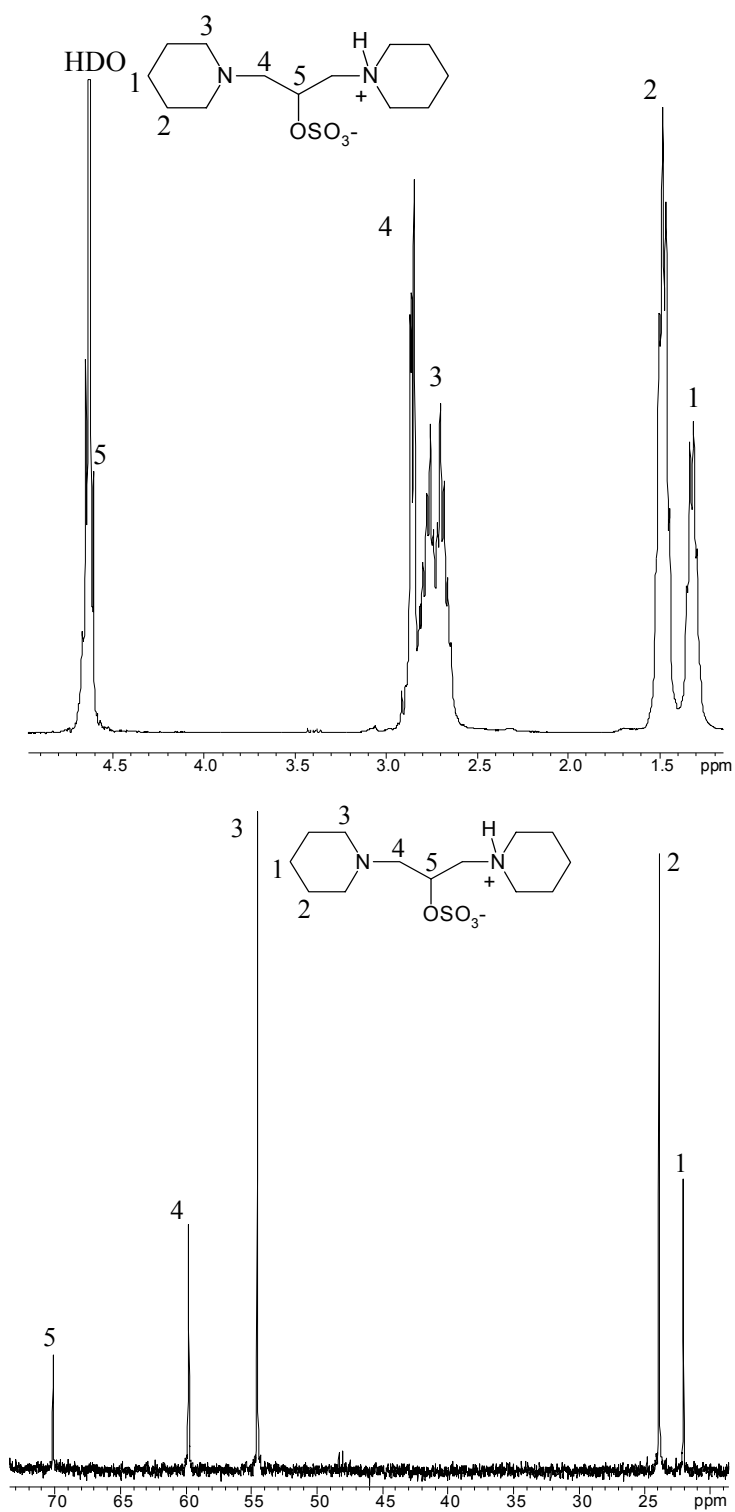


Figure 97. ¹H- (top) and ¹³C- (bottom) NMR spectra for DPSP and the corresponding assignments.

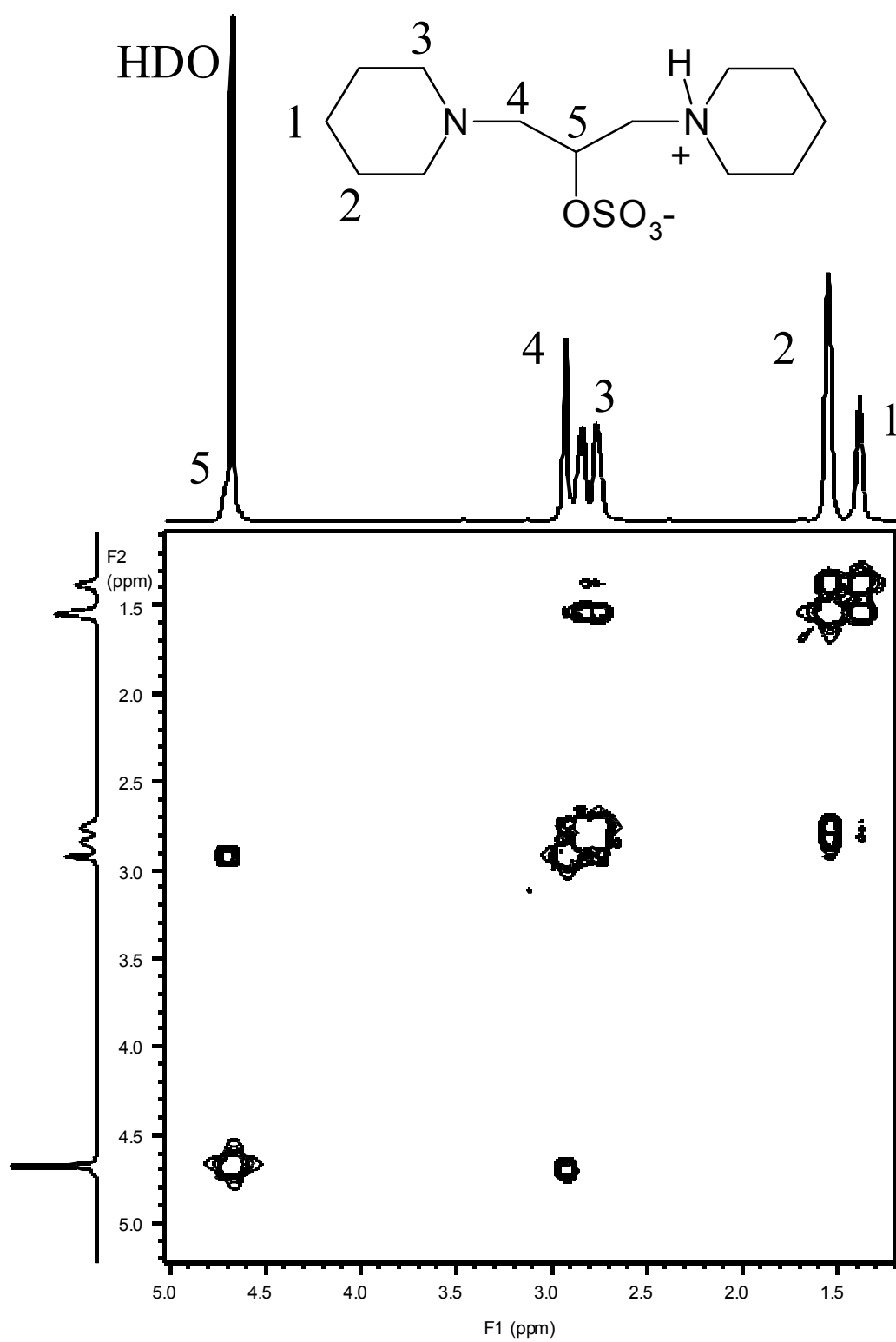


Figure 98. ^1H - ^1H COSY spectrum of DPSP with the corresponding assignments.

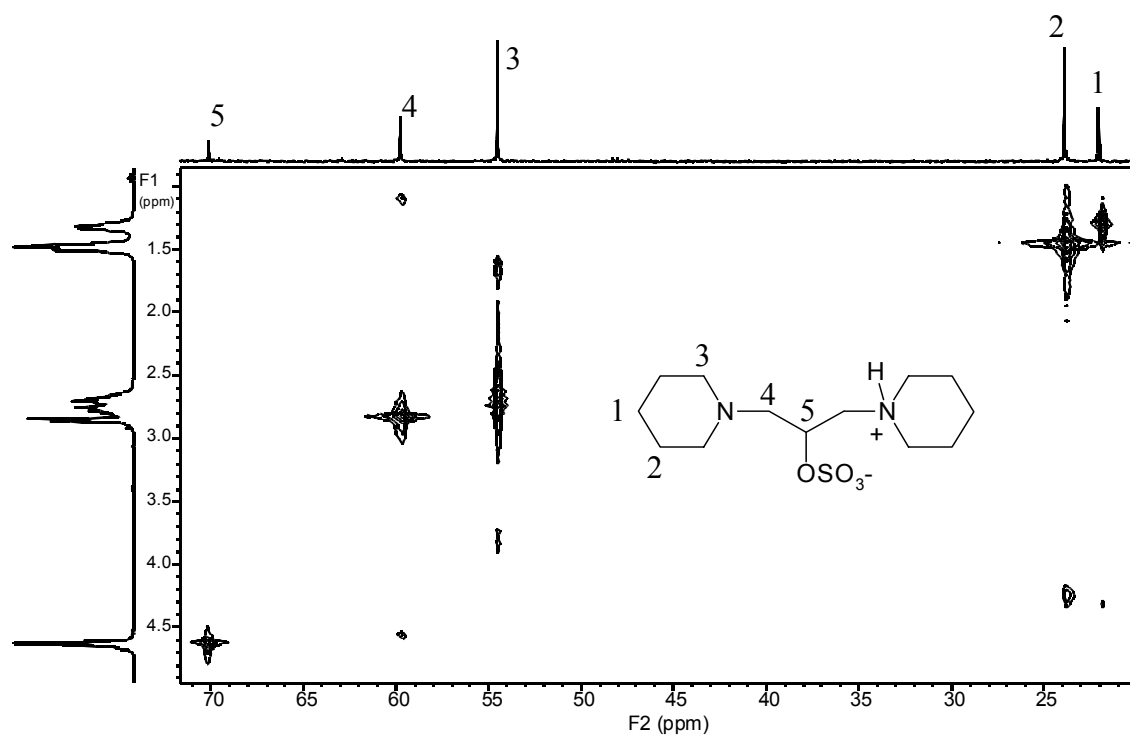


Figure 99. ^1H - ^{13}C HETCOR spectrum of DPSP and the corresponding assignments.

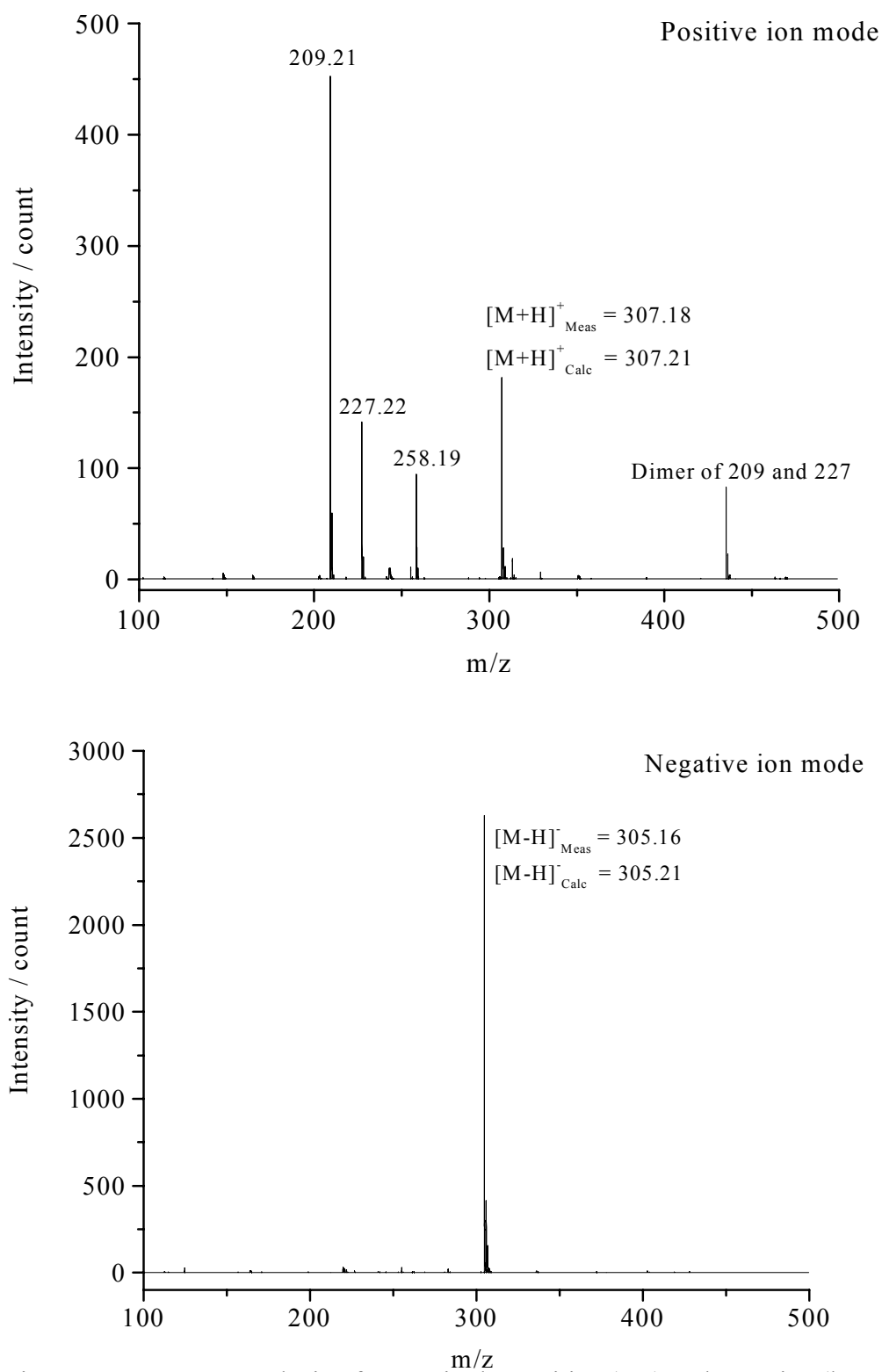


Figure 100. ESI-MS analysis of DPSP in the positive (top) and negative (bottom) ion modes.

Into the cool reaction mixture, add enough acetone to form a slurry of a thin consistency. Filter the slurry using a Buchner funnel and a suction flask. Remove acetone and THF under reduced pressure.

Step 2 (adapted from sulfation of BDAP and DMP). Fit a clean, 1 L, three-neck round bottom flask with an ice-water cooled condenser. Add 200 mL DMF to the flask, set the flask in an oil bath. Add the processed DPP from step 1 into the flask and heat to 65°C while stirring the solution with a mechanical stirrer. To the warm, stirring solution add 61.6 g (0.387 mol) SO₃•Pyr and continuously heat and stir the mixture at 65°C for 4 hours. Take the flask off of the oil bath and set it to cool on a cork O-ring with paper towels underneath (to absorb the oil).

Step 3. To the cooled reaction mixture, add 200 mL DMF and with the aid of a spatula, manually dislodge the solids and remove the chunks from the round bottom flask into a 2 L beaker. Add 300 mL DMF into the beaker and make a slurry of the solids. Filter the slurry using a Buchner funnel and a suction flask. Remove the solid cake and filter paper from the funnel and add them into another 2 L beaker and make a slurry with another 200 mL DMF. Repeat the steps until the DMF filtrate becomes pale yellow. Then, remove the solid cake and filter paper from the funnel and add them into another 2 L beaker and make a slurry with 300 mL of acetone. Filter the slurry, and make another slurry of the solids in 200 mL of ethanol, and filter again. Let the solids dry inside the fume hood.

Step 4. Dissolve the solids in a minimum volume (around 250 mL) of deionized water. Measure the pH of the solution and titrate it to pH=8.9 using a 10% LiOH solution (if the solution pH is below 8.9) or 2M H₂SO₄ (if the solution pH is above 8.9). Remove about half of the water using a rotovap with the water bath set at 65°C. Let the solution cool in the fume hood with continuous stirring for 24 hours. Filter the slurry, wash the solid cake with sufficient amounts of ice-cold ethanol a few times and let the cake dry in the fume hood. Analyze both the crystallization mother liquor and the solids by CE and repeat the crystallization from deionized water if necessary.

Remove more water from the crystallization mother liquor to get a second crop of crystals. Analyze each crop of crystals, and combine the similar ones. Repeat the concentration followed by crystallization steps until co-crystallization of DPSP and any of the salt contaminants is observed.

6.2.3.7 Recapitulation

A unique, basic isoelectric buffer, DPSP, has been synthesized from PIP and EH followed by reaction with SO₃•Pyr. According to the design of the molecule, the two amino groups in DPSP have close pK_a values, consequently DPSP has high buffering capacity and high conductivity in isoelectric state. The pI of DPSP is between 7.8 and 9.6 (calculated to be 8.9). DPSP has been obtained in its pure, isoelectric form and has been well characterized by 1D and 2D-NMR, ESI-MS and CE. DPSP has been successfully synthesized several times, in a 1 g scale batch to a 40 g scale batch.

7. CONCLUSIONS

7.1 TRISHUL

Polyacrylamide-based isoelectric membranes used in IET have worked well, but significant hydrolysis of the amide bond in the gels at high and low pH limits the utility of IET. To fully utilize the potentials of IET, hydrolytically stable, high- and low-pI isoelectric membranes are needed. A suitable isoelectric membrane for IET must be a hydrogel membrane (i) that has pores large enough to permit ions and macromolecules, such as proteins, to pass through and yet (ii) acts as an effective barrier against bulk transfer of liquids between the adjacent compartments and (iii) has immobilized acidic and basic functionalities that establish a buffered pH inside the membrane pores. Hydrogel membranes should be made using a hydrolytically stable polymer that (i) forms a hydrogel (thus is hydrophilic), (ii) can be crosslinked, and (iii) can be derivatized with acidic and basic functionalities. One such polymer is poly(vinyl alcohol), PVA. Low- and high-pI isoelectric hydrogel membranes were made using PVA.

7.1.1 Low-pI membranes

Hydrolytically stable, low-pI isoelectric hydrogel membranes were made by attaching an isoelectric buffer of a well-defined pI value to the PVA backbone and crosslinking the PVA strands, *in situ*. By this approach, the pH of the membrane is not significantly altered with slight changes in the amount of isoelectric buffer that is incorporated into the hydrogel. However, the pI of the membranes made using this approach cannot be tuned continuously as in polyacrylamide-based isoelectric hydrogels.

IDAPVA membranes were made using IDA, PVA and GDGE. ASPPVA membranes were made using ASP, PVA and GDGE. Similarly, GLUPVA membranes were made using GLU, PVA and GDGE. These membranes were tested in trapping and desalting experiments in the modified BF200IET unit. The pI value of IDAPVA membranes was determined to be between 1.7 and 2.0. The pI values of ASPPVA and GLUPVA membranes were determined to be between 2.0 and 2.6 and between 2.6 and 3.4, respectively.

All three hydrolytically stable, low-pI membranes were successfully used as the anodic membranes in IET experiments, with current densities as high as 67 mA/cm^2 , to trap, for at least 3 hours, small ampholytic molecules with pI values in the 3.9 to 10 range, and in desalting experiments to remove a strong electrolyte salt from a mixture of small ampholytes. They are promising, hydrolytically stable alternatives to the polyacrylamide-based membranes.

7.1.2 High-pI membranes

Sugars, cyclodextrins (CDs), and certain polyhydroxy compounds are very weak acids and have pK_a values between 11.5 and 14. Thus, it was hypothesized that high buffering capacity, high-pI, hydrolytically stable, isoelectric hydrogels can be made using PVA and any of these compounds. If at least two equivalents of such a high- pK_a moiety and at least one equivalent of a permanently cationic quaternary ammonium functionality were attached to the PVA backbone and the PVA was crosslinked, high-pI isoelectric hydrogels would be formed.

Hydrolytically stable, high-pI QCQPVA hydrogels were obtained by incorporating quaternary ammonium derivatives of β -CD (QCD) into a crosslinked PVA hydrogel. High-pI CDQPVA membranes were made by directly grafting quaternary ammonium groups (in the presence of β -CD) onto a crosslinked PVA hydrogel. Similarly, high-pI QPVA hydrogels were made by direct grafting of quaternary ammonium groups onto a crosslinked PVA hydrogel.

All three membranes had pI values greater than 11. These high-pI hydrogels served as effective cathodic membranes in isoelectric trapping experiments of small ampholytic compounds. These new, high-pI isoelectric hydrogels are very stable: the membranes have been used successfully even after storage for several months, at 4 °C. These membranes have been used in over 150 successful experiments for the rapid IET separation of both small ampholytic molecules and proteins. The membranes tolerated contact with very alkaline catholytes and withstood very high current densities (up to 80 mA/cm² has been tested), high power loads (up to 240 W/1.5 mL compartment volume has been tested), and long, continuous IET separations (up to 12 hours has been tested). They are promising alternatives for polyacrylamide-based membranes when good hydrolytic stability is required at high pH.

7.2 MOSES

With the advent of pH-biased IET, there is a demand for a series of isoelectric buffers (or isoelectric biasers) that act as good carrier ampholytes, with pI values covering the useful pH 2-10 range. By adding an ideal isoelectric biaser in IET, the conductivity of the receiving stream can be increased. Consequently, less potential

drops across the receiving stream and more drops across the feed stream. As a result, separation rates increase.

An ideal isoelectric biaser would have high buffering capacity and high conductivity in isoelectric state, as a consequence of having two closely spaced pK_a values. Most carboxylic acids have pK_a values in the 0.8 to 4.8 range and most amines have conjugate acid pK_a values in the 8 to 11 range. Thus, it is obvious that isoelectric buffers that are good ampholytes cannot be made by simply coupling one carboxylic acid unit with one amine unit. This also eliminates most common amino acids (glycine, β -alanine, etc.) from the list of good biasers.

7.2.1 Low-pI isoelectric buffers

Isoelectric buffers having two weak acid units coupled to one strong base unit (such as a quaternary ammonium functionality) or weak base unit (such as an amine group) can have close pK_a values that buffer at the pI, thus qualifying as good carrier ampholytes. Buffers with a quaternary ammonium functionality on the molecule are resistant to N-oxidation and are thus preferred. Such compounds are not commercially available, thus, it was important to synthesize them.

An opportunistic synthesis scheme is to take an iminodicarboxylic acid such as MIDA and alkylate the amino group. Thus, BCDAH was synthesized from MIDA and IM. The pI of BCDAH is between 1.5 and 1.7, being the most acidic isoelectric buffer so far reported (previously, cysteic acid was the most acidic buffer with a pI of 1.85 [71,72]). BCDAH has been obtained in its pure, isoelectric form and has been well characterized by 1D and 2D-NMR, ESI-MS, CE and X-ray crystallography.

Since iminodicarboxylic acids with pI values higher than MIDA's are not available, a *de novo* approach was needed for the synthesis of higher pI derivatives. An isoelectric buffer with two carboxylic acids (both structurally symmetric and asymmetric) can be made if a secondary amine is reacted with two equivalents of the a haloalkylcarboxylic acid (or its salt or its ester). This synthesis scheme has greater flexibility and broader applicability in terms of the derivatives that can be synthesized compared to the opportunistic approach. A major disadvantage of the synthesis scheme is that the isoelectric buffer is obtained in the salt form (due to the base and the released halide) requiring an additional salt removal step.

BCPDEAH, a unique, acidic isoelectric buffer has been synthesized from DEA and EBB. The pI of BCPDEAH is between 3.4 and 3.9, making BCPDEAH the least acidic isoelectric buffer so far reported (for buffers whose pI is between the pK_a values of the two carboxylic acids, glutamic acid was the least acidic with a pI of 3.2). BCPDEAH has been obtained in its pure, isoelectric form by IET, and has been well characterized by 1D and 2D-NMR, ESI-MS and CE. An additional characteristic of these buffers (and others that can be made using this synthesis scheme) is their resistance to N-oxidation, not found in isoelectric buffers reported in the literature.

7.2.2 High-pI isoelectric buffers

The highest aminocarboxylic acid pK_a value is at 4.3 (6-aminohexanoic acid) and thus, the pI value of the highest pI derivative could only be below that. High buffering capacity, higher pI value isoelectric buffers cannot be made using one amine and one carboxylic acid (though the pI value would be high) due to the large ΔpK_a . Since pK_a

values for amines range from 8.58 (morpholine) to 11.01 (piperidine), isoelectric buffers that are good carrier ampholytes can be made using amines, similarly to the carboxylic acid-based buffers. If two weak base groups (such as amines) and one acidic group (either strong or weak acid group) were linked into one molecule, the pI value of the compound will fall between the pK_a values of the two amine groups ($pI = (pK_{a2} + pK_{a3})/2$).

An opportunistic approach to synthesize amine-based isoelectric buffers is to sulfate the alcohol group of a species with two amine groups and one alcohol group. The pI will fall between the pK_a values of the two amine groups and the sulfate group will act as a permanently anionic functionality. Although rare, two such compounds with the two amine groups of close ΔpK_a values, are commercially available.

A unique, basic isoelectric buffer, BDASP, has been synthesized from BDAP and $SO_3 \cdot Pyr$. The pI of BDASP is between 7.8 and 9.6 (calculated to be 8.0). BDASP has been obtained in its pure, isoelectric form and has been well characterized by 1D- and 2D-NMR, ESI-MS, CE and X-ray crystallography. BDASP has been successfully synthesized several times, in a 1 g scale batch to a 40 g scale batch. However, a *de novo* approach was needed to make amine-based isoelectric buffers of different pI values.

To synthesize a series of amine-based isoelectric buffers using amines of different pK_a values, and according to the structure described above, an appropriate difunctional linker, epichlorohydrin was used to bind the two amine moieties and form an alcohol group in the process. The alcohol group was then sulfated using $SO_3 \cdot Pyr$.

A unique, basic isoelectric buffer, DMSP, has been synthesized from MOR and EH followed by reaction with $\text{SO}_3\cdot\text{Pyr}$. The pI of DMSP is between 4.6 and 6.1 (calculated to be 5.8). For isoelectric buffers where the pI value is between the pK_a values of two amino groups (such as in lysine with a pI of 9.9) DMSP is the least basic isoelectric buffer reported so far. DMSP has been obtained in its pure, isoelectric form and has been well characterized by 1D and 2D-NMR, ESI-MS, CE and X-ray crystallography. DMSP has been successfully synthesized several times, in a 1 g scale batch to a 500 g scale batch.

Also, BDPSP, another unique, basic isoelectric buffer has been synthesized from DPA and EH followed by reaction with $\text{SO}_3\cdot\text{Pyr}$. The pI of BDPSP is between 7.8 and 9.6 (calculated to be 8.7). BDPSP has been obtained in its pure, isoelectric form and has been well characterized by 1D- and 2D-NMR, ESI-MS and CE.

Another unique, basic isoelectric buffer, DPSP, has been synthesized from PIP and EH followed by reaction with $\text{SO}_3\cdot\text{Pyr}$. The pI of DPSP is between 7.8 and 9.6 (calculated to be 8.9). DPSP has been obtained in its pure, isoelectric form and has been well characterized by 1D- and 2D-NMR, ESI-MS and CE. DPSP has been successfully synthesized several times, in a 1 g scale batch to a 40 g scale batch.

REFERENCES

- [1] Ivory, C.F., *Sep. Sci. Technology* 2000, 35, 1777-1793.
- [2] Krivankova, L., Bocek, P., *Electrophoresis* 1998, 19, 1055-1062.
- [3] Simpson, R.J., *Proteins and Proteomics : A Laboratory Manual*, Cold Spring Harbor Laboratory Press, Cold Spring Harbor, NY, 2003.
- [4] Vesterberg, O., Svensson, H., *Acta. Chem. Scand.* 1966, 20, 820-834.
- [5] Williams, R.R., Waterman, R.E., *Proc. Soc. Exptl. Biol. Med.* 1929, 27, 56-59.
- [6] Kolin, A., *J. Chem. Phys.* 1955, 23, 407-410.
- [7] Martin, A.J.P., Hampson, F., US Patent 4,243,507, 1981.
- [8] Faupel, M., Barzaghi, B., Gelfi, C., Righetti, P.G., *J. Biochem. Biophys. Methods* 1987, 15, 147-161.
- [9] *IsoPrime Manual*, Amersham Pharmacia Biotech., San Francisco, CA, 1999.
- [10] Bjellqvist, B., Ek, K., Righetti, P.G., Gianazza, E., Gorg, A., Westermeier, R., Postel, W., *J. Biochem. Biophys. Methods* 1982, 6, 317-339.
- [11] Dossi, G., Celentano, F., Gianazza, E., Righetti, P.G., *J. Biochem. Biophys. Methods* 1983, 7, 123-142.
- [12] Righetti, P.G., *Laboratory Techniques in Biochemistry and Molecular Biology*, Vol. 20, Elsevier Science Publishing Company, Inc., New York, NY, 1990.
- [13] Righetti, P.G., Barzaghi, B., Faupel, M., *J. Biochem. Biophys. Methods* 1987, 15, 163-176.
- [14] Barzaghi, B., Righetti, P.G., Faupel, M., *J. Biochem. Biophys. Methods* 1987, 15, 177-188.
- [15] Righetti, P.G., Barzaghi, B., Luzzana, M., Manfredi, G., Faupel, M., *J. Biochem. Biophys. Methods* 1987, 15, 189-198.
- [16] Glukhovskiy, P., Landers, T.A., Vigh, Gy., *Electrophoresis* 2000, 21, 762-766.
- [17] Shave, E., Vigh, Gy., *J. Chromatogr. A*, 2002, 989, 73-78.

- [18] Herbert, B., Righetti, P.G., *Electrophoresis* 2001, 21, 3639-3648.
- [19] Zou, X., Speicher, D.W., *Anal. Biochem.* 2000, 284, 266-278.
- [20] Invitrogen Corp., December 18, 2003,
<http://www.invitrogen.com/content.cfm?pageid=9719&CMP=ILC-ZOOMFRACTIONATOR&GPN=LAST>.
- [21] Proteome Systems Ltd., December 15, 2003,
<http://www.proteomesystems.com/Catalogue/Profile.asp?ProductID=74>
- [22] Ogle, D., Ho, A., Gibson, T., Rylatt, D.B., Shave, E., Lim, P., Vigh, Gy., *J. Chromatogr. A* 2002, 979, 155-161.
- [23] Cretich, M., Pirri, G., Carrea, G., Chiari, M., *Electrophoresis* 2003, 24, 577-581.
- [24] McMurry, J., *Organic Chemistry*, Brooks/Cole, Pacific Grove, CA, 2000.
- [25] Chiari, M., Nesi, M., Roncada, P., Righetti, P.G., *Electrophoresis* 1994, 15, 953-959.
- [26] Shave, E., Vigh, Gy., *Electrophoresis* 2004, 25, 381-387.
- [27] Horvath, Zs., Corthals, G.L., Wrigley, C.W., Margolis, J., *Electrophoresis* 1994, 15, 968-971.
- [28] Vesterberg, O., *Acta Chem. Scand.* 1969, 23, 2653-2666.
- [29] Pospichal, J., Tietz, D., Ittyerah, T.R., Halpern, D., Chrambach, A., *Electrophoresis* 1991, 12, 338-341.
- [30] Gilges, M., Kleemiss, M.H., Schomburg, G., *Anal Chem* 1994, 13, 2038-2046.
- [31] Belder, D., Deege, A., Husman, H., Kohler, F., Ludwig, M., *Electrophoresis* 2001, 22, 3813-3818.
- [32] Purss, H.K., Caulfield, M.J., Solomon, D.H., Sommer-Knudsen, J., *Electrophoresis* 2003, 24, 12-19.
- [33] Wenger, P., de Zuanni, M., Javet, P., Gelfi, C., Righetti, P.G., *J. Biochem. Biophys. Methods* 1987, 15, 177-188.
- [34] Leeds, M., *Kirk-Othmer Encyclopedia of Chemical Technology*, 2nd ed., Vol. 21, John Wiley & Sons, Inc., New York, NY, 1970.

- [35] Herrmann, W.O., Haehnel, W., US Patent 1,672,156, 1928.
- [36] Sundararajan, P.R., *Polymer Data Handbook - Poly(vinyl alcohol)*, Oxford University Press, Inc., New York, NY, 1999.
- [37] Peierls, E.S., *Mod. Plastics* 1941, 18, 53.
- [38] Wiley Intersciences, February 22, 2003,
<http://www.mrw.interscience.wiley.com/kirk/articles/vinymart.a01/frame.html>
- [39] Zsardon, B., Fenyvesi, E., *Proc. 1st Int. Symp Cyclodextrins* 1981, 327-336.
- [40] Szetli, J., Fenyvesi, E., Zoltan, S., Zsardon, B., Tudos, F., US Patent 4,274,985, 1981.
- [41] Mocanu, G., Vizitiu, D., Carpov, A., *Journal of Bioactive and Compatible Polymers* 2001, 16, 315-342.
- [42] Jones, R.V., US Patent 2,623,037, 1951.
- [43] Reynolds, D.D., Kenyon, W.O., *J. Am. Chem. Soc.* 1950, 72, 1584-1598.
- [44] Lagache, M., *Ann. Chim.* 1956, 13, 5-52.
- [45] Ettore, K., Varadi, P., *Anal Chem* 1962, 34, 752-757.
- [46] Houtz, R.C., US Patent 2,341,553, 1951.
- [47] Wright, J.F., Minsk, L.M., *J. Am. Chem. Soc.* 1953, 75, 98.
- [48] Tsuda, M., US Patent 3,329,664, 1967.
- [49] Martell, A.E., Smith, R.M., *Critical Stability Constants*, Vol.1 , Plenum Press, New York, NY, 1974.
- [50] Martell, A.E., Smith, R.M., Motekaitis, R.J., *Updated Critical Stability Constants Database*, Chemistry Department, Texas A&M University, College Station, TX, 1996.
- [51] Gas, B., Coufal, P., Jaros, M., Muzikar, J., Jelinek, I., *J. Chromatogr. A* 2001, 905, 269-279.
- [52] Group of electromigration separation processes, November 21, 2003,
<http://www.natur.cuni.cz/~gas>.

- [53] Masuda, T., Kitahara, K., Aikawa, Y., Arai, S., *J. Chromatogr. A* 2002, 961, 89-96.
- [54] Rong, D., D'Souza, V.T., *Tetrahedron Letters* 1990, 31, 4275-4278.
- [55] Lee, Y., Liu, T., *Electrophoresis* 1996, 17, 333-340.
- [56] Bruggink, C., *Proceedings of the 7th AVH Association Symposium* 2000, 3-9.
- [57] Tian, S., Zhu, H., Forgo, P., D'Souza, V.T., *J. Org. Chem.* 2000, 65, 2624-2630.
- [58] Pitha, J., Rao, C.T., Lindberg, B., Seffers, P., *Carbohydr. Res.* 1990, 200, 429.
- [59] Khan, A.R., Forgo, P., Stine, K.J., D'Souza, V.T., *Chem. Rev.* 1998, 98, 1977-1996.
- [60] Šebesta, R., Sališová, M., *Enantiomer* 1999, 4, 271-277.
- [61] Zhong, N., Ohvo-Rekilä, H., Ramstedt, B., Slotte, J.P., Bittman, R., *Langmuir* 2001, 17, 5319-5323.
- [62] Solms, V.J., Egli, R.H., *Helv. Chim. Acta* 1965, 48, 1225-1228.
- [63] Szejtli, J., Zsardon, B., Fenyvesi, E., Szilasi, M., Tudos, F., *Hung. Teljes HU* 22,968 1982.
- [64] Mitsubishi Petrochemical Co., Ltd. JP Patent 58,167,613, 1983.
- [65] Mitsubishi Petrochemical Co., Ltd. JP Patent 59,164,728, 1984.
- [66] Otta, K., Fenyvesi, E., Zsardon, B., Szejtli, J., Tudos, F., *Proc. Int. Symp Cyclodextrins Ist* 1981, 357-362.
- [67] Sansho Co., Ltd., December 18, 2003, <http://www.sansho.co.jp/>
- [68] Van Slyke, D.D., *J. Biol. Chem.* 1922, 52, 525-536.
- [69] Fullarton, J.R., Kenny, A.J., *Biochem. J.* 1970, 116, 147-149.
- [70] Hjertén, S., Liao, J., US Patent 5,464,517, 1995.
- [71] Stoyanov, A., Righetti, P.G., *J. Chromatogr. A* 1997, 169-176.
- [72] Righetti, P.G., Bossi, A., Gelfi, C., *J. Cap. Elec.* 1997, 4, 47-59.
- [73] Stoyanov, A., Righetti, P.G., *Electrophoresis* 1998, 19, 1674-1676.

- [74] Bossi, A., Olivieri, E., Castelletti, L., Gelfi, C., Hamdan, M., Righetti, P.G., *J Chromatogr. A* 1999, 853, 71-82.
- [75] Beckers, J., *Electrophoresis* 2003, 24, 548-556.
- [76] Katritzky, A.R., Duell, B.L., Seiders, R.P., Durst, H.D., *Langmuir* 1987, 3, 976-982.
- [77] Moriarty, R., International Patent WO 94/19366, 1994.
- [78] De Mesmaeker, N. S., Merényi, R., Viehe, H.G., *Tetrahedron Letters* 1987, 28, 2591-2594.
- [79] Remizov, A.L., *Zhurnal Obshchei Khimii* 1964, 34, 3187-3192.
- [80] Jenner, G., *New J. Chem.* 1995, 19, 173-178.
- [81] Minch, M.J., Chen, S-S., Peters, R., *J. Org. Chem.* 1978, 43, 31-33.
- [82] Comber, R.N., Hosmer, C.A., Brouillette, W.J., *J. Org. Chem.* 1985, 50, 3627-3631.
- [83] Salvatore, R.N., Nagle, A.S., Schmidt, S.E., Jung, K.W., *Organic Letters* 1999, 1, 1893-1896.
- [84] Heine, H.W., Greiner, R.W., Boote, M.A, Brown, B.A., *J. Am. Chem. Soc.* 1953, 75, 2505-2506.
- [85] Macka, M., Johns, C., Grosse, A., Haddad, P., *Analyst* 2001, 126, 421-425.
- [86] Tait, R.J., Skanchy, D.J., Thompson, D.P., Chetwyn, N.C., Dunshee, D.A., Rajewski, R.A., Stella, V.J., Stobaugh, J.F., *J Pharm. Bio. Anal.* 1992, 10, 615-622.
- [87] Tait, R.J., Thompson, D.P., Stella, V.J., Stobaugh, J.F., *Anal. Chem.* 1994, 66, 4013-4018.
- [88] Jung, M., Francotte, E., *J. Chromatogr. A* 1996, 755, 81-88.
- [89] Haftendorn, R., Ulbrich-Hofmann, R., *Tetrahedron* 1995, 51, 1177-1186.
- [90] Stalcup, A.M., Gahm, K.H., *Anal. Chem.* 1996, 68, 1360-68.
- [91] Suss, F., Poppitz, W., Sanger-van de Griend, C.E., Scriba, G.K., *Electrophoresis* 2001, 22, 2416-2423.

- [92] Vincent, J.B., Sokolowski, A.D., Nguyen, T.V., Vigh, Gy., *Anal. Chem.* 1997, *69*, 4226-4233.
- [93] Vincent, J.B., Kirby, D.M., Nguyen, T.V., Vigh, Gy., *Anal. Chem.* 1997, *69*, 4419-4428.
- [94] Cai, H., Nguyen, T.V., Vigh, Gy., *Anal. Chem.* 1998, *70*, 580-589.
- [95] Zhu, W., Vigh, Gy., *Anal. Chem.* 2000, *72*, 310-317.
- [96] Maynard, D.K., Vigh, Gy., *Carbohydrate Research* 2000, *328*, 277-285.
- [97] Busby, M.B., Maldonado, O., Vigh, Gy., *Electrophoresis* 2002, *23*, 456-461.
- [98] Li, S., Vigh, Gy., *Electrophoresis* 2003, *24*, 2487-2498.
- [99] Bazito, R.C., El Seoud, O., *Carbohydrate Research* 2001, *33*, 95-102.
- [100] Williams, B.A., Vigh, Gy., *Anal. Chem.* 1996, *68*, 1174-80.

VITA

Sanjiv Kumar Shankerdass Lalwani was born on November 26, 1977 in Manila, Philippines. He attended St. Francis of Assisi School for his primary education and University of San Carlos, Boys School for his secondary education, both in Cebu City, Philippines. Sanjiv then attended University of San Carlos in Cebu City, Philippines from June 1994 to March 1998 where he received his Bachelor of Science degree in chemistry. His thesis was entitled Photometric Determination of Nitrite Using Reverse Flow Injection Analysis, under the directorship of Dr. Josephine M. Castañares. From May 1998 to June 2000, Sanjiv taught college freshman and organic chemistry courses while co-advising research in the Flow Injection Analysis group at the University of San Carlos. He commenced his graduate studies in August 2000 at Texas A&M University, under the directorship of Prof. Gyula Vigh. His permanent address is E. Luisa Apt., Don Pedro Rodriguez St., Capitol Site, Cebu City, Philippines 6000.